THE HONG KONG POLYTECHNIC UNIVERSITY

DEPARTMENT OF

BUILDING SERVICES ENGINEERING

SUSTAINABLE THERMAL COMFORT

LEUNG, Suet Ha

A thesis submitted in partial fulfillment of the requirement

of the Degree of Doctor of Philosophy

September, 2007

CERTIFICATE OF ORIGINALITY

I hereby declare that this thesis is my own work and that, to the best of my knowledge and belief, it reproduces no material previously published or written, nor material that has been accepted for the award of any other degree or diploma, except where due acknowledgement has been made in the text.

Signature : _____

Name : __Leung Suet Ha__

ABSTRACT

Ex-Premier Hon. Lee Guan Yew at the end of last Century, voted the invention of air-conditioning system as the greatest invention in 20th Century for Far East Asians because these systems keep indoor users comfortable in indoor spaces. The thermally comfortable environment helps to boost up the economy in Asia. ASHRAE Standard 55 on 2004 which is based on the late Professor Fanger's comprehensive thermal comfort theory provides the engineers a model to design and control the indoor thermal environment optimally. In geographically temperate regions, indoor cooling is the main issue for keeping an optimum thermal comfort environment

A survey conducted by Chan et al (1996) in the Hong Kong air-conditioned offices revealed that the thermal environment is not satisfactory. Two main reasons are identified in this project - distributive nature of the thermal environmental parameters and local culture. The former is not, and probably in many situations, cannot be properly controlled to match the thermal loading with the cooling capacity. The later influences the thermal comfort management protocol inducing unacceptability.

In this thesis, two approaches are used to rectify the situation. Firstly, from further analysis of the large data base compiled by Chan et al., the most influential distributive natures are found to be the spatial and temporal distribution of the air temperature and the distribution of clo. It is further found that the Hong Kong people are almost 2°C lower indulged as compared to ASHRAE Standard thermal comfort zone. The findings lead to a new sequence of design, test and commissioning and

operation of the air-side systems in setting the optimum air temperature for control, fine tuning of the air distribution and control, and operation of the systems. An envelop of air temperature which is formed by the two extreme distribution functions at air temperature linked by the range of temperature swing is proposed as a new target of air temperature control function. In this integrated approach, education, space air tightness, air and water balances and company culture on clothing clo are all taken into account.

Secondly, this study explores the feasibility of raising the air temperature in indoor space. Thermal comfort is maintained by increasing the velocity. Energy saving by replacing chilled water energy with fan energy is not the main target. In traditional thermal comfort management, cooled supply air is the main tool. In this study, loss of thermal comfort satisfaction due to the raised supply air temperature is compensated by higher air velocity and room air by-pass. A higher air velocity is produced by a special design of the fan coil system which is an integration of a traditional fan coil and an inverter control fan. The inherent deficiency of wall mounted thermostat can be reduced. Furthermore, a periodic fluctuation of air velocity is rendered possible which further enhances the thermal comfort. Hence, the new system is named “Harmonious Fan Coil System”. The system is analyzed and found feasible by site testing and ample computational fluid dynamic computations.

ACKNOWLEDGEMENT

I wish to dedicate this thesis to the late Professor Ole Fanger. I met Professor Fanger in the conference of ICEE2005 in YStad, Sweden on the June, 2005. Professor Fanger used to be a star in any conference and was difficult to get close because he used to be surrounded by a group of admirers, not to mention that I was only a fresh research student in his area of expertise. When I managed to say hello and introduced myself to him, I was overwhelmed by his benevolent smile. I then met him one other time in Lisboa in the conference of Healthy Building 2006. Everytime when I approached him, he was so patient listening to the description of my work and returning with encouraging suggestions which filled me with absolute confidence. The day that when I received the news of his passing away last year, I was absolutely overtaken. Today the anguish of grief subsides. Despite of my pride in completing this thesis for the efforts spent, there is still a portion of emptiness because Professor Fanger would never be able to read it. The condolence is, I successfully survive the anxious, lonely and occasionally remorseful moments of the research years and that I have not failed the stimulating reassurance given by this gentleman.

This work would not have been possible without the support and encouragement of my chief supervisor, Prof. Daniel W.T. Chan. Thanks for his enthusiastic encouragement and guidance. He also gave helpful consultation and valuable suggestions and information during the course of this work.

I would also like to thank Prof. SK Tang, my co-supervisor for his help on keeping the progress in pace with plan.

Cold magic are thanked for the hardware and technical support for the development of the harmonious fan coil units.

The Campus Development Office and the Facility Management Office of the University are thanked for their support in the implementation and assistance in the implementation of the harmonious fan coil system in the University campus.

Special appreciation is expressed to all the members of Indoor Environment Quality (IEQ) team for their assistance on laboratory preparation, site measurement and the development of the harmonious fan coil system.

It is acknowledged that Mr. Stephen Ng assists in the sound level measurement of the fan both in laboratory and site office and Miss Sonia Li for proofreading the thesis.

I would also like to thank Dr. Zhao Bin of Tsinghua University in assisting the application of user defined functions on the CFD simulation.

At last, my greatest thanks are to my family, for their love and support during the study.

TABLE OF CONTENTS

Page

Certification of Originality i

Abstract ii

Acknowledgements iv

Tables of contents vi

List of Figures xii

List of Tables xix

Chapter 1: Introduction 1

1.1 Brief Review of Conventional Thermal Comfort 3

1.1.1 Historical development of thermal comfort 3

1.1.2 Recent development in the philosophy of thermal comfort 10

1.2 Thermal Comfort Standards 13

1.2.1 ASHRAE Standard 55 13

1.2.2 ASHRAE Fundamentals Handbook (2005) – Thermal Comfort 15

1.2.3 ISO 7730 (2005): Moderate thermal environments 16

1.3 IEQ model 17

1.4 Review of dynamic air movement 18

1.4.1 Impact of dynamic air movement on thermal comfort studies 18

1.4.2 Impact of airflow fluctuation frequency on thermal sensation 19

1.5 Thermal comfort in reality 21

1.5.1 The forgotten perception 21

1.5.2 Spatial and Temporal Distribution 22

1.5.3 Chamber tests versus real human behaviour in tempering control systems 23

1.6 Impact on Health and energy consumption 23

1.6.1 Operation and maintenance engineers avoiding complaints 23

1.6.2 Operating temperature are too cool 23

1.6.3 Energy consumption 24

1.6.4 Blue Sky campaign – ethical and political requirement for a better-controlled thermal comfort environment. 25

Chapter 2:Objectives, Structure of Thesis and Methodology 26

2.1 Objectives of This Research 26

2.2 Structure of this thesis 27

2.3 Methods and Tools 30

2.3.1 Thermal Comfort Calculator Development 31

2.3.2 Analysis of the thermal comfort through parameters 32

2.3.3 Computation program 34

2.3.4 A Comprehensive Data Base for In-office Thermal Comfort Survey 41

2.3.5 Measurement systems 41

2.3.6 Development of the Harmonious Fan Coil System 43

2.3.7 Mathematical techniques 44

2.4 The application of CFD in thermal comfort issue 45

2.4.1 Transient calculation 47

2.4.2 User define function 51

2.4.3 Converge criteria 49

2.4.4 Overall calculation procedure 49

2.4.5 Validation 51

Chapter 3: Air temperature distribution in Hong Kong office buildings 52

3.1 Distribution characteristics of the thermal comfort parameters in Hong Kong 53

3.1.1 Description of the Large-Scale Survey in Hong Kong Offices 53

3.1.2 Validity of the Database 54

3.2 Distribution characteristics of the Database 56

3.3 Interpretation of the Ensemble Distribution 59

Chapter 4: Preference of In-office Air Temperature in Air-conditioned Offices 69

4.1 Neutral Temperature and Preferred Temperature of the Hong Kong Office Users 69

4.1.1 Neutral and preferred temperatures 69

4.1.2 The battle of 25.5°C 69

4.2 General discussion of clo 71

4.3 Methodology in clo survey in Hong Kong Offices 73

4.4 Normalization of preferred temperature by clo 75

4.4.1 Spoiled White Collars in Hong Kong 80

4.5 I_{cl} Equations 84

4.6 Impact of I_{cl} on PPD 87

4.7 A Survey of the Bank Air Temperature and of I_{cl} Bank Staff 92

4.7.1 Thermal comfort conditions in banks 92

4.7.2 Strategy proposed in the Press Conference 94

4.7.3 The Devil's Advocate Argument for Escalating Indoor Temperature 97

4.8 Summary 99

Chapter 5: Development of Harmonious Fan Coil Unit 100

5.1 Site description 101

5.2 Design process 103

5.2.1 Room characteristic 103

5.2.2 Cooling load calculation 104

5.2.3 Water side system 105

5.2.4 Air side system design 109

5.3 Education of Thermal Comfort to Office Staffs 116

5.4 Testing and Commissioning of System and Equipments 117

5.4.1 Functional tests 117

5.4.2 Flow characteristic measurement 117

5.4.3 Acoustic measurement 119

5.4.4 Air tightness measurement 125

5.4.5 Water balancing 130

Chapter 6: Experimental Study Results and Discussion in Test Rooms 134

6.1 Measurement Setup 135

6.2 Measurement system and procedures 139

6.2.1Velocity measurement 140

6.2.2 Temperature distribution measurement 142

6.3 Data Analysis 143

6.3.1 Airlfow analysis 143

6.3.2 Temperature variation analysis 148

6.3.3 Thermal comfort perception 149

6.4 Results and Discussion 150

6.4.1 Results summary 150

6.4.2 Temperature fluctuation and swing 154

6.4.3 Energy Spectrum Analysis 155

6.4.4 Draught Sensation 156

6.4.5 Effect of mixing ratio of air supply 161

Chapter 7: Computational Fluid Dynamic Analysis 166

7.1 Simulation Room Description 167

7.2 Boundary condition 168

7.3 CFD result validation 175

7.4 Simulation of fluctuating airflow with different frequencies 180

7.5 Summary 185

Chapter 8: Conclusion 190

8.1 Proposed 3-Steps Protocol for Setting the Optimum Indoor Temperature 191

8.2 Clothing style of Hong Kong People 192

8.3 Development of harmonious fan coil system 193

8.4 CFD simulation 194

8.5 Further study 195

Reference 197

Appendix A: Temperature measurement results

Appendix B: Power spectrum analysis for measurement

Appendix C: Relationship between air temperature and air velocity

Appendix D: CFD governing equation

LIST OF FIGURES:

Page

Figure 1.1: PMV-PPD model (ASHRAE, 2004) 8

Figure 1.2: Proposed Adaptive Comfort Standard (ACS) for ASHRAE Std. 55, applicable for naturally ventilated buildings. 12

Figure 1.3: Thermal comfort zone (ASHRAE, 2004) 14

Figure 1.4: Air speed required to offset increased temperature (ASHRAE, S55-1992) 14

Figure 1.5: Allowable mean air velocity as a function of air temperature and turbulence intensity. (ASHRAE, 2004) 16

Figure 1.6: The relationship between human thermal comfort sensation to frequency of air velocity fluctuation 20

Figure 2.1: Example of computation process described as tree 32

Figure 2.2: Illustration of the digit (0-1) parameters checklist 33

Figure 2.3: Sample checklist indicating the alternative computation ways with asterisks 33

Figure 2.4: Structural diagram of the computation program 35

Figure 2.5: Index page of parameters checklist 37

Figure 2.6: Page for calculating the parameter S_{sk} 37

Figure 2.7: Page for calculating the parameter α_{sk} 38

Figure 2.8: Page for calculating the parameter Q_{bl} 38

Figure 2.9: Page for calculating the parameter A_D 39

Figure 2.10: Return to calculate the parameter S_{sk} 39

Figure 2.11: Page for calculating the parameter ET* 40

Figure 2.12: Calculation procedure of SIMPLE algorithm 51

Figure 2.13: Iteration process involve user define functions 54

Figure 2.14: Overall iteration process for transient simulation 56

Figure 3.1: Illustration of the cut in and cut out situation in real office environment. 60

Figure 3.2: Interpretation of the spatial and temporal envelope 62

Figure 3.3: Spatial and temporal distribution envelope 62

Figure 3.4: Relationship of percentage of dissatisfaction with the operative temperature 65

Figure 3.5: Relationship of percentage of dissatisfaction with the ambient temperature 66

Figure 3.5: Swing of operative temperature against predicted percentage of dissatisfaction 67

Figure 3.6: Swing of ambient temperature against predicted percentage of dissatisfaction 67

Figure 4.1: Distribution of the indoor climatic measurement of the large database 72

Figure 4.2: Distribution of clothing insulation for office occupants in summer in Hong Kong 73

Figure 4.3: Probit models shows the preferred temperature on Hong Kong people 76

Figure 4.4: Mean thermal sensation votes compared to means predicted thermal sensation 77

Figure 4.5: Comfortable air temperatures for occupants with different clothing insulation. 78

Figure 4.6: Optimal operative temperature as a function of clothing and activity 81

Figure 4.7: Operative Temperature vs I_{cl} in ASHRAE 55 - PMV 82

Figure 4.8: Preferred operative temperature under various clothing insulation 85

Figure 4.9: PPD against T_o at different I_{cl} as Compare to the Ensemble Regression. 88

Figure 4.10: Impact of I_{cl} on T_o ^oC at minimum PPD 90

Figure 4.11: Minimum PPD (%) versus I_{cl} 91

Figure 4.12: Correlation between temperature and total colony counts (Chan et al., 2007) 98

Figure 4.13: Correlation between relative humidity and total colony counts (Chan et al., 2007) 98

Figure5.1: Floor plan of a faculty office in POLYU for installation of harmonious fan coil unit 102

Figure 5.2: Photo of the faculty office in PolyU campus for installation of harmonious fan coil unit system 102

Figure 5.3: Floor plan and furniture layout of the single office for installation the harmonious fan coil unit system 103

Figure 5.4: Internal wall up to the upper floor slap to reduce the latent load 104

Figure 5.5: Chilled water pipe layout plan in the faculty office 106

Figure 5.6: Chilled water pipe layout in the faculty office 106

Figure 5.7: Schematic showing a branch of balancing valve 107

Figure 5.8: Flow chart for proportional balancing procedure 108

Figure 5.9: Illustration of the Harmonious fan coil unit Type 1 110

Figure 5.10: Block diagram of air flow in Type I system 110

Figure 5.11: Illustration of Harmonious fan coil unit Type II system 111

Figure 5.12: Block diagram of air flow in Type II system 111

Figure 5.13: Configuration of the Fan Speed Control Unit 112

Figure 5.14: Block diagram of the control algorithm of the fan speed control unit 113

Figure 5.15: Circuit diagram of the “Fan Speed Control Unit” 114

Figure 5.16: Interface of the HFCU control interface for the temperature transducer 115

Figure 5.17: Controlling parameters of the Fan Speed Control Unit 115

Figure 5.18: Lunch talk meeting to the faculty staffs 116

Figure5.19: Propeller fan for make up air application 117

Figure 5.20: Measurement of volumetric flow rate of the propeller fan 118

Figure 5.21: measurement result of the supply voltage to the volumetric flow rate of the propeller fan 118

Figure5.22: Measurement arrangement of sound level 120

Figure 5.23: Laboratory of Sound measurement 120

Figure 5.24: Propeller fan lining up with acoustic insulation 121

Figure 5.25: Sound measurement result before acoustic insulation 122

Figure 5.26: Sound measurement result after acoustic insulation 123

Figure 5.27: Sound measurement taken in office after installation 124

Figure 5.28: RAD-7 for radon measurement 125

Figure 5.29: MatLab program for air change rate calculation 126

Figure 5.30: Flowchart of the calculation procedure of the air change rate by radon method 128

Figure 5.31: Computation results of the infiltration rate 129

Figure 5.32: Simplified schematic of the chilled water system of the faculty office 139

Figure 6.1: Measurement layout of the single office room equipped with HFCU Type I system (drawing not in scale). 136

Figure 6.2: Photo of measurement setup in the single office room equipped with HFCU Type I system 137

Figure 6.3: Measurement setup of mobile velocity measurement column. 141

Figure 6.4: Relationship of thermostat set point temperature and swing amplification between sitting area and the wall-mounted thermostat location 155

Figure 6.5: Simultaneous records of instantaneous temperature at four points located at a distance of 20mm between each other at a point within the occupied zone of a room with exhaust mechanical ventilation and window slots where large local temperature gradients were expected (Melikov et al. 1997). 156

Figure 6.6: Draught risk (%) without centrifugal fan operation 157

Figure 6.7: Draught risk (%) with centrifugal fan operation 157

Figure 6.8: Draught risk (%) with centrifugal fan and fluctuating frequency 158

Figure 6.9: Correlation between air temperature and air velocity at set point 22℃ and med fan speed. 159

Figure 6.10: Correlation between air temperature and air velocity at set point 24℃ and hi fan speed. 159

Figure 6.11: Correlation between air temperature and air velocity at set point 26℃ and med fan speed. 160

Figure 6.12: Correlation between air temperature and air velocity at set point 24℃, 15 to 30Hz frequency and med fan speed. 160

Figure 6.13: Correlation between air temperature and air velocity at set point 24℃, 30 to 45Hz frequency and hi fan speed. 161

Figure 6.14: Relationship between space temperature swing and mixing ratio at set point temperature 22^{o}C 163

Figure 6.15: Relationship between space temperature swing and mixing ratio at set point temperature 24℃ 163

Figure 6.16: Relationship between space temperature swing and mixing ratio at set point temperature 26℃ 164

Figure 6.17: Relationship of space mean temperature and set point temperature deviation and mixing ratio at set point temperature 22℃ 164

Figure 6.18:Relationship of space mean temperature and set point temperature deviation and mixing ratio at set point temperature 24℃ 165

Figure 6.19: Relationship of space mean temperature and set point temperature deviation and mixing ratio at set point temperature 26℃ 165

Figure 7.1: The geometry of the simulation model 168

Figure 7.2: The geometry of the supply and return diffuser 169

Figure 7.3: Measured value of the supply air temperature profile 170

Figure 7.4: Measurement result with regression curve in confidence interval between 5-95%. 173

Figure 7.5: Comparison of CFD and measurement results over height 176

Figure 7.6: Temperature profile for the measured and the simulation result 178

Figure 7.7: Temperature and the velocity contour of different planes of the base case. 179

Figure 7.8. Supply velocity profile (0.2Hz) 181

Figure 7.9: Contour of temperature and vector of velocity magnitude of 184

different plan (0.2Hz)

Figure 7.10: Airflow fluctuation characteristics comparison of simulation and measurement at the sitting position 186

Figure 7.11: Airflow fluctuation characteristics comparison of simulation and measurement at the sitting position 187

Figure 7.12: Airflow fluctuation of supply vs sitting location (0.2Hz) 188

Figure 7.13: Airflow fluctuation of supply vs sitting location (0.2Hz) 188

Figure 7.14: Power spectrum density of airflow fluctuation – air supply vs thermostat (0.2Hz) 189

Figure 7.15: log- power spectrum density of airflow fluctuation – air supply vs thermostat (0.2Hz) 189

Figure 7.16: Power spectrum density of airflow fluctuation – thermostat vs sitting place (0.2Hz) 190

Figure 7.17: log-power spectrum density of airflow fluctuation – thermostat vs sitting place (0.2Hz) 190

LIST OF TABLES

Page

Table 1.1: List of parameters for Fanger's model 5

Table 1.2: The repose to steady and fluctuating air flow 20

Table 1.3: List of neutral temperature in Hong Kong and other countries 22

Table 3.1: Summary of the 11 office buildings surveyed 54

Table 3.2: Summary of sensors on the measurement system of the mobile car 54

Table 3.3: The descriptive statistical result of the survey in Hong Kong and Kalgoorlie-Boulder 56

Table 3.4: The result of the statistical test of mean air temperature, mean radiant temperature and relative humidity. 57

Table 3.5: Results of the probability distribution function curve and equation 58

Table 4.1: Equations in ASHRAE fundamental chapter 8 involving clothing parameters 84

Table 4.2: Neutral temperature at different clo values 86

Table 4.3: Equations for PPD and To in different Icl 89

Table 4.4:Survey of Air Temperature in Banks in Hong Kong 93

Table 4.5:Survey of Air Temperature in Seven Banks in Wan Chai District 93

Table 5.1: Cooling load calculation of the faculty office 105

Table 5.2: As-built measurement result of volumetric flow rate 119

Table 5.3: Summary of the proportional balancing result 131

Table 5.4: Energy saving before and after water balancing 133

Table 6.1 Cooling load estimation of the measurement period 138

Table 6.2: Summary of test cases in the single office room 139

Table 6.3: Summary of volumetric flow rate of the HFCU system in different test combinations in the single office room 140

Table 6.4: List of measured parameters and sensors on mobile stack 141

Table 6.5: Testing standard adopted in the measurement 143

Table 6.6: Summary table of temperature swing, velocity swing, swing reduction rate, turbulence intensity, equivalent frequency and percentage of dissatisfaction at set point temperature 24℃. 151

Table 6.7: Summary table of temperature swing, velocity swing, swing reduction rate, turbulence intensity, equivalent frequency and percentage of dissatisfaction at set point temperature 22℃. 152

Table 6.8: Summary table of temperature swing, velocity swing, swing reduction rate, turbulence intensity, equivalent frequency and percentage of dissatisfaction at set point temperature 26℃. 153

Table 6.9: Swing amplification between thermostat location and space 154

Table 6.10: Temperature swing and mixing ratio under different test cases 162

Table 7.1: Result of the curve fitting of the supply air temperature profile 172

Table 7.2: Table of ANOVA analysis 172

Table 7.3: Boundary condition of the simulation 173

Table 7.4: Summary of simulation cases 180

CHAPTER 1: INTRODUCTION

Building services engineers cut the first corner of indoor environmental quality (IEQ) in 1973 when the oil embargo triggered a new era in energy conservation. At that time, the Hong Kong government encouraged setting the air-conditioned room temperature in the summer to 25.5^{o}C. When the oil embargo became history, the indoor air temperature design criterion became market-driven again. For a typical commercial building, the design room air temperature is 24^{o}C based on the summer thermal comfort zone proposed by the American Society of Heating, Refrigerating and Air-Conditioning Engineers (ASHRAE) standard 55. In "Grade A" buildings, building operators prefer a lower design temperature of 23.3^{o}C in order to minimize the number of thermal comfort complaints. However, many building operators further set the room air temperature to 21-23^{o}C, and some of the coldest interiors in the world can be found in Hong Kong.

In recent years, the issue of raising indoor temperatures has been discussing regularly in Hong Kong and other Asian areas. "The Hong Kong's cold war heats up" as reported in CNN headline news on June 30, 2005 (CNN, 2005.6.30) raised international concerns about the freezing indoor environments during the hot and humid mid-summer months. Hong Kong's green groups carried out campaigns to gauge what Hong Kong residents felt about the frigid air, and received many complaints about the chilly breeze in restaurants, shops and offices in their city of 6.9 million people. This is an alarming indication of the need to raise room temperatures to a comfortable level – neither too hot nor too cold. Since October 2004, the Hong Kong government has been advocating for the public to set air-conditioned temperature to 25.5^{o}C during the summer. In June 2005, the Hong Kong

government launched a “No freezing summer” campaign to urge the private sector to follow suit. However, 25.5^{o}C may not be everyone’s preferred temperature, as each individual has his or her own clothing preferences and knowledge of thermal comfort and indoor quality. For most Hong Kong residents, it is easier to put on more clothes rather than take off extra layers, so there is a great demand for lower temperatures within indoor spaces.

In response to the recent government campaign, this research study aims to develop a protocol for setting room temperature control criteria and to support the Government’s campaign on energy conservation by raising indoor temperature. The protocol aims to establish an optimum temperature setting to achieve the intended thermal comfort satisfaction level. Further energy-saving opportunities examined include the adoption of a more casual dress code and of fan assisted ventilation concept.

1.1 Brief Review of Conventional Thermal Comfort

Humans have always striven to create a thermally comfortable environment. This is reflected in building traditions around the world - from ancient history to present day. Today, creating a thermally comfortable environment is gaining more concern as one of the most important parameters in designing an indoor space where the majority of people usually spend more than 20 hours of their days – at home, at the workplace or during transportation.

1.1.1 Historical development of thermal comfort

Thermal comfort has been investigated since the early 19th century in America. During that era, heating ventilation systems proved problematic and created uncomfortable environments for occupants. The American Society of Heating and Ventilating Engineers (ASHVE) was established in Pittsburgh to study ways to create a better indoor thermal environment. These early researchers mainly focused on the working thermal conditions in industries or in hot environments.

In the 1930s, numerous commercial buildings were built and complaints about the cold airflow within working spaces began to amass. Houghten et al. (1938) initiated investigation of the relationship between air temperature, air speed and air cooling. In later years, research studies extended to residential buildings and other working areas while thermal comfort, in particular over-cooling, was still the main complaint indoors. Today's Hong Kong is still facing the same problem of too-cold interior spaces.

Throughout the last century, thermal comfort models were developed because they quantitatively (based on large surveys of people) describe the ranges of conditions where people will feel thermally comfortable in buildings. There are two prevailing thermal comfort models which are:

- the comfort model originally proposed by Fanger or Predicted Mean Vote (PMV) model,
- and the recent model which takes into account the adaptation to the prevailing climate of occupants of buildings (Adaptive Comfort Model).

Predicted mean vote (PMV) – Predicted percentage of Dissatisfaction (PPD) model

Most indoor thermal comfort criteria in worldwide building designs are based on the PMV-PPD relationship. The predicted mean vote (PMV) by Professor Fanger (1970), as presented in ASHRAE (2001) and International Standard ISO 7730 (ISO, 1994), is the index of thermal comfort most widely used for assessing moderate indoor thermal environments. It was based on steady heat transfer theory, and was calibrated against Nevins' (1966) and McNall's (1967) data. Fanger applied classical heat transfer theory and empirical studies to derive the general comfort equation incorporating four basic environmental parameters (air velocity, mean radiant temperature, relative humidity and air temperature) and two personal parameters (clothing and activity level). It predicts the expected comfort vote on the ASHRAE seven-point scale of subjective warmth (cold (-3), cool (-2), slightly cool (-1), neutral (0), slightly warm (1), warm (2) and hot (3)). The idea behind this comfort model is

to encounter the imbalance between the heat flow required for optimum comfort at the specified activity and the heat flow from the body to the environment.

List of parameters for Fanger's model:

Index	Parameter	Description
1	f_{cl}	clothing area factor, dimensionless
2	t_{cl}	clothing surface temperature, ^oC
3	t_r	mean radiant temperature, K
4	h_c	convective heat transfer coefficient, $W/(m^2K)$
5	t_a	ambient temperature, ^oC
6	p_a	water vapor pressure in ambient air, kPa
7	R_{cl}	thermal resistance of clothing, m^2 K /W
8	V	wind velocity, m/s
9	I_{cl}	thermal resistance, clothing, clo unit
10	W	rate of mechanical work accomplished, W/m^2
11	M	rate of metabolic heat production, W/m^2
12	L	thermal load on body, W/m^2

Table 1.1: List of parameters for Fanger's model

The equations for the predicted mean vote are as follows:

$$\begin{aligned} M - W = {} & 3.96\times10^{-8} f_{cl}\left[(t_{cl}+273)^4 - (\overline{t_r}+273)^4\right] + f_{cl}h_c(t_{cl}-t_a) \\ & + 3.05\left[5.73 - 0.007(M-W) - p_a\right] + 0.42\left[(M-W) - 58.15\right] \\ & + 0.0173M(5.87 - p_a) + 0.0014M(34 - t_a) \end{aligned} \quad (1.1)$$

Where

$$t_{cl} = 35.7 - 0.0275(M - W) - R_{cl}\left\{\begin{matrix}(M - W) - 3.05[5.73 - 0.007(M - W) - p_a] \\ -0.42[(M - W) - 58.15] - 0.0173M(5.87 - p_a) \\ -0.0014M(34 - t_a)\end{matrix}\right\}$$

(1.2)

$$h_c = \begin{cases} 2.38(t_{cl} - t_a)^{0.25} & 2.38(t_{cl} - t_a)^{0.25} \succ 12.1\sqrt{V} \\ 12.1\sqrt{V} & 2.38(t_{cl} - t_a)^{0.25} \prec 12.1\sqrt{V} \end{cases} \quad (1.3)$$

$$f_{cl} = \begin{cases} 1.0 + 0.2I_{cl} & I_{cl} \prec 0.5clo \\ 1.05 + 0.1I_{cl} & I_{cl} \succ 0.5clo \end{cases} \quad (1.4)$$

The general formula for predicted mean vote is:

$$PMV = [0.303\exp(-0.036M) + 0.028]L \quad (1.5)$$

where the seven-point scale of PMV is:

+3	Hot
+2	Warm
+1	Slightly warm
0	Neutral
-1	Slightly cool
-2	Cool
-3	Cold

Taking a holistic approach, this comfort equation describes the connection between the measurable physical parameters and thermal sensation as experienced by the normal person. The equation provides a useful operational tool to evaluate the offered thermal comfort conditions by measuring physical parameters.

The equation also reveals that the temperature of surfaces in an enclosure greatly influences people's thermal sensation while the relative humidity level only has a moderate influence on an individual's thermal sensation.

Since discomfort may occur when the skin is wet (sweat, water, etc.), Gagge et al (1969) produced an equation for skin wettedness (w) which can be used as a test to exclude conditions which satisfy the comfort equation:

$$w = 0.06 + 0.94\frac{E_{rsw}}{E_{\max}} \tag{1.6}$$

where E_{rsw} and E_{max} are the evaporative heat loss (W/m^2) for regulatory sweat and maximum of it.

When upper limit of w depends on metabolic rate, therefore limit is estimated using:

$$w = 0.0021M + 0.15\,. \tag{1.7}$$

Realizing the sensation vote predicted was only the mean value drawn from group of people, Fanger extended the PMV to predict the proportion of any population who will be dissatisfied with environment. This is the well-known curve PMV-PPD (predicted percentage dissatisfied) produced by Fanger (1972). The graph, as illustrated in Figure 1.1 (ASHRAE, S2004 and ISO7730), demonstrates the PPD as a function of the PMV of a group of people, who have similar clothing and activities. Therefore, PMV-PPD model could predict the PMV spatial distribution and be

applied to design indoor thermal environments. However, the PMV index is only valid under steady-state condition and cannot be applied for temporal distribution; that is, temperature and air velocity variations with time.

The general form of Predicted Percentage of Dissatisfaction (PPD) is:

$$PPD = 100 - 95\exp\left[-\left(0.03353PMV^4 + 0.2179PMV^2\right)\right] \tag{1.8}$$

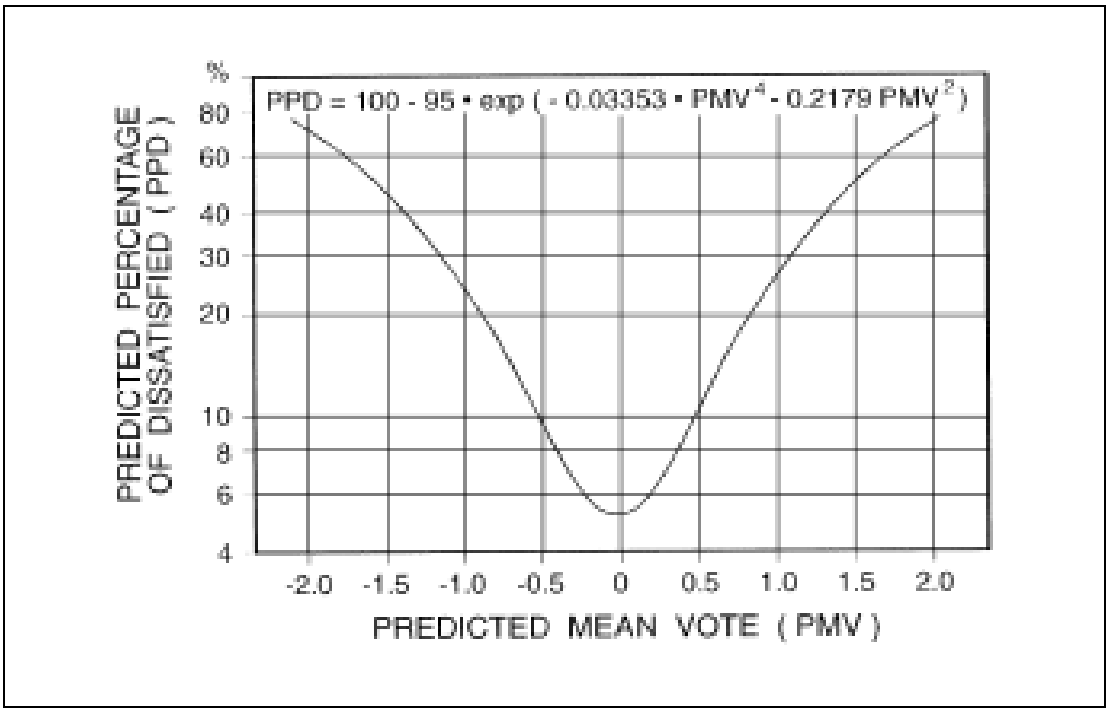

Figure 1.1: PMV-PPD model (ASHRAE, S2004 and ISO7730)

Percentage of Dissatisfaction due to Draft

Draught, as defined in ISO 7730, is unwanted local cooling of the skin caused by air movement. The effect of turbulence intensity (Tu) on draught discomfort was addressed long ago by Mayer (1987) and Fanger et al. (1988). Tu was incorporated into a model that predicts the percentage of dissatisfaction due to draught as a function of mean air velocity, air temperature and turbulence intensity (Fanger and

Melikov et al., 1988). This model was first adopted in ASHRAE 55-92.

$$PD = (34 - t_a)(v - 0.05)^{0.62}(0.37 \cdot v \cdot Tu + 3.14) \ [\%] \tag{1.9}$$

$$\text{where } Tu = \frac{SD_v}{\overline{V}} \cdot 100\% \tag{1.10}$$

This model is only valid for sedentary, thermally neutral individual dressed in normal clothing. Some researchers extended the draught model, incorporating the effect of higher activity level to the draft sensation. Toftum (1994) further enhanced the model to account for the draft risk by adding the terms of skin temperature, workload and metabolic rate as follows:

$$PD = \left(T_{sk} - T_a\right)\left(\overline{V} - 0.05\right)^{0.6223}\left(3.143 + 0.37 \cdot \overline{V} \cdot Tu\right)\left[1 - 0.013 \cdot \left(M - W - 70\right)\right] \tag{1.11}$$

Toftum et al. conducted an intensive study on the human response to air movement in 2003. This study concludes that the PD model overestimates the predicted dissatisfaction level by the difference of the effects of activity level and the thermal sensation. It also indicates that for an individual feeling cool or slightly cool, a low air velocity will make them an uncomfortable feeling compared to those feeling neutral or warmer. The dissatisfaction due to draft increases 2-3 times with a one unit change on the thermal sensation scale, from neutral to slightly cool. The same report also found that there is no difference in sensitivity to draft for individual feeling warm or slightly warm.

Percent Satisfied (PS) model

Fountain et al. (1994) developed a "percent satisfied" (PS) model for predicting the percentage of satisfaction of an individual in an office environment when local control of air movement is available. This can predict the percentage of dissatisfied individuals when local air movement control is not available and not enough air movement is provided. The model was developed based on laboratory experiments where the temperature was controlled to stay within a range of 25.5^{o}C to 28.5^{o}C. The PS model is as follows:

$$PS = 1.13\sqrt{t_o} - 0.24t_o + 2.7\sqrt{\overline{V}} - 0.99\overline{V} \qquad (1.12)$$

1.1.2 Recent development in the philosophy of thermal comfort

Adaptive model

Extensive field research based on a global database of 21,000 measurements for which the data was gathered by de Dear et al. (1998) reveals that buildings with natural and hybrid ventilation are evaluated differently. Especially during months with higher outdoor temperatures, higher indoor temperatures in such buildings are more acceptable than what Fanger's model predicts. In this extent, people's expectation of the building's climate, based on the outdoor temperature of that particular day and of preceding days plays an important role of adaptation mechanisms.

The Adaptive Comfort Standard (ACS) developed by de Dear (2004) was included in the latest revision of ASHRAE Standard 55 (2004). The scope of the ACS option is limited to naturally ventilated spaces in which the thermal conditions of the space may be influenced by the occupants, primarily by the opening of windows. The adaptive model is a model that relates indoor design temperatures or acceptable temperature ranges to outdoor meteorological or climatological parameters. (Figure 1.2)

ACS also serves as an alternative to the PMV-based method in ASHRAE Standard. 55. The outdoor climatic environment for each building was characterized in terms of mean outdoor dry bulb temperature $T_{a,out}$, instead of ET*. Optimum comfort temperature, T_{comf}, was then similar to the regression based on mean $T_{a,out}$:

$$T_{comf} = 0.31 \cdot T_{a,out} + 17.8 \qquad (1.13)$$

Many researchers have conducted field studies to enhance the ACS model (Humphreys, 1975; 1978; 1979; Nicol, 1993; de Dear, 1998; Nicol & McCartney, 2001). To cope with the recent development of sustainable building design norms, the ACS model is recommended to the real-life comfort requirements and to reduce cooling energy demands at the same time. However, the use of the ACS approach is proposed only for non-mechanically conditioned buildings which are not commonly found in Hong Kong and other urban cities in China.

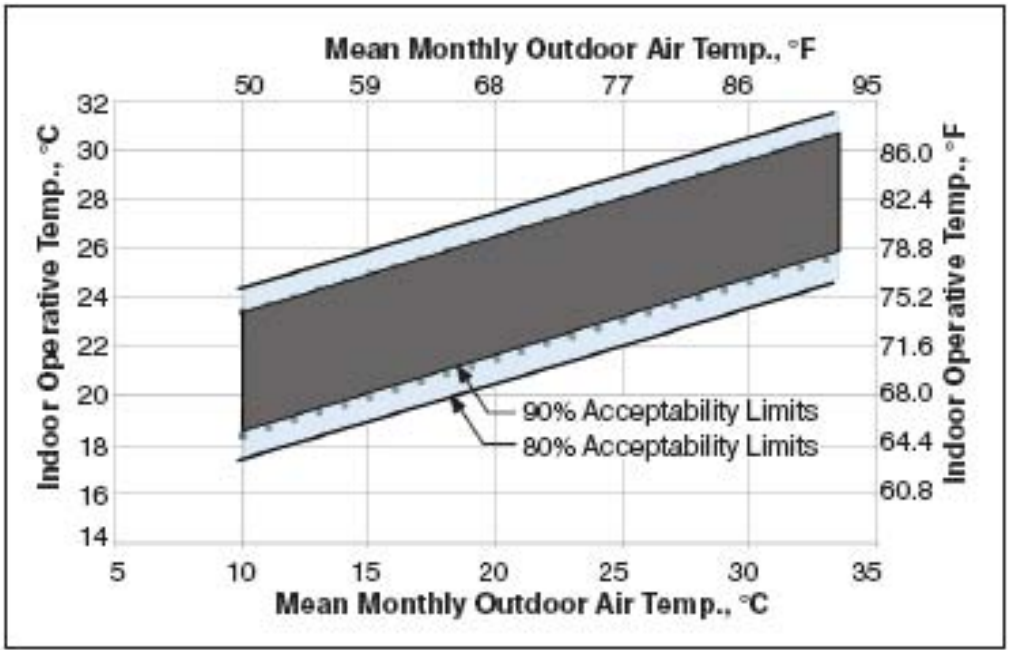

Figure 1.2: Adaptive Comfort Standard (ACS) for ASHRAE Standard 55 (2004), applicable for naturally ventilated buildings.

1.2 Thermal Comfort Standards

Optimum indoor air temperatures have often been the subject of debate, and suggested limits or guidance values for buildings have been proposed for many years by number of professional institutions. Global institutions include the American Society of Heating, Refrigerating and Air Conditioning Engineers (ASHRAE) in the USA, the Chartered Institute of Building Services Engineers (CIBSE) in the UK, national standards organizations, the ISO as well as the European Committee for Standardization. All have produced standards concerning on thermal comfort.

1.2.1 ASHRAE Standard 55

Since the 1980s, ASHRAE Standard 55 specifies thermal conditions acceptable to a majority of a group of occupants exposed to the same conditions within a space. The Standard defines "majority" such that the requirements are based on 80% overall acceptability with 10% dissatisfaction criteria for general thermal comfort, plus an additional 10% dissatisfaction that may occur on average from local thermal discomfort.

ASHRAE Standard 55-04 further adopts Fanger's PMV-PPD model (Fanger, 1970) and methods of calculation to determine the comfort zone (as illustrated in Figure 1.3). The thermal comfort zone describes the combinations of temperature and humidity with PPD is less than 10% and PMV ranges between -0.5 and 0.5.

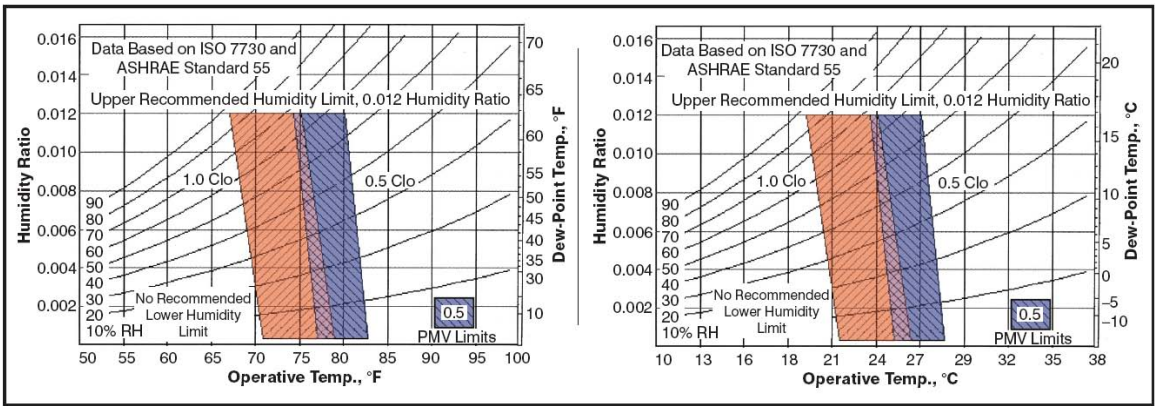

Figure 1.3: Thermal comfort zone (ASHRAE 55, 2004)

Although precise relationships between air speed and improved comfort have not yet been established, the operative temperature limits in a thermal comfort zone are based on a limit of air speed less than 0.2 m/s. However, higher air speeds can be beneficial for improving comfort at higher temperatures. Figure 1.4 below illustrates the required air speed to offset the increment of air temperature.

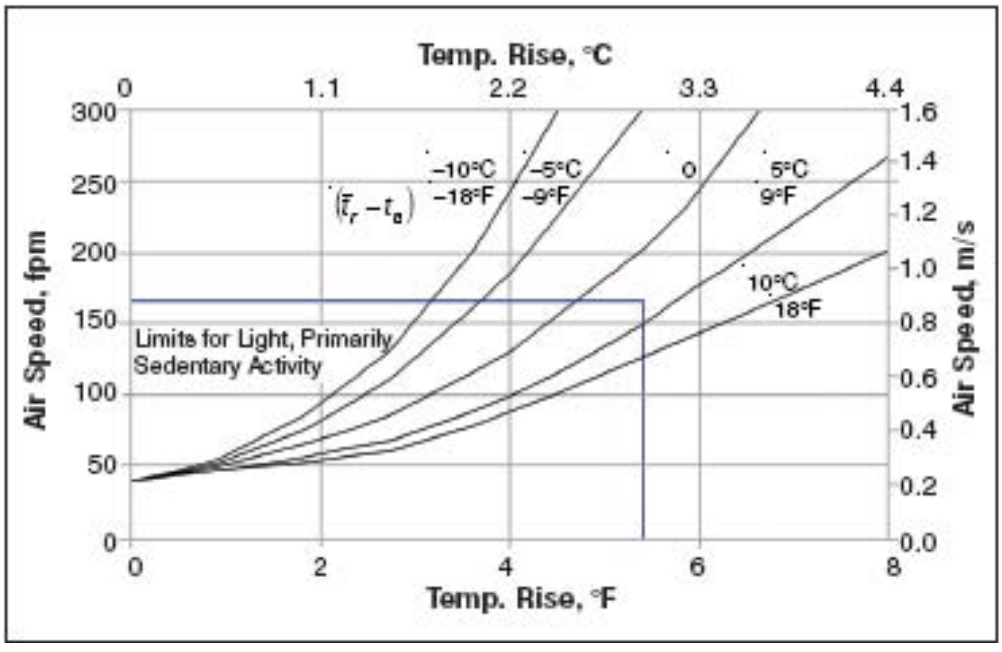

Figure 1.4: Air speed required offsetting increased temperature (ASHRAE 55, 2004)

This graph is important for commercial buildings that are primarily in cooling mode, where there are opportunities to reduce energy use while improving comfort. This can be achieved by allowing the temperature to rise slightly towards the higher end of the comfort zone, while giving people the opportunity to individually control air movement through task ventilation systems, personal or ceiling fans, or operable windows. This figure is valid for slightly clothed people with clothing insulations between 0.5 to 0.7 clo (ASHRAE S55-04). For example, assuming the mean radiant temperature to be close to the air temperature, the maximum temperature rise would be about 3^{o}C with elevated air speed of 1.2 m/s.

1.2.2 ASHRAE Fundamentals Handbook (2005) – Thermal Comfort

The handbook discusses the thermal comfort issue in detail, and includes 92 equations involving over 130 parameters. The models for thermal comfort are concerned with steady-state conditions in all aspects of human thermal comfort, including issues from the fundamental physical thermal environment to human physiological conditions. Computation methods are later applied to estimate the acceptable range of thermal conditions for each particular situation, rather than defaulting to the simpler graphic comfort zone, where assumptions might not match their conditions.

1.2.3 ISO 7730 (2005): Moderate thermal environments

ISO 7730 provides an analytical method for assessing moderate environments and is based on the predicted mean vote and predicted percentage of dissatisfied (PMV-PPD) indices (Fanger, 1970), and more recent works concerning draughts (draught risk model) (Olesen, 1985; Fanger et al., 1989). The Standard considers that an individual's thermal sensation is related to the body's thermal balance as influenced by clothing insulation and metabolic rate, as well as the environmental parameters: air temperature, radiant temperature, humidity and air velocity.

In addition to ASHRAE Standard, ISO 7730 provides guidance in terms of levels of dissatisfaction. This includes dissatisfaction caused by whole-body discomfort, draughts and other local effects.

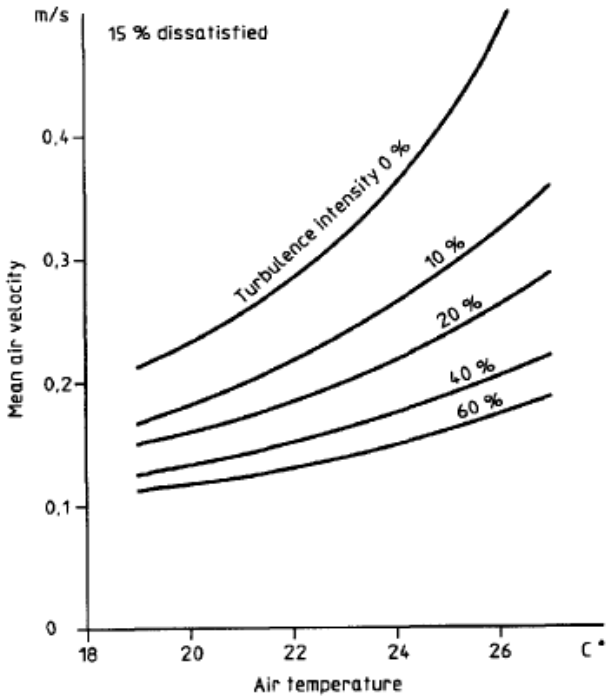

Figure 1.5: Allowable mean air velocity as a function of air temperature and turbulence intensity (ASHRAE 55, 2004)

1.3 IEQ model

Conventional studies on the indoor environment address each indoor comfort index separately. More recently, the equivalence of the discomfort caused by different physical qualities has been considered. In a study performed by Fanger et al., the discomfort caused by indoor air pollution, thermal load and noise was investigated. It was found that when the operative temperature was in the range of 23 to 29^0C, a 1^0C change in operative temperature was found to have the same effect on human comfort as a noise level of 3.9dB (Fanger et al., 1988). Some researchers have embraced the concept of total environmental quality and used multivariate regression analysis to establish a thermal comfort models based on field measurements (Gan and Groome, 1994).

It was realized that effective control of indoor environment requires an integrative understanding of indoor environmental parameters including thermal comfort, indoor air quality, aural comfort and visual comfort. A compact IEQ logger has been developed for continuous monitoring of the IEQ performance in buildings (Chan et al., 1998). A new composite IEQ index was used to integrate the basic indoor environmental qualifiers in air-conditioned offices; they are thermal comfort, indoor air quality and aural comfort. It expresses the holistic satisfaction level of the occupant to the indoor environment in terms of the essential physical indoor environmental parameters. A survey carried by Mui et al. (2003) indicated that thermal comfort receives most complaints among the four basic environmental components. The derived IEQ equation are:

$$PDIEQ = 0.42 \times PDTC + 0.09 \times PDIAQ + 0.28 \times PDAC \quad (1.14)$$

where :

PDTC = percentage of dissatisfaction of thermal comfort

PDIAQ = percentage of dissatisfaction of indoor air quality

PDAC = percentage of dissatisfaction of aural comfort

1.4 Review of dynamic air movement

1.4.1 Impact of dynamic air movement on thermal comfort studies

Thermal comfort and air movement have been studied as early as the 1920s in America. In the 50s, Rohles et al. (1974) carried out the first laboratory study on the relationship between air movement and human thermal sensation. 90 subjects were tested under a perforated ceiling air supply in a test chamber. Rohles indicated that skin temperature had relatively stronger correlation with the thermal sensation of subjects. He proposed a summer thermal comfort zone with 0.8m/s as the maximum allowable air velocity.

When the oil embargo triggered off a new era in energy conversation in 1973, ceiling fans and static table fans gained a great attention, leading to studies on their effects upon thermal comfort. Rohles, Konz and Jones (1983) investigated the extenders of the summer comfort zone based on the cooling effect of forced convection by ceiling fans. Rohles concluded that induced turbulent flow could benefit the thermal

sensation and extends the comfort range to as high as 29.4^{0}C (at 50% RH) when the mean air velocity exceeds 0.8m/s.

In the same year, Konz et al. further investigated the effect of cyclic and static fans, and flow direction on thermal sensation. Cyclic fans were found to be more favorable than static fans in extending the summer comfort zone.

Scheatzle, Wu and Yelloot (1986) suggested that the upper comfort limit proposed by Rohles et al. (1983) may be further extended for humilities lower than 50%, but reduced for higher humidity.

The above studies reveal that maintaining proper relative humidity and keeping fluctuating airflow are advantageous to positive thermal sensation.

1.4.2 Impact of airflow fluctuation frequency on thermal sensation

In 1989, Tanable et al. investigated the effect of periodic airflow. Subjects were tested under seven different characteristic airflows including sinusoidal wave (10s-60s period), random wave, constant, impulse waveform with mean velocity in the range of 0.5-2m/s. Sinusoidal waveform was found to create a stronger cooling effect. Tanabe (1994) carried further tests on the effects of frequency with mean air velocity controlled at 0.2m/s. The results, summarized in the table below, indicate that response to steady and fluctuating airflow are different, and fluctuating airflow could create a greater cooling feeling and sensation.

Subject response	Constant airflow	Fluctuating airflow
Thermal sensation	-0.13	-0.31
Comfort sensation	-0.34	-0.39
Mean skin temperature	33.8	33.8
Airflow satisfaction %	47%	64%
Cooling effect satisfaction %	4.7%	10.9%

Table 1.2: The reponse to steady and fluctuating air flow (Tanabe, 1994)

Tanabe and Kimura also studied the sinusoidal varying airflows of 0.017, 0.033 and 0.10Hz in climate chamber experiments, resulting in a greater perceived cooling effect than random, constant or pulsed air movements with the same velocity. These frequencies, however, are too slow to cause the maximum cooling effect in the results of Fanger and Pedersen (1977) shown in Figure 1.6 below.

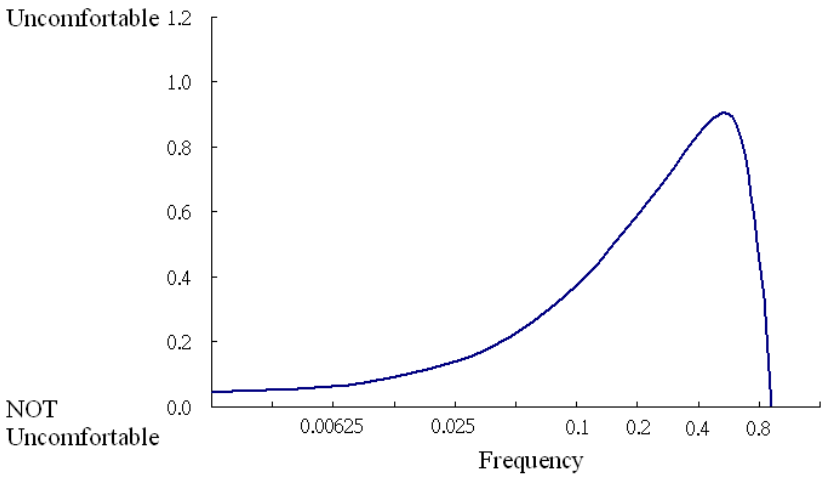

Figure 1.6: The relationship between human thermal comfort sensation to frequency of air velocity fluctuation (Fanger and Pedersen, 1977)

This was confirmed by Zhou and Melikov (2002) and Zhou et al. (2002), who found an equivalent frequency in the range of 0.2Hz to 0.6Hz to be the most uncomfortable. The equivalent frequency of a randomly fluctuating air velocity was defined as the frequency of sinusoidal velocity fluctuations with the same ratio of the standard deviation of acceleration to the standard deviation of air velocity as in the random velocity fluctuations.

1.5 Thermal comfort in reality

Currently, we have more than 100 years of thermal comfort research to draw upon, and should put these ideas and findings into practice.

1.5.1 The forgotten perception - Metaphor of 'cold air system'

When establishments began using air conditioning systems in the 1950s, Hong Kong locals began calling it a "cold air system", hence indicating an expected sense of coolness. Since then, the call for colder indoor air temperatures has become a deeply entrenched part of the local culture in Hong Kong.

In mid 1990's, Chan et al. carried a large-scale survey on Indoor Environmental Quality (IEQ) in air-conditioned offices in Hong Kong (Chan et al., 1998). The study included 1158 workstations covering 30,000m^2. The extensive survey found that 60% of the 1193 workstations in Hong Kong offices are fell within the comfort zone suggested by ASHRAE Standard 55 (Chan et al., 1998). Further analysis of the acceptability and clothing code suggested that indoor users in air-conditioned offices

prefer 1.5°C lower than temperatures recommended by ASHRAE Standard 55 (Chan et al., 1998). Chan et al. ascribed this phenomenon as an induced expectation of the Cantonese translation of the term 'air-conditioning system' as literally meaning 'cold air system'. Another survey by Chan et al. also suggested that the neutral temperature in Hong Kong is 1.5^{o}C lower compared with other research worldwide as summarized in the table below. Both observations show a great potential of escalation of temperature in air-conditioned indoor space in Hong Kong buildings.

Researchers	City	Neutral Temp. (^{o}C)
Auliciems & de Dear (1985)	Northern Australia	24.2
Schiller et al. (1988)	San Francisco (USA)	22.3
Busch (1989)	Thailand	24.6
de Dear et al. (1991)	Singapore	24.2
de Dear & Fountain (1994)	Townsville (Australia)	24.2
Chan et al. (1995)	Hong Kong	23.5

Table 1.3: List of neutral temperature in Hong Kong and other countries

1.5.2 Spatial and Temporal Distribution

W.K. Chow (1994) carried measurements in three typical air-conditioned rooms to compare the mean air velocity and turbulent intensity. Several conclusions were drawn: (1) the maximum turbulent intensity is greater than 90%, (2) it is not appropriate to derive thermal comfort from mean air velocity, (3) ADPI is not enough to represent the air flow spatial distribution and cooling sensation of an individual over a large area. Therefore, distribution approach is proposed to study the true thermal comfort in space.

1.5.3 Chamber tests versus real human behavior in tempering control systems

As is often the case in thermal comfort research, we have an apparent contradiction between field-based survey and laboratory research. These conflicts come from the main differences of distribution of thermal comfort parameters and 'real' human behavior in daily life. In real-life application, temperature control is always a problematic issue since there are many variable thermal comfort parameters such as the effects of clothing distribution and transient loading variation.

1.6 Impact on Health and energy consumption

1.6.1 Operation and maintenance engineers avoiding complaints

Carrying forward the wrong perception of 'cold air system' in Hong Kong, expectations of 'cold' environment made it much easier for people to put on more clothes rather than taking off extra layers. Thus, engineers and building owners prefer setting the indoor temperature cooler to reduce occupants' complaints.

1.6.2 Operating temperature is too cool

As reported in recent news (Ming Po, 2007.06.29), large indoor/outdoor temperature differentials could be one possible cause of the sudden rise of flu and cold cases in ShenZhen in Mainland China. Due to global warming, the average maximum outdoor temperatures in the summers in the highly dense city of Hong Kong reaches an alarming 31.2^{o}C in June, 2007 which is 0.9^{o}C higher the historical average value..

Large temperature differences between indoors and outdoors could easily cause sudden increase in heat loss rate due to sensible and latent heat transfer by wet clothes stuck to the front and back of a human body.

1.6.3 Energy consumption

According to Electrical and Mechanical Services Department of The Government of the Hong Kong SAR (EMSD of HKSAR) – Energy Efficiency and Conservation Newsletter "EnergyWits" (2005), *"If everyone adjusts the air-conditioned room temperature by 1 degree Celsius in the summer, we can save about $1 billion in electricity expenditure annually."* There is a high potential for energy conservation just from the escalation of indoor temperature. EMSD further concluded that implementation of the 25.5^{o}C campaign had effectively cut down the power consumption of five government venues with an average power reduction of 4.2% ("EnergyWits", 2006). Further energy saving potential can be sought by increasing air velocity (Rohles, 1983; Tanable et al., 1989, 1994) and by imposing fluctuating velocity (Fanger et al., 1977; Tanabe, 1997)

Sonne, Parker and Cocoa (1998) in a study of simple household usage of fan-assisted air-conditioning, estimated an energy-use reduction of up to 15%. While the estimation is not conclusive, two vital points are raised. The keys to successful energy conservation are raising the air temperature set point as compared to no fan operation, and education users have in choosing correct operation modes.

So, Tse and Suen (2006) implied energy could be saved with fan-assisted air-conditioning operation without sacrificing the Predicted Mean Vote (PMV). They

also developed a “Fan-Lamp” device to facilitate fan-assisted air-conditioning operation. This proposed the need for fans in indoor applications. However, table and ceiling fans are not very common in buildings, in particular the commercial buildings in Hong Kong. This research introduces a new fan-assisted air-conditioning concept.

1.6.4 Blue Sky campaign – ethical and political requirement for a better-controlled thermal comfort environment.

This research study supports the Hong Kong Blue Sky campaign and the theme of “Fresh Air, Cool City”, emphasizing the setting of air-conditioned room temperatures in the summer to a target temperature of 25.5^{o}C. The proposed one-line indoor temperature escalation protocol that will give comprehensible guidelines to raise indoor temperatures, supporting the government’s “No freezing summer” campaign. To rectify the misconception of “cold” air being more desirable, the true thermal comfort and indoor air quality concept should be clearly introduced and addressed. It is a vital step to educate Hong Kong residents about the environmental benefits of casual dress codes.

CHAPTER 2: OBJECTIVES, STRUCTURE OF THESIS AND METHODOLOGY

2.1 Objectives of This Research

The review of Professor Fanger's thermal comfort model in Chapter 1 clearly indicates that thermal comfort theory is well established. It will be shown in Chapters 3 and 4 that the large-scale in-office survey conducted by Chan et al. in Hong Kong in-office environments is very different from those conducted in neighbouring cities. Over 60% of workstations were found to be over-cooled. One glaring question raised is - are Hong Kong in-office workers more comfortable? Furthermore, on achieving sustainable thermal comfort, are we able to improve the situation in practice if the thermal comfort conditions are unhealthy and/or can we enhance the situation in practice if the thermal comfort conditions are considered satisfactory? These questions form the basis of the objectives in this research project. Achievement of sustainable thermal comfort operation would result in raising intended thermal comfort satisfaction levels while consuming the least possible energy.

The objectives in this study are:

1. To further analyze the physical ,physiological and psychological aspects in real office environment
2. To develop an operational procedure for temperature setting of offices
3. To optimize temperature and air velocity to tune the system for the more energy efficient point

4. To achieve sustainable thermal comfort environment by develop a novel Harmonious fan coil system
5. To verify the CFD simulation with full scale measurement
6. To verify of PMV comfort assessments with real comfort votes from thermal comfort survey.
7. To perform extensive computational fluid dynamics (CFD) with development of appropriate user-defined functions to verify the applicability of the harmonious fan coil system in practice, and develop the CFD as a designed tool for sustainable thermal comfort operations.

2.2 Structure of this thesis

Chapter 1. Literature review

This chapter gives a review of the classic thermal comfort and to summarize recent developments on thermal comfort sensation and operation enhancement. The application of this model in practice is also observed. The deficiency and difficulty in complying with the classic model are also discussed. This appreciation forms the basis of developing an approach and design of a new system for sustainable thermal comfort.

Chapter 2. Objectives, Structure of Thesis and Methodology

This chapter lays down the objectives and structure of this thesis. The methodology and tools used in this study are described either in brief for later elaboration or described comprehensively to allow clear discussion of the results. It is sufficient to

say that this study is not purely a development of a protocol for sustainable thermal comfort. It is also a piece of social work in negotiating with individuals, including users, engineers, architects, contractors and manufacturers.

Chapter 3. Probability Functions of the Key Thermal Comfort Parameters

Using statistical techniques, probability functions of several key thermal comfort parameters are modeled. The erroneous interpretation of an ensemble of the distribution functions of some thermal comfort parameters are discussed, which underscores the hidden problems in sustainable thermal comfort operations. The potential use of these survey-generated probability functions in fuzzy logic control is highlighted.

Chapter 4. Preference of In-office Air Temperature in Air-conditioned Offices

One of the dilemmas in thermal comfort control in Hong Kong is the negligence of the clothing culture of the users in offices and its impact. This chapter is dedicated to exploring the relationship of preferred air temperature and air temperature with respect to the insulation factor of clothing. One surprising result is that PPD cannot be compensated with a reduction in operative temperature. A protocol for setting optimum temperature in air-conditioned offices is proposed.

Chapter 5. Development of the Harmonious Fan Coil System

This chapter discusses the design details of the Harmonious Fan Coil Unit (HFCU), which renders fan-assisted air-conditioning feasible in offices. It also describes the extensive preparation work for manufacture, system design, site preparation, system

preparation, site testing and commissioning, tuning of control system, and user education. The HFCU are installed in two offices.

Chapter 6. Measurement Results and Discussion in Test Rooms

This chapter describes measurement systems, the measured results and subsequent analyses. The measurement results support the feasibility of HFCU using fan energy in lieu of cooling energy. The room air by-pass also reduces the temperature swing at work stations. The measurement systems and analyses can be developed into commissioning protocols and methodology in finding room characteristics for thermal comfort control purposes.

Chapter 7. Computational Fluid Dynamic Analysis

This chapter describes using CFD as an analytic tool for thermal comfort study of the HFCU systems. It also illustrates the technique developed for analysis under the dynamic nature of the system and environment.

Chapter 8. Conclusion

Finally, this chapter summarizes the completion of the objectives. The Three Step approach in Chapter 4 and the HFCU render the sustainable thermal comfort successful. The conclusion also highlights the limitation of this first generation system and proposes ways for enhancement to make the system commercially viable.

2.3 Methods and Tools

The scope of work in this thesis is very extensive. It embraces mathematical tools in statistics (Chapter 3 and 4) and computational fluid dynamics (Chapter 7). The current technology in air-conditioning systems is deficient in providing alternative mechanisms for sustainable thermal comfort. It is one of the objectives in this study to design such systems for this purpose (Chapters 5 and 6). Finally, an observation why building services engineers cannot play a better role in sustaining the appropriate thermal comfort satisfaction is the lack of comprehensiveness in the thermal comfort model itself, rendering the evaluation of thermal comfort parameters difficult. Hence, it is in the very beginning of this study that a thermal comfort calculator (Chapter 2.3.1-2.3.3) is developed to facilitate many of the studies in this research study.

Other than development of the academic contexts in this project, this is a constructive exercise probing into the physiological and psychological responses of human subjects towards the mental balance of their sensations and thermal comfort environment. It is interesting to incorporate an educational strategy into this research, once believed to be a purely engineering problem of sustainable thermal comfort. It is also quite an experience considering the extensive efforts in solicitation and supervisory meetings with the supporting manufacturer and contractors, as well as the endless contract meetings with the Facility Management Office and Campus Development Office of the Hong Kong Polytechnic University. The following sub-sections in Section 2.3 highlights the methods, tools and system developments used in this research study.

2.3.1 Thermal Comfort Calculator Development

A thermal comfort calculator was developed to facilitate the calculation of various thermal comfort parameters, and to benefit comprehensive review and understanding of thermal comfort models. There are several available programs which were developed by other researchers, (e.g. thermal comfort tool by ASHRAE (1997); PMV tool by SquareOne research (2006) ; Wincomf by Fountain and Huizenga (1995)); however, they only base on Fanger's PMV model and some attain Gagge's two node model. All of them cannot give a throughout consideration for other thermal parameters.

In the computational tool developed in this thesis is mainly based on ASHRAE Fundamentals Handbook (2005) – Thermal Comfort discusses the thermal comfort issue in detail, which including 92 equations involving over 130 parameters. The models for thermal comfort concern with steady-state conditions in all aspects of human thermal comfort, including issues from the fundamental physical thermal environment to human physiological conditions. Computation method is applied to estimate the acceptable range of thermal conditions for every particular situation, rather than defaulting to the simpler graphic comfort zone, where assumptions might not match their conditions. The hierarchy of the computational process is shown in Figure 2.1.

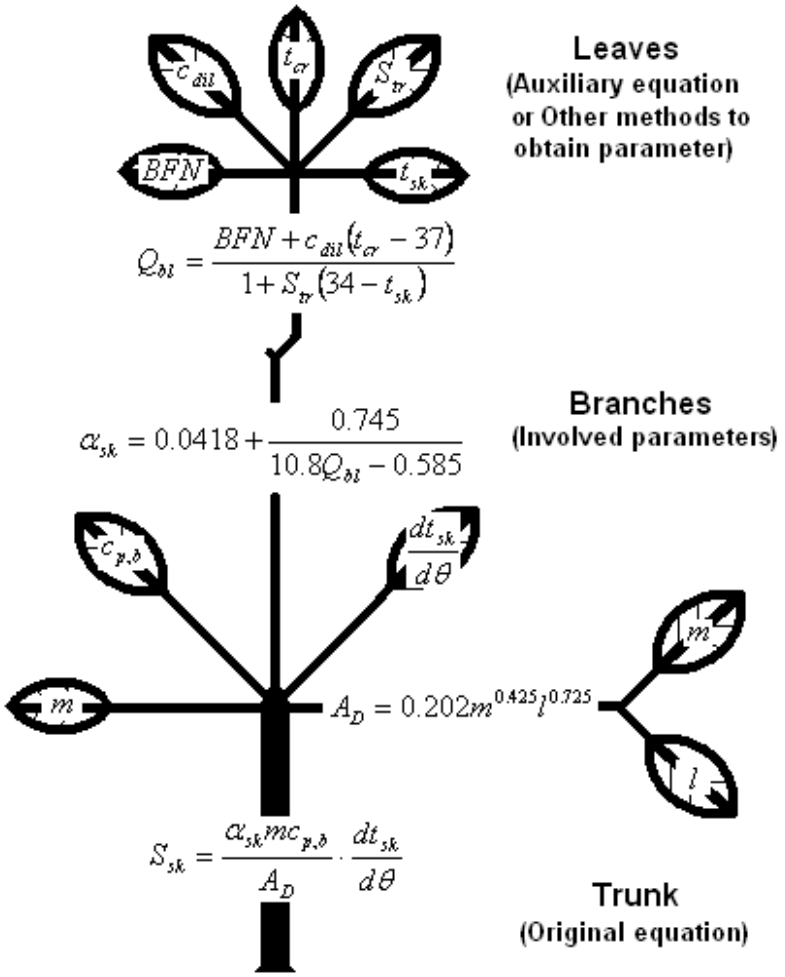

Figure 2.1: Example of computation process described as tree

2.3.2 Analysis of the thermal comfort through parameters

Creating a parameter checklist in a spreadsheet, including all the parameters' symbol and description listed. Also, it indicates which equations the parameters live, by the digit "**1**" as the object of equation and "**0**" as the subject. Through the digit (**0-1**) checklist, the trail of parameters or the components of the equations are clearly illustrated. Part of the sample checklist is shown in Figure 2.2.

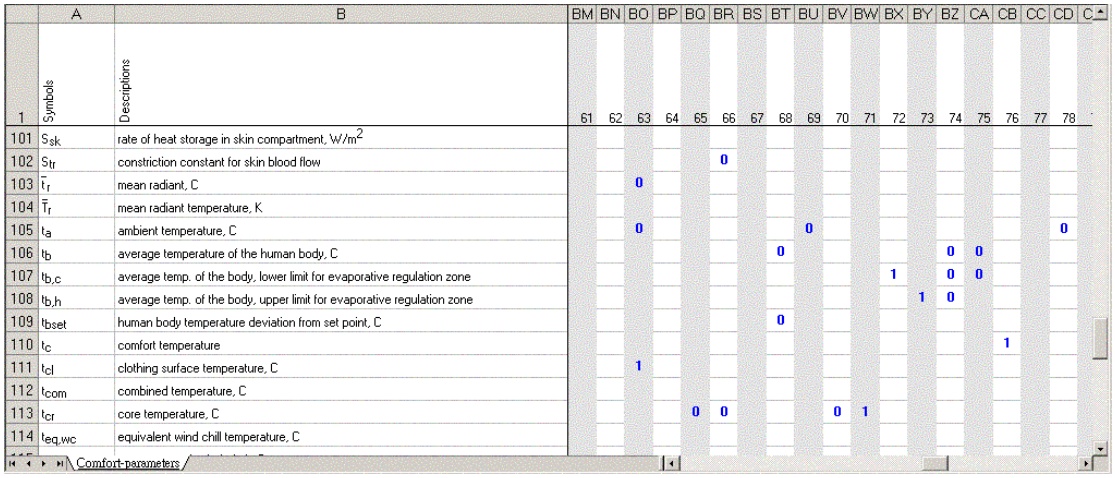

1	Symbols	Descriptions	61	62	63	64	65	66	67	68	69	70	71	72	73	74	75	76	77	78
101	S_{sk}	rate of heat storage in skin compartment, W/m^2																		
102	S_{tr}	constriction constant for skin blood flow						0												
103	$\bar{t}_r$	mean radiant, C			0															
104	$\bar{T}_r$	mean radiant temperature, K																		
105	t_a	ambient temperature, C			0						0									0
106	t_b	average temperature of the human body, C								0						0	0			
107	$t_{b,c}$	average temp. of the body, lower limit for evaporative regulation zone												1		0	0			
108	$t_{b,h}$	average temp. of the body, upper limit for evaporative regulation zone													1	0				
109	t_{bset}	human body temperature deviation from set point, C								0										
110	t_c	comfort temperature																1		
111	t_{cl}	clothing surface temperature, C			1															
112	t_{com}	combined temperature, C																		
113	t_{cr}	core temperature, C					0	0				0	1							
114	$t_{eq,wc}$	equivalent wind chill temperature, C																		

Comfort-parameters

Figure 2.2: Illustration of the digit (0-1) parameters checklist

Instead of the trace of the parameters, applicable alternative computation ways for obtaining the required parameters are indicated with asterisks in the checklist. The methods include physical measurements, survey, coefficients from reference tables/charts, and derivation through other equations, etc. (Sample checklist illustrated in Figure 2.3)

1	Symbols	Descriptions	measurable	with Mobile Stack	with Manikin	with other equipmer	survey	Coeff. / Const	derivation by equation	computation methodology
104	$\bar{T}_r$	mean radiant temperature, K	x	x					x	eqt 50 (environmental parameters)
105	t_a	ambient temperature, C	x	x						
106	t_b	average temperature of the human body, C	x		x				x	eqt 68: $t_b = (1 - \alpha_{sk})\, t_{cr} + \alpha_{sk}\, t_{sk}$
107	$t_{b,c}$	average temp. of the body, lower limit for evaporative regulation zone					x		x	eqt 72 (2-node model)
108	$t_{b,h}$	average temp. of the body, upper limit for evaporative regulation zone					x		x	eqt 73 (2-node model)
109	t_{bset}	human body temperature deviation from set point, C								t_{bset} set to zero when negative
110	t_c	comfort temperature					x		x	eqt 76 (adaptive model)
111	t_{cl}	clothing surface temperature, C	x			x			x	eqt 59 (steady-state energy balance)
112	t_{com}	combined temperature, C							x	eqt 31 (total skin heat loss)
113	t_{cr}	core temperature, C	x		x					
114	$t_{eq,wc}$	equivalent wind chill temperature, C						x	x	eqt 81, table 11 (wind chill index)
115	t_{ex}	temperature of exhaled air, C							x	eqt 22 (respiratory loss)
116	t_g	black globe temperature, C	x	x						
117	T_N	surface temperature of surface N, K	x			x				

Comfort-parameters

Figure 2.3: Sample checklist indicating the alternative computation ways with asterisks

2.3.3 Computation program

A prototype computation program was developed on the Visual C#.NET interface for steady performance and better appearance. The advantages of the computation program include the user-friendly preset directive calculation process and the auto-transfer of subject parameters calculation result. These make the studying process clear and convenient. The directive calculation process also guides users to get the result in the simplest and most effective manner.

The computation program is developed as a graphical user interface (GUI), including the components of parameter index, preset directive computation, parameter database and graphical references. The parameter database stores the value of parameters and supports data for the computation. In addition to the load/save function, the database can be loaded from a default set as well as saving the result from computation. Directive computation is preset in the program, which leads users to get results in a straightforward and efficient manner. Furthermore, it provides a selection of equations for the computation if more than one equation is available. If the required subject parameters are unknown, users would be directed to the particular subject parameter calculation page while transferring the result to the computation afterwards. For cases such as the calculation of the parameter of ADPI, statistical data from a measurement dataset is required; database space is available for insertion. Meanwhile the database would be analyzed. The function of iteration is also available for the computation of parameters like t_{cl}, ET*, t_{oh}, t_{com}, etc. Moreover, graphical references are provided, including coefficients, tables, figures and charts. (The structural diagram of the computation program is illustrated in Figure 2.4)

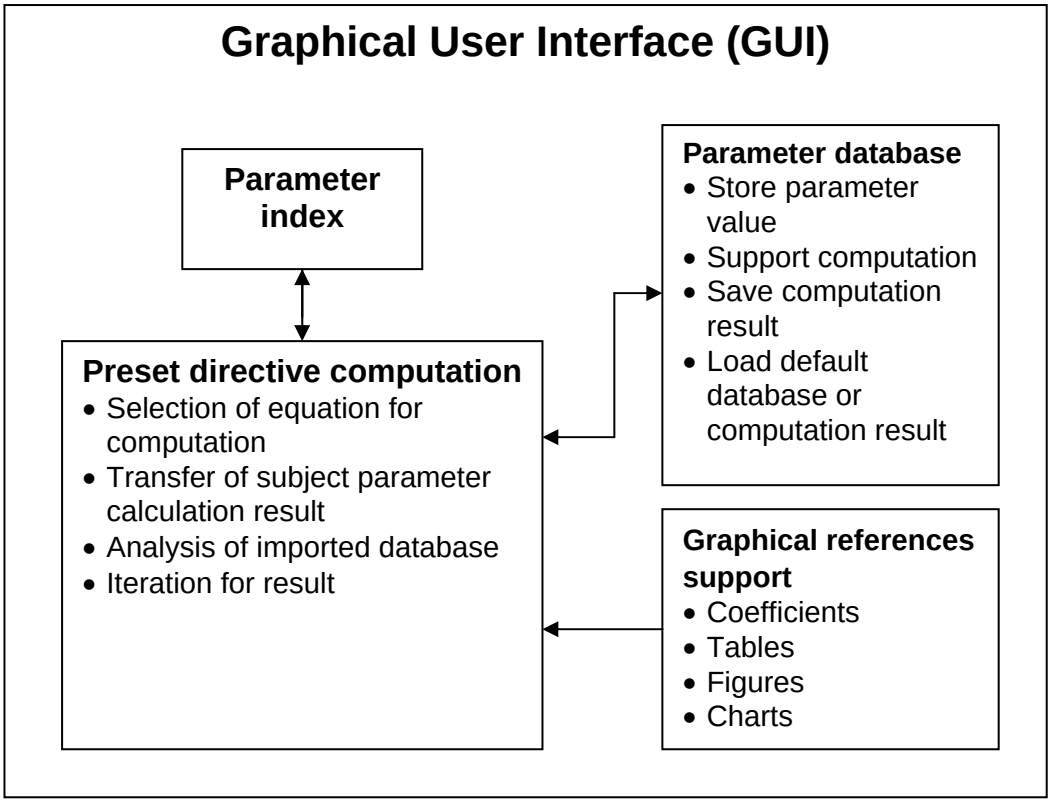

Figure 2.4: Structural diagram of the computation program

Again, the example of calculating the rate of heat storage in skin compartment (S_{sk}) is applied to introduce the computation program. The parameters involved in thermal comfort computation are listed in the index page (illustrated in Figure 2.5). Selecting the parameters to be studied, users would be directed to the page for calculation. Figure 2.6 illustrates the page for calculating the parameter S_{sk}. The equation is shown and the blanks for filling in the values of the five subject parameters are available. “Edit” icons are available to find the subject parameters if they are unknown. For example, users could click the icon at the right of the blank if α_{sk} is unknown. Figure 2.7 illustrates the page for calculating the parameter α_{sk}. The parameter Q_{bl} is required for computation. Similarly, click the icon to find Q_{bl} if it is

unknown. Figure 2.8 illustrates the page for calculating the parameter Q_{bl}. Five subject parameters are involved in the calculation, while the values of an average person are given for three of them. The remaining parameters (human body core temperature and skin temperature) can be measured. Therefore, getting the result of Q_{bl}, the parameter of α_{sk}, can be obtained. In the calculation of the parameter A_D (as illustrated in Figure 2.9), all subject parameters for the calculation of S_{sk} are obtained. The results attained in each subject parameter calculation page can then be transferred to the object parameter calculation page (as illustrated in Figure 2.10), and the result of the parameter S_{sk} can be acquired.

For some special cases, such as the computation of t_{cl}, ET* (as illustrated in Figure 2.11), t_{oh}, and t_{com}, iteration is required. If users try to calculate this manually, they will have to repeat the calculation process numerous times to obtain an accurate result. With the aid of the computation program, the value of subject parameters only have to be inserted once and iteration would proceed to obtain an accurate result with a difference of less than $1e^{-6}$.

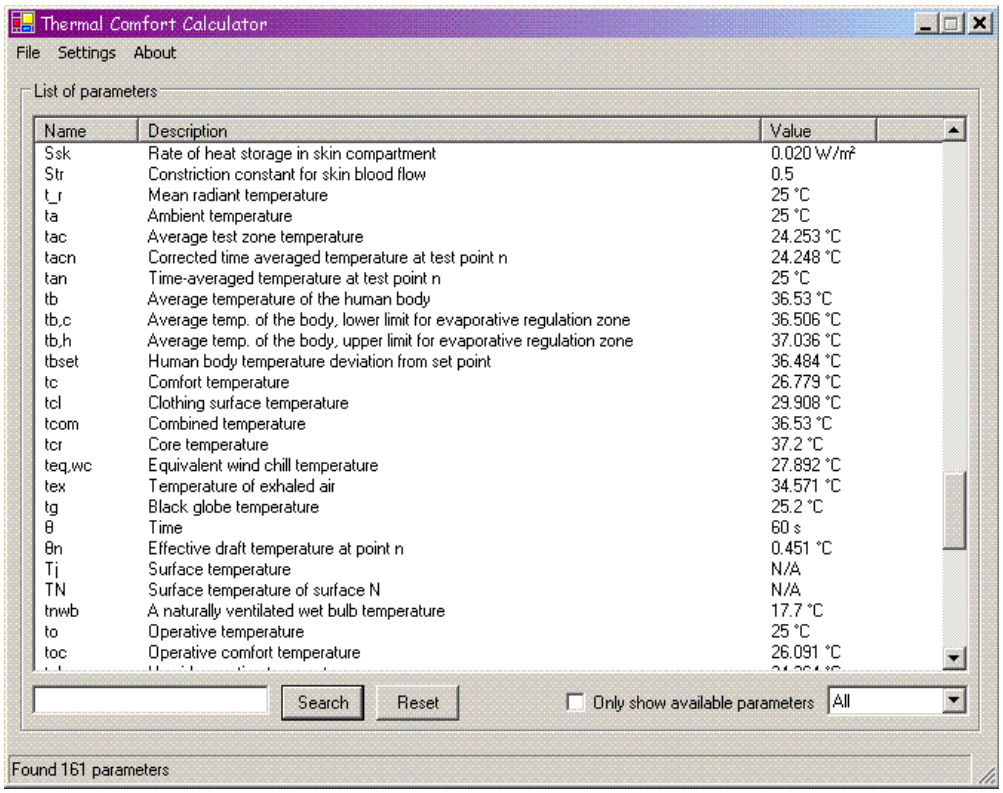

Figure 2.5: Index page of parameters checklist

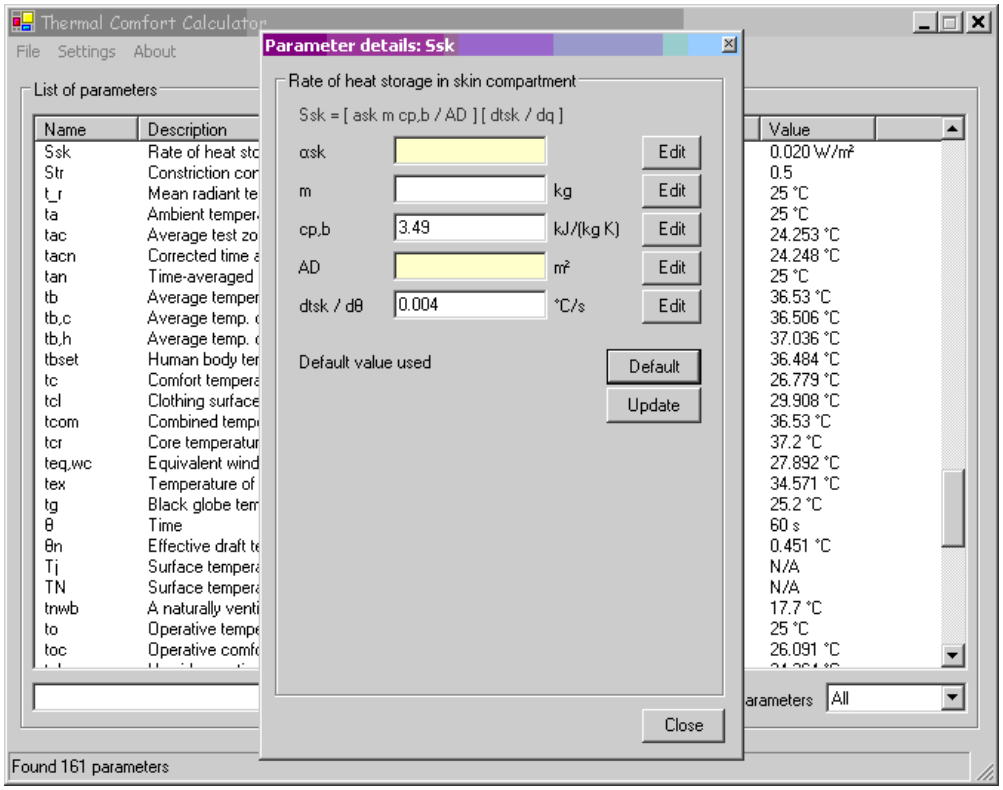

Figure 2.6: Page for calculating the parameter S_{sk}

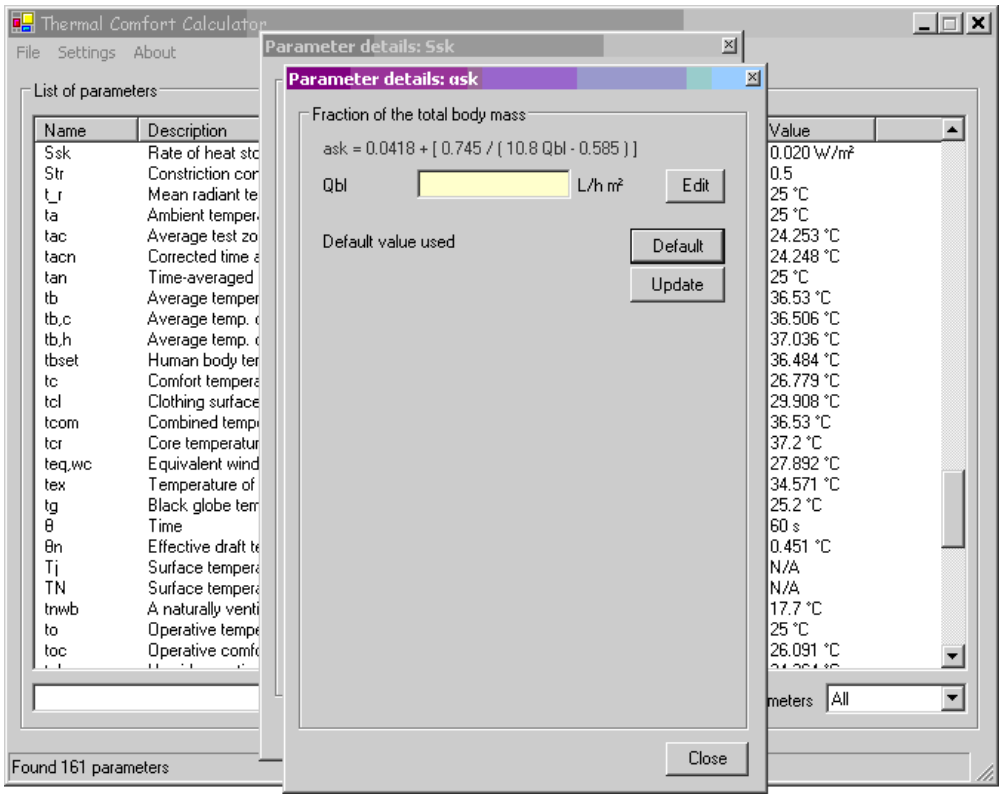

Figure 2.7: Page for calculating the parameter α_{sk}

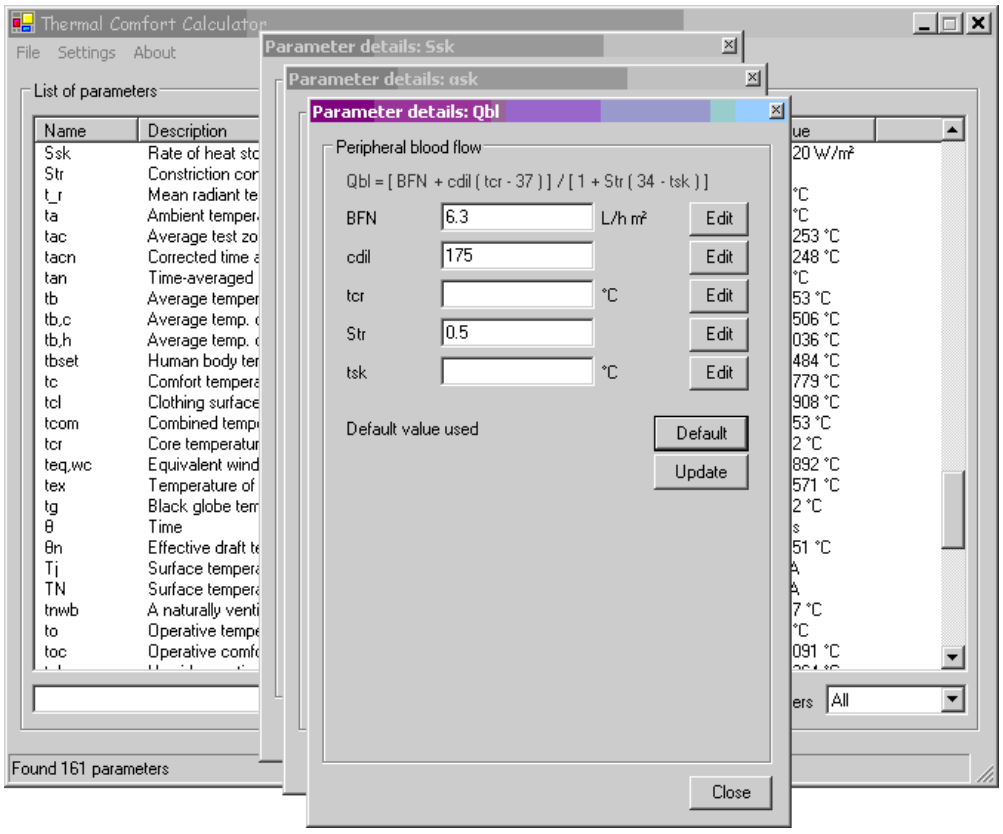

Figure 2.8: Page for calculating the parameter Q_{bl}

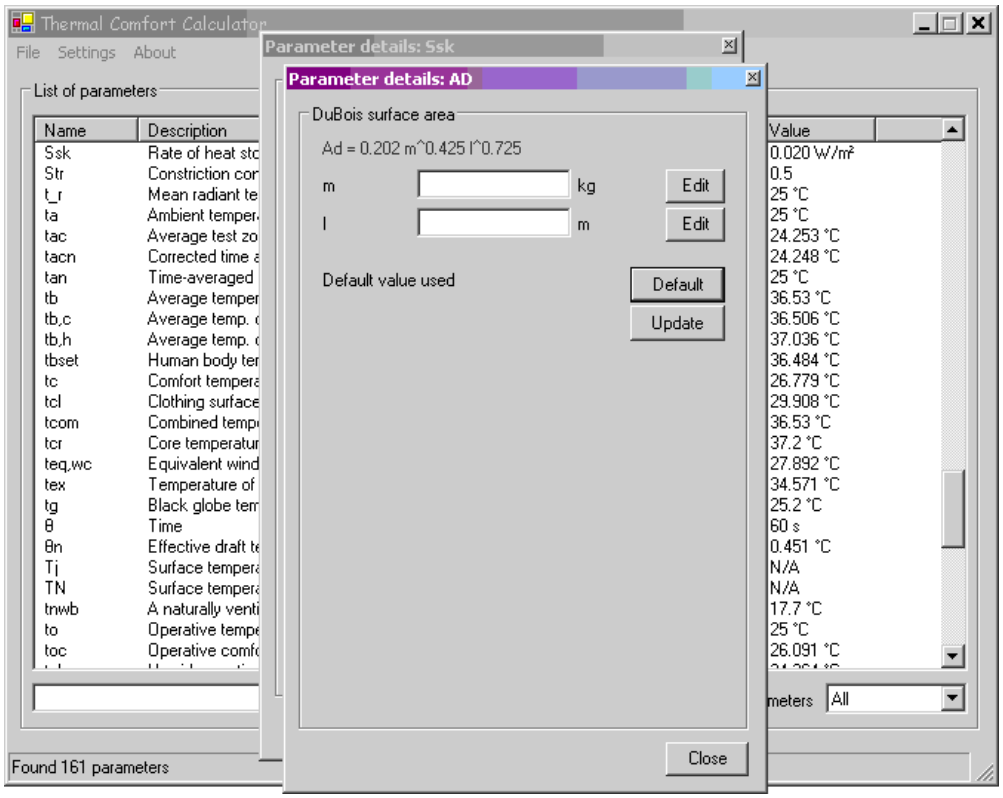

Figure 2.9: Page for calculating the parameter A_D

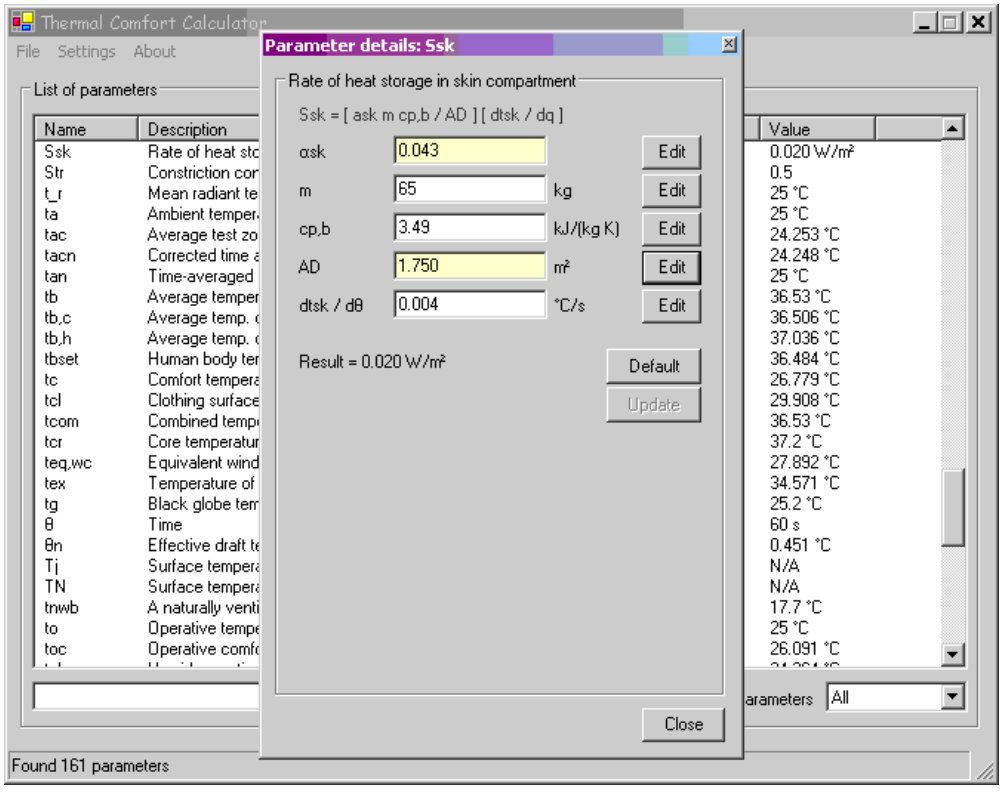

Figure 2.10: Return to calculate the parameter S_{sk}

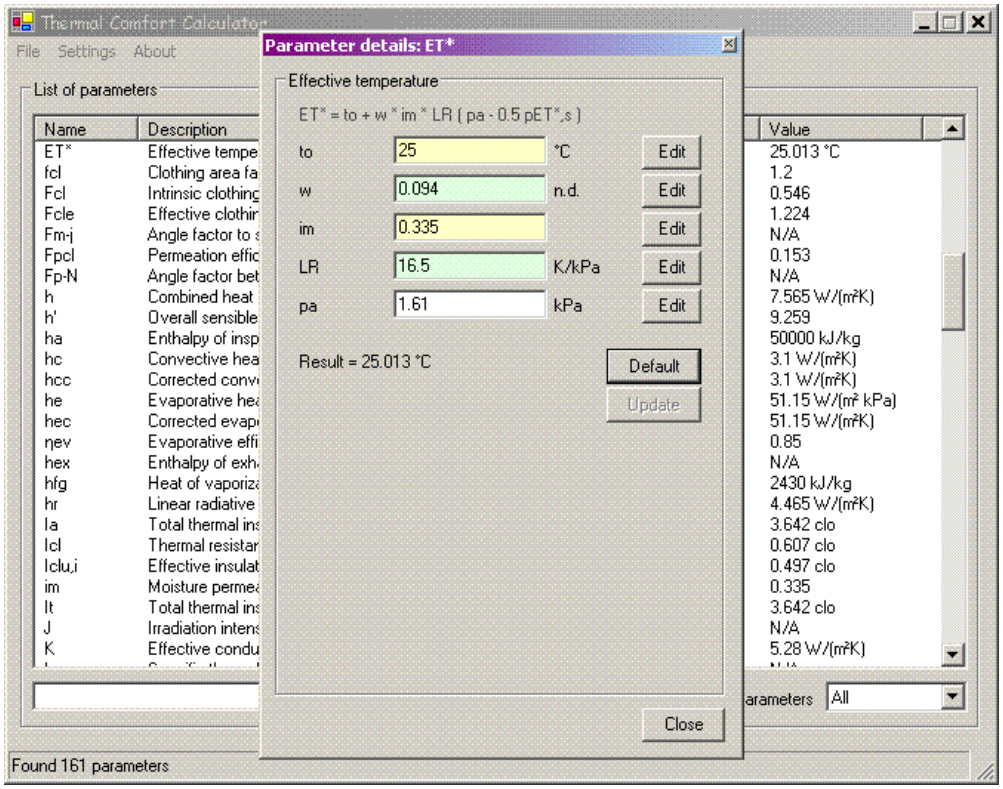

*Figure 2.11: Page for calculating the parameter ET**

2.3.4 A Comprehensive Data Base for In-office Thermal Comfort Survey

Chan et al. (1998) conducted a comprehensive in-office study of indoor environmental quality and sick building syndrome. The details of the survey are described in Section 3.2.1. In this study, the database is further analyzed on a deeper level. This second-order analysis of the database has generated very interesting results on the human sensation preferences, especially the impact of clothing culture. The outcome forms the basis of sustainable thermal comfort strategies and initiates the development of a new harmonious fan coil system (HFCU) which adopts the fan-assisted air-conditioning.

2.3.5 Measurement systems

Through the analysis of model equations of the thermal comfort model, the 130 thermal comfort parameters as stated in ASHRAE Handbook Fundamental Chapter 8 on Thermal Comfort are divided into four types:

- Measurement
- Survey data
- Derivatives
- Coefficients, constants and assumed values

Prior to the design of the HFCU, measurements had been carried out in a household apartment and a secondary school, and a protocol was drafted for the feasibility study of fan assisted air-conditioning to conserve energy, submitted to Electrical and Mechanical Services Department (EMSD) of HKSAR. These measurements form

the basis of the detailed design of the HFCU. However, as these measurements were not conducted in offices, the results are not shown so that this thesis can focus on the discussion of sustainable thermal comfort in an office environment. Nevertheless, the former measurements provide a chance to develop a series of measurement systems and protocols for thermal comfort analysis under dynamic situations. The measurement is then used to calculate the derivatives.

Specifically, two main systems are used:

i. Mobile Stack

Mobile stack is a highly flexible and specific measurement platform for the investigation of indoor air quality. It is designed for measuring the air and thermal parameters at different vertical levels, i.e. feet (0.1m), sitting body (0.6m), sitting head or standing body (1.1m), standing head (1.7m), as recommended in ASHRAE 55. The parameters include room air temperature, global temperature, relative humidity, air velocity, carbon dioxide concentration.

ii. Leakage Test System

This system comprises a radon meter and a carbon dioxide sensor and logger system. The leakage test is based on a curve-fitting technique under multiple minimum error iterations to determine the emission rates of radon gas in space, which in turn is used to determine the leakage rate in an enclosed space. This leakage test method is derived from a modelling technique to measure radon emission rate (Tung et al., 2006). In the leakage test measurements, metabolic carbon dioxide is used as a test agent to verify the measurements.

Details of these measurement systems and instrumentation will be presented in the appropriate chapters.

2.3.6 Development of the Harmonious Fan Coil System

Following a comprehensive site measurement in developing a protocol for fan-assisted air-conditioning for thermal comfort in a residential apartment and a classroom of a secondary school, the approach of using fan energy in lieu of cooling energy was found to be feasible in optimizing thermal comfort. Publication of these results and protocol is under preparation. They are not presented in this thesis because the focus of this thesis is on air-conditioned offices.

Usually, desk top fans are suggested for fan-assisted air-conditioning. However, the air flow field generated is normally difficult to control without draft risk and cannot be trusted to cause no nuisance upon its location and operation. Therefore, a harmonious fan coil system was designed and tested in the Dean's Office and the office of a Professor in the University. Further details are described in Chapter 5. It took tremendous effort to solicit support and to supervise the manufacturing of the system with the manufacturer. Convincing the Facility Management Office and the Campus Development Office that the system is superior in attaining a sustainable thermal comfort was also a lengthy endeavour. Finally, it is worth mentioning that this development takes these into account:

- educating the users for an acceptable thermal comfort,
- making the office space air tighter,
- changing the practice of water-balancing to compensate over-sizing of the fan

coils,

- preparing the fans (reducing noise generation),
- furnishing the control systems,
- supervising the contractors and
- testing and commissioning the systems.

2.3.7 Mathematical techniques

Probability distribution modelling

One of the key issues causing discomfort is the spatial and temporal distribution of the thermal comfort parameters. Therefore, more in-depth analysis of these distributions will help to identify problem areas and to seek solutions.

Signal Processing

In recent studies of thermal comfort, air velocity acceleration (Zhou, 1999) and air flow turbulence (Fanger, 1988) are considered important factors. In the new development of the HFCU, a harmonious (frequency varying) air flow component can be imposed on the mean flow. Auto-correlation analysis serves as a mean to calculate the air flow characteristics in the room.

Computational Fluid Dynamics

The use of computational fluid dynamics is two-fold. Firstly, it helps to study the new system under more scenarios than measurements. Secondly, it is capable of being developed as a tool for design and operation conditions of the HFCU. In this

project, much effort has been spent in development of this tool. It also takes much effort to develop User Defined Functions for analysis of the HFCU under varying boundary conditions. Therefore, a briefing of the technique was deemed necessary and is presented in Section 2.4

2.4 The application of CFD in thermal comfort issue

CFD has demonstrated a wide variety in the application of indoor environment simulation. Researchers applied CFD in many areas, for example in laboratories (Nielsen, 1974; Lu, 1996), case studies (Waters, 1986; Chow, 1996) and its usage in building design (Markatos, 1983; Jones, 1987). Numerous thermal comfort studies have been conducted with the use of CFD tools. Prediction of air movement and thermal comfort condition in mechanical ventilated office was conducted in 1994 (Awbi, 1994) with acceptable accuracy after validating with field measurement. Gan make use of CFD tool to investigate the local thermal discomfort in a displacement ventilation system (Gan, 1995) The inference of air diffusion models to the air flow and thermal comfort in an indoor environment was investigated which concluded that the ADPI is not enough to describe the air diffusion performance or the draft risk (Chung, 1995). The effect of humidity on indoor environment was investigated in 2001. (Teodosiu, 2003)

Cheong (Cheong, 2003) used CFD to predict airflow pattern, indoor air quality and the thermal comfort level indicated by PMV and PPD in a lecture theatre in Singapore, with the comparison of measurement data and subjective response of building occupants.

In a CFD simulation, not only is the indoor environment to be simulated, but the influence of human to the occupied space can also be included. The indoor comfort level was simulated with the evaluation of a thermal manikin in order to solve the thermal comfort problem in different working place environments (Nilsson, 2003), which found that the result corresponds with measurements made in the real environment. The effect of the rising air stream due to the heat generated by the building occupants is also simulated to find its effect on indoor air quality and the thermal comfort level (Murakami, 1997; Murakami, 1998; Hayashi, 2002, Sorensen, 2003).

In the whole thesis, one real office is simulated using computational fluid dynamics. In this chapter, the theory of the simulation is introduced. All applied techniques and the selected models are also illustrated. The fundamental conservation of mass, momentum, turbulence modeling, the boundary types, discretization method, transient simulation, user defined function, convergence criteria for the two cases are discussed in this chapter.

A commercial CFD code “FLUENT” (FLUENT, 2003) is used for the simulation of the indoor environment. The numerical scheme employed belongs to the finite volume group and adopts integral from of the conservation equations. The solution domain is subdivided into a finite number of contiguous control volumes and conservation equations are applied to each volume. Surface and volume integrals are approximated using suitable quadrature formulae. The mathematical formulation adopted is showing in Appendix A.

2.4.1 Transient calculation

Iteration time advancement scheme is applied in all transient simulations. In a one-time step, iterations are carried out until all the solutions reach the convergent criteria or reach the maximum number of iterations per time step set before. When compared to the non-iterative time advancement scheme, iterative time advancement scheme can reduce the splitting error for different variables throughout the calculation.

2.4.2 User defined function

The application of the user-defined function is to add additional calculation procedures or to allow the setting of their own physical properties of the simulation cases. This function can be interactive between the FLUENT main program and the user-defined programs.

All the simulations used the segregated solver, and the following figures describe the dynamic relation between different modules of user-defined functions.

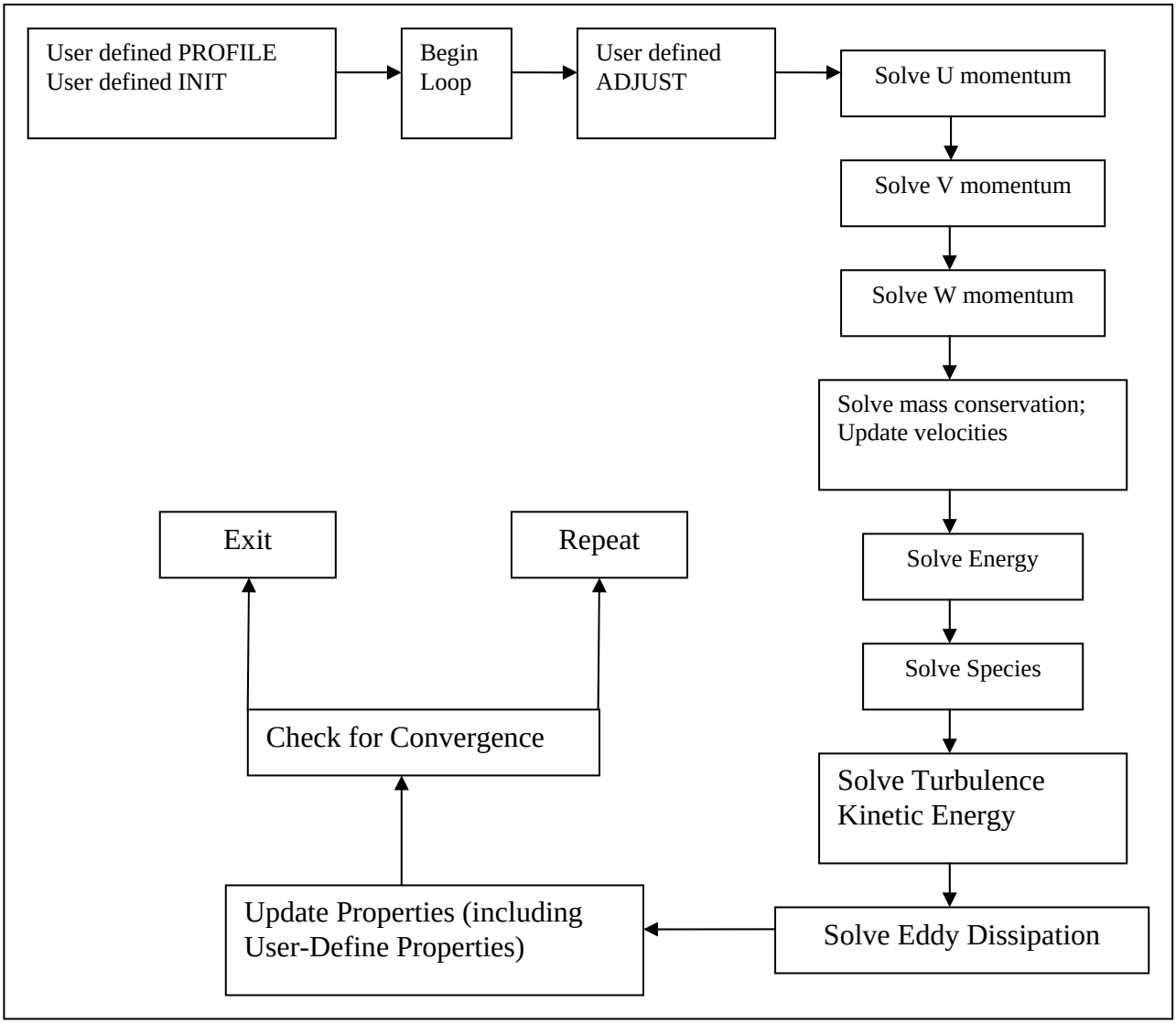

Figure 2.13: Iteration process involve user define functions

In the office simulation, under-defined functions are applied. The modules functions "ADJUST" and "PROFILE" are used to customize the boundary condition and read out the stored value of the face in the domain.

2.4.3 Convergent criteria

The convergence criterion for continuity, x, y, z velocity is 1×10^{-3}; for energy calculation, the convergence criterion is 1×10^{-6}.

2.4.4 Overall calculation procedure

In conclusion, the overall calculation procedures involving user-defined function, time iterative advancement scheme and SIMPLE algorithm in the simulation are shown in the following flowchart:

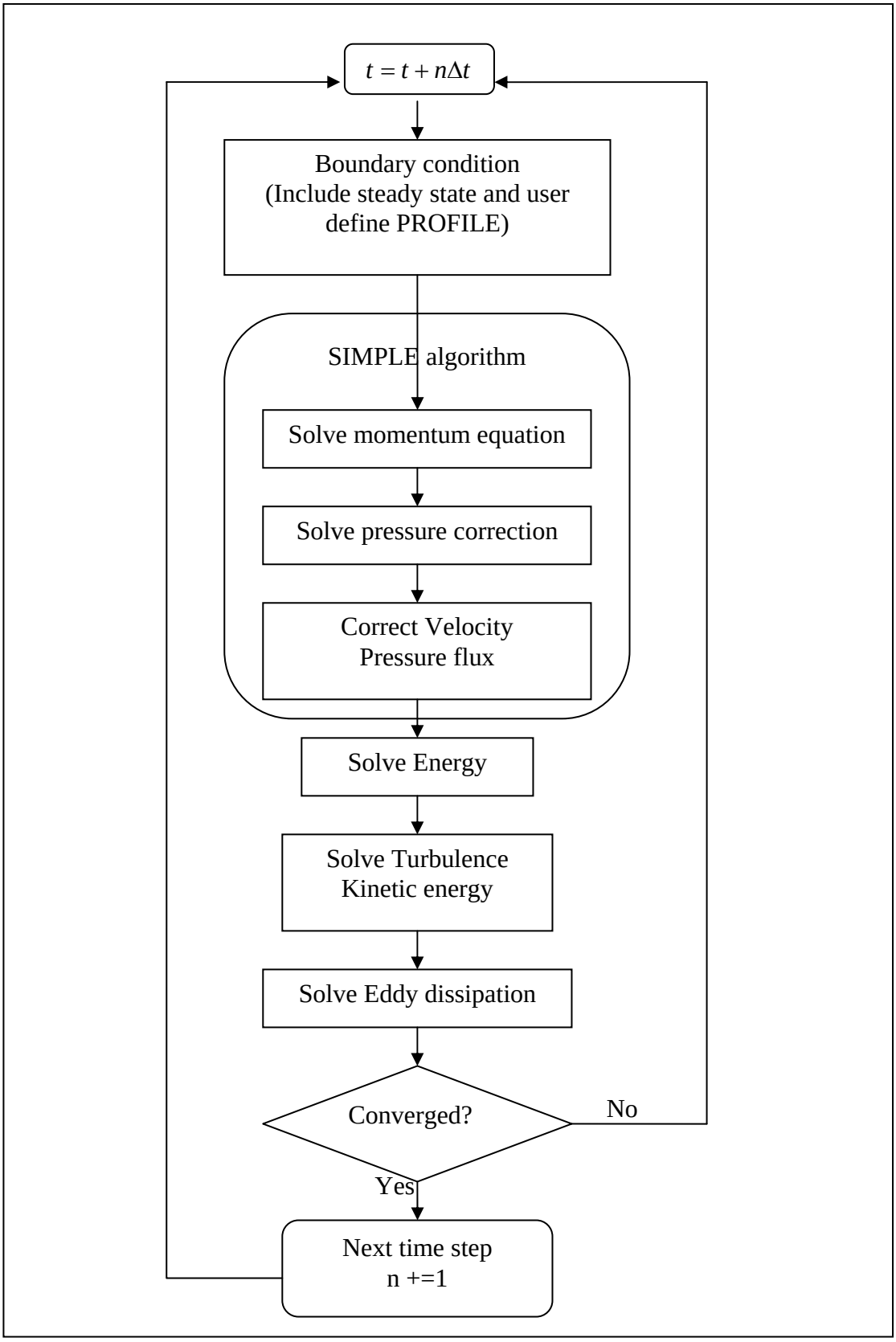

Figure 2.14: Overall iteration process for transient simulation

2.4.5 Validation

All the simulation models are validated by data measured. For steady state simulations, vertical profiles of temperature and velocity are employed to check validity. For the transient simulation, the profile of temperature against time and the vertical profile of velocity compared against the time-rated average velocity data from measurements are used for the validation.

CHAPTER 3: AIR TEMPERATURE DISTRIBUTION IN HONG KONG OFFICE BUILDINGS

Hong Kong is a city in a sub-tropical area, and intensive cooling is often required during the hot summer months. Outdoor humidity is also quite high, and the mean temperature during the summer reaches 28.8^{o}C. (HKO, 2007) For reasons of ease and economy, only air temperature is controlled while relative humidity is allowed to vary wildly. For most engineers, the indoor thermal comfort design criterion is simply 24^{o}C. In reality, this setting is only a safe choice within the summer thermal comfort zone according to the ASHRAE Standard 55(2005) and within normal range of I_{cl}. The common practice in thermal comfort design is to assume all rooms or space served by one piece of equipment is a single zone. The distribution characteristics are taken care of by the ADPI (air distribution performance index). In this chapter, the distribution functions of the key parameters (air temperature, relative humidity and radiant temperature) were found. An air temperature distribution envelope was used to define the distribution characteristics of this very important parameter (important in the sense that traditionally this is the parameter used for controlling the thermal comfort environment). This distribution envelope can be used to identify the degree of non-compliance to the range of PMV as determined by a pre-determined PPD, a business decision in the investment of indoor thermal comfort environment.

3.1 Distribution characteristics of the thermal comfort parameters in Hong Kong

3.1.1 Description of the Large-Scale Survey in Hong Kong Offices

A large-scale thermal comfort survey was conducted in selected Hong Kong office buildings. This large-scale thermal comfort survey was carried by Chan et al. (1998) in the summer of 1996. The selected building details and the type of air conditioning systems served are shown in Table 3.1. Two identical mobile carts were built, each equipped with three arrays of sensors to measure the air temperature, globe temperature, relative humidity and air velocity. The sensors of the measurement system are listed in Table 3.2.

Building code	Type of tenant	Number of Questionnaires	Air conditioning type	Floor plan layout
1	private	59	FCU	Open plan
2	private	206	FCU	Open plan
3	private	30	FCU	Mixed
4	private	363	FCU	Open plan
5	private	96	FCU	Mixed
6	civil	67	CAV+VAV	Mixed
7	private	43	VAV	Open plan
8	civil	139	VAV	Open plan
9	private	95	VAV	Open plan
10	private	92	CAV+FCU	Mixed
11	private	8	FCU	Mixed

Key: CAV: Constant air volume

VAV: Variable air volume

FCU: Fan coil unit

Table 3.1: Summary of the 11 office buildings surveyed

Quantity	Sensor		Accuracy
	Description	Position	Calibrated
Air temperature	Shielded thermistor	0.1m,0.6m, 1.1m	±0.1^{o}C over range 17^{o}C to 26^{o}C
Globe temperature	Thermistor	0.1m,0.6m, 1.1	±0.1^{o}C (M) for thermistor
Relative humidity	Digital psychrometer	0.6m	±1% RH (M) for range 0 to 100%
Air speed	Omni-directional constant temperature anemometer	0.1m,0.6m, 1.1	±5%,0.005m/s (M)

* M: Manufacturer calibrated and checked by inter-comparison

Table 3.2: Summary of sensors on the measurement system of the mobile cart

3.1.2 Validity of the Database

The database was analysed in line with other international reports such as de Dear (1998). In this chapter, further analysis of the distribution characteristics of the air temperature, relative humidity and radiant temperature will be conducted. Different statistical tests are applied to find the distribution function of the probability distribution. Correlation coefficient, constant variance test (Levene's test) Durbin-Waston statistics and the normality test (for error analysis). (Sigma plot, 2003)

The Hong Kong survey is very similar to the study in Kalgoorlie-Boulder, Australia. Table 3.1 extracted from Chan et al. demonstrates that the survey in Hong Kong has the same characteristics. Given the compliance to international standards on measurements and analyses, the study was considered valid and represented the thermal comfort conditions in Hong Kong. Although the survey was conducted in the mid-1990s', a later smaller-scale survey in offices confirmed that the situation are still very similar (Mui and Chan, 2003). Therefore, the database is still pertinent for more in-depth analysis in this study.

When compared with the results of field measurement carried out in Kalgoorlie-Boulder, Australia (Cena, 2001), while the mean air temperature, mean radiant temperature and mean relative humidity were 23.4^{o}C, 24.0^{o}C and 41.5% as also shown in Table 3.3. It shows that the variation for the three parameters in Hong Kong is smaller than that of Kalgoorlie-Boulder. With the exception of lower mean air temperature in Hong Kong, all the other parameters' averages are higher then that of Australia.

	No. of sample	Range	Minimum	Maximum	Mean	Std. deviation	Variance
Air temperature	1158	8.44	17.6 (19.1)	26.05 (30.5)	21.74 (23.4)	0.97 (1.4)	9.33
Radiant temperature	1158	7.97	20.34 (20.2)	28.31 (32.8)	23.27 (24.0)	1.10 (1.4)	1.216
Relative humidity	1158	33.8	37.9 (24.5)	71.7 (66.1)	55.0 (41.5)	4.95 (8.8)	24.52

( ) is the result of the Kalgoorlie-Boulder

Table 3.3: The descriptive statistical result of the survey in Hong Kong and Kalgoorlie-Boulder

3.2 Distribution characteristics of the Database

The distribution functions of the three parameters were found. As all engineers know, there exists a distribution of the thermal comfort parameters even if a zone is designed to be a single one with uniform performance across the space. Different statistical tests were applied in order to find out a suitable distribution function for the thermal comfort parameters. The results are shown in Table 3.4. The results of the probability distribution of the survey data are shown in the Table 3.5. Points represent the real data of the survey and the lines are the probability distribution models for each of the parameters.

Parameter	PDF	R	R sqr	Adj Rsqr	PRESS	Durbin-Waston	Normality test	Constant variance test
Air temperature	Log-normal	0.99	0.99	0.99	0.0022	1.9831	0.3148,0.1498	Passed (P=0.1807)
Radiant temperature	Modified Gaussian	0.99	0.99	0.99	0.0021	1.9360	0.3053, 0.1746	Passes (P=0.3894)
Relative humidity	Lorentzian	0.98	0.97	0.96	0.048	1.9767	0.3232, 0.2488	Passed (P=0.1863)

Table 3.4: The result of the statistical test of mean air temperature, mean radiant temperature and relative humidity.

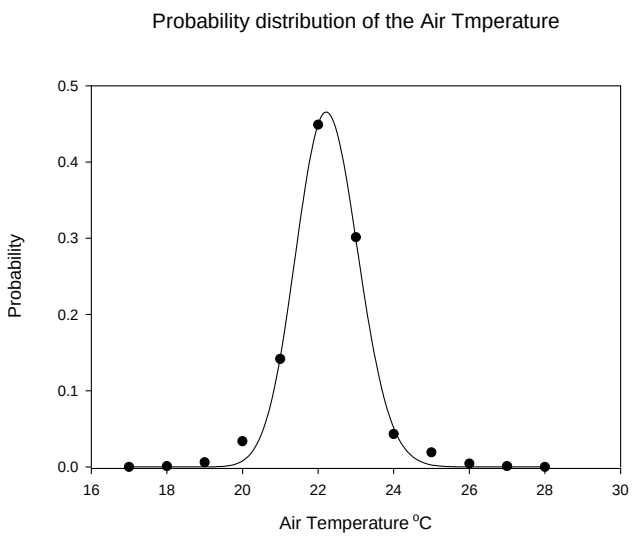	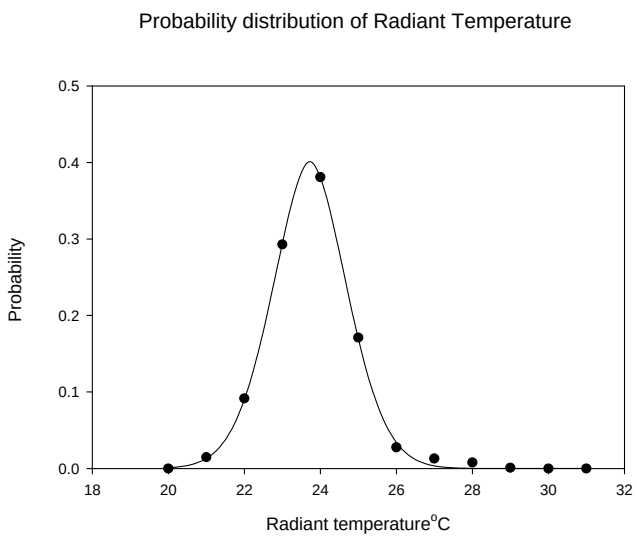	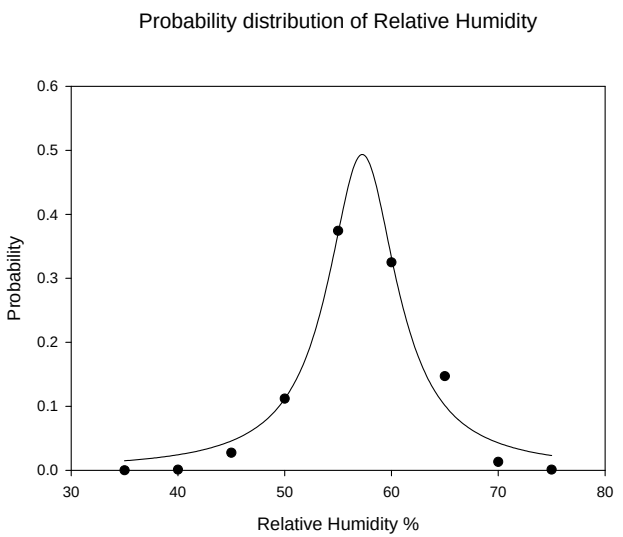
$P(Ta) = 0.4657e^{\left[-0.5\left[\frac{\ln\left(\frac{Ta}{22.2167}\right)}{0.038}\right]^2\right]}$	$P(Tr) = 0.4013e^{-0.5\left(\frac{\lvert Tr-23.7263\rvert}{0.9433}\right)^{1.8122}}$	$P(RH) = \frac{0.4937}{1+\left(\frac{RH-57.2669}{3.9284}\right)^2}$

- The probability distribution of the survey data

— The probability function

Table 3.5: Results of the probability distribution function curve and equation

These distribution functions are very useful in setting up a fuzzy logic control algorithm. Traditional fuzzy logic algorithms normally assume triangular or Z membership functions as a control. This project proposes these distribution functions for such purposes. Actually, the original aim in this study is to produce such an algorithm. More in-depth analysis of the database reveals that in a real-life situation, Fanger's thermal comfort model is not properly understood in practice. It is also shown in the large-scale study that 60% of the work stations were surveyed as experiencing temperature on the cool side as compared to the thermal comfort zone defined by ASHRAE Standard 55-2004. Therefore, the foci in this study are to investigate the interactive responses and culture of indoor occupants to thermal comfort environment and to propose solutions to sustainable thermal comfort control. Nevertheless, the approach of setting membership functions for fuzzy control is an important step in operating sustainable thermal comfort conditions. A proposal for such development is shown at the end of this chapter, which will be left for further study beyond the scope of this thesis.

3.3 Interpretation of the ensemble distribution

In typical office environment, a significant temperature swing is easily found. It could be explained by the cooling load from time to time. This is normal for room served by fan coil units system due to the cut in and cut out condition of the chilled water. Figure 3.1 shows a measured data to illustrate the chilled water cut in and cut out situation. The cut in action interprets that the detected air temperature reaches the designed set point temperature. The supply chiller water valve for the terminal will open at that point. The temperature of the room would gradually increase until it

reaches the minimum allowable temperature set point. The valve will then turn off for the terminal; this is the cut out point.

The temperature profile at the position of the thermostat, supply air diffuser, and two other points within the room are recorded. From they graph, it is shown that the temperature fluctuation of the thermostat (ΔT_{sensor}) is smaller then the space. There is an amplification of the swing and here it is calculated as:

Amplification factor of thermostat swing $A = \frac{S_{space}}{\Delta T_{sensor}}$

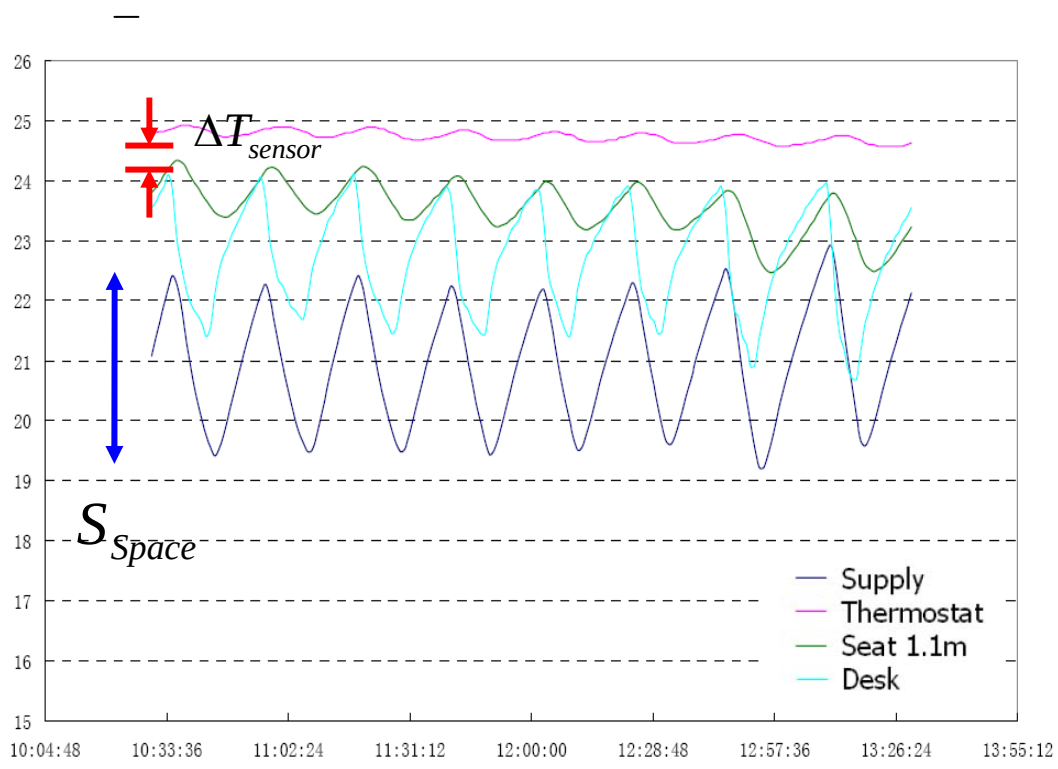

Figure 3.1: Illustration of The cut in and cut out situation in real office environment

A more advanced consideration from this distribution function is that it represents the envelope of spatial and temporal variations in an office. Assuming the temperature distribution in space is settled at a spatial distribution function. When there are cut in and cut out process in the terminal side, the space temperature will increase and decrease accordingly. The spatial distribution function will move to the left (increasing supply air temperature) when fan coil unit system cuts in; in contrast, the distribution function will move to the right when the thermostat detects the upper limit set point. Therefore, the spatial distribution function will swing across time. Figure 3.2 demonstrates several snapshots for the spatial distribution of the zone at different incidental time slot. The spatial distribution function swing across time forms the ensemble spatial and temporal temperature envelope as shown in Figure 3.3. The upper distribution (the red line) and the lower distribution (black line) form the boundary of the thermal comfort envelope. This envelope can be applied in designing and controlling the performance of air conditioning system meeting the desired thermal comfort zone.

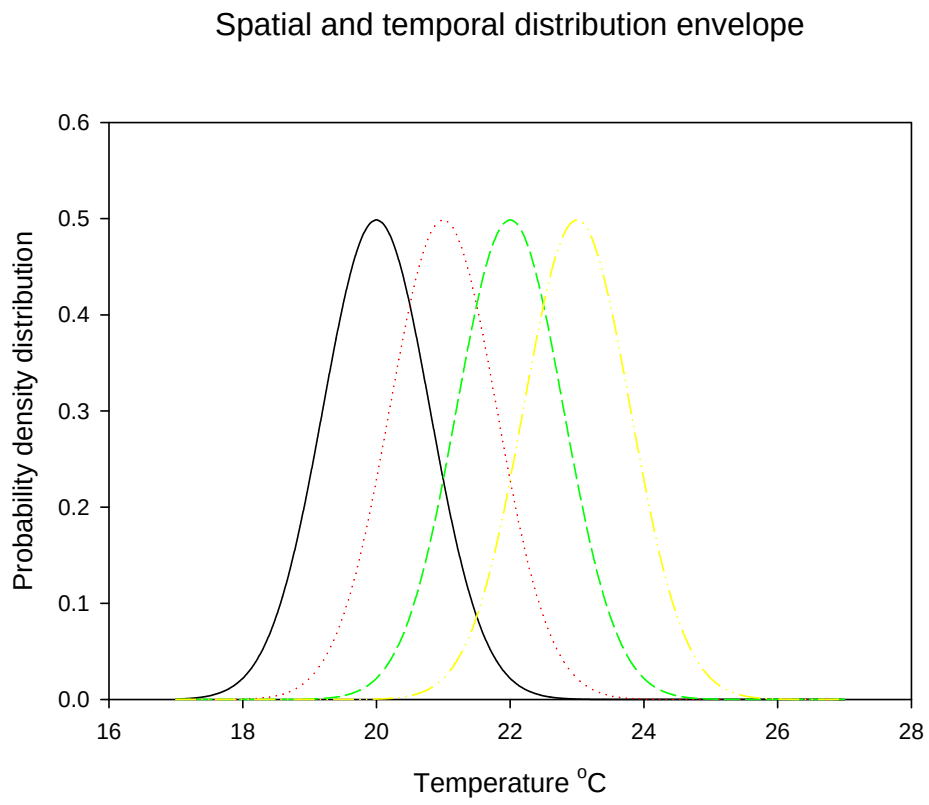

Figure 3.2: Interpretation of the spatial and temporal envelope.

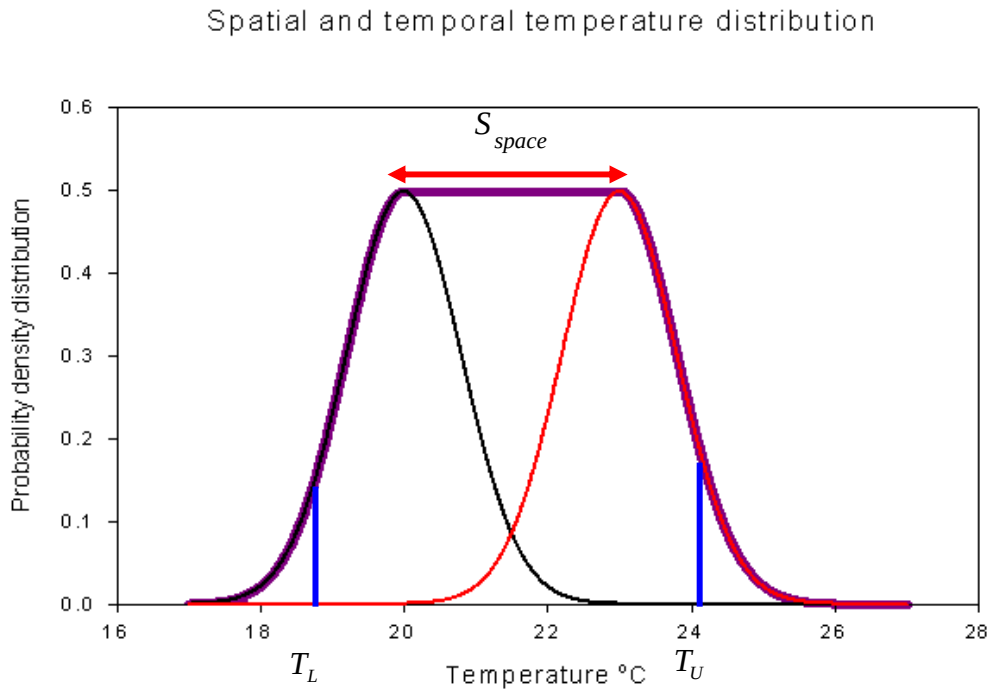

Figure 3.3: Spatial and temporal distribution envelope

In Figure 3.3, the T_L and T_U represent the higher temperature limit of air temperature of the zone having the design thermal comfort condition to the occupant. The value of the T_L and T_U can be found in thermal comfort standard. The area beyond the temperature range can be calculated by the following equations:

Lower area: $$\frac{1}{\sigma_L\sqrt{2\pi}}\int_{T_L}^{\mu_L} e^{[-\frac{1}{2}\left[\frac{x-\mu_L}{\sigma_L}\right]^2]}\,dx = \frac{1-PPD}{2} \tag{3.1}$$

Upper area: $$\frac{1}{\sigma_U\sqrt{2\pi}}\int_{\mu_U}^{T_U} e^{[-\frac{1}{2}\left[\frac{x-\mu_U}{\sigma_U}\right]^2]}\,dx = \frac{1-PPD}{2} \tag{3.2}$$

The ensemble envelop could be used to determine and predict the predicted percentage of dissatisfaction level calculated by computing the percentage of area out of the temperature range under the distribution function. The level could be compared with the desired thermal comfort criteria.

As shown in Figure 3.3, the S_{Space} is the range of the temperature variation within the thermal comfort and is also the control range of the thermostat. In reality, the variable S_{Space} is a function of the investment on the thermostat selection.

The spatial distribution is a function of the supply air circulation. Therefore, it can be fine-tuned by the adjustment of air diffusers. The performance in this respect is indexed by ADPI (air diffusion performance index). On the other hand, the extent of movement of the distribution function is measured by the temperature swing, a function of the performance of the thermostat control system.

The satisfaction with thermal comfort in an office would depend on this envelope falling within the range of temperature acceptance of the office. This is a function of both ADPI and control swing. However, in practice the two indices are dealt with separately. ADPI is the set criteria at design. Temperature swing depends on the willingness to invest. This segregation of performance is a consequence of improper understanding of the thermal comfort and the embedded dynamic nature of the distribution functions of temperature.

The situation is even more complicated at an individual work station as the thermal sensation of each individual is different. This scenario is further complicated by the company culture of dress codes. In all the thermal comfort parameters, I_{cl}, the insulation factor of clothing, is a parameter which is not controllable by the design engineers. In fact, in many thermal comfort surveys, especially when many air-conditioned spaces are involved, the distribution of the thermal comfort parameters is interpreted as an ensemble. In this section, this erroneous interpretation has already been indicated. The I_{cl} issue is particularly serious if omitted in the interpretation of the results. In fact, it is these misunderstandings that led to the very unsuccessful thermal comfort control in air-conditioned offices in Hong Kong. Therefore, the impact of I_{cl} on thermal comfort model is worth discussing in more detail in Chapter 4.

Figure 3.2 shows the distribution function of PPD against T_o. The same distribution function is shown against T_a in Figure 3.6.

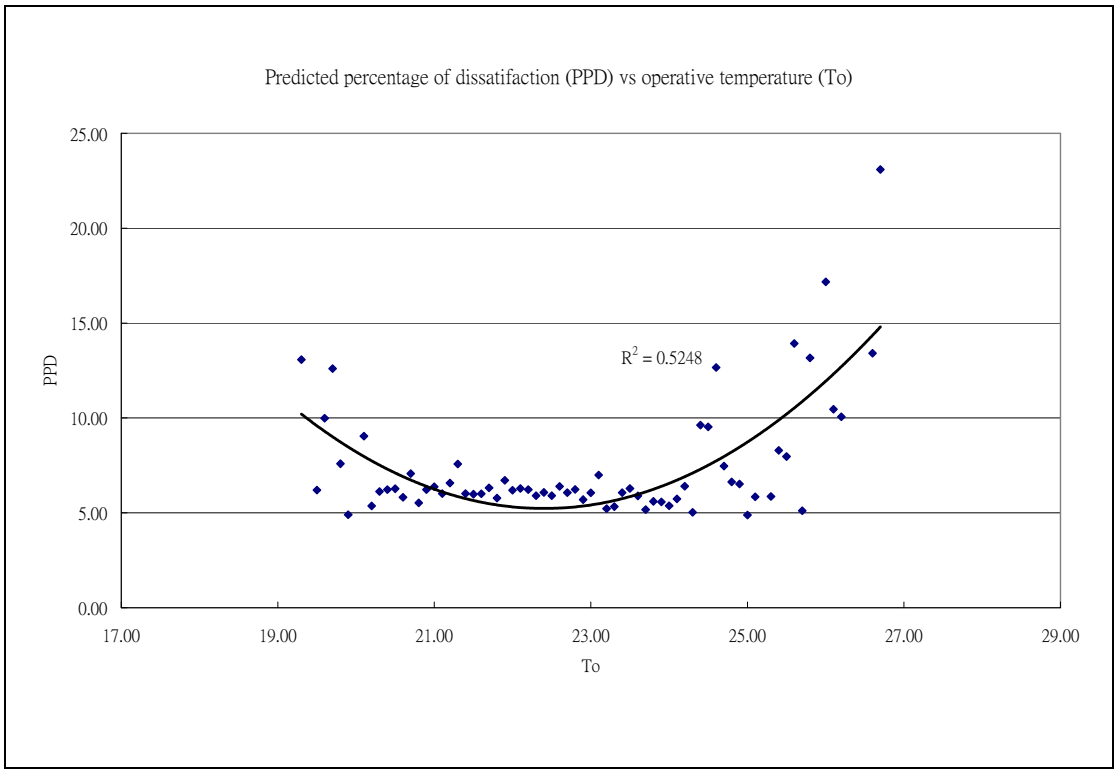

Figure 3.2 Relationship of percentage of dissatisfaction with the operative temperature

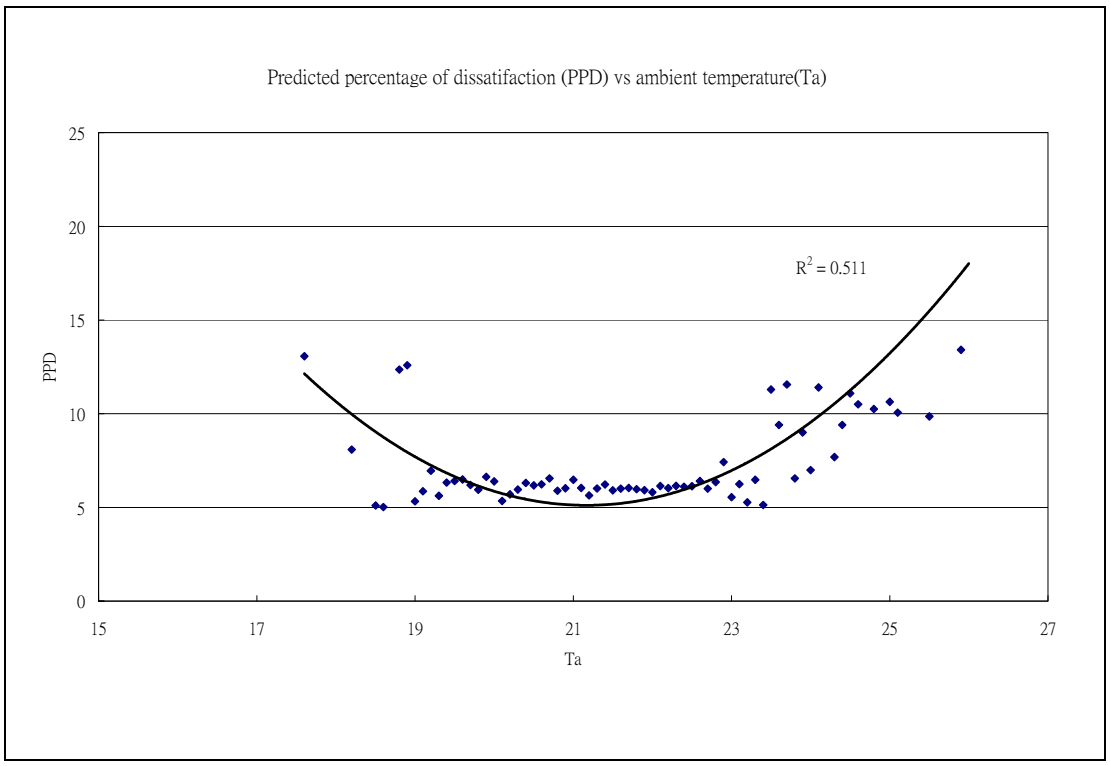

Figure 3.3 Relationship of percentage of dissatisfaction with the ambient temperature

The PPD is best set by the investor based on his willingness to buy quality materials to meet his potential clients' expectations. If 10% PPD is the normal target, at first hand, the choice of range of T_o would be between 19.5 and 25.5°C and T_a will be between 18.5 and 24°C. Figures 3.4 and 3.5 are the corresponding ranges of acceptable T_o and T_a at different PPD.

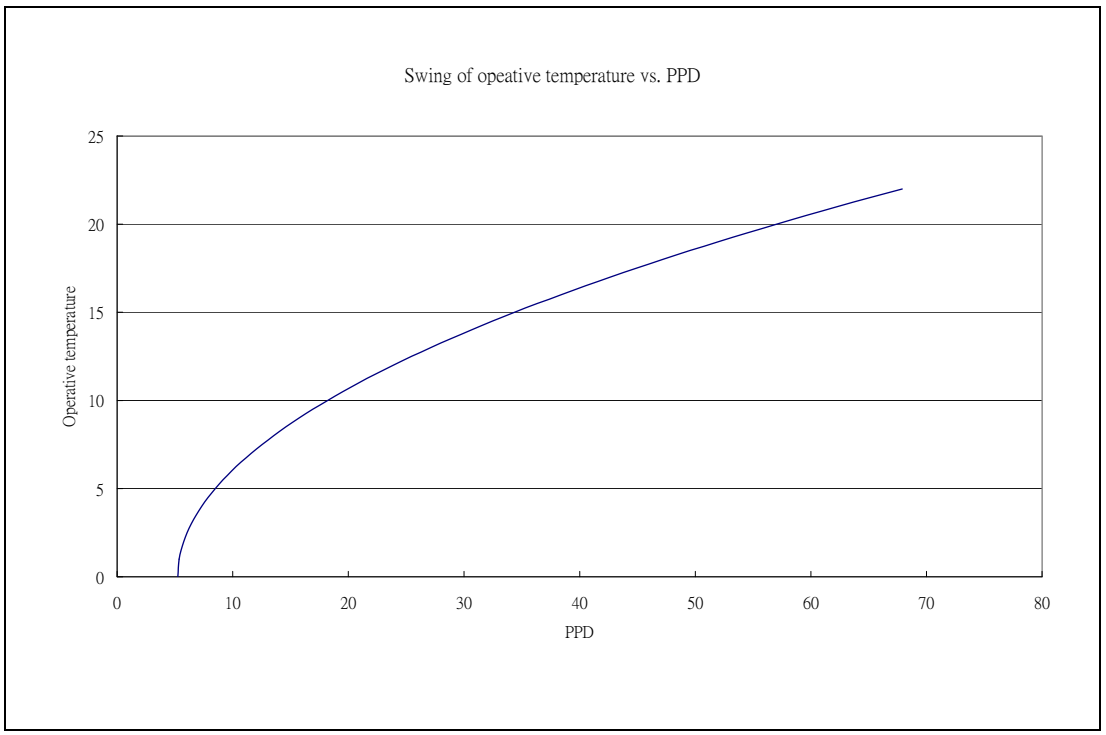

Figure 3.4: Swing of operative temperature against predicted percentage of dissatisfaction

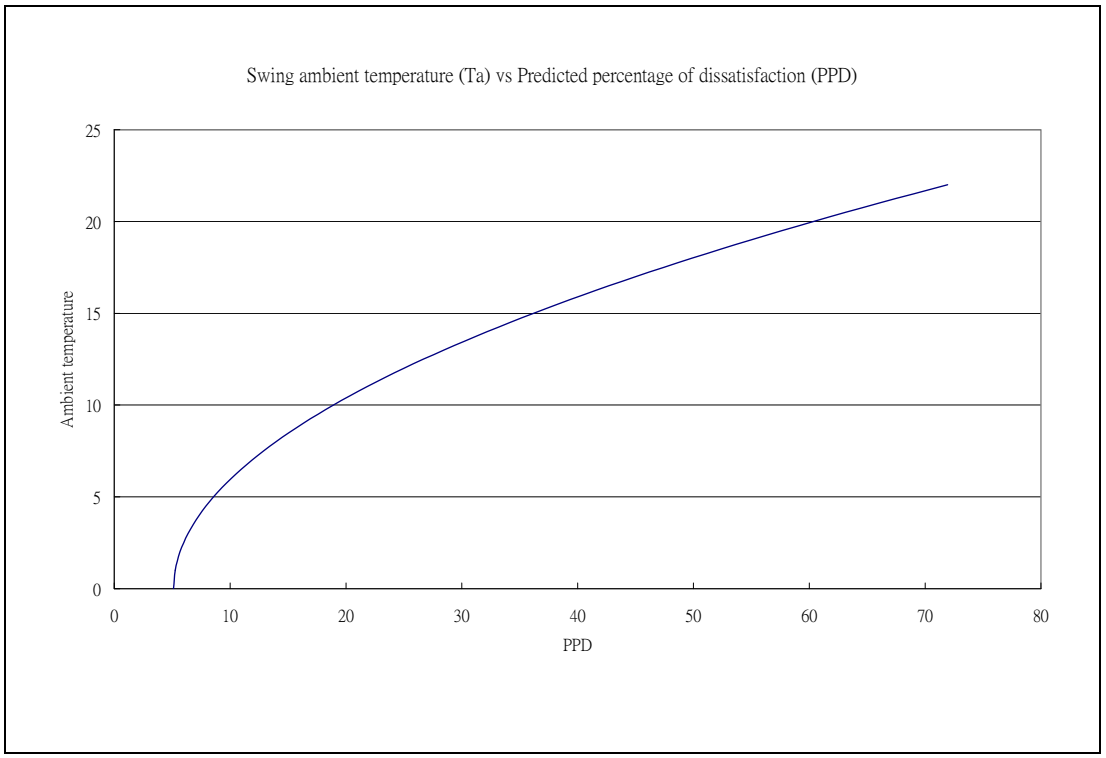

Figure 3.5: Swing of ambient temperature against predicted percentage of dissatisfaction

This wider temperature range of acceptance as compared to Fanger's thermal comfort model was ascribed to the differences between real site measurements and chamber tests (Chan et al., 1998). However, it is shown in Section 4.6 of Chapter 4 that it is the ensemble of clothing which drowns the impact of colthing to PPD. Hence, the interpretation of the ensemble is seriously erroneous in thermal comfort control. As further discussed in Chapter 4, to an individual, the range of temperature acceptance would only be 2°C. In this sense, both the ADPI and swing would have to be tightened up. The former is a function of the thermal load distribution and supply air circulation. The latter relates to the total thermostat control system. If the combined spatial and temporal envelope is to be limited to 2°C, the cost of such an operation can be very high. It is no wonder that even though the thermal comfort model has been well developed for several decades, thermal comfort remains the most dissatisfied quality among the four basic thermal comfort qualifiers, namely thermal comfort, indoor air quality comfort, visual comfort and aural comfort.

After the elaborative discussion on impact of clothing on thermal comfort in Chapter 4, Chapter 5 and onward will describe the details of an innovative harmonious fan coil system design attempting to solve the above-mentioned problem other than achieving the aim for sustainable thermal comfort.

CHAPTER 4: PREFERENCE OF IN-OFFICE AIR TEMPERATURE IN AIR-CONDITIONED OFFICES

4.1 Neutral Temperature and Preferred Temperature of the Hong Kong Office Users

4.1.1 Neutral and preferred temperatures

In the large scale in-office survey described in Chapter 3, it has already shown that only 34.9% of the surveyed workstations in Hong Kong office are within the thermal comfort zone. The neutral temperature was found to be 23.5 °C. The preferred temperature was found to be 22.5 °C. These temperatures were determined from the ensemble of the sample. This chapter attempts to normalize the preferred temperature of the Hong Kong office users by clo values derived from their clothing. This will then help infer the 'thermal comfort culture' in air-conditioned offices. Two implications arise from this result. First, if the in-office spaces in Hong Kong are colder than other developed cities, what are the causes? Second, how we can possibly adjust Hong Kong office users' thermal sensations and make the city more sustainable?

4.1.2 The battle of 25.5°C

In 1973, the first post-Second World War energy crisis occurred. Fossil fuel costs rocketed sky high when the Middle East War triggered an oil embargo, and building

services engineers were under great pressure to conserve energy. Actions were taken by the Hong Kong Government, campaigning for citizens to raise the indoor air temperature in air-conditioned spaces to 25.5°C (or 78°F), which is in the high end of the thermal comfort zone designated by ASHRAE Standard 55-1992. However, thermal comfort sensation is not a function of air temperature alone. The campaign was not successful as this temperature requirement was not legally enforced, and the raise in temperature brought no benefit to tenants whose rent covered air-conditioning service. This campaign was soon forgotten when high fuel costs were eased subsequent to peace in the Middle East.

In Hong Kong, there are three typical design criteria of indoor air temperature in air-conditioned offices, for three types of users. The normal temperature is 24°C. For Grade A buildings, owners maintain temperatures at 23.3°C to reduce high temperature complaints. In all Government projects, the specification calls for 25.5°C to be consistent to the Government's effort in conserving energy.

In the 1980s, most buildings featured intelligent service systems for energy management. In the 1990s, the concept of a healthy building became a main concern. Due to the local humid climate and reasons analyzed in the later sections in this chapter, buildings, including Government structures, were not enthusiastic about setting air temperatures to 25.5°C during this period.

In the mid-2000s, environmental threats due to global warming were imminent. Raising temperatures to 25.5°C became a pertinent issue once again. This time, environmental groups such as Friends of the Earth have joined the campaign, giving it more leverage. Unfortunately, without associated protocol in achieving this goal, and given Hong Kong's social culture, local year-round weather conditions as well

as other thermal comfort parameters, this induced even more reluctance from the building industry.

By understanding the preferred temperature normalized to the clo values of the Hong Kong people, control measures can be developed on sustaining thermal comfort with escalated temperature. This chapter concentrates on the analysis of the effect of clo on preferred temperature.

4.2 General discussion of clo

The general picture of the indoor climatic condition can be showed in Figure 4.1. This shows that only 34.9% of the indoor climate is within the thermal comfort shown according to ASHRAE Standard 55 - 1992. 61.6% of the sample point are having a lower temperature then the zone.

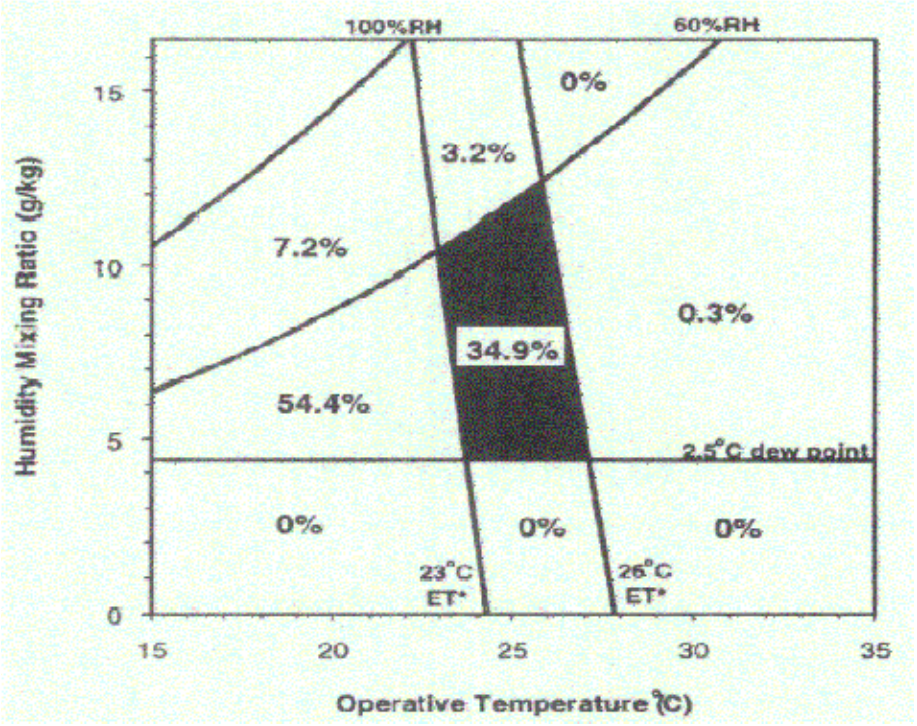

Figure 4.1: Distribution of the indoor climatic measurement of the large database (Chan et al, 1998)

Clo is an index to represent the insulation factor of the heat transfer between one's skin and the thermal environment. In the ASHRAE handbook, more then 13 equations involving the clothing parameters in assessment of thermal comfort indices. Due to the complicated assessment of these values with clo, in this research project, the impact of clo to the indoor thermal comfort environment is evaluated by the extensive survey as described in Chapter 3. In practice, indoor thermal environment is almost exclusively controlled by regulating indoor air temperature. As shown in the survey, relative humidity can be kept between 50% to 60% ,air velocity can be kept between 0.1 m/s to 0.15 m/s. The use of indoor air temperature (t_a) is more realistic in reflecting the thermal environmental problems in Hong Kong offices.

4.3 Methodology in clo survey in Hong Kong Offices

Clo values of various clothing are defined in ASHRAE Standard 55 - 2004. In the survey, a comprehensive list of clothing items was listed. The clothing conditions for each surveyed subject were recorded in the form. The overall clo value for each subject was evaluated according to ASHRAE Standard 2005. The distribution of the of clo values in the summer survey is shown in Figure 4.2.

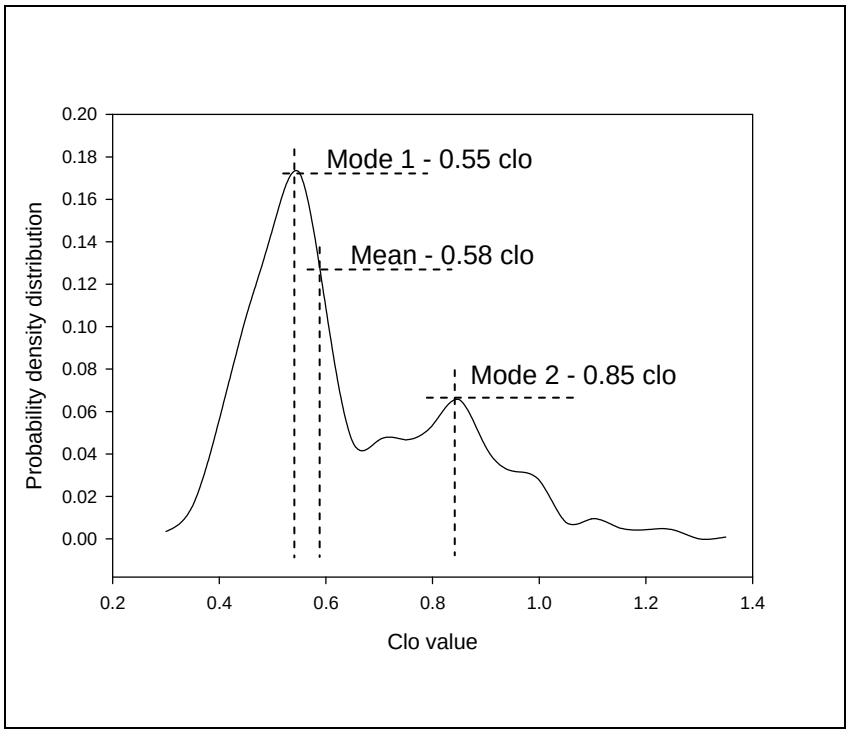

Figure 4.2: Distribution of clothing insulation for office occupants in summer in Hong Kong

Two peaks of clo values were found at 0.55 and 0.85. The former correspond to the usual indoor dressing code in Hong Kong offices. The latter is not surprising as indoor air temperatures are on the cold side, as found in this same survey

(refer to Table 3.5). Another reason for a higher clo value is due to the company culture, which results in a strict dressing code requiring ties and jackets for men, and suits and jackets for women.

User behavior is important in getting thermal comfort control right and clothing has an important factor on people's perception of the indoor environment. Normally, air temperature is set by the dress code of the office, keeping other factors unchanged. Or that the air temperature should be a function of the clo values. In Hong Kong air-conditioned offices, the higher clo values are partly due to the company culture necessitating more restrictive clothing. However, it was observed that this clo values distribution is important in two aspects:

i. The dress culture in Hong Kong offices is more formal than that of its neighbouring countries, such as mainland China, Taiwan, Singapore, Malaysia, Indonesia and even Japan during the summer. For example, the Japanese Government encourages employees to dress casually in Government campaigns called "CoolBiz" for indoor temperatures to be maintained at 28°C (CoolBiz, 2006). In mainland China, the indoor air-conditioned spaces are kept at 26°C as mandated by law (GVBchina, 2005). As a result of these countries' efforts, executives and administrators are very casually dressed. Hong Kong's air-conditioner users are essentially using energy to cool off under their layers of clothing.

ii. Normally, the clo dictates the preferred indoor air temperature for setting PMV. However, due to the uncontrollable air temperature at low values, air-conditioned office users have to put on jackets to accommodate to the cooler temperatures. This not only squanders energy, but renders thermal conditions inside air-conditioned offices very unhealthy. This health impact is particularly deleterious when a perspiring individual enters a 'cold' office on a hot summer day. The first cold draft perhaps instantly eases the discomfort from the heat. However, 10°C (e.g. 30°C against 20°C) temperature difference will weaken the immunity system and cause sickness according to the wise of traditional Chinese medical theory (DMA, 2005). The lowered indoor humidity will cause increased evaporation of sweat, inducing an even higher rate of heat loss. Finally, sweat-soaked clothing will cling to the chest and back, causing an uncomfortable and unhealthy situation which further lowers the immunity level, making the individual more prone to opportunistic diseases. This situation is commonly referred to as 'air-conditioning sickness'.

4.4 Normalization of preferred temperature by clo

In Chan et al. analysis of the temperature preferences of Hong Kong users, the preferred value was found from a McIntyre-type question (McIntyre , 1980) in the questionnaire. The question provided three choices:

- Prefer warmer
- No change
- Prefer cooler.

The results from Chan et al (1998) study shown in Figure 4.3 illustrating the preferred temperature of Hong Kong people in summer condition. Considering the data set as an ensemble without identifying influencing factors, the preferred temperature is 22.5°C which is 1°C lower than the neutral temperature found from regressing the thermal sensation vote against T_o which is shown in Figure 4.3 (Chan et al., 1998).

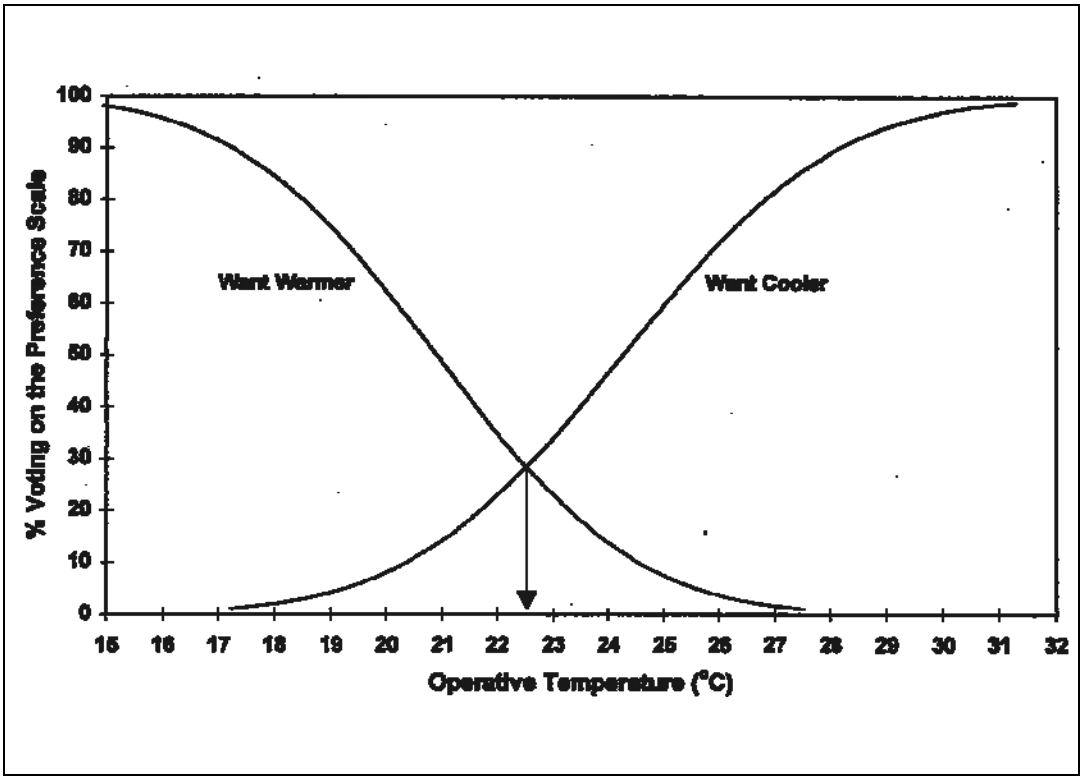

Figure 4.3: Probit models shows the preferred temperature on Hong Kong people (Chan et al., 1998)

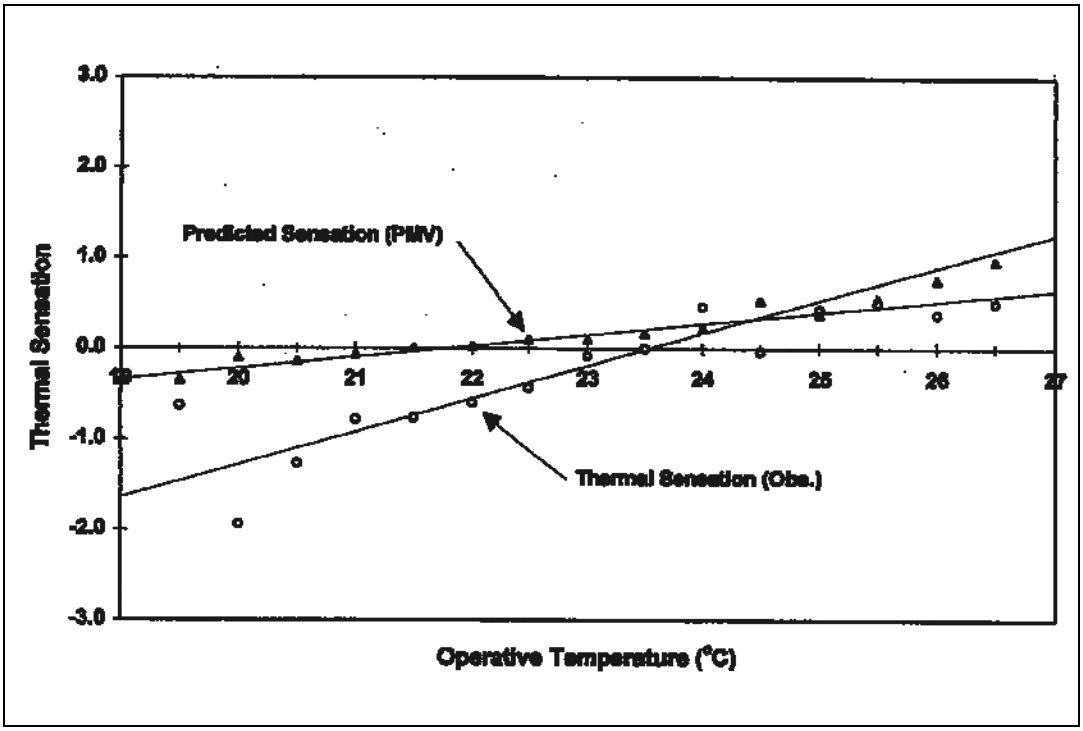

Figure 4.4: Mean thermal sensation votes compared to means predicted thermal sensation (Chan et al., 1998)

The survey results seem to imply that while people are at thermal mental balance with the environment, if given a choice, Hong Kong indoor users in an air-conditioned environment would prefer the temperature to be 1 °C lower than what has been observed as 'neutral'.

To investigate this point further, the database was binned with air temperature. Air temperature was chosen because this finding was used as an educational tool to campaign for temperature increase in offices. To obtain the preferred air temperature at different clo values, the data set was binned with 1^0C air temperature increment; the weighted average of clo values for the group preferred warmer environments and the group that preferred cooler were then found. The results are plotted in Figure 4.5. The derived linear regression equation is:

$$T_a = -16.672 I_{cl} + 32.289 \quad (4.1)$$

where T_a = indoor air temperature

I_{cl} = clothing value (ASHRAE 55, ISO 7730)

The correlation coefficient (R^2 = 0.9589) indicates quite a significant correlation with observations in the survey.

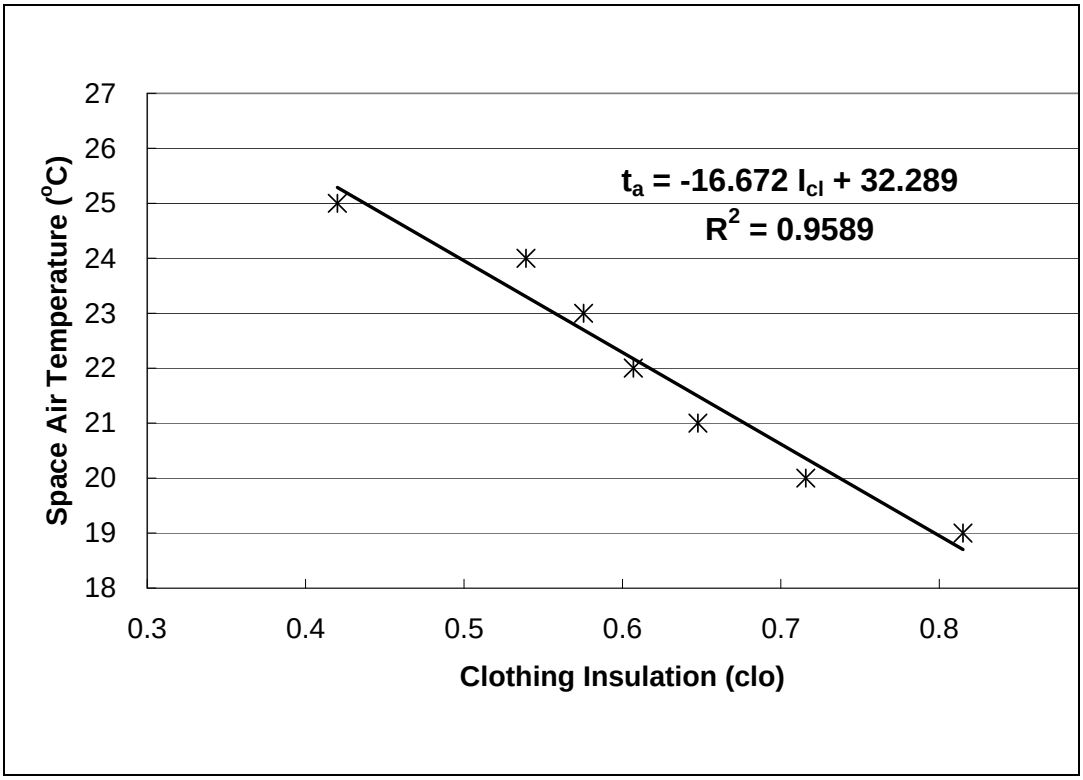

Figure 4.5: Comfortable air temperatures for occupants with different clothing insulation.

This result is significant that this is the preferred temperature at a specified I_{cl} in air-conditioned Hong Kong offices. The significance of this curve resolves the disputes about setting a unique indoor air temperature set point. While policy-makers move for escalated temperatures, this observed preference of the

Hong Kong people should be taken seriously if company clothing culture is not altered. It also points out that if Hong Kong were to be more serious about energy saving in thermal comfort; reducing clothing insulation will be a very effective method.

4.4.1 Spoiled White Collars in Hong Kong

The air temperature versus clo plot reveals the differences in the perceptions of Hong Kong indoor users and internationally accepted thermal sensation. Figure 4.7 is the superposition of Figure 4.4 on the ASHRAE Thermal Comfort Model PMV family curves. The red horizontal line represents the people having a sedentary activity level, their optimal operative temperature versus clo value as suggested by ASHRAE standard. The blue line is from survey data with the same activity level as the blue line, but the preferred operative temperature against different clo value. It can be seen that the preference of the Hong Kong indoor people would be ‘sensed’ in the cooled side by the international ‘sensation’. For the same clo value, when compared to what international standard recommended, Hong Kong people tends to want a lower temperature.

The interpretation is more obvious when these points are superimposed on the activity curves (ASHRAE 55, ISO 7730) in Figure 4.6. At these preferred points, assuming PMV = 0, the preferred operative temperature at the same clothing conditions would satisfy workers at higher activity levels.

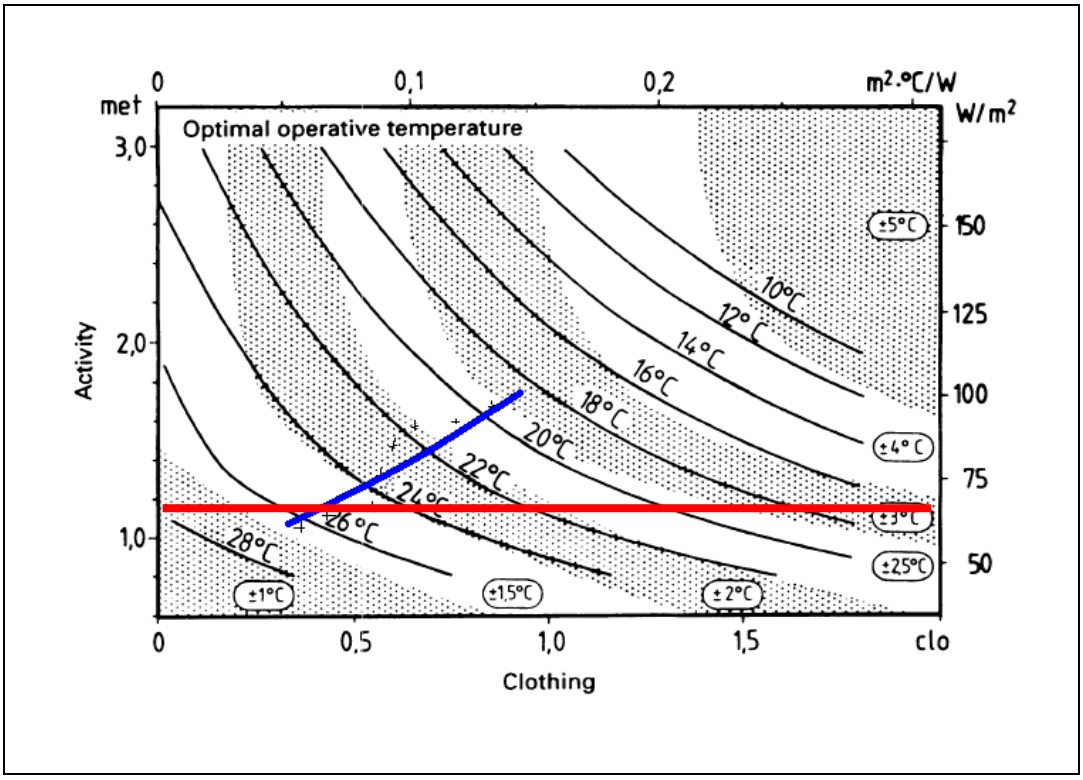

Figure 4.6: Optimal operative temperature (corresponding to PMV = 0) as a function of clothing and activity (ISO, 1995)

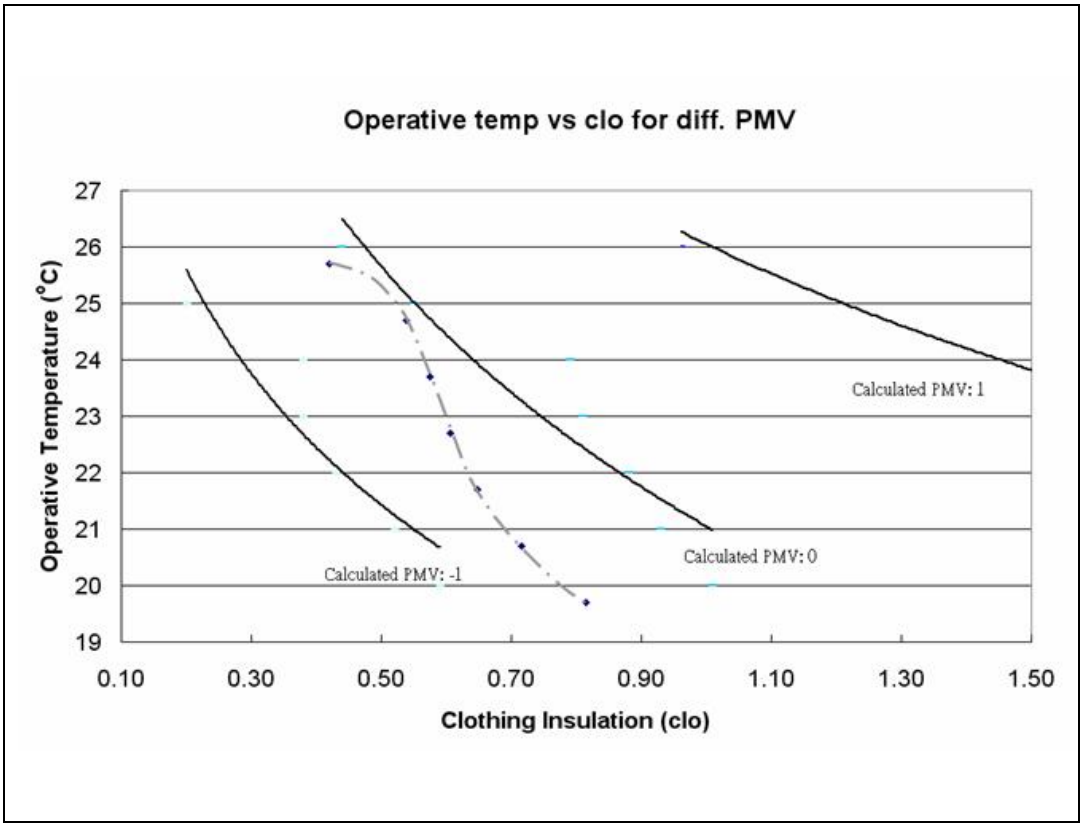

Figure 4.7: Operative Temperature vs I_{cl} in ASHRAE Standard 55 (2004)

Two hypotheses are proposed here to explain how Hong Kong white collar workers in air-conditioned offices are spoiled in preferred thermal comfort conditions.

1. Air-conditioned systems have been used extensively for indoor environmental quality comfort since the 1960s'. The Cantonese, the main ethnic group in Southern China, were amazed by the cooled air from air conditioning systems in the hot summer months and erroneously named it literally as 'cold air system'. Since then, the mental expectation in an air-conditioned space is 'cold' air accompanied by an expected cool sensation. In real official environment, Facility managers find fewer complaints with a cool environmental rather than a hot one. As there are no

incentives for an escalated temperature in the rental fee structure, there is a general quest by tenants for a cooler environment based on the psychological rationale of ‘more for the same maintenance cost’.

2. The negative feedback of a cooler environment dictates the clothing habits of air-conditioned space users. As decades pass, people get used to putting on a jacket during the hot summer months to feel thermally satisfied in the cooler environment.

The above two hypotheses can been simply explained by the “adaptive” theory by de Dear (1997). In short, the Hong Kong people are adapted to a relative colder environment where they have been exposed It is interesting that the occupants wear more cloths to intend to keep thermally comfortable balance and that the heavier clothing drive them to request for a lower climate condition. Meanwhile, facility manager tends to set a lower temperature in order to reduce complains from client.

In realizing the cost of the lower temperature preference, there is room for improvements to make the thermal environment more sustainable so that:

1. indoor office workers find the thermal environment more acceptable and become less prone to health problems;

2. it is feasible to escalate the control air temperature set point.

4.5 I_{cl} Equations

In Figure 4.4, the ensemble regression equation for vote vs To is

$$\text{Mean summer ASHRAE vote} = 0.3618 * T_o - 8.5154 \quad (4.2)$$

It can be observed in this graph that at higher temperatures, survey subjects tend to vote lower from the linear regression model and at lower temperature to vote higher from the regression model. Considering Figure 4.2, people with significantly different clo values can stay in the same office with the same thermal condition without obvious dissatisfaction (complaints). This complies with the usual practice in thermal comfort studies which deem votes between slightly warm (+1) and slightly cool (-1) to be acceptable. In other words, we can endure a range of 2°C within our sensation of thermal comfort. Therefore, the regression model and the observed points are more in line between 21.5 to 23.5°C. At lower temperatures, the subjects are expected to wear more. Hence, the regression model predicts a lower vote than observed. At the other temperature extreme, the subjects are expected to wear less. Hence the regression model predicts a higher vote than observed.

To test this hypothesis for linear correlation, the data points are binned by clo valves between 0.4 and 0.7, in 0.1 increments. The data groups were then binned with T_o and plotted in Figure 4.8. The ASHRAE Thermal Comfort model at constant clo values are also plotted in the same graph for comparison purposes.

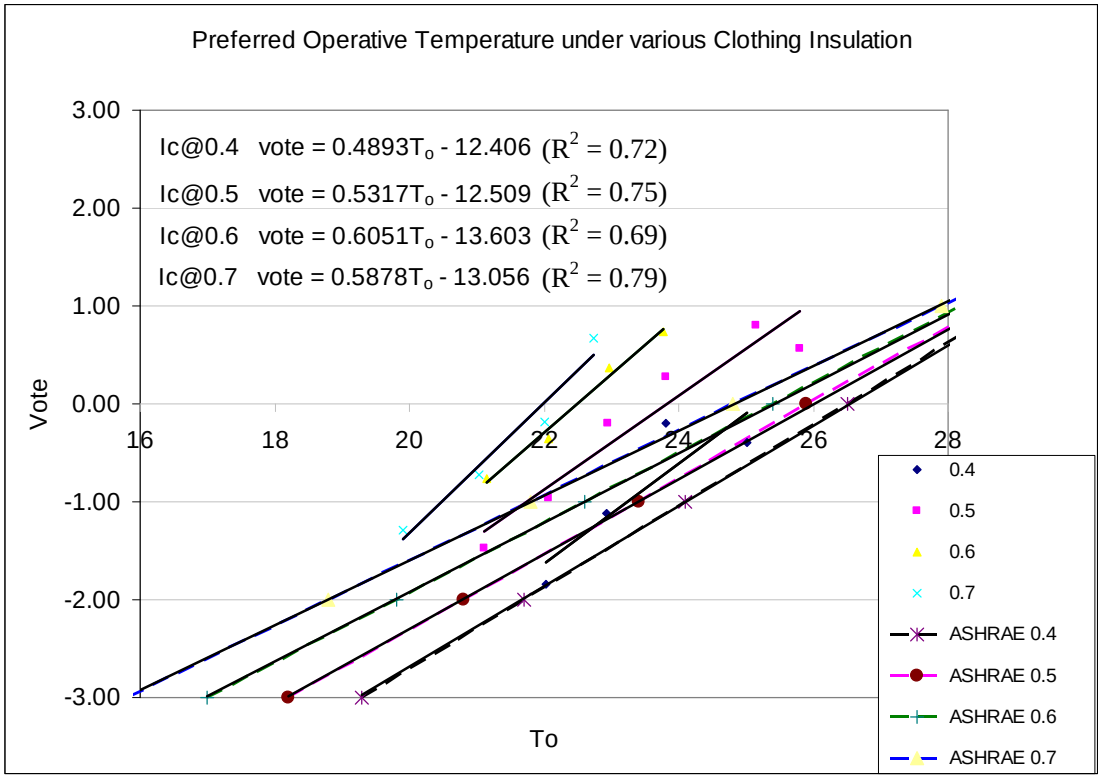

Figure 4.8: Preferred operative temperature under various clothing insulation

Two-tailed test is applied to test the hypothesis that x (T_o) contributes no information for the prediction of y (vote) using the straight line model against the alternative that the two variables are at least linearly related.

Four I_{cl} equations are regressed with 99% confidence interval:

I_{cl} at 0.4,

$$\text{Vote} = 0.4893\ T_o - 12.406 \qquad (4.3)$$

I_{cl} at 0.5,

$$\text{Vote} = 0.5317\ T_o - 12.509 \qquad (4.4)$$

I_{cl} at 0.6,

$$\text{Vote} = 0.6051\ T_o - 13.603 \qquad (4.5)$$

I_{cl} at 0.7,

$$\text{Vote} = 0.5878\ T_o - 13.056 \qquad (4.6)$$

Neutral temperature at different clo values are shown in Table 4.2

I_{cl} (clo)	**Neutral temperature T_o °C**	**Preferred temp T_o °C**	**PMV for Preferred temp. using derived I_{cl} equations**
0.4	25.2	26.1	0.46
0.5	23.8	24.4	0.27
0.6	22.5	22.7	0.15
0.7	22.0	21.1	-0.62

Table 4.2: Neutral temperature at different clo values

The neutral temperature as predicted by the I_{cl} equations and the preferred temperature predicted by the linear regression are consistent in the sense that the PMV are within the comfort range for 90% satisfaction (ASHRAE Standard 55). The consistency is expected because they are generated from the same surveyed data. It is also consistent with the claim that Hong Kong white collar workers (office workers) are ‘spoiled’ to the cool side as compared with international standard.

The I_{cl} equations are more useful in setting the optimum operative temperature without changing the company culture, which is a business decision. The key points are:

1. The operative temperature should aim to be compatible with the dress code of the company.

2. The ‘sensation’ can be adjusted to the warmer side, given proper advice in thermal comfort education and the promotion of environmental ethics.

To illustrate the usefulness of these conclusions, these results are used to explain to the public the inconsistent temperature adjustment in banks.

4.6 Impact of I_{cl} on PPD

Section 3.4 discusses the usual erroneous interpretation of the ensemble in the large scale survey. However, as in previous sections in this Chapter, the huge data base provides data on more detail study of human responses with respect to clothing. In the following sections, all the PPD are analyzed based on the Chan et al. surveyed data and the clo value indicates the clothing insulation of the occupant only, excluding the insulation effect of the furniture. An additional 0.1-0.15 clo value has to be added to I_{cl} when considering a chair or other furniture as an insulation..

The PPD curves for different I_{cl} bin groups between 0.4 to 1.0 are superimposed on the PPD ensemble curve in Figure 4.9. It is seen that the temperature ranges of acceptance are much smaller and are more in compliance to Fanger’s prediction.

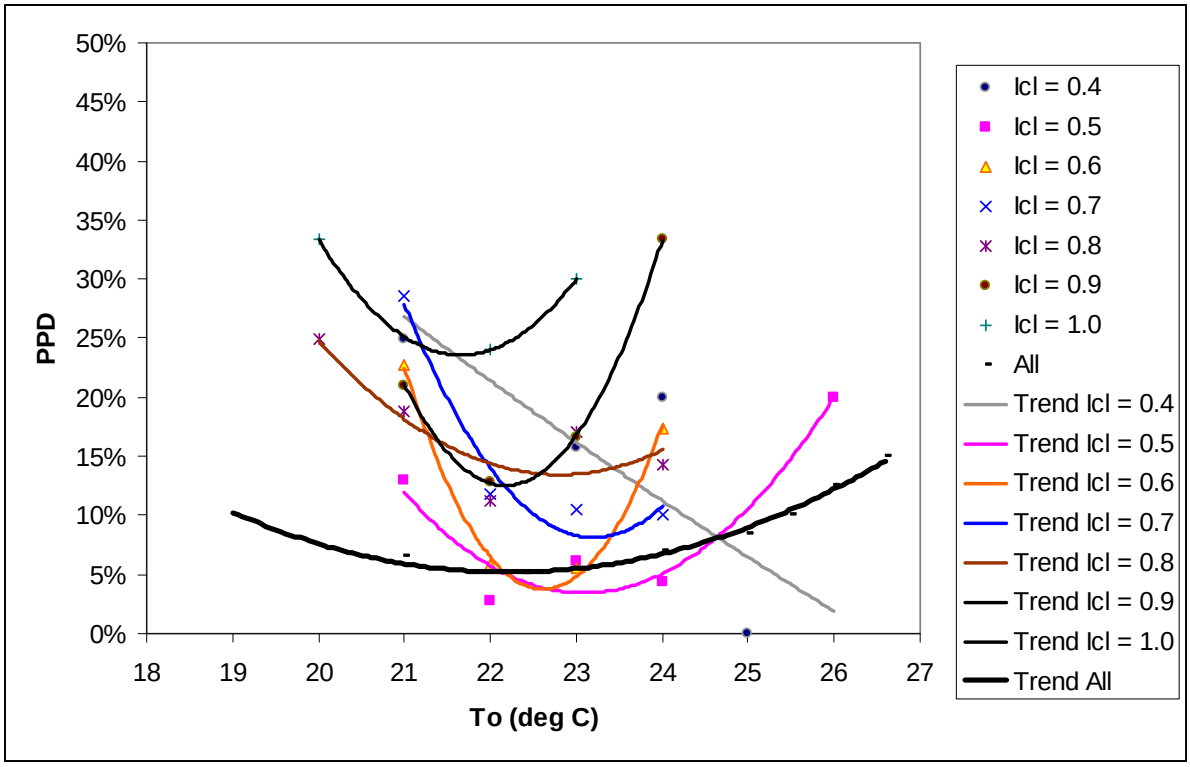

Figure 4.9: PPD against T_o at different I_{cl} as Compare to the Ensemble Regression.

The relationship between the PPD and To with different clo value are regressed and the result is shown in the following tables. Except clothing insulation with 0.4, other are fitted by a quadratic equation and the R square value is more then 0.77, which shows that with different value of clothing insulation, the pattern of the PPD to operative temperature is similar.

$$PPD = aT_o^{\,2} + bT_o + c \qquad (4.7)$$

Icl	a	b	c	R^2	n
0.5	0.0195	-0.9009	10.432	0.9172	35
0.6	0.0721	-3.2611	36.909	0.9957	212
0.7	0.0407	-1.8885	21.988	0.9539	139
0.8	0.0144	-0.6586	7.6434	0.7765	32
0.9	0.0622	-2.7604	30.729	0.999	33
1	0.0356	-1.54	16.911	1	24
All	0.0087	-0.4146	5.0261	0.6205	475

Table 4.3: Equations for PPD and T_o in different I_{cl}

For I_{cl} = 0.4, another pattern is found:

$$PPD = -1.1676 Ln(T_o) + 3.8231 T_o$$

(4.8)

With R^2 = 0.6511.

The different in the pattern can be explained by the number of samples for the I_{cl} =0.4. This value represents a very little clothing and it is not a normal practice in Hong Kong for people wearing so little in office.

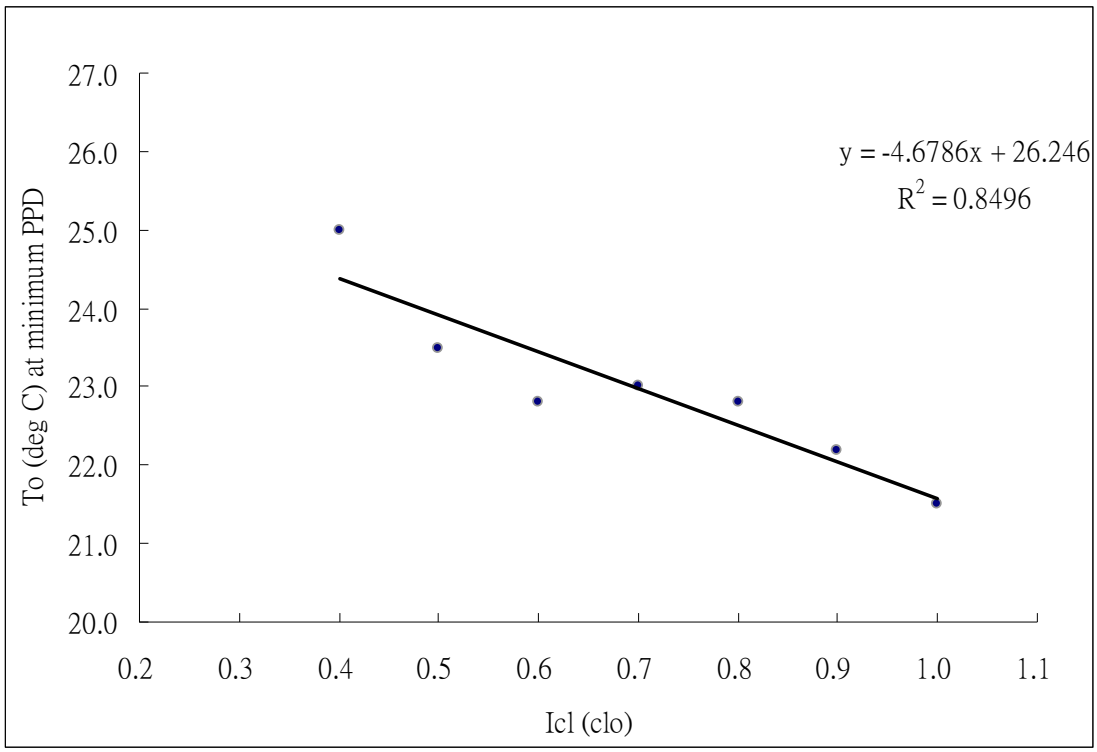

Figure 4.10: Impact of I_{cl} on T_o ºC at minimum PPD

Figure 4.10 further reveals that I_{cl} has an impact on T_o at minimum PPD. These values are in close agreement with Table 4.2 for neutral temperatures generated from the I_{cl} equations.

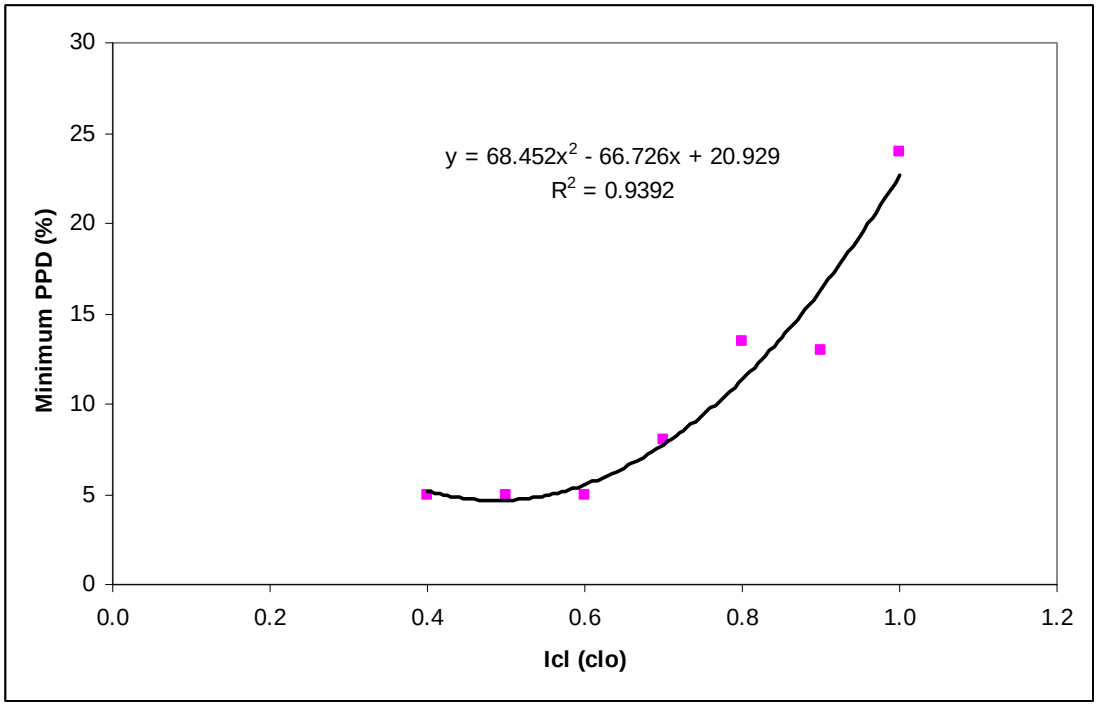

Figure 4.11: Minimum PPD (%) versus I_{cl}

Another interesting observation of the impact of clothing on PPD is shown in Figure 4.11. The minimum PPD increases quadratically with I_{cl}. The high correlation coefficient of 0.94 is surprising. In this graph, any PPD below 5% is set to 5% in accordance to Fanger's PPD and PMV model. It shows that in air-conditioned office in a temperate region, it is difficult to maintain a low PPD with high insulation factor of the clothes. It might be explained analytically by the heat transfer model of human being under thick clothes. It could be the time lag, inertia of the clothes and more likely, the enclosure of the main veins around the neck, under the arms and between thighs which makes the heat release much more difficult and hence causing discomfort even if the ambient temperature is kept low.

It is therefore obvious that I_{cl} plays an important role in thermal comfort control. It is also overwhelming to see that formal dresses in air-conditioned offices are not desirable and that the associate discomfort is difficult to release. The most optimum ranges of I_{cl} is between 0.4 to 0.6 which corresponds to light dressing of short sleeve shirts with open collar with at most long trousers.

4.7 A Survey of the Bank Air Temperature and of I_{cl} Bank Staff

4.7.1 Thermal comfort conditions in banks

On the 30th of August 2007, Green Sense, a local environmental lobby, held a press conference criticizing local banks for adjusting air temperatures below the currently Government recommended level of 25.5°C in response to the global quest of energy conservation.

Tables 4.4 and 4.5 contain temperature data recorded in summer at the banks in question.

At the same time, the observation of the I_{cl} of the uniform of 0.8-1.0. Extrapolating the I_{cl} equations, the temperatures at East Asia Bank and Hangseng Bank would be beyond the slightly cool PMV while the rest seems to fit to the uniforms. However, all temperatures are much too cool for walk-in customers with an I_{cl} of 0.4 at PMV between -1.2 and -3.

Bank	Number of branches	Average T_a°C
Hong Kong and Shanghai Bank	12	23.2
East Asia Bank	12	22.5
Chartered Bank	11	23.1
Hangseng Bank	13	22.7
Bank of China	20	23.0
	Total:68	*Average: 22.9*

Table 4.4: Survey of Air Temperature in Banks in Hong Kong carried in summer 2007 (SCMP, 2007)

Bank	Average T_a°C
Hong Kong Bank	21.1
East Asia Bank	19.8
Chartered Bank	22.8
Hangseng Bank	18.8
Bank of China (Hong Kong)	21.9
DBS Bank	20.8
Wing Lung Bank	22.7

Table 4.5: Survey of Air Temperature in Seven Banks in Wan Chai District carried in summer 2007 (Green Sense, 2007)

This scenario points out another dilemma in thermal comfort control, especially in public places. For people coming in and out of air-conditioned spaces frequently, the current practice of thermal comfort control in Hong Kong will induce discomfort as well as possible sickness when sweating occurs in outdoor

and suddenly dried up in indoor cold environment.

4.7.2 Strategy proposed in the Press Conference

Using the analysis on impact of I_{cl} on thermal comfort discussed in earlier sections, the following points were made clear to the public in the conference:

i. the researchers have no intention of revoking the clothing culture of the banks in this project;

ii. the banks should be consistent in their pledge of environmental friendliness, and the clothing style the management imposed on their staff, is wasting energy in cooling clothing;

iii. the banks should control the thermal environment so that it is suitable to their staff and clients; the I_{cl} of all expected users are important;

iv. the public are educated to expect thermal comfort rather than cold circulating air, and the term for air-conditioning systems should be reinstated. In doing so, the public should conceive ‘slightly warm’ as acceptable thermal comfort sensation;

v. everyone has an environmental obligation to conserve energy to reduce the impact on global warming, and the Hong Kong people should align with the world with an optimum thermal comfort setting.

A strategic 3-step protocol for more sustainable thermal comfort operation in air-conditioned office is proposed as follows:

Step 1.

Setting of the optimum indoor air temperature –

This is done by understanding the company culture in terms of a demographic analysis for all expected users in the premises, and a survey of the physical environmental conditions. The set of I_{cl} equations are used as guidelines. The optimum air temperature for office set point is then determined taking into account other thermal comfort parameters such as metabolic rate, radiant temperature, relative humidity, air speed, air turbulence intensity and expected range of PMV for the intended percentage of dissatisfaction.

Step 2.

Adjustment of clothing code –

If a company is serious about sustainable thermal comfort, the management can redesign uniforms or encourage staff to wear proper but simple (neat casual) uniforms or clothing. All staff can also be educated with the right thermal comfort sensation. The former has been proven that the temperature can be adjusted 2°C higher. The latter can be another 2°C up. This brings the temperature back to the optimum target of 26°C, which is in agreement of the ‘Blue Sky’ campaign by the Hong Kong Government of Special Administration Region.

Step 3.

System Enhancement.

In Chapter 3, it has already demonstrated that due to spatial and temporal distributions, the operative temperature envelope falls out of the acceptable range at the intended predicted percentage of dissatisfaction. Modifying the temperature control system will reduce the swing. Recommissioning (re-balance) the air distribution system will reduce the spread (higher ADPI). Both actions will modify the distribution envelope and bring it within the range of acceptance.

Further enhancement can be attained by replacing partially cooling by chilled water energy with cooling by fan energy, more commonly referred to as a fan assisted air-conditioning system. This is in response to a call by a local authority, the Electrical and Mechanical Engineering Department. Literature survey shows that this approach is possible. Recent research also supports the fact that air speed fluctuation enhances thermal comfort. This approach has been taken up and put into application trials. The Chapters that follow describes this in detail and analyses its feasibility.

4.7.3 The Devil's Advocate Argument for Escalating Indoor Temperature

The campaign by EMSD to set the indoor air temperature to 25.5°C since the energy crisis in 1973 has been a failure. It started to gain some success when petrol prices rose precipitously in 2006, and when global warming impacts became obvious. However, many engineers are still very skeptical because they bear the responsibility of righting these problems, as well as the brunt of complaints.

The main objections are:

i. If 25.5°C is taken with a spread of ±1.5°C, there are bound to be places with air temperatures of 27°C, which appears to be too high. In fact, many engineers neglect the fact that the operative temperature can be another half degree higher.

ii. The relative humidity would increase with reduction in cooling.

iii. The bacteria and fungi counts will increase.

Points (i) has been dealt with in Chapter 3. Point (ii) will be dealt with by tightening the space to reduce infiltration and will be further discussed in later chapter. Point (iii) has no ground with an increment of a few degrees. This is also supported by recent survey in the University campus carried by Chan et al. that the relative humidity (45 - 70%) and temperature (21 – 27^{o}C) have no significant correlation with total bacteria and fungi counts. (Figures 4.12 and 4.13)

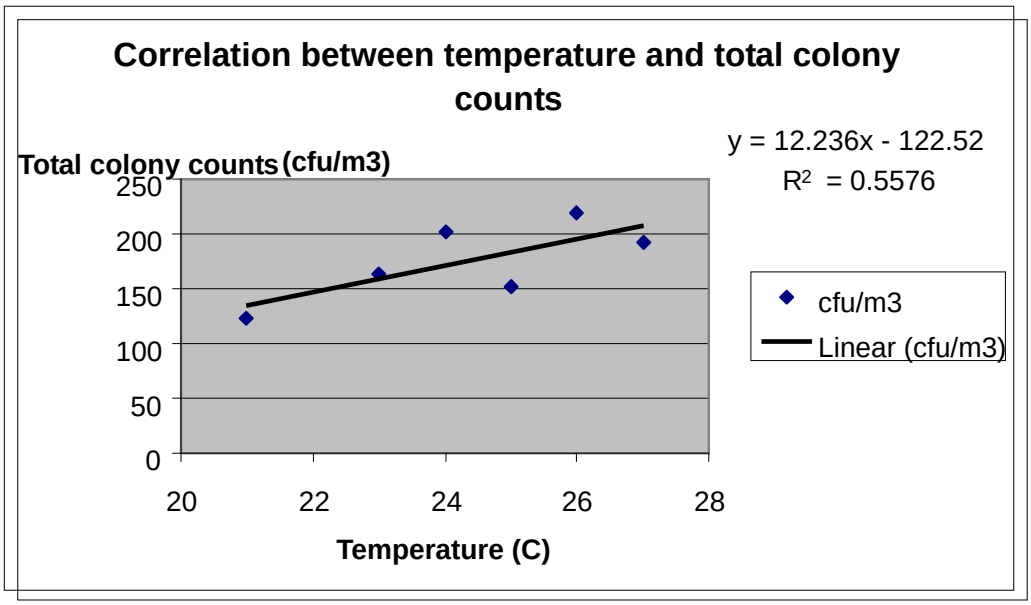

Figure 4.12: Correlation between temperature and total colony counts (Chan et al., 2007)

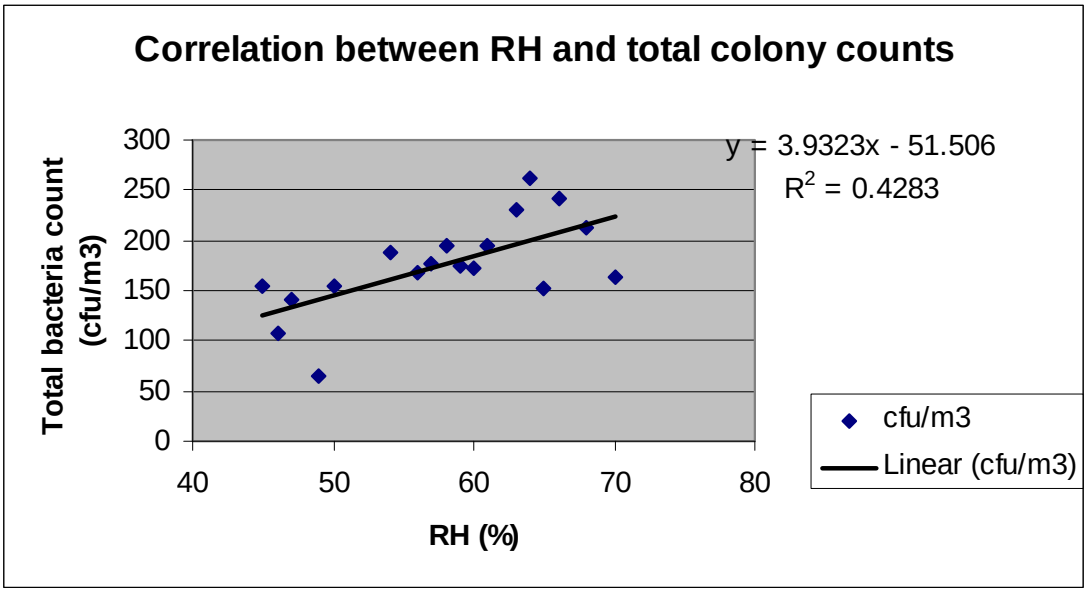

Figure 4.13: Correlation between relative humidity and total colony counts (Chan et al., 2007)

4.8 Summary

I_{cl} is found to have great impact in influencing thermal comfort control, which is very much ignored in practice of thermal comfort design. It causes a dilemma in controlling the indoor thermal comfort environment in air-conditioning offices. Also, due to an error in the initial perception of air-conditioning systems in the 1960s, indoor air temperatures are set erroneously low. The findings in the large scale survey by Chan et al. that Hong Kong is overcooled can now be explained.

The survey of the air temperature in banks by Green Sense agreed with the above hypothesis. A formal dressing code in the banks is perceived to give clients a formal and reliable reception. Unfortunately, clients are also exposed to an environment that lowers their immune system. This is due to an ignorance of a more in-depth understanding of the thermal comfort model. The analysis in this Chapter provides clues to solve the problem.

The 3-step protocol for sustainable thermal comfort setting and operation is a breakthrough for optimum thermal comfort control. It opens up the possibility of studies of system support and enhanced thermal comfort which will be discussed in the following chapters.

CHAPTER 5: DEVELOPMENT OF HARMONIOUS FAN COIL UNIT

The 25.5^{o}C scheme proposed by EMSD to Hong Kong residents is problematic. The major objective of the plan is simply setting the thermostat to 25.5^{o}C, and not much information was provided to the public. It created much public criticism about whether 25.5^{o}C is a comfortable temperature setting. The Hong Kong Economic Times reported that EMSD had to order fans to relieve staff complaints about warm office environments under the policy of 25.5^{o}C (Hong Kong Economic Times, 2006). This reflects the lack of a proper protocol of promoting escalation of indoor air temperature as well as proposal of feasible engineering solutions.

Step 3 of the proposed 3-step protocol in this research study proposes a series of system enhancement works including developing a fan assisted air-conditioning system. In this Chapter, feasibility of the engineering solutions will be described in detail. The fan-assisted unit is developed to provide a “harmony” environment to achieve sustainable thermal comfort, that is to increase the indoor temperature thus saving energy but without scarf icing people thermal comfort. In later sections, the new development is named “harmonious” fan coil unit system.

Two real sites were chosen for the installation of an innovative harmonious fan coil unit (HFCU) which apply the fact that air speed with fluctuation enhances thermal comfort. The HFCU system is designed to allow a rise in the temperature set point, which can reduce energy use without surrendering the thermal comfort conditions of building occupants.

Several actions have been taken to achieve the goal:

1. increasing air tightness of the room to reduce the latent load;

2. rebalancing the water side system for more effective use of energy;

3. design of a harmonious fan coil system to deliver dynamic air movement;

4. education of a proper understanding of thermal comfort.

5.1 Sites description

The two application sites were undergoing large-scale renovations. The first site was a faculty office in University campus which consists of six individual office rooms and one mini open plan office. The designed number of occupants is eleven and the total floor area is 111m^2. The mini open plan office (refer to zone 2 in floor plan in Figure 5.1) was selected for the installation of one HFCU system. This test site is used to demonstrate the proposed series of design, testing and commissioning procedures for implementing a new HFCU system.

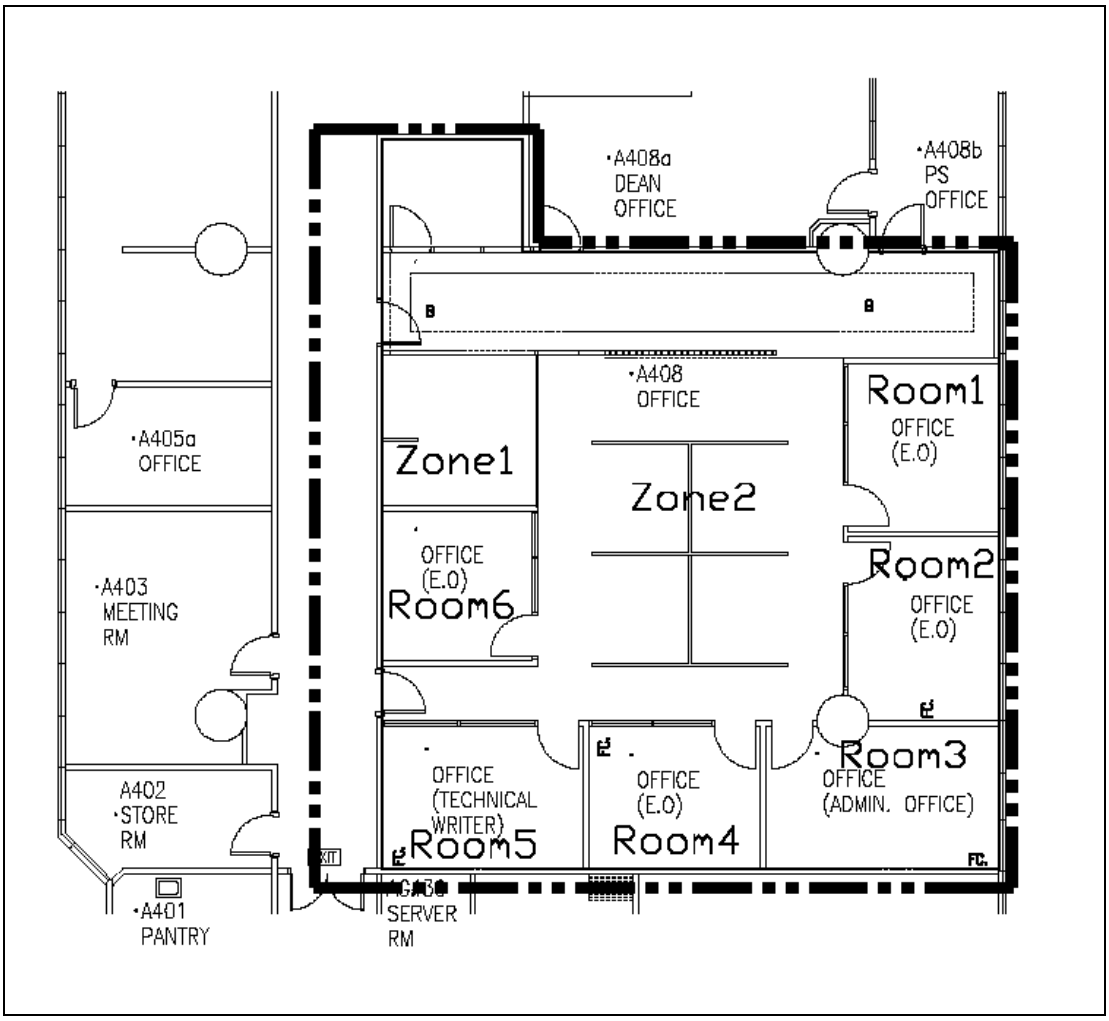

Figure 5.1: Floor plan of the faculty office in PolyU campus for installation of harmonious fan coil unit system

Figure 5.2: Photo of the faculty office in PolyU campus for installation of harmonious fan coil unit system

The other room is a typical single (one-person) office in the same University campus. The room dimension is of 2.8m x 3.8m x 2.5m and the one-side window size is 2.7m x 1.2m. The false ceiling and furniture layout plan are shown in Figure 5.2. This site is used for detailed experiments and simulation in later Chapters.

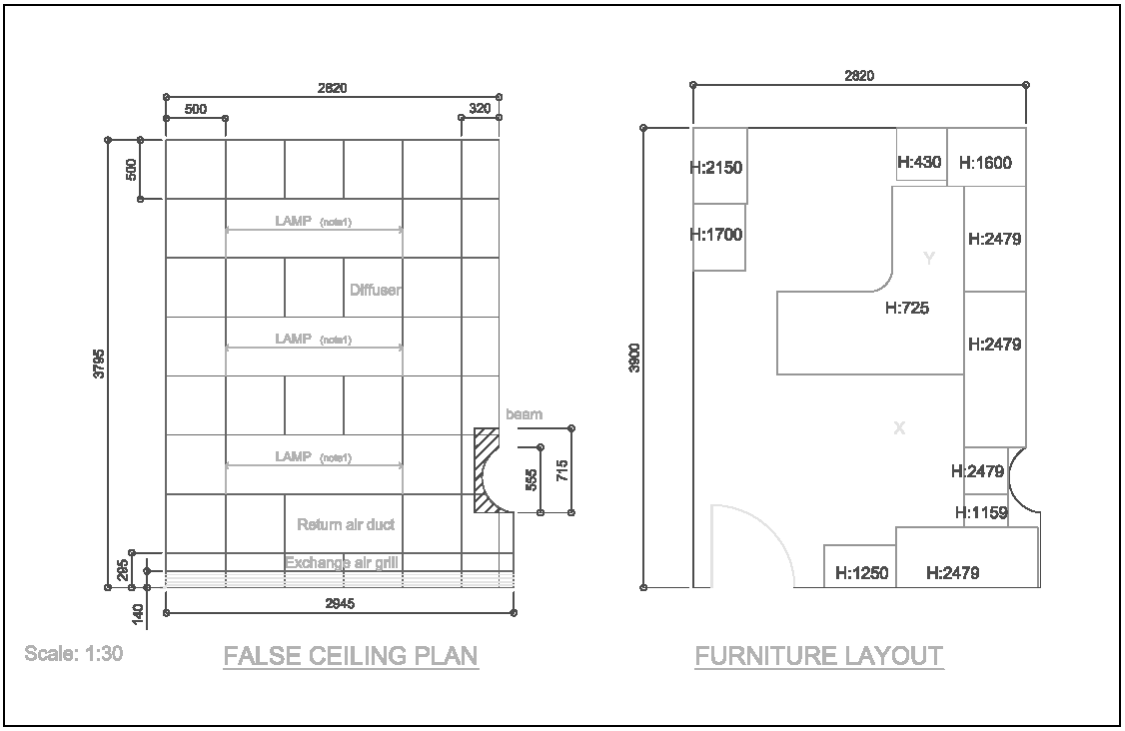

Figure 5.3: Floor plan and furniture layout of the single office for installation the harmonious fan coil unit system

5.2 Design process

5.2.1 Room characteristics

Typical air-conditioned building shells in Hong Kong could maintain the indoor space at 50-70% relative humidity. However, one often neglected issue in attempt to enhance the thermal comfort condition indoor and to raise the indoor temperature set point is the unwanted infiltration. Unwanted air infiltration especially in the warm

seasons from the outdoors into the building through various cracks and openings in exterior walls could increase the latent load of the room. The greatest air infiltration generally occurs around the window and door frames and can be eliminated by caulking and weather stripping. In addition, the sites' boundaries and internal rooms were constructed with full height walls up to the upper floor slab. Moisture from neighbor offices through false ceiling is avoided.

Figure 5.4: Internal wall up to the upper floor slap to reduce the latent load

5.2.2 Cooling load calculation

It is not surprise to note that the previously installed fan coil units of the rooms were significantly oversized. The new sizing of fan coil units are based on the detailed space cooling load calculation using the simulation software HTB2 (Alexander, 1996). Table 5.1 lists the estimated cooling load at individual rooms and zones based on the constructions of full height internal walls and partitions, tinted windows to reduce the radiant load.

	Area (m^2)	Estimated cooling load (KW)
Room1	9.4	1692
Room2	10.3	1854
Room3	12.4	2232
Room4	9.1	682.5
Room5	10.7	802.5
Room6	8.4	630
Zone1	8.7	652.5
Zone2	41.5	3112.5

Table 5.1: Cooling load calculation of the faculty office

5.2.3 Water side system

Hydronic balancing insures that design chilled water flows can be obtained and makes the cooling capacity available to all terminals. Improper balancing of the chilled water system would lead to undesired chilled water flow through the fan coil unit.

Special arrangement of the chilled water pipes was implemented in the faculty office as illustrated Figures 5.5-5.7. The balancing valves for the eleven fan coil units were allocated in one accessible location for the convenience of testing and balancing, as well as future maintenance. Balancing valves were installed for each terminal such that balancing for the design flow condition guarantees adequate flow in each terminal. Flow greater than design may cause low flows in other terminals of the system generating complaints on discomfort. Unsteady flow supply to one terminal would cause room temperature fluctuation. (Petitjean, 2004)

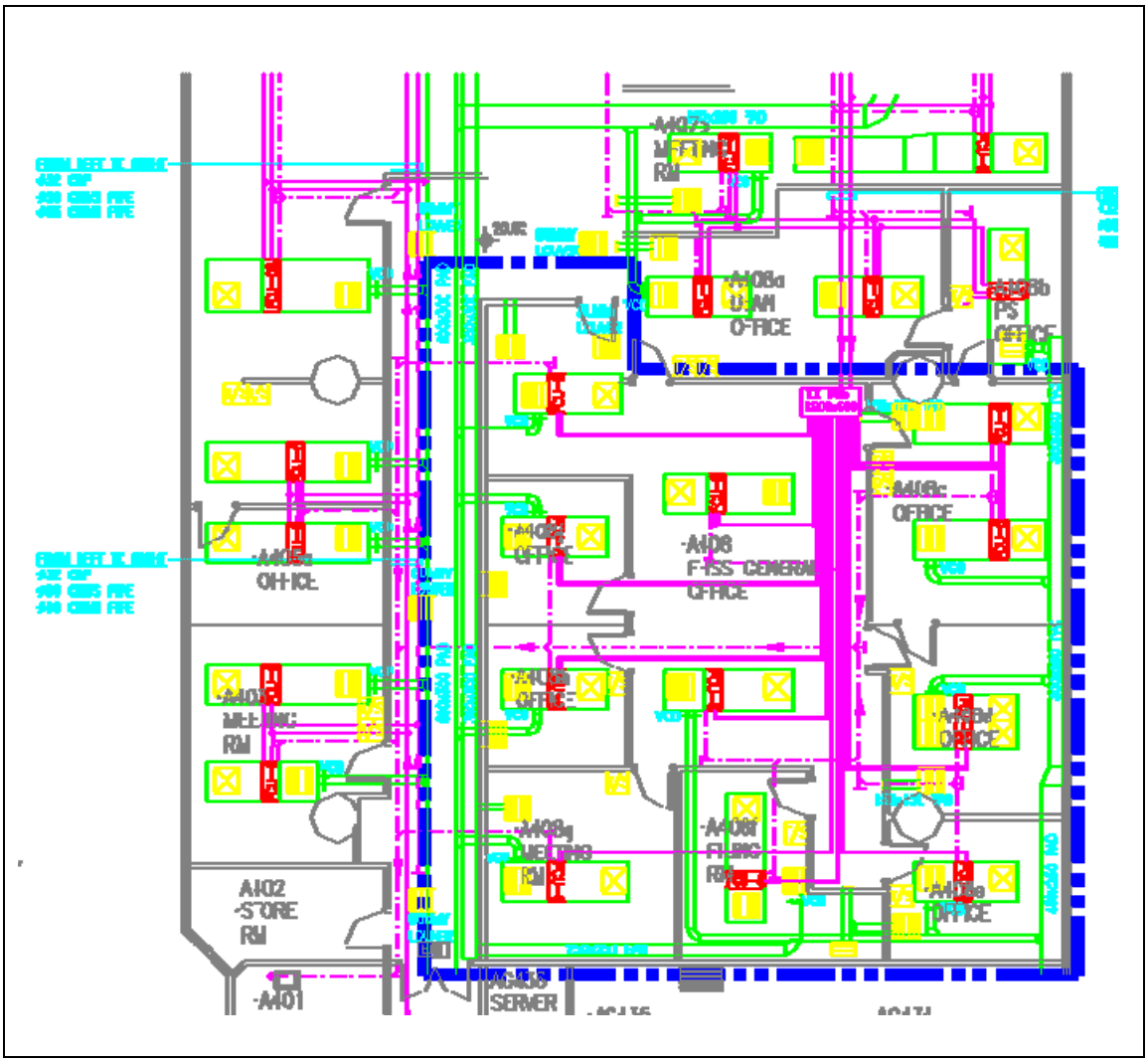

Figure 5.5: Chilled water pipe layout plan in the faculty office

Figure 5.6: Chilled water pipe layout in the faculty office

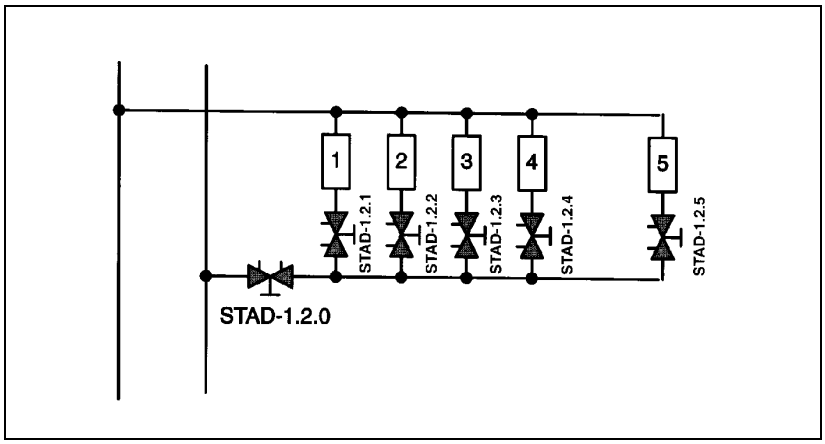

Figure 5.7: Schematic showing a branch of balancing valve

Proportional balancing was performed in the faculty office. The procedure for the balancing method is summarized in the following figure and flow chart. (Petitjean, 2004)

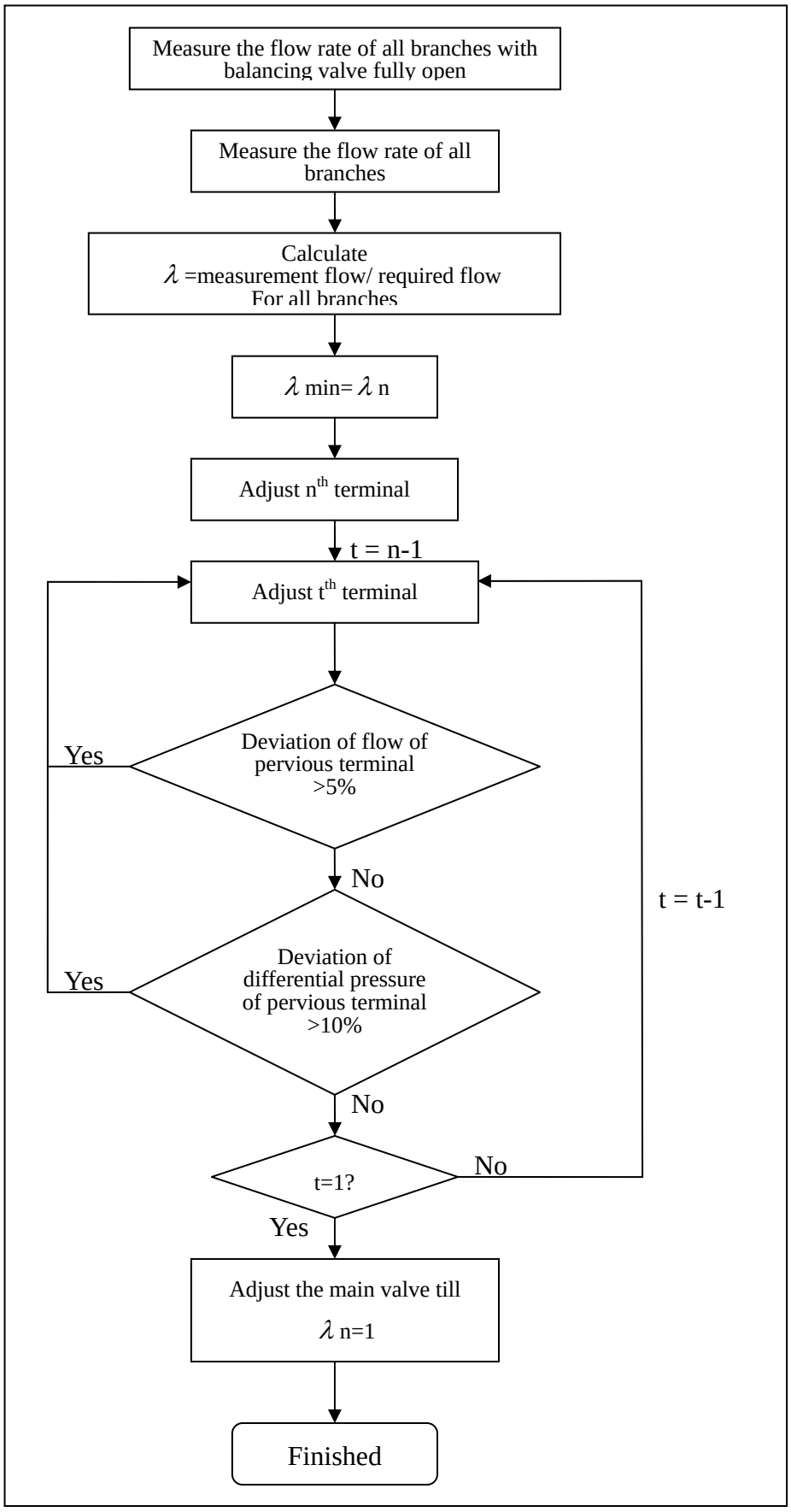

Figure 5.8: Flow chart for proportional balancing procedure

5.2.4 Air side system

Air balancing is another concern during design and construction. The fresh air supply ducted into each terminal was balanced by adjusting the damper in each branch in turn until the measured airflow equals the target airflow.

Other than the water and air balancing works, the key issue of the development of harmonious fan coil unit (HFCU) system is to attaining a fluctuating velocity to the environment, generating breeze-like airflow to the occupants. In the new HFCU design, an additional fan with frequency inverter was incorporated in a typical fan coil unit. Two types of harmonious fan coil systems were designed to install in the two sites respectively.

Type I (Harmonious Fan Coil Unit with Fan Box):

Type I is based on the traditional fan coil unit design with a air supply fan box installed in the supply channel for room air make up purpose. As illustrated in Figures 5.9 and 5.10, the fan box was situated in the air supply terminal and connected with a room air bypass channel to avoid drifting volumetric flow from the fan coil unit. The fan box performs like a mixing chamber for cooled air after coil and re-circulated room air. This way, the room's air can be re-circulated through both the fan coil unit and the room air by-pass, creating a better mixing in the room.

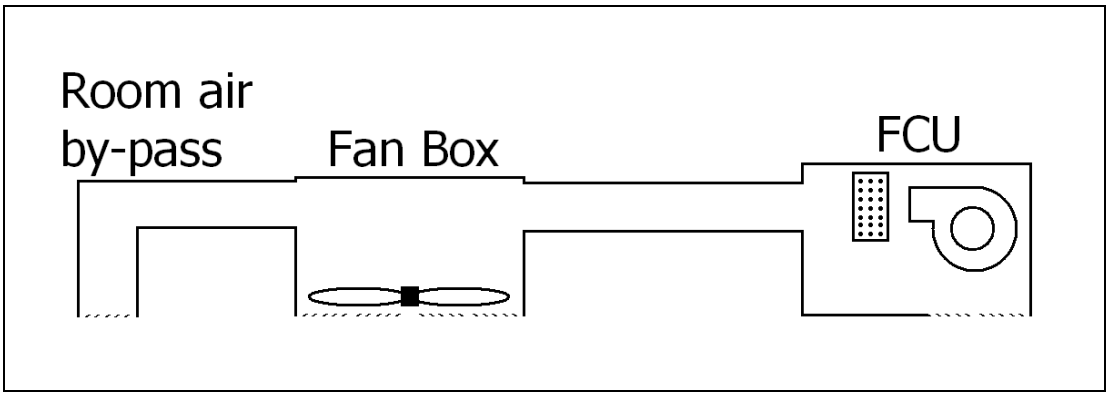

Figure 5.9: Illustration of the Harmonious fan coil unit Type 1

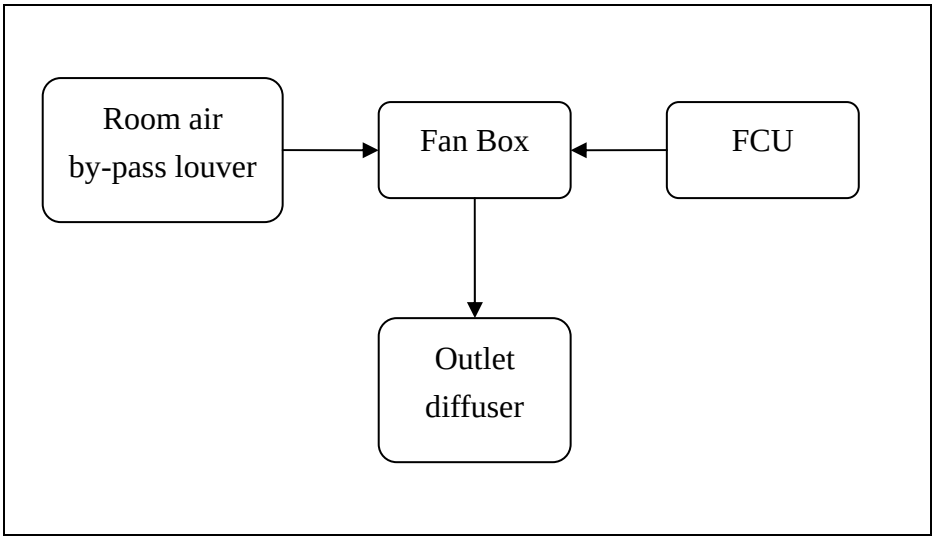

Figure 5.10: Block diagram of air flow in Type I system

Type II (Integrated Harmonious Fan Coil Unit):

Type II harmonious fan coil was also equipped with an additional harmonious fan, but its arrangement is different from that of Type I. Two centrifugal fans were installed in parallel. The FCU fan in front of the cooling coil runs at constant speed. The harmonious fan (without cooling coil) runs at variable speed controlled by the frequency inverter. The room air is recirculated through the return louver, and part of the air then passes though the cooling coil. The air mixes before delivery to the

occupied zone through a supply diffuser. This arrangement avoids fluctuating air flow rate flow through the coil and keeps the performance of heat transfer from the coil to the air constant. Figure 5.12 illustrates the air flow path of this Type II HFCU system.

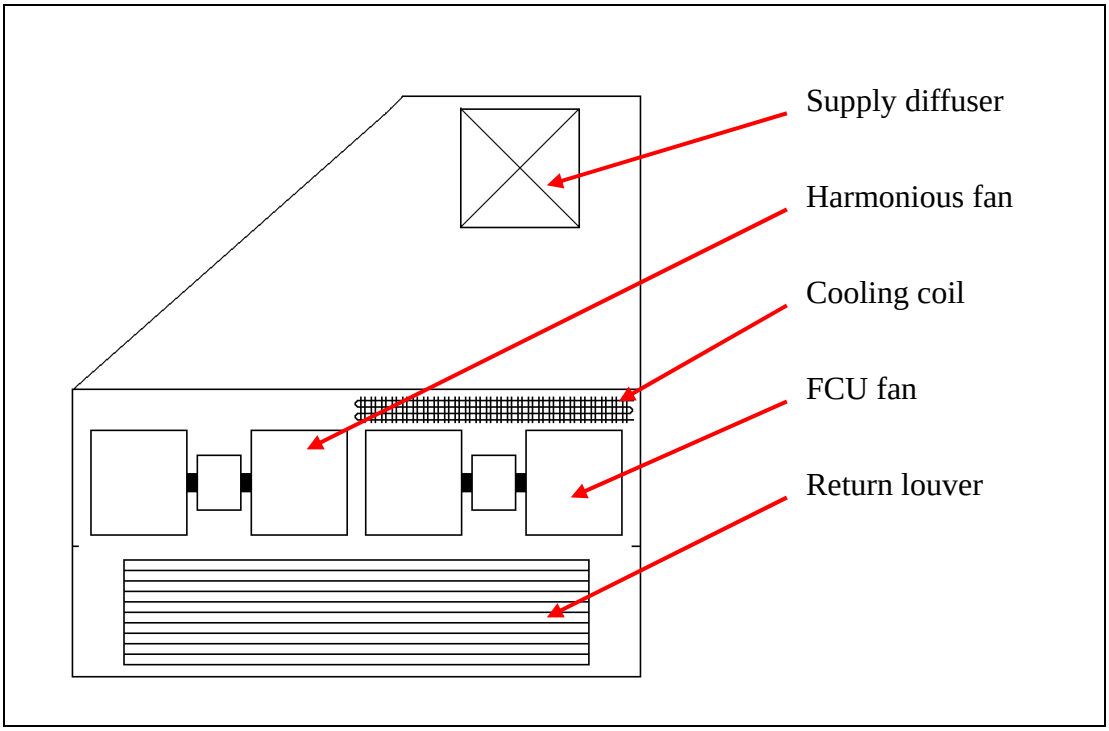

Figure 5.11: Illustration of Harmonious fan coil unit Type II system

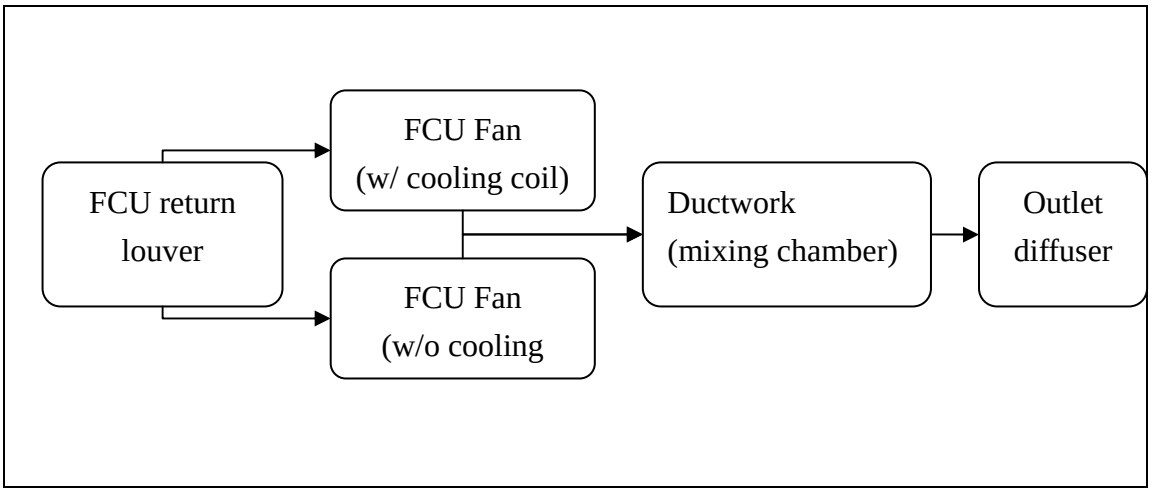

Figure5.12: Block diagram of air flow in Type II system

Frequency inverter

For both Type I and II systems, the additional fan is controlled by a “Fan Speed Control Unit” (FSCU). The FSCU is integrated by two main components – frequency inverter and temperature transducer. Rotational speed of the fan is controlled by the output power of the frequency inverter. The output power can be adjusted by two methods:

1) Manual adjustment

2) Analog DC voltage input.

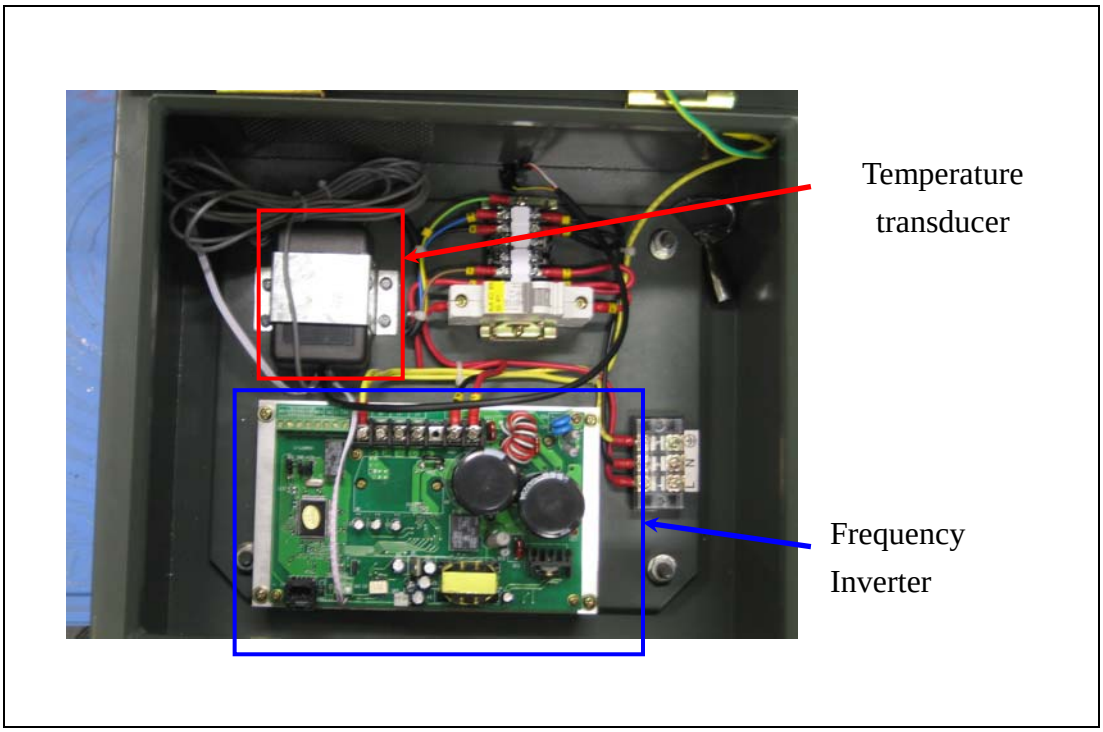

Figure 5.13: Configuration of the Fan Speed Control Unit

In this FSCU, the output power frequency was adjusted by the analog DC voltage input from the temperature transducer, which generated the analog DC signal. The following block diagram shows the operation flow of the transducer.

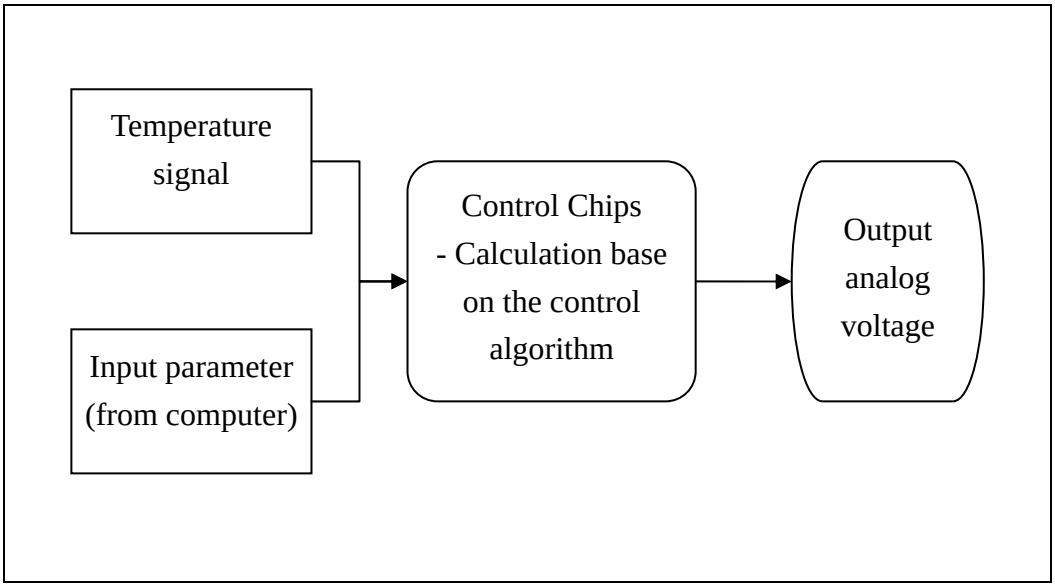

Figure 5.14: Block diagram of the control algorithm of the fan speed control unit

Control algorithm of the temperature transducer

The user can adjust the settings for controlling the harmonious fan through the developed HFCU control interface. Several parameters could be modified to adjust the period and amplitude of the velocity fluctuation: the minimum and maximum flow rate of the supplementary fan, the time from minimum to maximum flow rate and vice versa, and the time for constant flow rate at minimum and maximum flow rate (refer to Figures 5.15 - 5.17)

Different variations of velocity profiles with different temperatures can be set. A thermostat built on broad can detect the temperature and change the preset operation profile.

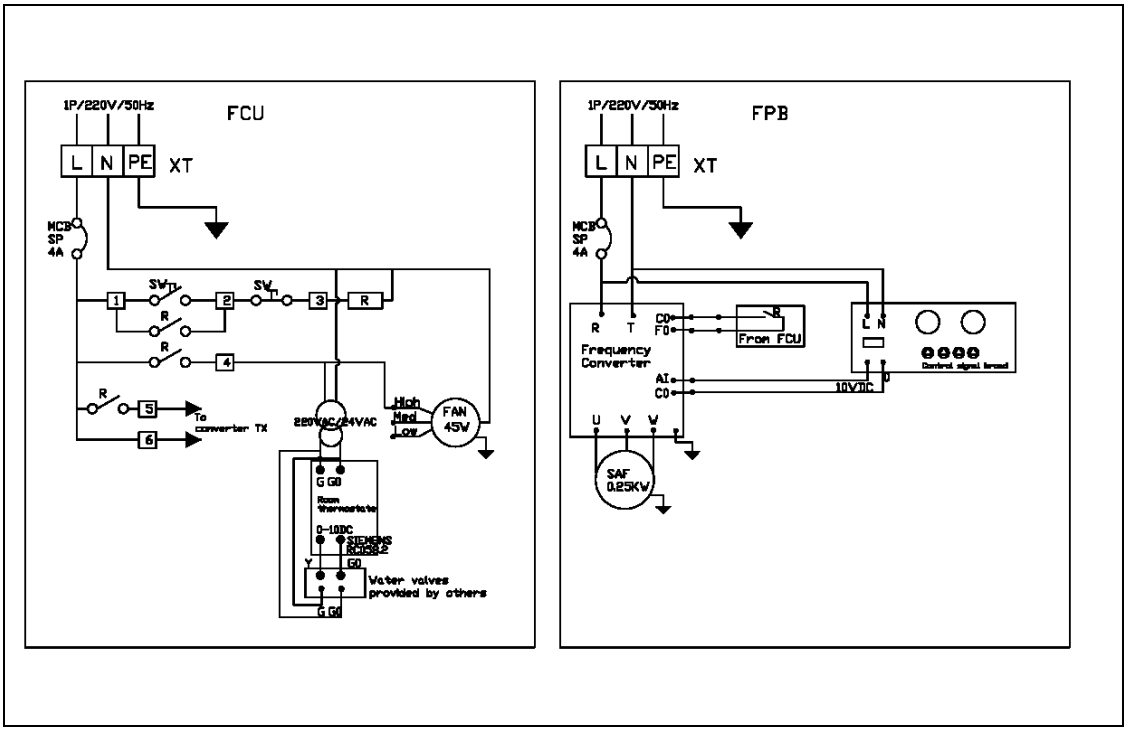

Figure 5.15: Circuit diagram of the "Fan Speed Control Unit"

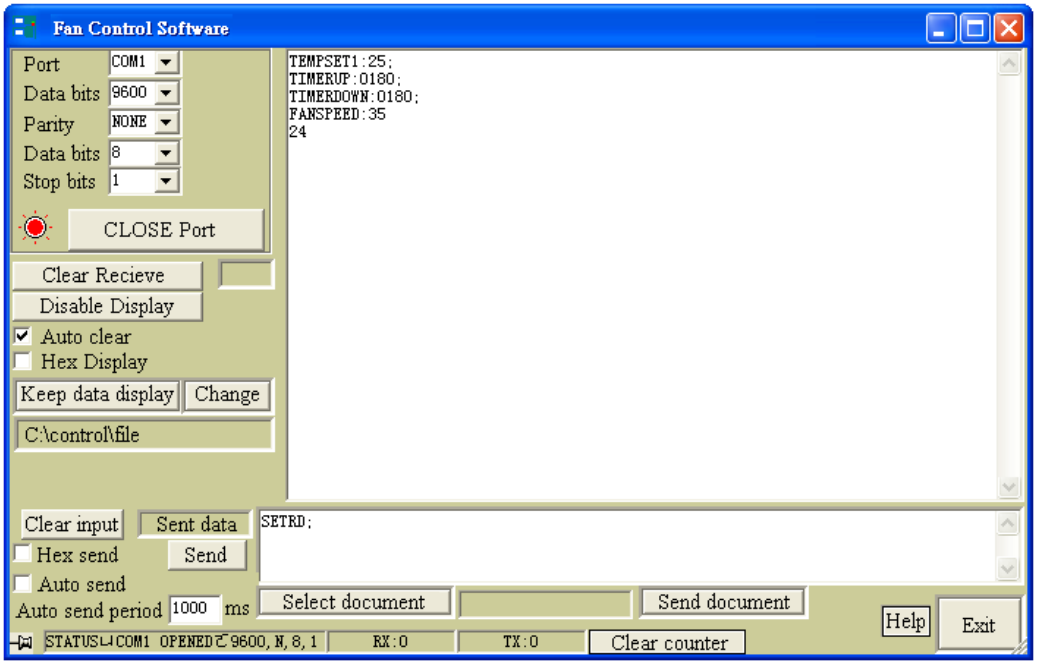

Figure 5.16: Interface of the HFCU control interface for the temperature transducer

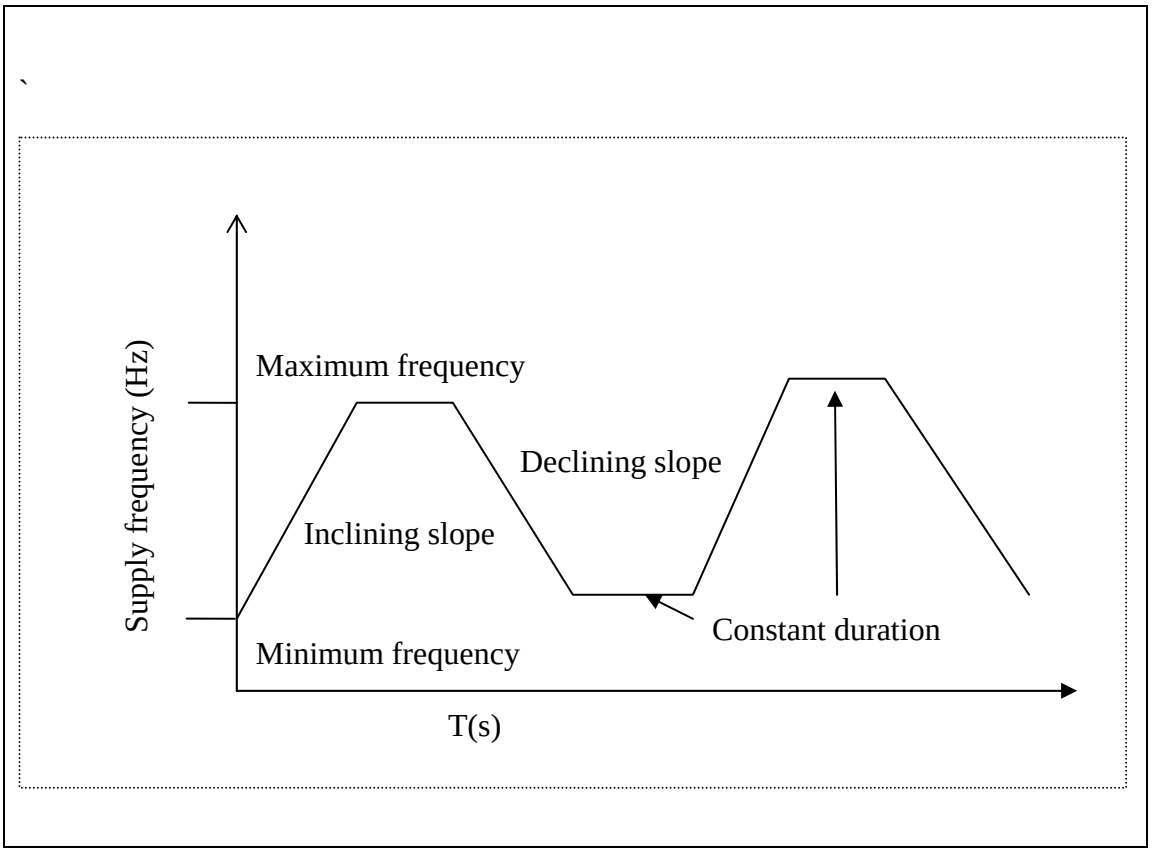

Figure 5.17: Controlling parameters of the Fan Speed Control Unit

5.3 Education of Thermal Comfort to Office Staffs

A lunch talk was given to the occupants of the office before they moved into the renovated sites. The purpose of the talk was to educate them with the correct concepts in thermal comfort and to explain the usage of the harmonious fan coil system. Messages for changing clothing styles and avoiding wearing too many layers were passed to them so that they could accept higher temperatures in the working environment.

Figure 5.18: Lunch talk meeting to the faculty staffs

5.4 Testing and Commissioning of System and Equipments

5.4.1 Functional tests

A high static propeller fan (Figure 5.19) was selected for the application of makeup air. Four blades were incorporated in the fan. The fan operated in a three phases at 220V with rated input current 1.7A. According to the ASHRAE handbook, this type of fan can be used for makeup air application. (ASHRAE, 2004)

Figure5.19: Propeller fan for make up air application

The flow rate of the fan and the additional noise level induced by the fan was measured in the laboratory.

5.4.2 Flow characteristic measurement

The flow rate for the proposed system is not constant, but varies from time to time. Therefore, a frequency inverter was installed to adjust the rotational speed of the fan. In this case, the relationship of the flow rate for different supply voltages was studied. The measurement was taken by Flowhood model number CFD-850L manufactured by Shortridge instruments (Shortridge, 2007). The result is shown in the following figure.

Figure 5.20: Measurement of volumetric flow rate of the propeller fan

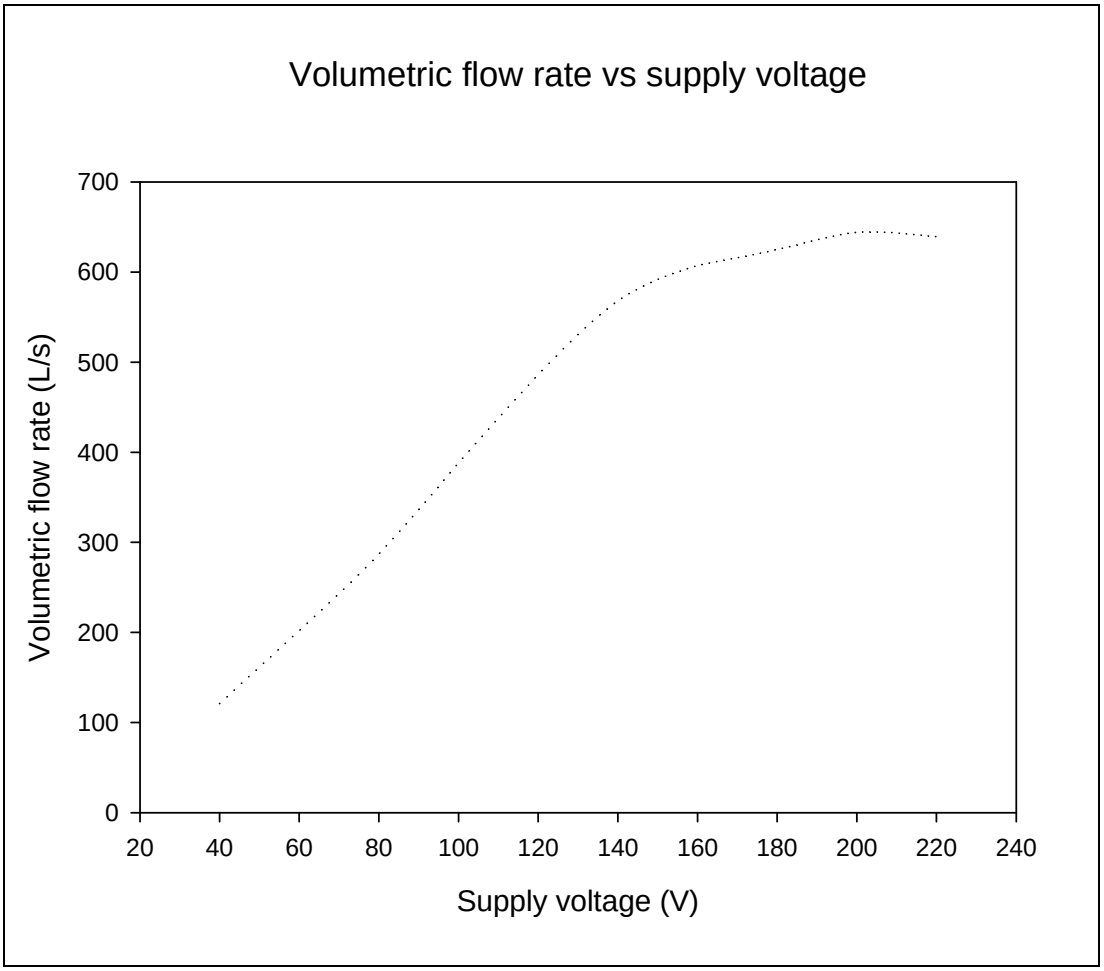

Figure 5.21: measurement result of the supply voltage to the volumetric flow rate of the propeller fan

After installation, the flow rate of the system was measured again for commissioning purposes. The following table summarizes the flow rate in different operation modes.

FCU Speed	Frequency of input power (Hz)	Total flow rate (L/s)	FCU flow rate (L/s)	2nd fan flow rate(L/s)	Mixing Ratio
Low	0	104	104	0	0
Low	35	332	104	228	2.19
Low	45	346	104	242	2.32
Med	0	139	139	0	0
Med	30	338	139	199	1.43
Med	35	367	139	228	1.64
High	0	166	166	0	0
High	30	365	166	199	1.19
High	40	408	166	242	1.45

Table 5.2: As-built measurement result of volumetric flow rate

5.4.3 Acoustic measurement

The additional use of the fan is supposed to increase the sound level in the occupied room. Therefore, before the installation, the propeller fan was tested to evaluate its induced sound level. The measurement equipment used was Sound Level Meter B&K 2260 (Bruel & Kjaer, 2007). The measurement setup is shown in the following diagram. The height of the measurement point was on the same level as the centriod of the fan. The background noise level before and after the sound measurement was measured such that the only the noise from the fan was indicated in the measurement results.

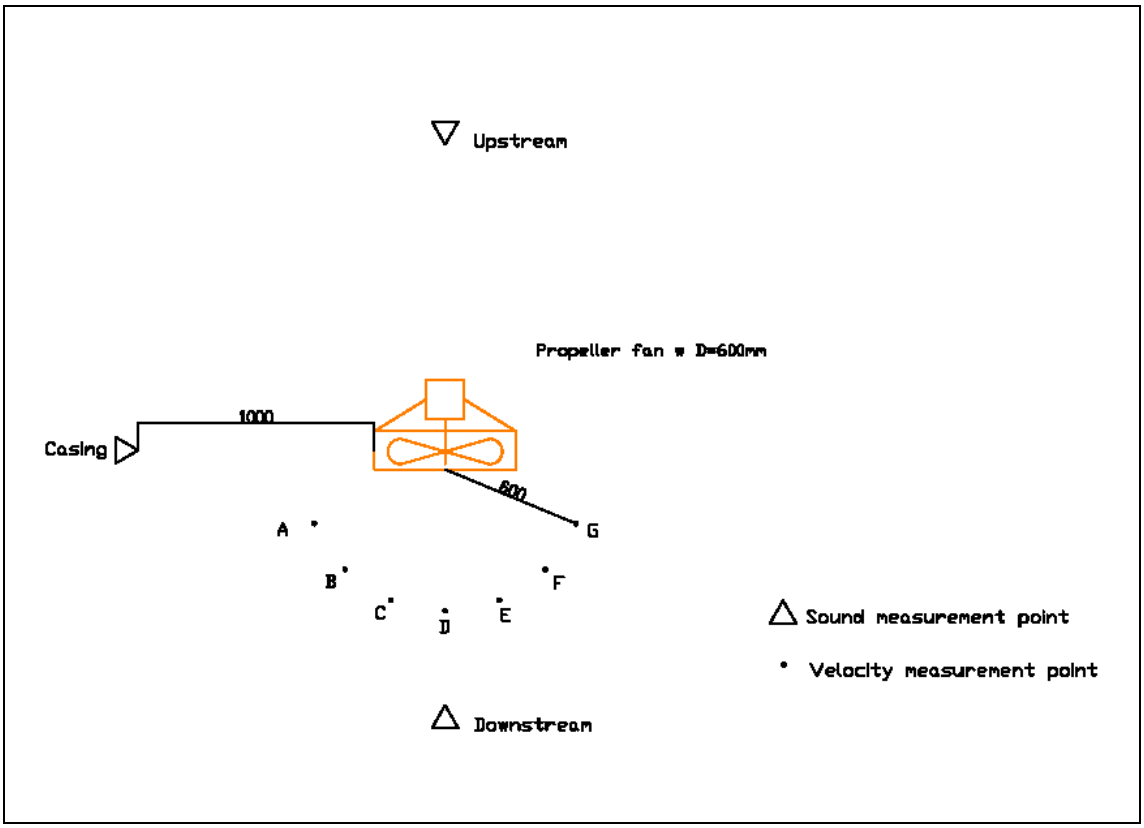

Figure5.22: Measurement arrangement of sound level

Figure 5.23: Laboratory of Sound measurement

The results of the sound levels generated by the propeller fan are illustrated in the following figures. From the measurement data, high frequency noise dominates in the sound spectrum and indicates that installation of the fan may be acoustically uncomfortable to the occupant. As a result, acoustic insulation was equipped in the casing of the propeller fan as shown in Figure 5.24. Sound measurements were taken again after lining up the acoustic insulation, and the results shown in Figure 5.26.

Figure 5.24: Propeller fan lining up with acoustic insulation

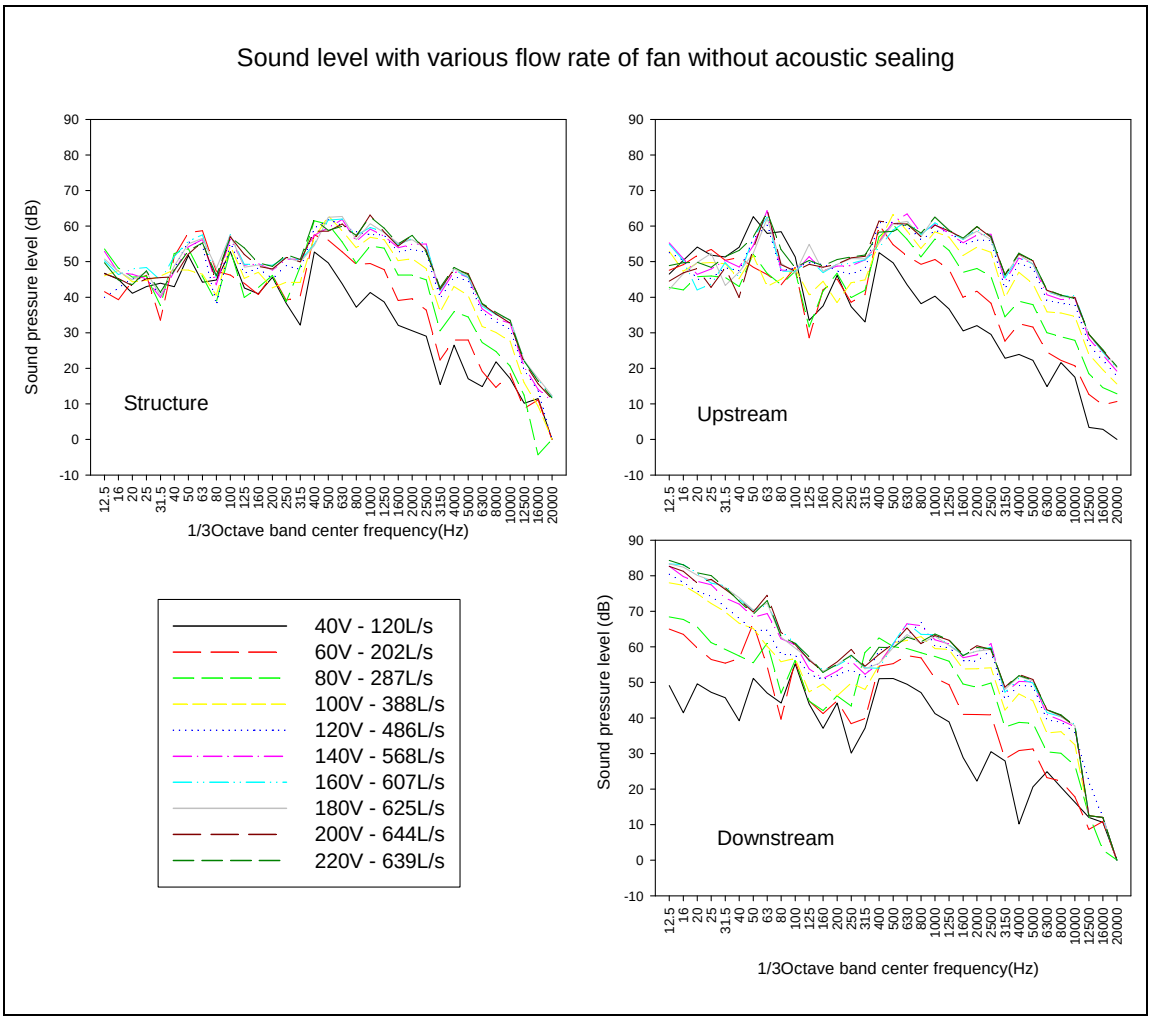

Figure 5.25: Sound measurement result before acoustic insulation

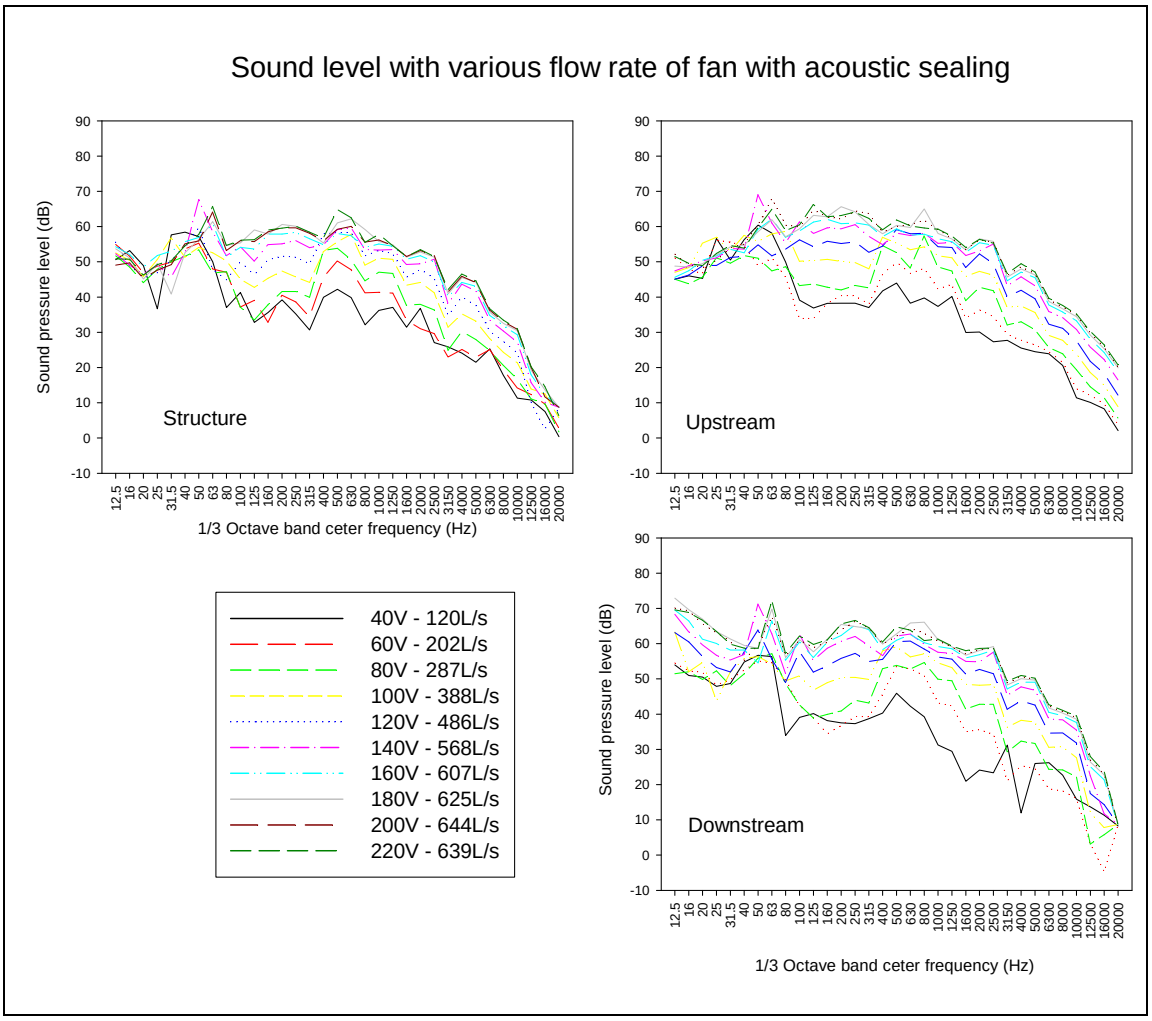

Figure 5.26: Sound measurement result after acoustic insulation

When compared to the result of the sound measurement before and after installation of the acoustic lining, it was found that high frequency noise, which is more sensitive to the human ears, was reduced.

Sound measurements were taken again in the office after the installation work was completed. Figure 5.27 shows the result of the noise measurement in the office.

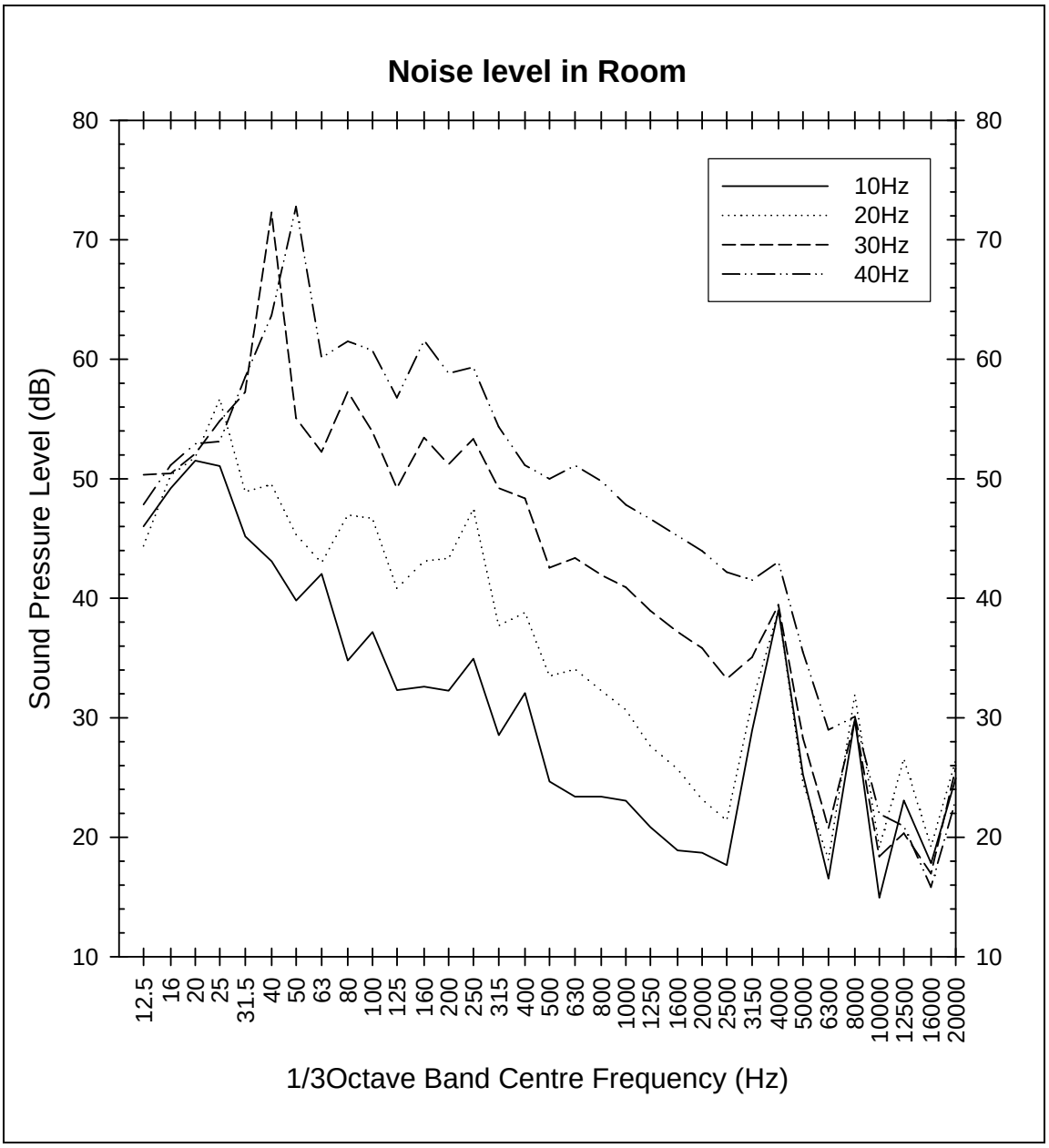

Figure 5.27: Sound measurement taken in office after installation

5.4.4 Air tightness measurement

Tung et al (2006) suggested an innovative way to calculate the air change rate with the use of radon measurement. By using this method, the radon level was monitored overnight as the radon builds up during the night as no fresh air is supplied to the zone. The dramatic drop is measured once the fresh air is provided again in the morning. With this data, the air change rate of the zone can be quantified. A computer program written by MatLab was employed to compute the air change rate and the calculation procedure are shown in Figure 5.30. The radon levels were measured by *RAD7* Electronic Radon Monitor manufactured by DURRIDGE (DURRIDGE, 2006).

Figure 5.28: RAD-7 for radon measurement

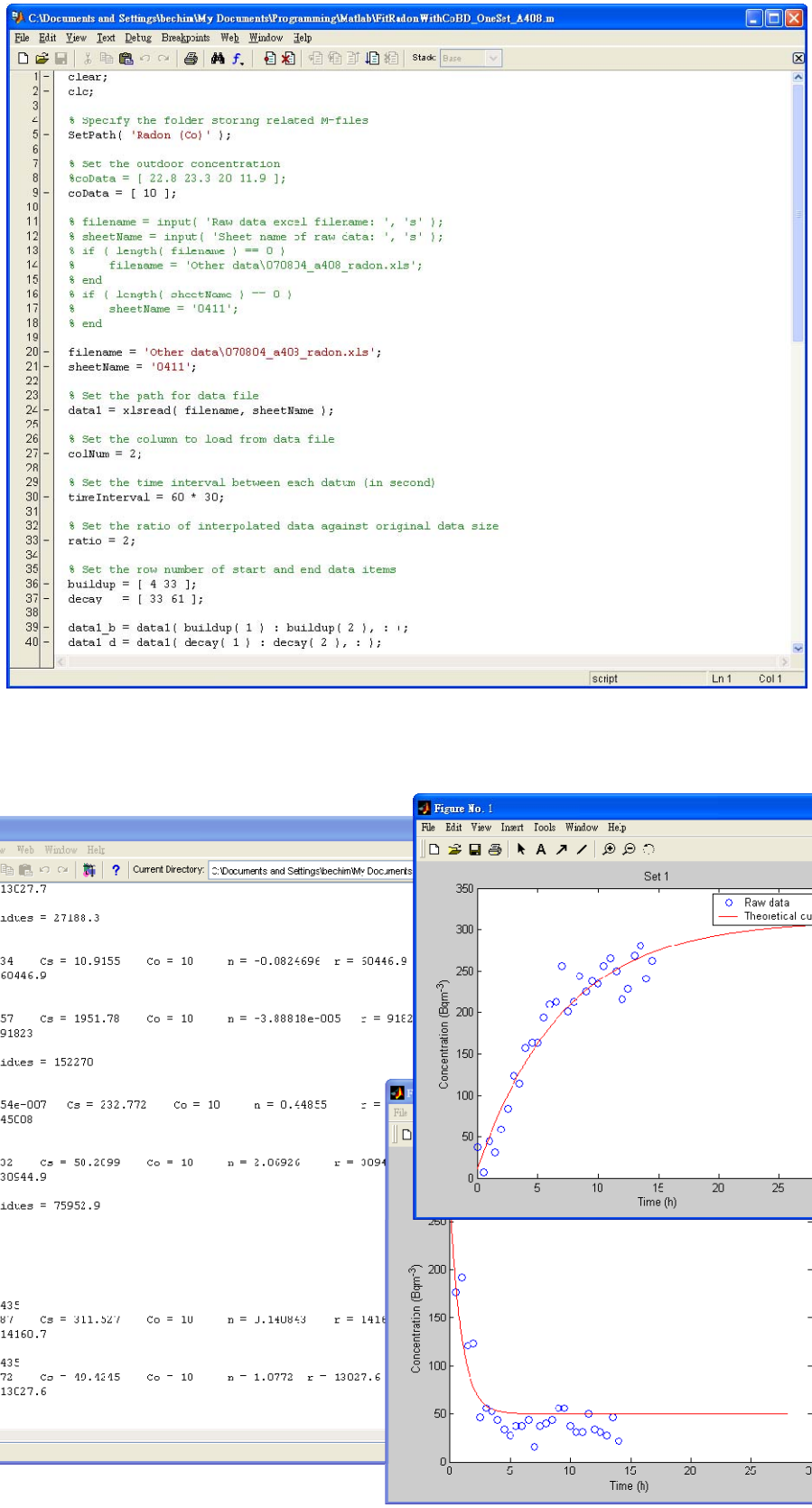

Figure 5.29: MatLab program for air change rate calculation

The measurement result is illustrated in Figure 5.31 with the calculate air change rate of the site. Six other typical offices in University campus were measured by the same method for comparison of air tightness. The results indicate that the infiltration rate of the faculty office was the lowest. The installation of caulking and weather stripping, full height walls were effective in preventing the unwanted air filtration and thus significantly reduce the latent load of the rooms and zones.

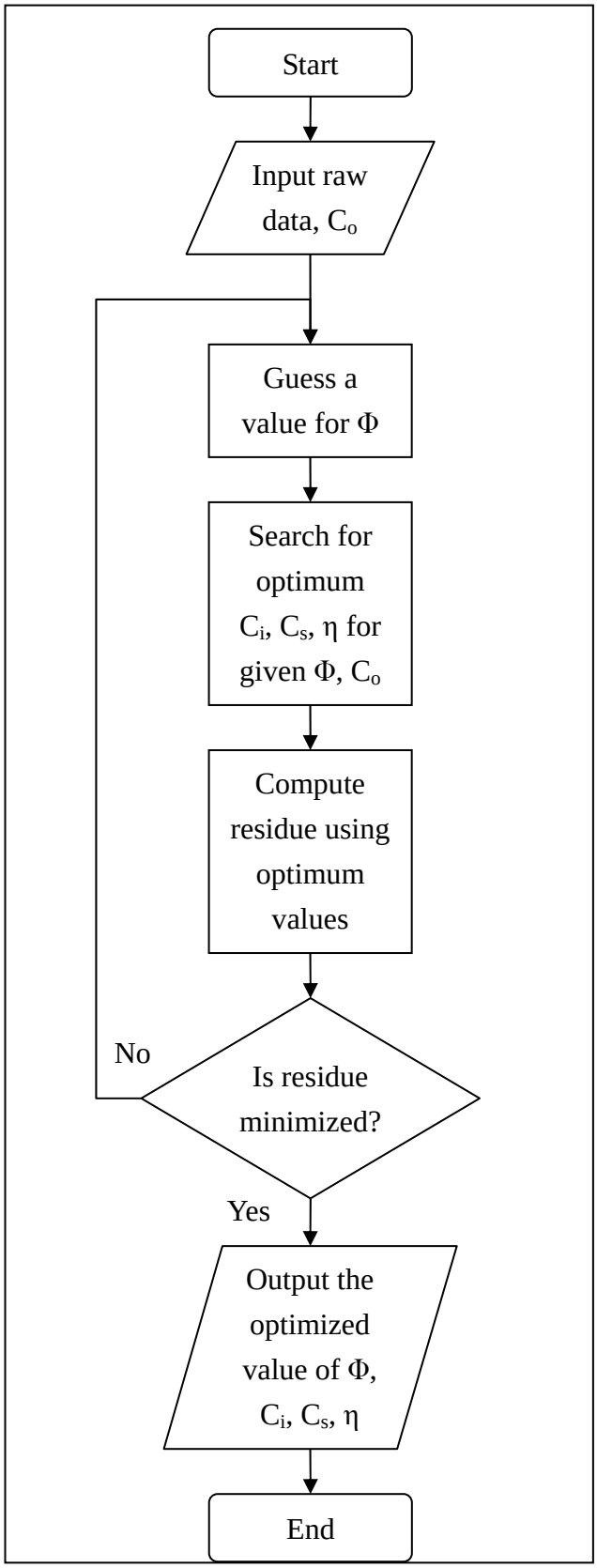

C_o = *outdoor radon concentraton (Bq/m^3)*

Φ = Specific radon production rate of "Reading Section" (Bq/m^{3}h)

C_i = initial concentration of radon (Bq/m^3)

C_s = steady concentration of radon(Bq/m^3)

η =Radon decay constant and effective aur exchange rate (h^{-1})

Figure 5.30: Flowchart of the calculation procedure of the air change rate by radon method

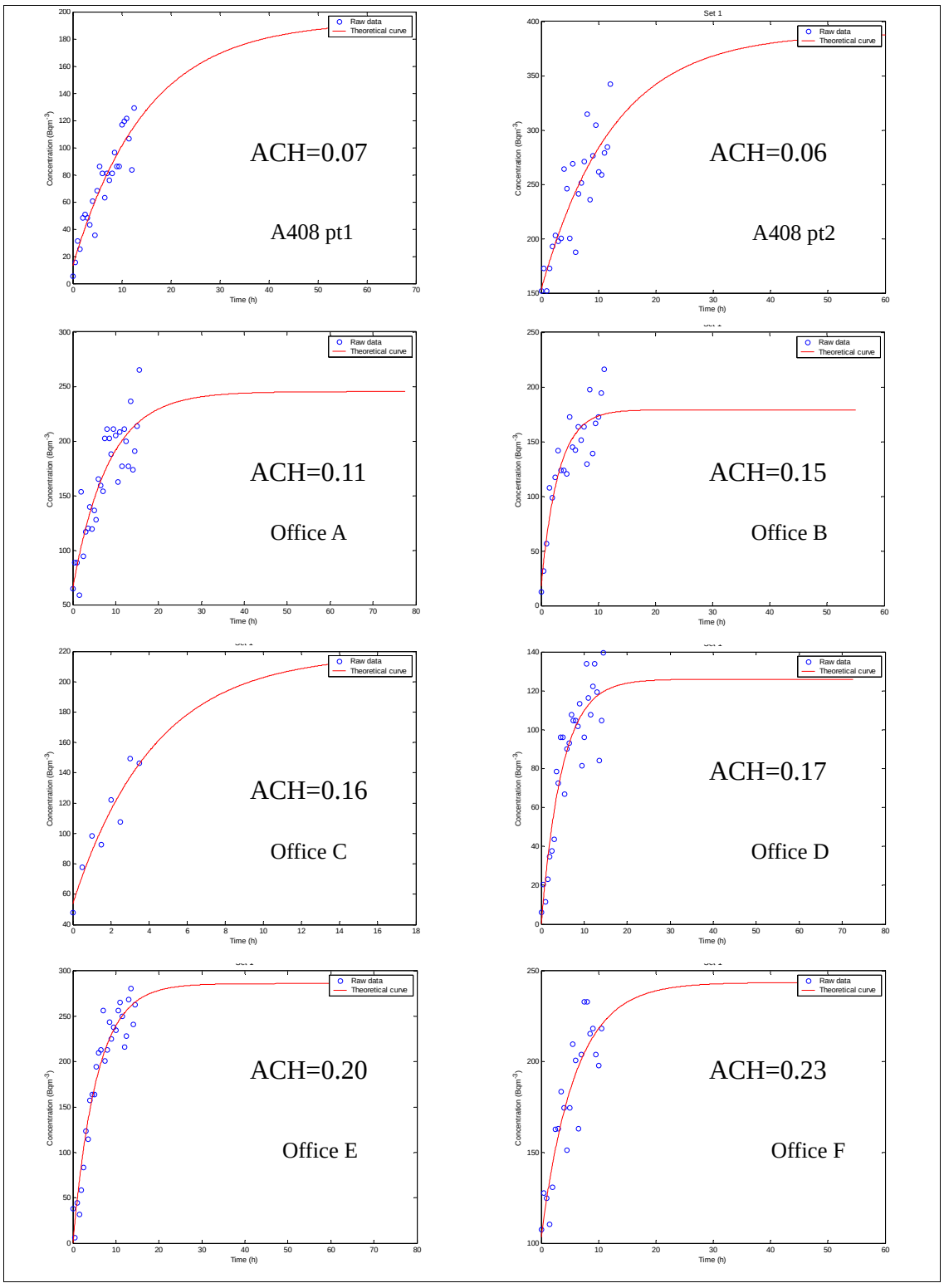

Figure 5.31: Computation results of the infiltration rate

5.4.5 Water Balancing

The module consists of 10 functional fan coil units with different rated flow rates. Each was equipped with a manual balancing valve. A differential pressure controller and a manual balancing valve were installed at the main return and supply respectively to investigate the impact of energy saving for a hydronic system.

Figure 5.32 shows a simplified schematic of the model under study. Number 5 is not shown, as it as not in use (fully shut). Valve A and B are so-called partner valves. Valve A is for flow measurement and resistance adjustment, while Valve B is a differential pressure controller which regulates itself to maintain a constant differential pressure across A and B.

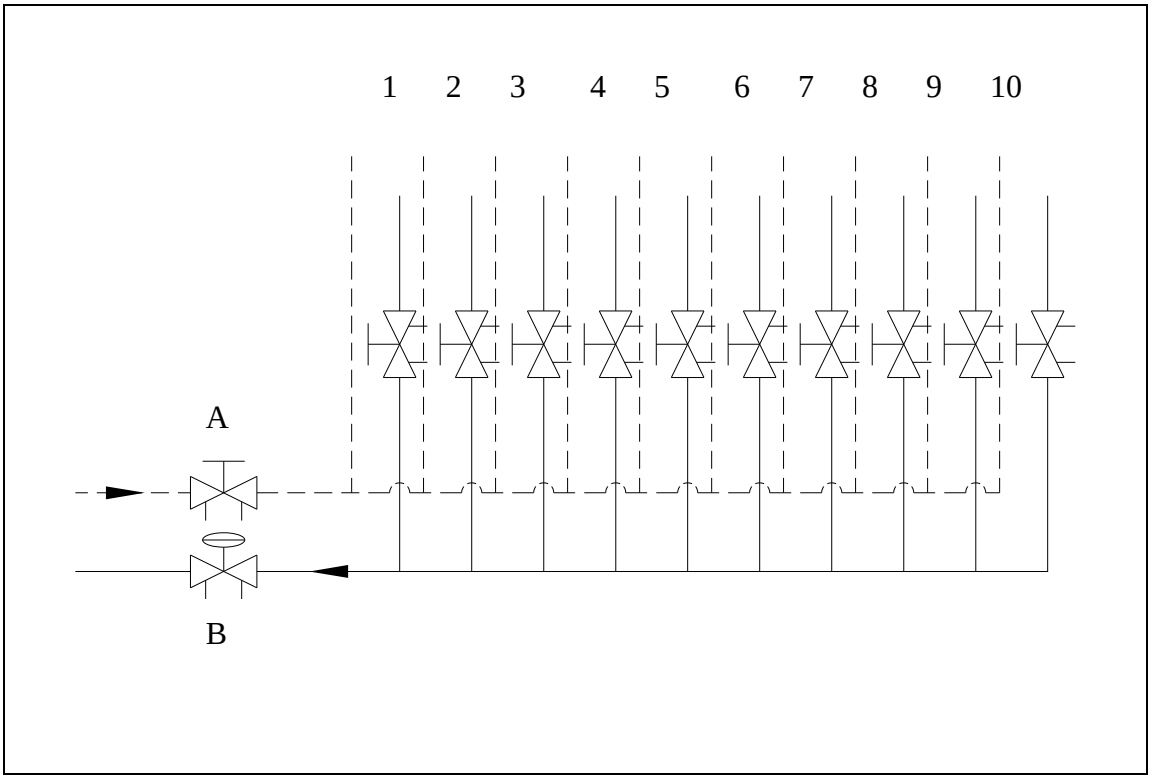

Figure 5.32: Simplified schematic of the chilled water system of the faculty office

Balancing results:

The module was balanced using the proportional balancing method with a computerized balancing instrument. Every balancing valve was set so as to obtain the design flow of each FCU. The total flow was obtained by measuring the manual balancing valve at the main supply. After adjusting Valve B (differential pressure controller) to get the desired total flow, the result was 0.60 l/s, which was 95% of the design flow, 0.63 l/s. A differential pressure controller at the return was installed to keep the system unaffected by pressure disturbances during operation. At the same time, the water temperature difference was recorded and it was 7°C (supply water temp.: 7°C , return water temp.: 14°C). Hence, by using the equation 5.1, the instantaneous cooling power output was 17.5 kW (4.98 RT).

$$P = \frac{q \cdot \Delta T}{0.86} \tag{5.1}$$

Label	Room	Setting turns
1	FCU 8 - Corridor	0.5
2	A408c	1.5
3	FCU 10 - Open plan	3.0
4	A408d	1.5
5	Not used	N/A
6	A408e	2.0
7	A408f	0.5
8	A408g	0.5
9	A408h	0.5
10	FCU 9 - Cabinet	0.5
11	Copy room	0.5

Table 5.3: Summary of the proportional balancing result

Simulation results:

To simulate a situation in which the system is unbalanced, all balancing valves corresponding to FCUs were opened to its maximum position by turning the hand wheels. Meanwhile, the settings of valves at the main supply and return remained the same. The total flow was then taken and it was 0.90 l/s which was 143% of the designed total flow. As expected, the return water temperature was lower than 14°C. The water temperature differential at that time was 6°C (supply water temp.: 7°C, return water temp.: 13°C). Using the same formula, the cooling power output was 22.5 kW (6.4 RT). Hence, there was a waste of 50% in total flow and 28.5% in cooling power output.

Fault detection:

During the balancing process, a couple of faults were detected. For instance, three out of ten ON/OFF control valves were malfunctioning and had to be opened manually. Moreover, a gate valve connecting a FCU at the open pan office was shut. These faults were found with the help of the balancing instrument used.

With an unbalanced system, a certain percentage of overflow in one part of the system implies a certain percentage of underflow in other parts of the system. Underflow of a system or a coil makes it difficult, even impossible, to obtain the room temperature at night in design condition.

With regards to energy efficiency, the 28.5% cooling power saving is significant. The result was due to the over-sizing of terminal unit. An overflowing circuit takes more heat than a balanced circuit. Furthermore, it reduces the control ability of the system to keep a room temperature constant within the limits.

	After balancing	**Before balancing**
Supply water temp.	7°C	7°C
Return water temp.	13°C	14°C
water temperature differential (q)	6°C	7°C
instantaneous cooling power output (P)	17.5 kW (4.98 RT)	22.5 kW (6.4 RT)

Table 5.4: Energy saving before and after water balancing

CHAPTER 6: EXPERIMENTAL STUDY RESULTS AND DISCUSSION IN TEST ROOM

Experimental studies were carried out to support the feasibility of HFCU system in term of system enhancement - the Step 3 of the proposed 3-step protocol. The room air by-pass was turned through the adjustment of secondary centrifugal “harmonious” fan to study its effect on temperature swing at work stations. The measurement systems and analyses were developed into commissioning protocols and methodology in finding room characteristics for thermal comfort control purposes. As described in Chapter 5, the typical single office in the Hong Kong Polytechnic University campus was renovated to accommodate the experimental studies and later simulation modeling.

6.1 Measurement Setup

The measurement objectives are:

- to measure the boundary conditions (i.e. wall surface temperature, supply air temperature and air flow rate of AC unit and fan) for simulation modeling and for developing a tool for HFCU design in practice;
- to measure the spatial and temporal distribution of thermal comfort parameters (i.e. air temperature, relative humidity and air velocity) with and without imposing fluctuating airflow for developing the commissioning protocol and methodology in understanding room characteristics.

The room layout and arrangements of ventilation systems including the newly developed HFCU system are illustrated in Figures 6.1 and 6.2.

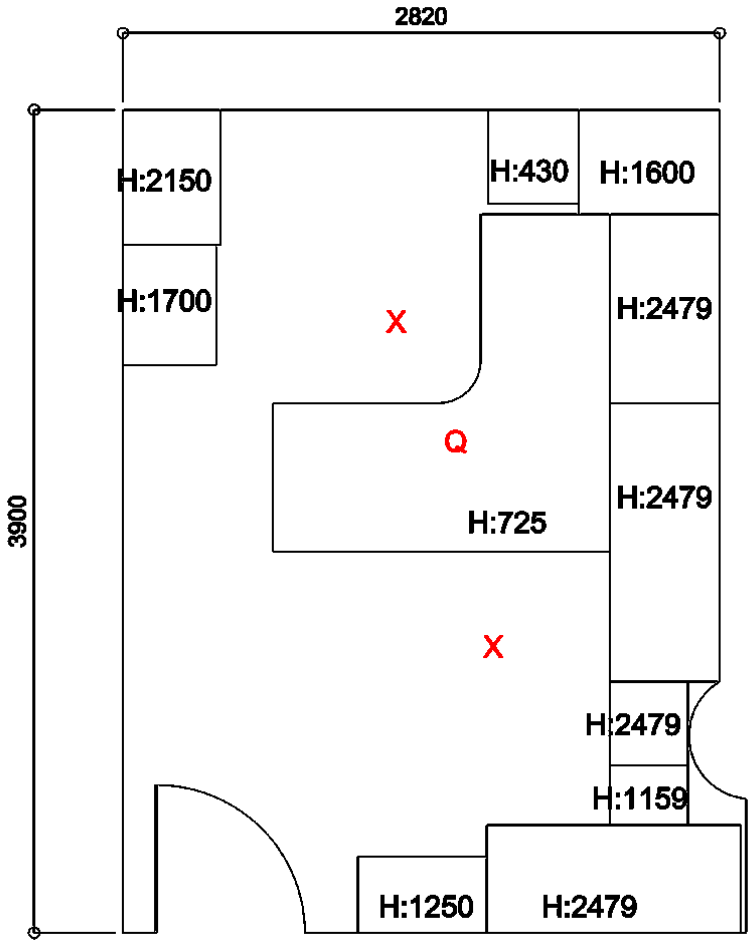

Figure 6.1: Measurement layout of the single office room equipped with HFCU Type I system (drawing not in scale).

Figure 6.2: Photo of measurement setup in the single office room equipped with HFCU Type I system

The test room had dimensions of 2.9m x 3.9m x 2.5m. The size of the window opposite to the door was 2m x 1.2m, with single glazing and UV protected window film. The glazing had a U factor of 5.91 W/(m^2.^{o}C). During the entire measurement period, the window blinds were closed to minimize the direct irradiation coming from the window and to avoid extra cooling load to the room. The average window cooling load was estimated at 79W/m^2 and the total window cooling load was 190W.

The external wall area was 2.6m^2 and the recorded temperature difference was 8.5^{o}C. The walls had a U factor of 0.45W/m^2K and contributed 10W cooling load to the room.

Three lighting fixtures each consisting of 2 x 1200mm T8 lamps with electronic ballast were installed. The heat load from the lighting fixture was 128W per fixture according to ASHRAE Standard 2005.

There was one desktop computer with two 20” monitors situated on the working desk contributing 165W cooling load in total. One laser printer was kept idle during the measurement period and brought 35W to the environment.

During the measurement, one person was assumed to be sat in front of the desk carrying out light office work. To simulate the equivalent sensible heat load of 70W from individual, a radiator with 70W was placed on the armed chair at the work station.

Cooling load in the room	**Heat (W)**	**Remark**
$Q_{internal\text{-}wall}$	0	Negligible as no significant temperature difference was record for the two sides of the internal walls.
$Q_{external\text{-}wall}$	10	
Q_{equip}	584	
Q_{person}	70	
Q_{window}	190	
Q_{Total}	854	75.5 (W/m^2)

Table 6.1 Cooling load estimation of the measurement period

6.2 Measurement system and procedures

Measurements were taken in two consecutive weekdays. During the measurement period, no one was allowed into the rooms. All the doors and windows were kept closed. The test cases are summarized as follow:

Cases	Thermostat set point temperature (℃)	Fan speed	**Fluctuating frequency (Hz)**
1	22	Lo	OFF
2	22	Lo	35
3	22	Lo	45
4	22	Med	OFF
5	22	Med	30
6	22	Med	35
7	22	Hi	OFF
8	22	Hi	30
9	22	Hi	40
10	24	Lo	OFF
11	24	Lo	35
12	24	Lo	45
13	24	Med	OFF
14	24	Med	30
15	24	Med	35
16	24	Med	15-30
17	24	Med	15-45
18	24	Med	30-45
19	24	Hi	OFF
20	24	Hi	35
21	24	Hi	40
22	24	Hi	15-30
23	24	Hi	15-45
24	24	Hi	30-45
25	26	Med	OFF
26	26	Med	30
27	26	Med	35
28	26	Hi	OFF
29	26	Hi	30
30	26	Hi	40

Table 6.2: Summary of test cases in the single office room

Further to the measurement of volumetric flow rate of the propeller or "harmonious" fan in the HFCU system as reported in previous Chapter, the total airflow rate in different test combinations were measured using the Flowhood model number CFD-850L manufactured by Shortridge instruments (Shortridge, 2007). The results are summarized in the following table.

Cases	FCU fan speed	Harmonious fan speed	**Air flow rate @ supply (L/s)**
1	Low	Off	100
2	Medium	Off	134
3	High	Off	175
4	Low	On (15Hz)	119
5	Low	On (30Hz)	283
6	Low	On (45Hz)	315

Table 6.3: Summary of volumetric flow rate of the HFCU system in different test combinations in the single office room

6.2.1 Velocity measurement

Two laboratory-grade mobile stacks were fixed in locations marked "X" in Figure 6.1. Each stack has four levels mounted with instruments (Figure 6.3). The data acquisition system comprises of a DaqBook Data Logging System. Table 6.4 summaries the mobile stack setup.

Figure 6.3: Measurement setup of mobile velocity measurement column.

Level from floor	Measured Parameters	Sensors
0.1 meter	air temperature	HOBO Onset data logger
	air velocity	TSI 8455 Air Velocity Transducers
0.6 meter	air temperature	HOBO Onset data logger
	air velocity	TSI 8455 Air Velocity Transducers
1.1 meter	air temperature	HOBO Onset data logger
	air velocity	TSI 8455 Air Velocity Transducers
1.7 meter	air temperature	HOBO Onset data logger
	air velocity	TSI 8455 Air Velocity Transducers

Table 6.4: List of measured parameters and sensors on mobile stack

6.2.2 Temperature distribution measurement

Hobo loggers were mounted on the mobile stack at heights of 0.1m, 0.6m, 1.1m and 1.7m for measuring the temperature vertical distribution (Figure 6.3). Three HOBO manufactured temperature monitoring loggers were mounted at air supply diffuser, return lover and near the wall-mounted thermostat. One TSI Q-Trak 8845 monitoring device was placed on the work station table, marked as "Q" in Figure 6.2.

The technical specifications of the instruments are as follow:

Air velocity transducer:	TSI 8455
Range:	0.127 – 50.8 m/s
Accuracy:	+/-2%
Response time:	0.2sec
Hobo Onset data logger:	U12-013
Temp range:	-20 – 70^{o}C
RH range:	5- 95 %
Accuracy:	+/- 0.35 ^{o}C, +/-2.5%RH
Resolution:	0.03 ^{o}C, 0.03%RH

The used instrument and sensors had research-grade accuracy, conforming to the relevant international standards set out below.

Standard	Use
ISO 7726	Thermal Environments - Instruments and methods for measuring physical quantities.
ISO 7730	Moderate thermal environments - Determination of the PMV and PPD indices and specification of the conditions for thermal comfort.
ASHRAE 55-2004	Thermal Environmental Conditions for Human Occupancy – measurement and comfort indices.
BS 1042 Part 2	Velocity-area method for air flow measurement in ducts.

Table 6.5: Testing standard adopted in the measurement

6.3 Data Analysis

6.3.1 Airlfow analysis

Air movement in rooms can be described by the mean velocity, $\bar{v}$, standard deviation of velocity, SD_v, turbulence intensity, Tu and energy spectrum, E(f), characteristic frequency, f_c, (Hinze 1975, Melikov et al. 1988) and a newly developed parameter – equivalent frequency f_e (Zhou 1999). The equations used for describing airflow characteristics are defined as follow:

The mean velocity measured over a period of time is:

$$\overline{V} = \frac{1}{\Delta\tau}\int_{\tau}^{\tau+\Delta\tau}|V|d\tau \quad \overline{V} = \frac{\sum_{i=1}^{n}|V_i|}{n} \tag{6.1}$$

where $|V_i|$ is the absolute velocity at time i (m/s), τ is time interval (s)

The variance of the air velocity record is

$$\sigma^2 = \frac{1}{\Delta\tau}\int_{\tau}^{\tau+\Delta\tau}(V-\overline{V})^2\, d\tau \tag{6.2}$$

And its standard deviation is

$$SD_v = \sqrt{\sigma^2} = \sqrt{\frac{\sum_{i=1}^{n}(v_i-\overline{v})^2}{n-1}} \tag{6.3}$$

Turbulence intensity:

Turbulence intensity, Tu, is one of the typical parameters for studying dynamic airflow. It describes the degree of fluctuation within a time period.

$$Tu = \frac{\sqrt{\overline{v'^2}}}{\overline{v}} \tag{6.4}$$

where v' is the fluctuant velocity (m/s)

Autocorrelation:

In turbulent flow, unsteady vortices appear on many scales and interact with each other. Turbulence causes the formation of eddies of many different length scales. An autocorrelation is used for finding repeating patterns in a signal, determining the presence of a periodic signal and identifying the missing fundamental frequency in an airflow propagation implied by its harmonic frequencies.

$$R_{ii}(T) = v_i'(t) \cdot v_i'(t+T) \tag{6.5}$$

$$\tilde{R}_{ii}(T) = \frac{\overline{v_i'(t) \cdot v_i'(t+T)}}{\overline{v_i}^2} \tag{6.6}$$

Power spectrum analysis

The power spectrum analysis can illustrate energy distribution of eddies with different frequencies. The negative slope of the logarithmic power spectrum curves β can be used as the index in the spectrum analysis (Zhou, 2006). Previous research indicates that the human-sensitive frequency region is between 0.01Hz and 1Hz. The density distribution of the variance over frequency, E(f), is the energy spectrum of the velocity fluctuation, and the integral of E(f) of all frequencies over the variance of the velocity. The spectra show energy distribution at different frequencies.

$$\int_0^\infty E(f) \cdot df = \overline{v'^2} \tag{6.7}$$

where f is the frequency of fluctuation.

The integral scale can be calculated from E(f) when f approaches zero (Hinze, 1975).

$$L = \frac{\bar{v} \cdot E(f)}{4\sigma^2} \tag{6.8}$$

The characteristic frequency of the largest eddies (Melikov et al. 1988) is

$$f_c = \frac{1}{2\pi\tau_i} \tag{6.9}$$

Characteristic frequency and energy spectra are used to describe the frequency of air velocity fluctuations.

Cross-correlation:

Cross-correlation (or sometimes "cross-covariance") is a measure of similarity of two airflow characteristics. It is a function of the relative time between the signals. According to Wiener–Khinchin theorem, the spectral density of the cross-correlation coherence reports a measure of the dependence of two airflow fluctuation signal:

$$\gamma^2 = \frac{E(|XY|^2)}{E(|X|^2)E(|Y|^2)} \tag{6.10}$$

where X and Y are the two airflow velocity function

Equivalent frequency

A new equivalent frequency was developed by Zhou (turbulence intensity is another characteristic parameter which demonstrates the turbulence amplitude of airflow):

$$f_e = \frac{1}{2\pi} \cdot \frac{SD_a}{SD_v} \tag{6.11}$$

Where SD_a and SD_v are the standard deviations of acceleration and velocity respectively and a is the acceleration of the velocity. They can be calculated with the following equations:

$$SD_v = \sqrt{\sigma^2} = \sqrt{\frac{\sum_{i=1}^{n}\left(V_i - \overline{V}\right)^2}{n-1}} = \frac{\int_0^{\frac{1}{2f}} A\sin(\omega\tau)d\tau}{2f_e} = 2\pi A \tag{6.12}$$

$$SD_a = \sqrt{\frac{\int_{\tau}^{\tau+\Delta\tau} a^2 d\tau}{\Delta\tau}} = \sqrt{\frac{\sum_{i=1}^{n} a_i^2}{n-1}} = \frac{\int_0^{\frac{1}{2f_e}} A\omega\cos(\omega\tau)d\tau}{2f_e} = \frac{2}{\pi} A\cdot\omega = 2\pi\cdot f_e \cdot SD_v \tag{6.13}$$

$$a = \frac{dV}{dt} \tag{6.14}$$

The determination of the equivalent frequency should be more than 10 minutes, such that 75% of the measurements will have a relative error less than 10%. Zhou found that most indoor air has an equivalent frequency between 0.2 and 0.6 Hz, and occupants are most sensitive to equivalent frequencies in the range of 0.2 to 0.6Hz.

6.3.2 Temperature variation analysis

The instantaneous value of air temperature, t:

Mean air temperature (over time), $\bar{t}$:

$$\bar{t} = \frac{1}{\Delta\tau}\int_{\tau}^{\tau+\Delta\tau} t\,d\tau \tag{6.15}$$

$$\bar{t} = \frac{\sum_{i=1}^{n} t_i}{n} \tag{6.16}$$

The standard deviation of the instantaneous air temperature, σ_t

$$\sigma_t^2 = \frac{1}{\Delta\tau}\int_{\tau}^{\tau+\Delta\tau} (t-\bar{t})^2\,d\tau \tag{6.17}$$

The RMS spectrum of the instantaneous air temperature

$$\int_{0}^{\infty} E(f)\,df = \sigma_t^2 \tag{6.18}$$

The ASHRAE S55-2004 specifies limits on cyclic operative temperature variation (i.e. where operative temperature repeatedly rises and falls within a period not greater than 15 minutes), expressed as an allowable peak-to-peak variation of 1.1^{o}C (2.0 ^{o}F).

6.3.3 Thermal comfort perception

To compare the results with the measurements, percentage of dissatisfaction due to draft (PD) was calculated to study the degree of induced unwanted air movement to the occupant. The equation is:

$$PD = (34 - T)(\overline{V} - 0.05)^{0.62}(3.14 + 0.37\overline{V}Tu)(\%) \quad (6.19)$$

where Tu is the turbulence intensity (%) is calculated by:

$Tu = \frac{SD_v}{\overline{V}} \cdot 100\%$ for measurement cases

$Tu = \frac{100(2k)^{0.5}}{\overline{V}}$ for simulation cases

For PD<100%, PD=100%.

Where k is the turbulent kinetic energy (J/Kg), T is the air temperature (^{o}C), $\overline{V}$ is the air velocity magnitude (m/s)

6.4 Results and Discussion

6.4.1 Results summary

The resulting derived parameters are summarized as in Tables 6.6 – 6.8. The graphs demonstrating the temperature variation in four measurement locations (supply diffuser, thermostat, seating position at 1.1m height and seating position at breathing zone level) are plotted in Appendix A. The power spectrum analysis for the measurement results are plotted in Appendix B.

Cases	Temp. swing (^{o}C)	Reduction of swing (%)	Vel. Swing (m/s)	Reduction of swing (%)	Temp. mean (^{o}C)	Vel. Mean (m/s)	Vel. Stdev	Tu (%)	PD of sitting area (%)	Dominant frequency	Equivalent frequency
Lo,24C,Fan Off	3.25	0.00	0.35	0.00	22.71	0.23	0.20	85.71	12.53	0.0078	0.0402
Lo,24C,45hz	2.06	36.62	0.30	14.29	24.15	0.27	0.04	14.87	12.15	0.0039	0.0509
Lo,24C,35hz	2.13	34.46	0.31	11.43	24.29	0.14	0.09	61.26	6.92	0.0039	0.0566
Med,24C,Fan Off	4.70	0.00	0.40	0.00	22.64	0.34	0.16	46.83	16.87	0.0117	0.0470
Med,24C,30hz	3.12	33.62	0.40	0.00	23.81	0.23	0.11	50.62	11.20	0.0078	0.0411
Med,24C,35hz	2.90	38.30	0.40	0.00	23.94	0.38	0.08	21.14	16.04	0.0058	0.0157
Med,24C,15-30hz	3.00	36.17	0.38	5.00	23.48	0.17	0.08	36.60	8.84	0.0039	0.0403
Med,24C,15-45hz	3.50	25.53	0.29	27.50	23.26	0.13	0.08	60.48	6.85	0.0078	0.0411
Med,24C,30-45hz	3.20	31.91	0.34	15.00	23.15	0.11	0.08	72.92	5.94	0.0078	0.0402
Hi,24C,Fan Off	4.85	0.00	0.57	0.00	22.97	0.40	0.18	45.43	18.45	0.0039	0.0509
Hi,24C,35hz	3.80	21.65	0.51	10.53	23.97	0.28	0.11	39.89	12.83	0.0039	0.0566
Hi,24C,40hz	3.25	32.99	0.30	47.37	24.07	0.24	0.06	15.04	11.18	0.0117	0.0470
Hi,24C,15-30hz	3.50	27.84	0.32	43.86	24.57	0.27	0.08	30.93	11.52	0.0039	0.0509
Hi,24C,15-45hz	3.10	36.08	0.25	56.14	23.35	0.19	0.10	52.47	9.90	0.0039	0.0566
Hi,24C,30-45hz	4.00	17.53	0.33	42.11	23.27	0.22	0.08	38.07	11.34	0.0117	0.0470

Table 6.6: Summary table of temperature swing, velocity swing, swing reduction rate, turbulence intensity, equivalent frequency and percentage of dissatisfaction at set point temperature 24℃.

Cases	Temp. swing (°C)	Reduction of swing (%)	Vel. Swing (m/s)	Reduction of swing (%)	Temp. mean (°C)	Vel. Mean (m/s)	Vel. Stdev	Tu (%)	PD of sitting area (%)	Dominant frequency	Equivalent frequency
Lo,22C,Fan Off	1.75	0.00%	0.32	0.00%	19.58	0.45	0.08	18.01	25.90	0.0039	0.0566
Lo,22C,45hz	1.23	29.71%	0.18	8.00%	21.82	0.17	0.03	20.04	10.31	0.0117	0.0470
Lo,22C,35hz	2.60	-48.57%	0.36	-2.29%	21.73	0.16	0.07	42.14	9.88	0.0039	0.0509
Med,22C,Fan Off	2.55	0.00%	0.40	0.00%	19.85	0.41	0.13	30.06	23.93	0.0039	0.0566
Med,22C,30hz	2.63	-3.14%	0.30	25.00%	21.04	0.38	0.05	12.42	20.58	0.0117	0.0470
Med,22C,35hz	1.68	34.12%	0.32	20.00%	21.75	0.26	0.08	29.59	14.75	0.0117	0.0470
Hi,22C,Fan Off	3.55	0.00%	0.41	0.00%	20.36	0.45	0.12	26.63	24.61	0.0039	0.0509
Hi,22C,30hz	2.87	19.15%	0.52	-26.83%	21.39	0.23	0.11	49.52	13.86	0.0039	0.0566
Hi,22C,40hz	2.37	33.24%	0.25	39.02%	21.44	0.44	0.05	12.33	22.14	0.0117	0.0470

Table 6.7: Summary table of temperature swing, velocity swing, swing reduction rate, turbulence intensity, equivalent frequency and percentage of dissatisfaction at set point temperature 22℃.

Cases	Temp. swing (^{o}C)	Reduction of swing (%)	Vel. Swing (m/s)	Reduction of swing (%)	Temp. mean (^{o}C)	Vel. Mean (m/s)	Vel. Stdev	Tu (%)	PD of sitting area (%)
Med,26C,Fan Off	4.85	0.00%	0.55	0.00%	22.97	0.23	0.22	94.31	12.27
Med,26C,30hz	3.25	32.99%	0.50	9.09%	26.22	0.18	0.13	72.11	7.00
Med,26C,35hz	3.17	34.64%	0.30	45.45%	26.19	0.26	0.06	20.97	9.38
Hi,26C,Fan Off	4.85	0.00%	0.68	0.00%	25.69	0.30	0.18	57.96	11.27
Hi,26C,30hz	3.85	20.62%	0.56	17.65%	26.22	0.26	0.09	35.02	9.38
Hi,26C,40hz	2.95	39.18%	0.40	41.18%	26.33	0.34	0.07	19.19	11.27

Table 6.8: Summary table of temperature swing, velocity swing, swing reduction rate, turbulence intensity, equivalent frequency and percentage of dissatisfaction at set point temperature 26℃.

6.4.2 Temperature fluctuation and swing

Figures in Appendix A illustrate the temperature swing temporal distribution in different locations. The largest temperature fluctuations occurred in the occupied sitting area (up to 6^{o}C). The amplification of temperature fluctuation was observed between sitting area and the wall-mounted thermostat location. At High speed air supply, the amplification of swing remained relatively high, but had no significant linear correlation. In contrast, the Low speed air supply had a significant linear correlation with the amplification ratio. These regression lines could be made use for effective thermostat control to reduce the swing of temperature at desired location. Table 6.9 and Figure 6.4 below demonstrate the amplification ratio in different cases.

Thermostat set point temperature (℃)	**FCU fan speed**	**Thermostat temperature swing (℃)**	**Space Temperature swing (℃)**	**Amplification**
22	High	0.26	3.55	13.50
24	High	0.29	5.40	18.62
26	High	0.44	6.15	13.98
22	Low	0.34	2.10	6.25
24	Low	0.34	3.40	10.06
26	Low	0.32	5.29	16.62
22	Medium	0.36	3.30	9.17
24	Medium	0.27	4.80	18.05
26	Medium	0.32	5.80	18.24

Table 6.9: Swing amplification between thermostat location and space

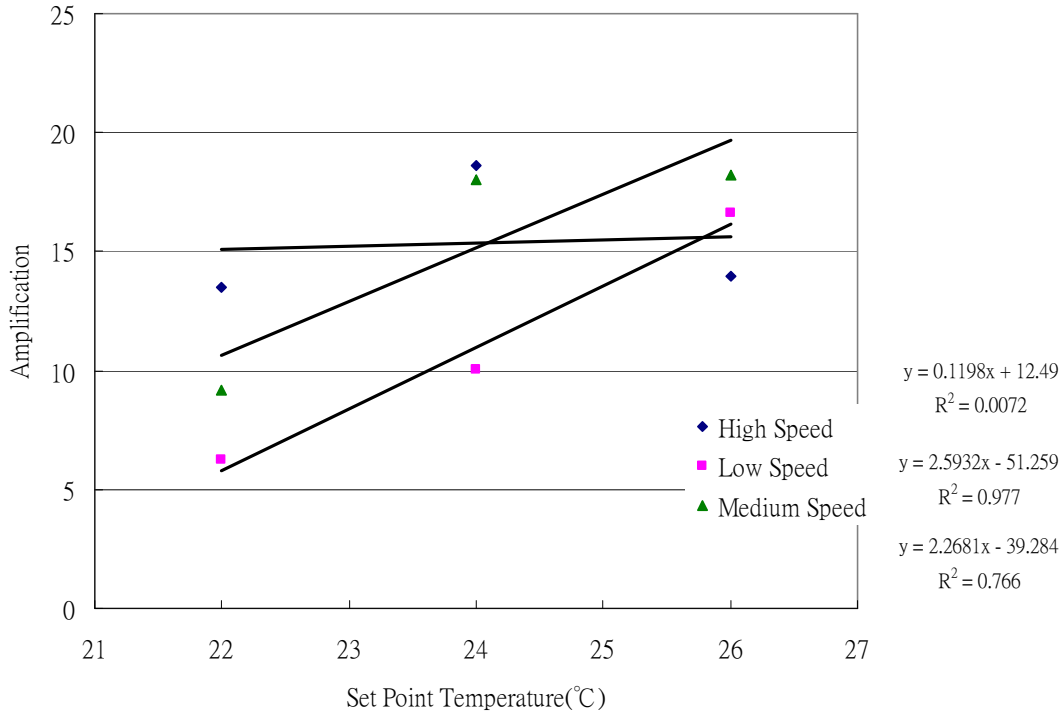

Figure 6.4: Relationship of thermostat set point temperature and swing amplification between sitting area and the wall-mounted thermostat location

6.4.3 Energy Spectrum Analysis

In real life, air temperature and velocity in indoor spaces is not static, even at closed points, as shown in Figure 6.5 (Melikov et al. 1997). The fluctuating air velocity and temperature may have an influence on the thermal sensation (Fanger and Pedersen 1977) along with periodical air velocity. The energy spectra of the measured velocity analyzed in this chapter indicated that the frequency of these fluctuating airflows was different. The dominant frequency and equivalent frequency are summarized in Tables 6.6 – 6.8.

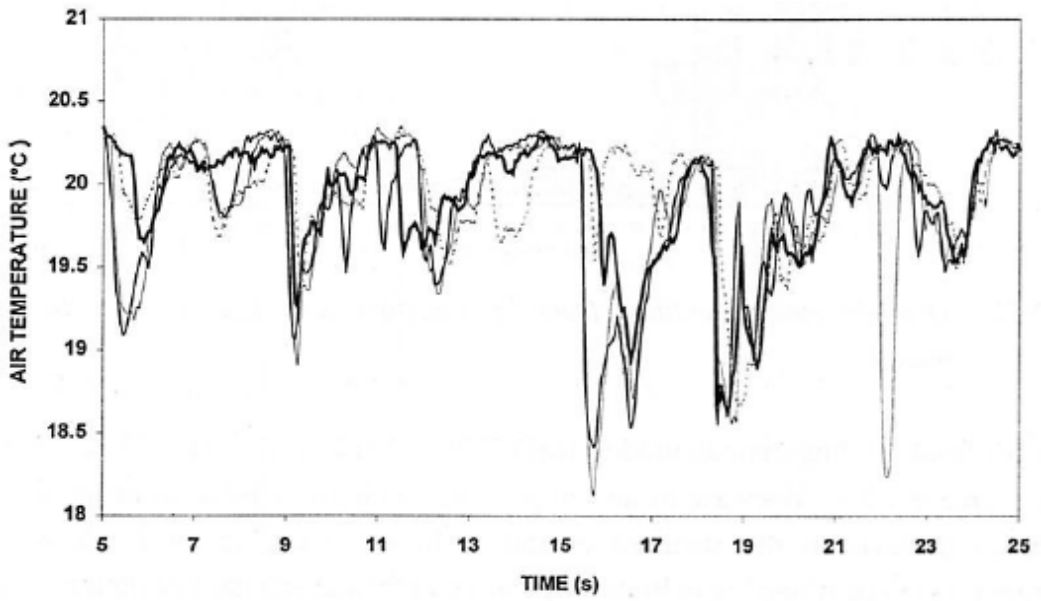

Figure 6.5: Simultaneous records of instantaneous temperature at four points located at a distance of 20mm between each other at a point within the occupied zone of a room with exhaust mechanical ventilation and window slots where large local temperature gradients were expected (Melikov et al. 1997).

6.4.4 Draught Sensation

According to the draught model (ISO 7730, 1995; ASHRAE Standard 55-05), the draught rate is calculated from the velocity and temperature values. Distribution of the draught rate is shown below. The mean of draught risk % in the two sitting positions decreases from 18% to 11% when HFCU was operated with centrifugal fan operation and fluctuating velocity (Figures 6.6 – 6.7)

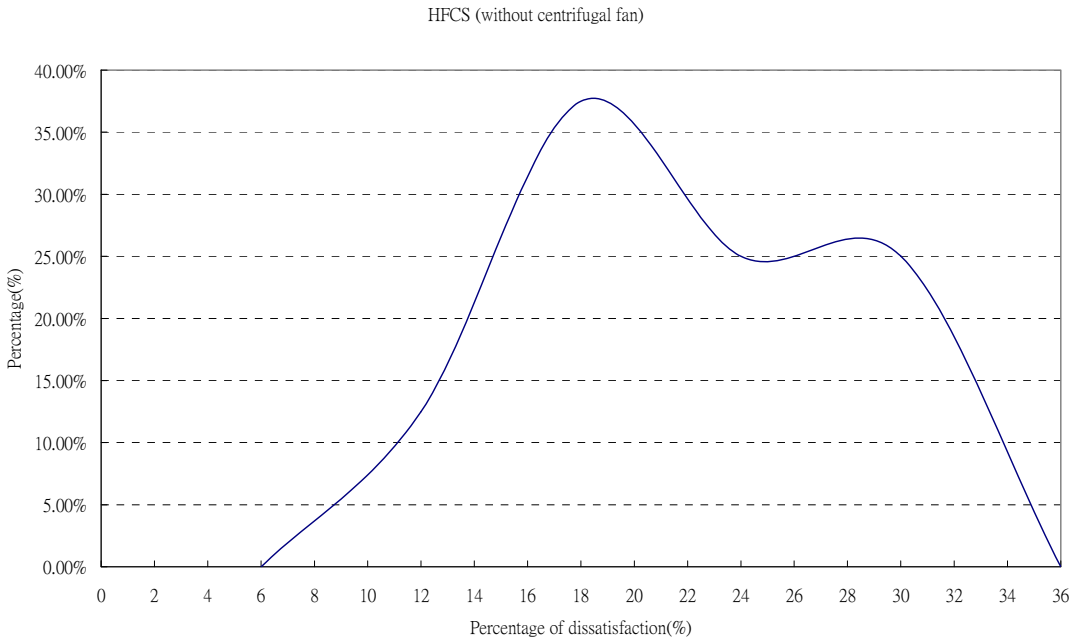

Figure 6.6: Draught risk (%) without centrifugal fan operation

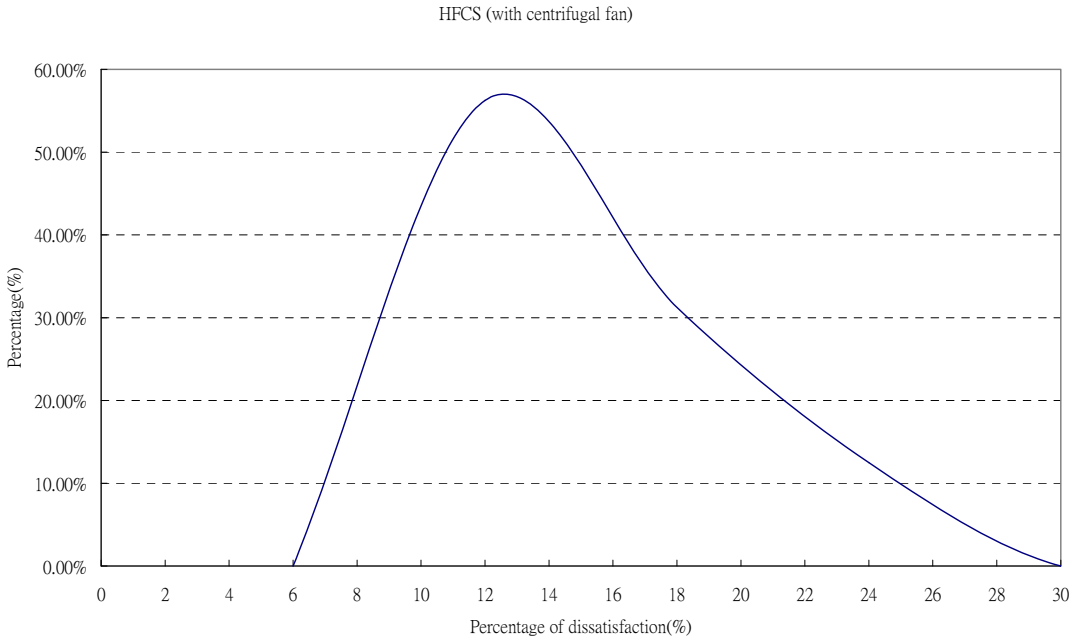

Figure 6.7: Draught risk (%) with centrifugal fan operation

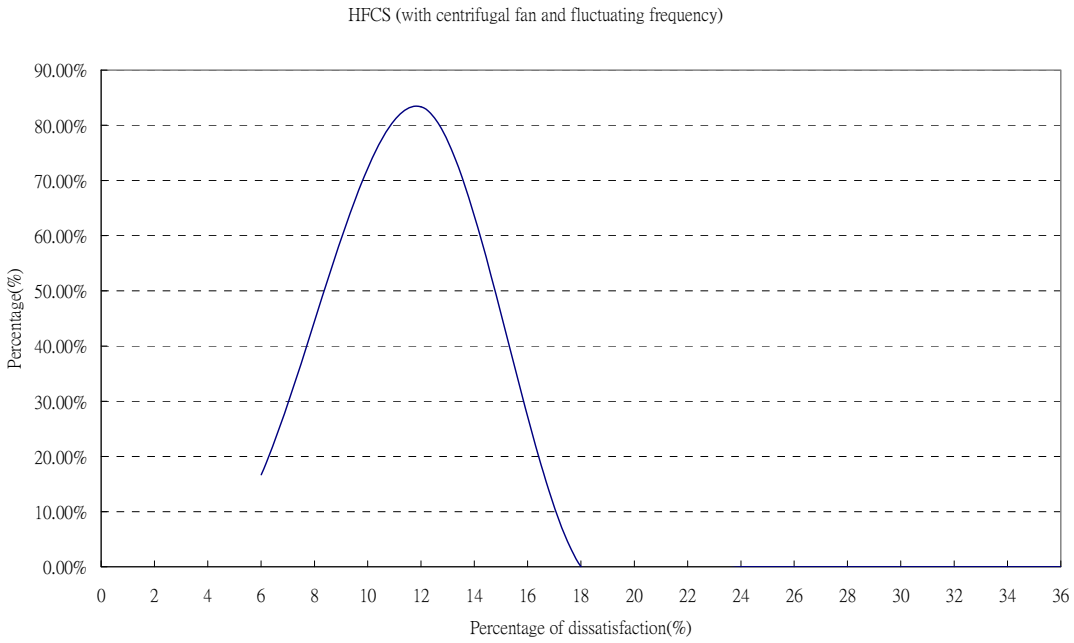

Figure 6.8 Draught risk (%) with centrifugal fan and fluctuating frequency

As known from the existing draught models (ISO 7730, 1995; ASHRAE Standard 55-05), the draught rate may increase with a decrease in air temperature, an increase in mean air velocity, or an increase in the standard deviation. In an occupied zone, air with a low temperature often combines with high mean air velocity and standard deviation as illustrated in Appendix C. Figures 6.9 – 6.11 demonstrate that the low temperature situation often meet with the high velocity. This will most probably cause a considerable draught sensation. The low air temperature should therefore be avoided in occupied zones to decrease the draught risk. Figures 6.12 and 6.13 demonstrate that fluctuating velocity air supply would help to compensate the draught risk by shifting the velocity profile.

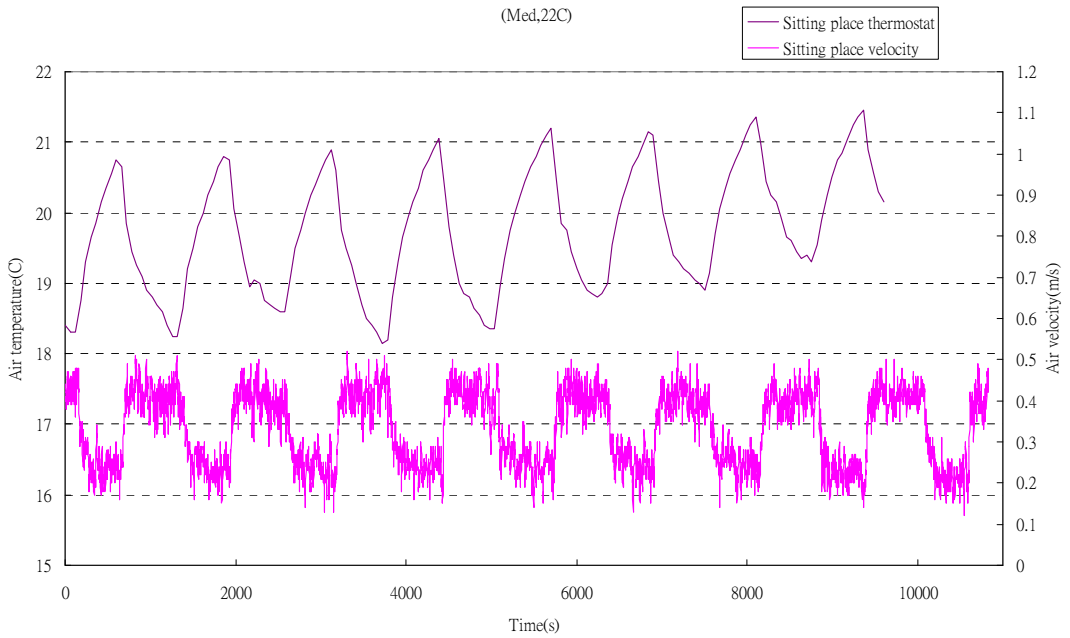

Figure 6.9: Correlation between air temperature and air velocity at set point 22℃ and med fan speed.

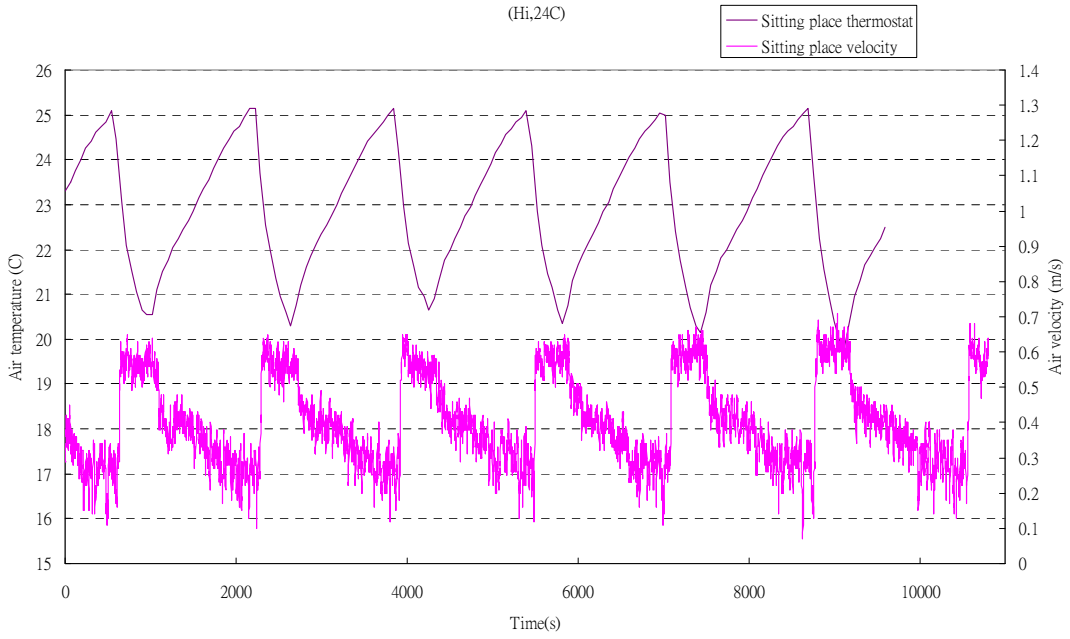

Figure 6.10: Correlation between air temperature and air velocity at set point 24℃ and hi fan speed.

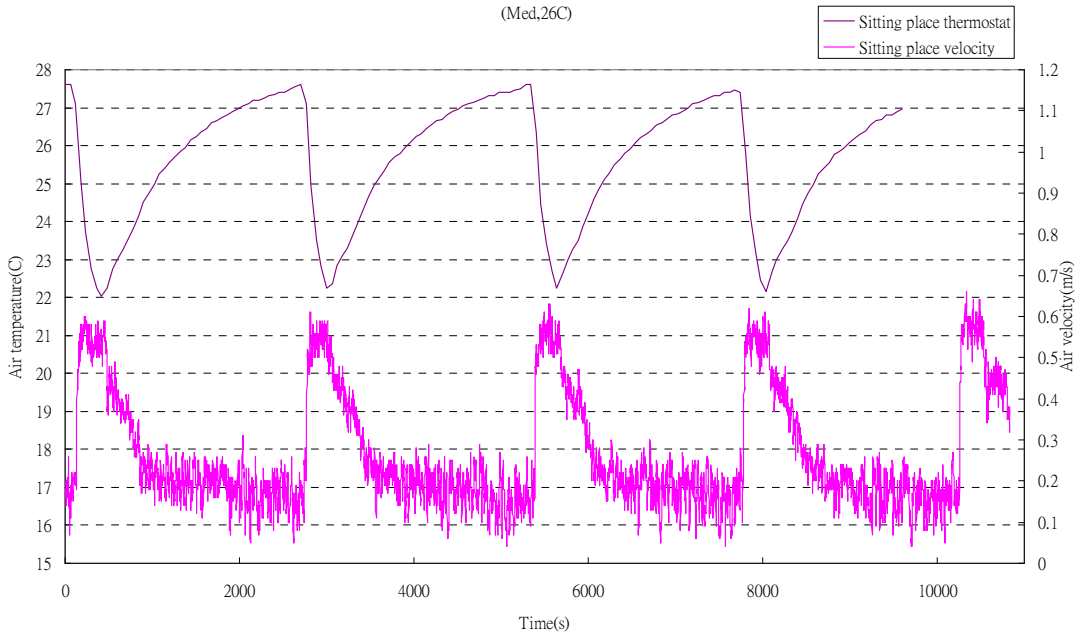

Figure 6.11: Correlation between air temperature and air velocity at set point 26℃ and med fan speed.

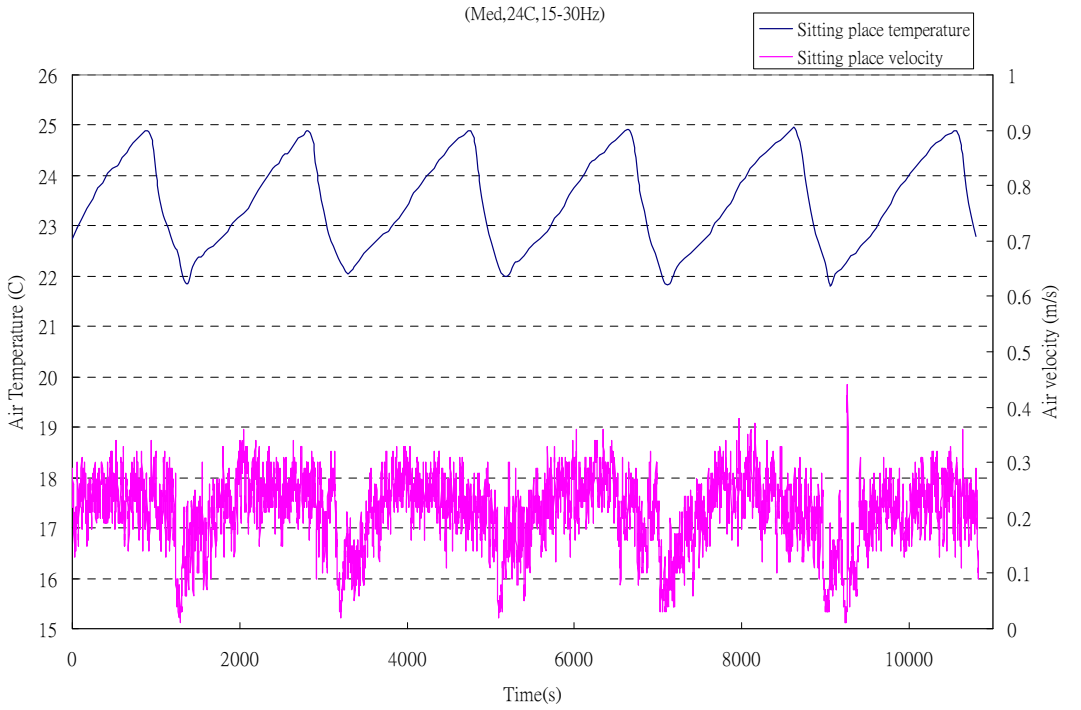

Figure 6.12: Correlation between air temperature and air velocity at set point 24℃, 15 to 30Hz frequency and med fan speed.

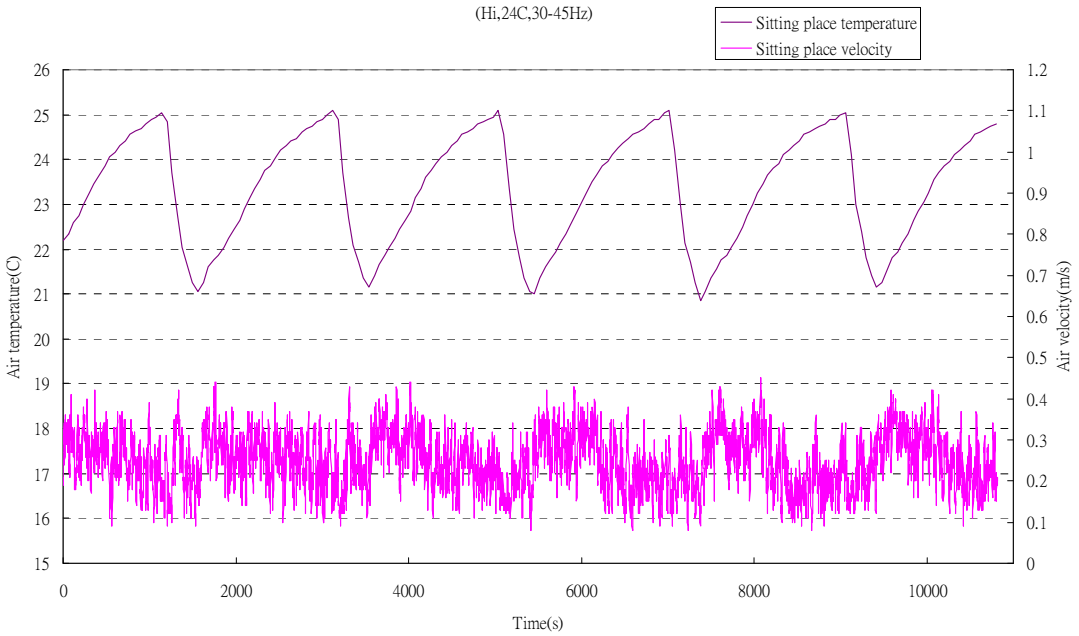

Figure 6.13: Correlation between air temperature and air velocity at set point 24 ℃, 30 to 45Hz frequency and hi fan speed.

In order to enrich this research on objective responses to dynamic behaviour of airflow in particular for the Hong Kong people, human experiments are proposed to be carried in future study. The influence of the five factors, mean air velocity, turbulence intensity, equivalent frequency, mean air temperature and airflow direction should be further evaluated.

6.4.5 Effect of mixing ratio of air supply

Another unique design of HFCU system is that the air supply volume could be varied by setting different frequencies of the secondary centrifugal fan; in return, setting the mixing ratio of the chilled cold air and bypass air could prevent the carry over problem and to maintain a proper humidity level indoor. The

relationship between mixing ratio and temperature swing is summarized in Table 6.9 below. Plotting the temperature differential of thermostat set-point and air temperature against the mixing ratio, increasing the mixing ratio is found to be effective to better control within the differential range of the temperature set point control. Meanwhile, increasing the mixing ratio could also reduce the temperature swing at the sitting position.

Test	Set point	FCU fan	Fan Box fan	Mixing ratio	Swing
1	22	Low	45	2.32	0.95
2	22	Low	35	2.19	2.60
3	22	Low	0	0	1.75
4	22	Medium	30	1.43	2.40
5	22	Medium	35	1.64	1.30
6	22	Medium	0	0	2.55
7	22	High	30	1.19	2.65
8	22	High	40	1.45	2.00
9	22	High	0	0	3.55
10	24	Low	45	2.32	2.15
11	24	Low	35	2.19	2.05
12	24	Low	0	0	3.25
13	24	Medium	30	1.43	3.05
14	24	Medium	35	1.64	2.90
15	24	Medium	0	0	4.70
16	24	High	30	1.19	3.80
17	24	High	40	1.45	3.25
18	24	High	0	0	4.85
19	26	Low	45	2.32	2.10
20	26	Low	35	2.19	2.65
21	26	Low	0	0	4.20
22	26	Medium	30	1.43	3.25
23	26	Medium	35	1.64	3.35
24	26	Medium	0	0	4.85
25	26	High	30	1.19	3.85
26	26	High	40	1.45	3.05
27	26	High	0	0	4.85

Table 6.10: Temperature swing and mixing ratio under different test cases

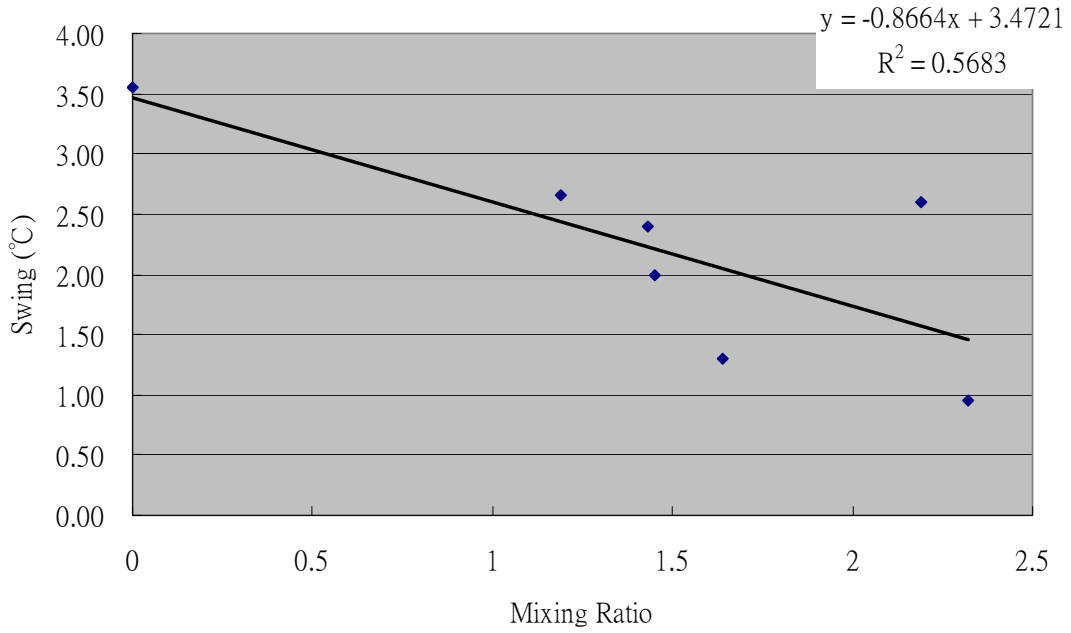

Figure 6.14: Relationship between space temperature swing and mixing ratio at set point temperature 22°C

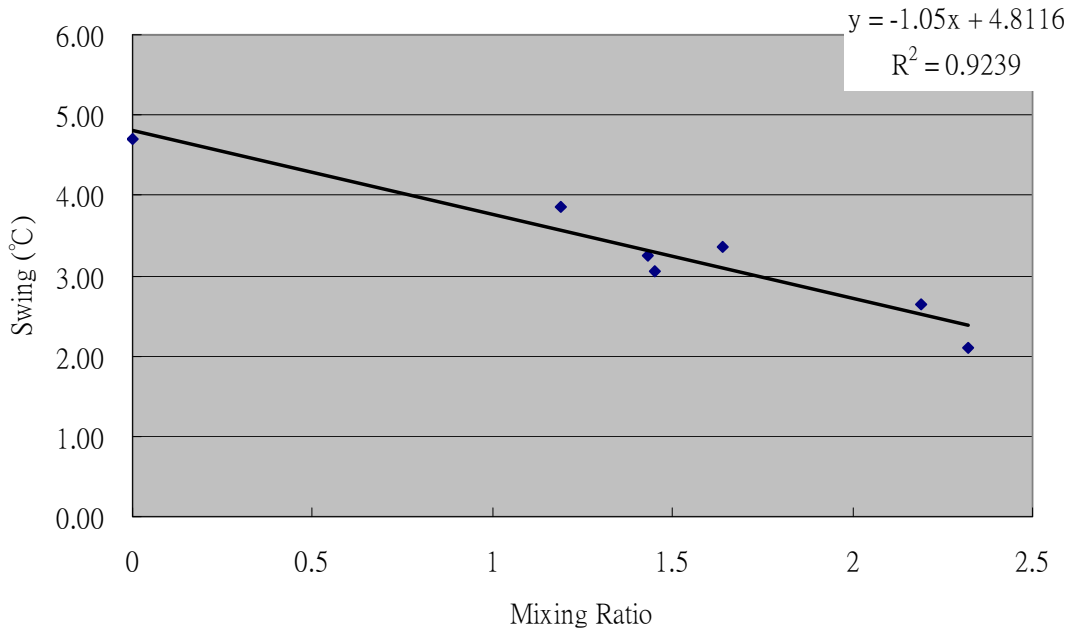

Figure 6.15: Relationship between space temperature swing and mixing ratio at set point temperature 24℃

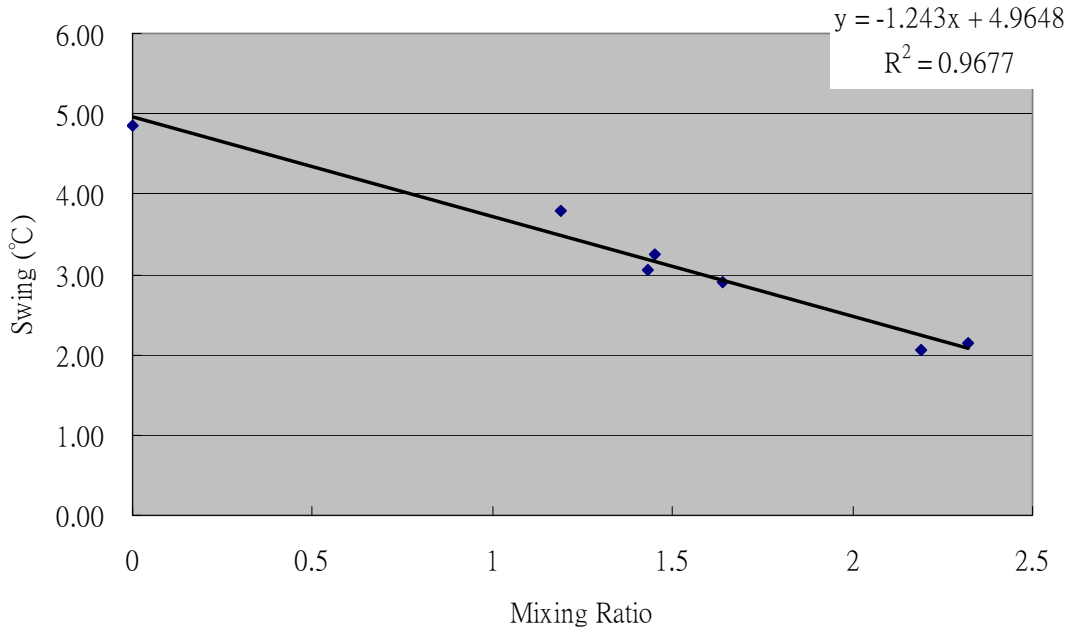

Figure 6.16: Relationship between space temperature swing and mixing ratio at set point temperature 26℃

Reduction of deviation between set point temperature and mean space temperature

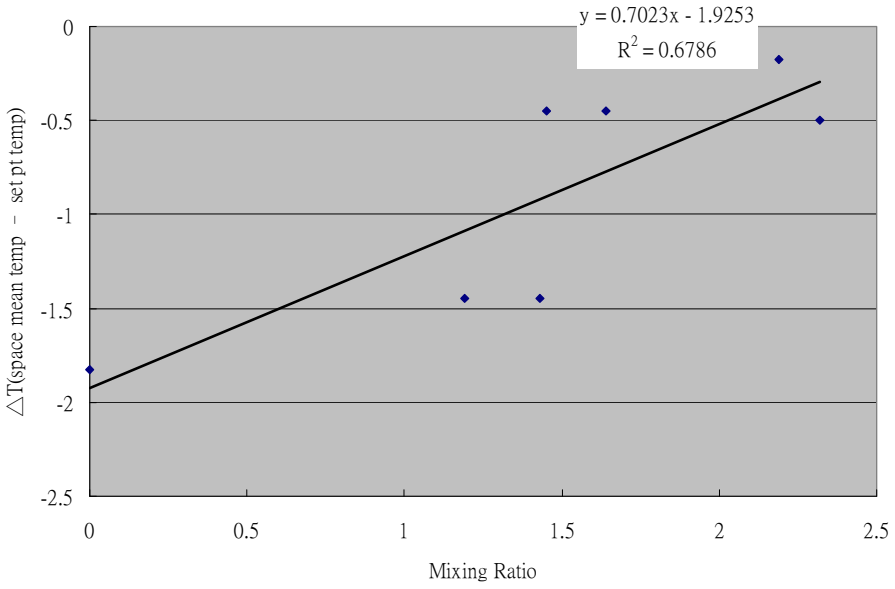

Figure 6.17: Relationship of space mean temperature and set point temperature deviation and mixing ratio at set point temperature 22℃

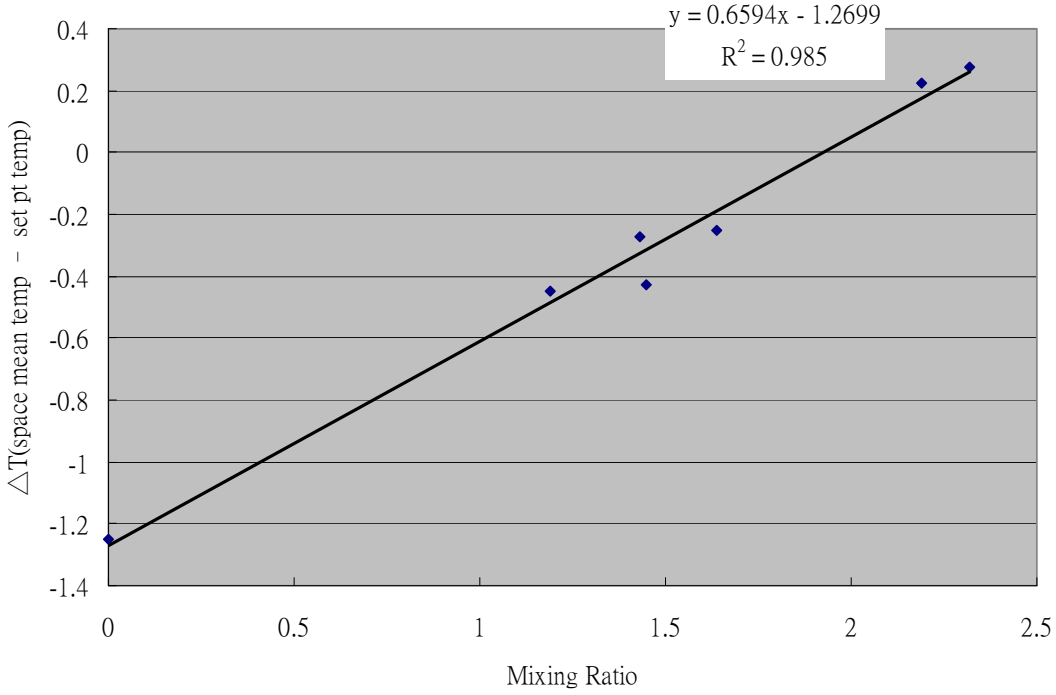

Figure 6.18:Relationship of space mean temperature and set point temperature deviation and mixing ratio at set point temperature 24 ℃

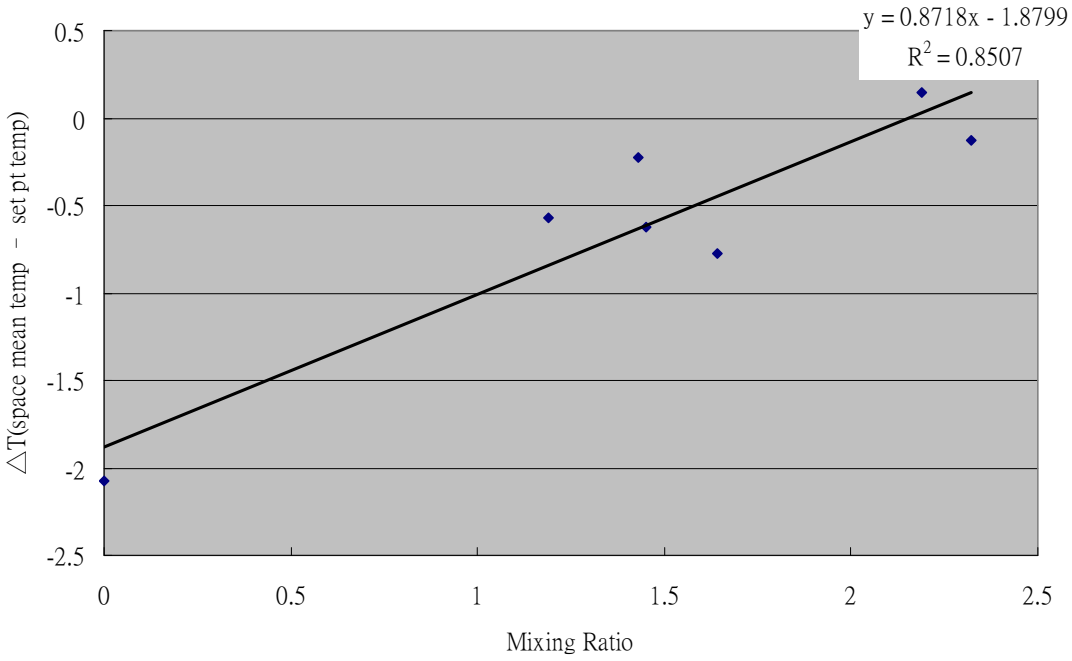

Figure 6.19: Relationship of space mean temperature and set point temperature deviation and mixing ratio at set point temperature 26 ℃

CHAPTER 7: COMPUTATIONAL FLUID DYNAMICS ANALYSIS

Researchers and engineers are paying more and more attention to the application of computational fluid dynamics (CFD) in setting a comfortable environment in building design. In this chapter, extensive computational fluid dynamics (CFD) with development of user-defined functions of airflow fluctuating parameters are investigated to verify the applicability of the harmonious fan coil system in practice, and to develop the CFD as a designed tool for sustainable thermal comfort operations.

A three-dimensional model was employed to report the harmonious fan coil system design in a typical office. Using the measured values as boundary conditions, the validation of the model and the result of different cases are analyzed in this chapter. This analytic tool also illustrates the technique developed for analysis under the dynamic nature of the system and environment.

7.1 Simulation model

In this Chapter, the simulation model was built based on the measurement results from Chapter 6. The model room is a typical single office in the Hong Kong Polytechnic University.

The simulation case consisted of 808199 tetrahedral meshes. For critical locations, for example, the diffuser and the region near wall boundary, smaller grids were applied. The grid actually divided the space into tiny little volume and after generating it, discrete algebraic equations were solved with the boundary condition settings. After initialization of the simulation, iterations were carried out until the convergence criteria were met. The convergence criteria was set to be 10^{-3} of sum of the absolute residual for the x,y,z momentum, continuity of mass, kinetic energy of turbulence and the dissipation rate of turbulence energy. For the convergence criteria of energy equation, it was set to 10^{-6}. For the transient simulation, the maximum number of iterations of time steps was 100 and the time for each time step was set to 1s.

The computations were carried out in a desktop computer with central processing unit of speed 2.67GHz, 2G random access memory (RAM). For the steady state simulation, each simulation takes about forty-eight hours and transient case takes about one week for several cycles of fluctuations of the supply air.

Figure 7.1: The geometry of the simulation model

7.2 Boundary condition

The measurement site was a one-person office with dimensions of 2.9m x 3.9m x 2.5m. There was no significance temperature difference between the two sides of all the internal walls as all other zones were also air conditioned. It was assumed that no heat gain came from the entire internal wall.

The surface temperatures of the wall, the office equipment, the person and also the light fixture were measured and set as the boundary condition in the simulation. The measurements also took into account the effect of irradiation due to the temperature differences among different surfaces. A square diffuser was simulated by the momentum method as it is impossible to simulate the real complex geometry for the diffuser (Chen, 1991). The boundary conditions for the diffuser needed the velocity magnitudes, the flow direction and also the turbulence intensity around the diffuser to be taken by site measurement. The vertical flow direction for a square diffuser was a 30^{o} bend away from the normal vertical of the plane. The horizontal component was in four directions which was perpendicular to one another as shown in the following picture.

Figure 7.2: The geometry of the supply and return diffuser

In normal operation of a fan coil unit, the moderating valve controls the flow rate of the chilled water supply to the fan coil unit. In this case, the supply air temperature varied from time to time. The temperature of the supply air, during the measurement, was measured by a hobo logger hung on the diffuser. The measured profile of the supply air temperature is shown in the following figure.

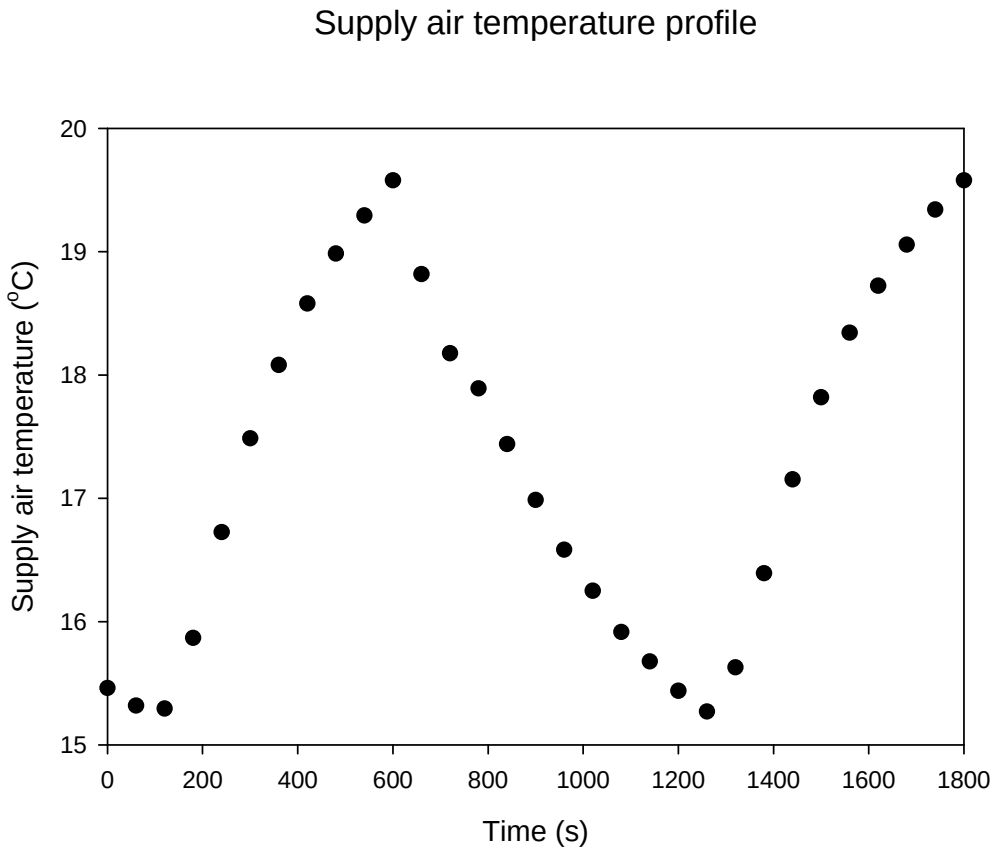

Figure 7.3: Measured value of the supply air temperature profile

Because the supply air temperature of a base case is not constant, user-defined function (UDF) was needed to set up the boundary condition. Thus, the measured temperatures needed to be fitted in a function form such that it can easier to written into the UDF.

Marquardt_Levenberg algorithm (Marquardt, 1963) was applied for the curve fitting of the supply air temperature for the fan coil unit. This is an iterative process starting with a randomly generated guess. The result is then checked if it fits the curve, and better fit data is generated until the residual sum of squares comes to a convergent condition. The following equation shows the predictive algorithm:

$$SS = \sum_{i=1}^{n} w_i \left(y_i - \hat{y}_i \right)^2 \qquad (7.1)$$

Where y_i is the observed data and $\hat{y}_i$ is the predicted data.

The selected step size was 100, tolerance was 0.000100 and the maximum number of iterations was set to be 100.

Standard error

CV(%) is coefficient of variation, similar to standard error but with normalization. It is calculated as:

$$CV(\%) = Std.error \times 100\, parametervalue \tag{7.2}$$

Dependency shows the degree of dependency that the value is between each other. It is calculated as:

Dependency = 1-(variance of the parameter, other parameters constant)/(variance of the parameter, other parameters changing)

As the (variance of the parameter, other parameters constant)/(variance of the parameter, other parameters changing) approaches zero, the higher the correlation between the two parameters.

The data is fit against:

$$y = y_o + a\sin\left(\frac{2\pi x}{b+c}\right) \tag{7.3}$$

The result of the curve fitting is as follows:

	Coefficient	Std. Error	CV(%)	Dependency	t	P
a	1.9703	0.0714	3.623	0.00336235	27.6040	<0.0001
b	1172.0594	15.9422	1.36	0.7148898	73.5192	<0.0001
c	5.3691	0.0669	1.247	0.7208331	80.2017	<0.0001
y_o	17.2776	0.0519	0.3003	0.0917311	333.0039	<0.0001

Table 7.1: Result of the curve fitting of the supply air temperature profile

Analysis of Variance

	DF	SS	MS	F	P
Regression	3	54.9420	18.3140	258.2864	<0.0001
Residual	25	1.7726	0.0709		

Table 7.2: Table of ANOVA analysis

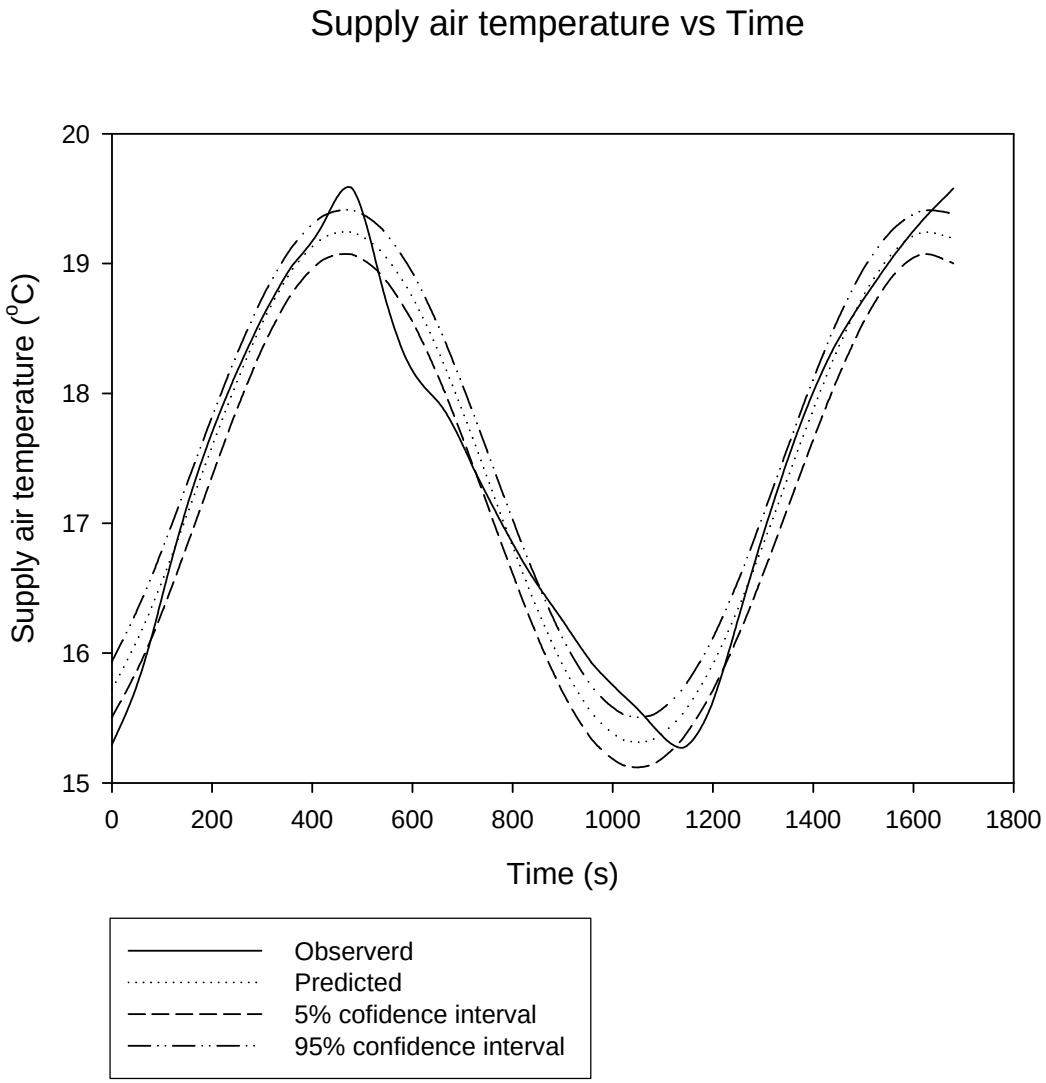

Figure 7.4: Measurement result with regression curve in confidence interval between 5-95%.

The above results show that the regression model can fully represent the measured data. Therefore, this function can be applied in writing the boundary condition user-defined function of the supply air temperature in the base case.

Other boundary conditions of the simulation cases are shown in the following table:

	Temperature (K)	**Heat flux (W/m^2)**
Window	305	79W/m2
Person	307	65W/m2
Printer	N/A	38.5W/m2
Light fixture	303	53.3W/m2
External wall	N/A	4W/m2
PC	N/A	135W/m2
Monitor	N/A	107W/m2

Table 7.3: Boundary condition of the simulation

7.3 CFD result validation

The validation was performed based on a typical case with a normal operating fan coil unit. The case was a constant air flow with varying supply temperature due to the moderating valve controlling the flow rate of the chilled water. Therefore the average value of the velocity and the transient profile were selected for the validation of the simulation result against the measured result.

Figure 7.6 shows the transient temperature profile and the comparison between the selected measurement data set and the simulation results. The eight points selected to represent the room's characteristics include the quest location, occupant location, thermostat surface, center of the room, supply and return of the fan coli unit.

Figure 7.5 shows the comparison of the CFD model with the time average velocity of the measured result. The velocity of the room was relatively low with values in the range of 0.01-0.1m/s. Although there were discrepancies between the simulation and the measured result at some points, the agreement between them is acceptable. These discrepancies were due to the measurement uncertainty of the hot wire anemometer.

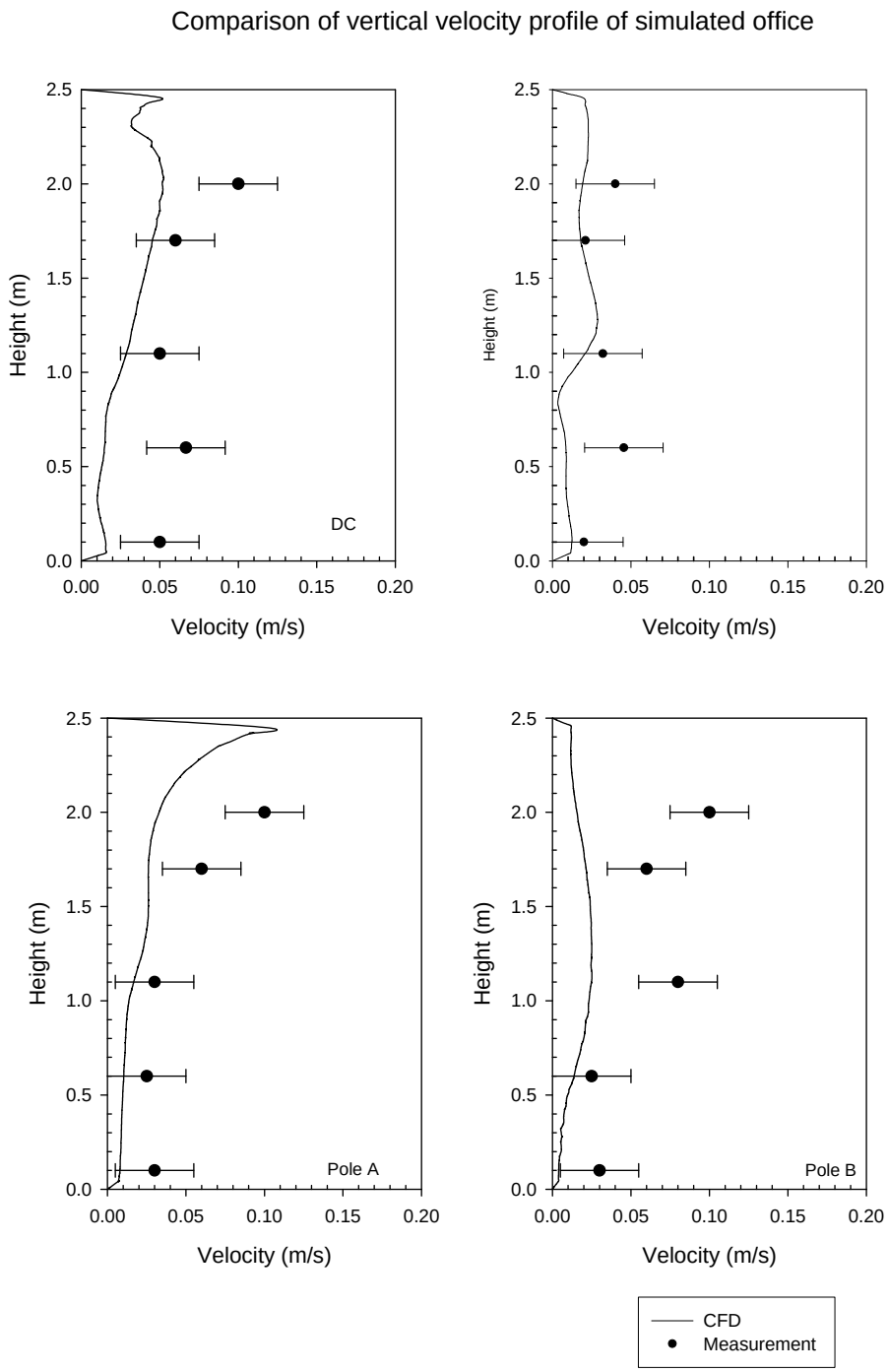

Figure 7.5: Comparison of CFD and measurement results over height

Figure 7.6 demonstrates fluctuation of the room temperature due to the changes of varying supply air temperature following the modulating chilled water supply. The result shows that the fluctuation was the largest in the center position of the room. This can be explained by the fact that distance between the point and the supply

diffuser was the shortest. Therefore, the fluctuation was deeply influenced by supply air temperature variations. The highest temperature profile was recorded in the thermostat location, as it was the most downstream location from the supply.

When compared to the profile of seating position A (y=0.6m) and seating position B (y=1.1m), It shows that the temperature of seating position (y=1.1m) was generally higher since the heat plume of the human increased the temperature to a higher level for the same location.

All simulation models were validated by data measured. For steady state simulations, vertical profiles of temperature and velocity were employed to check validity. For the transient simulation, the profile of temperature against time and the vertical profile of velocity compared against the time-rated average velocity data from measurements were used for the validation.

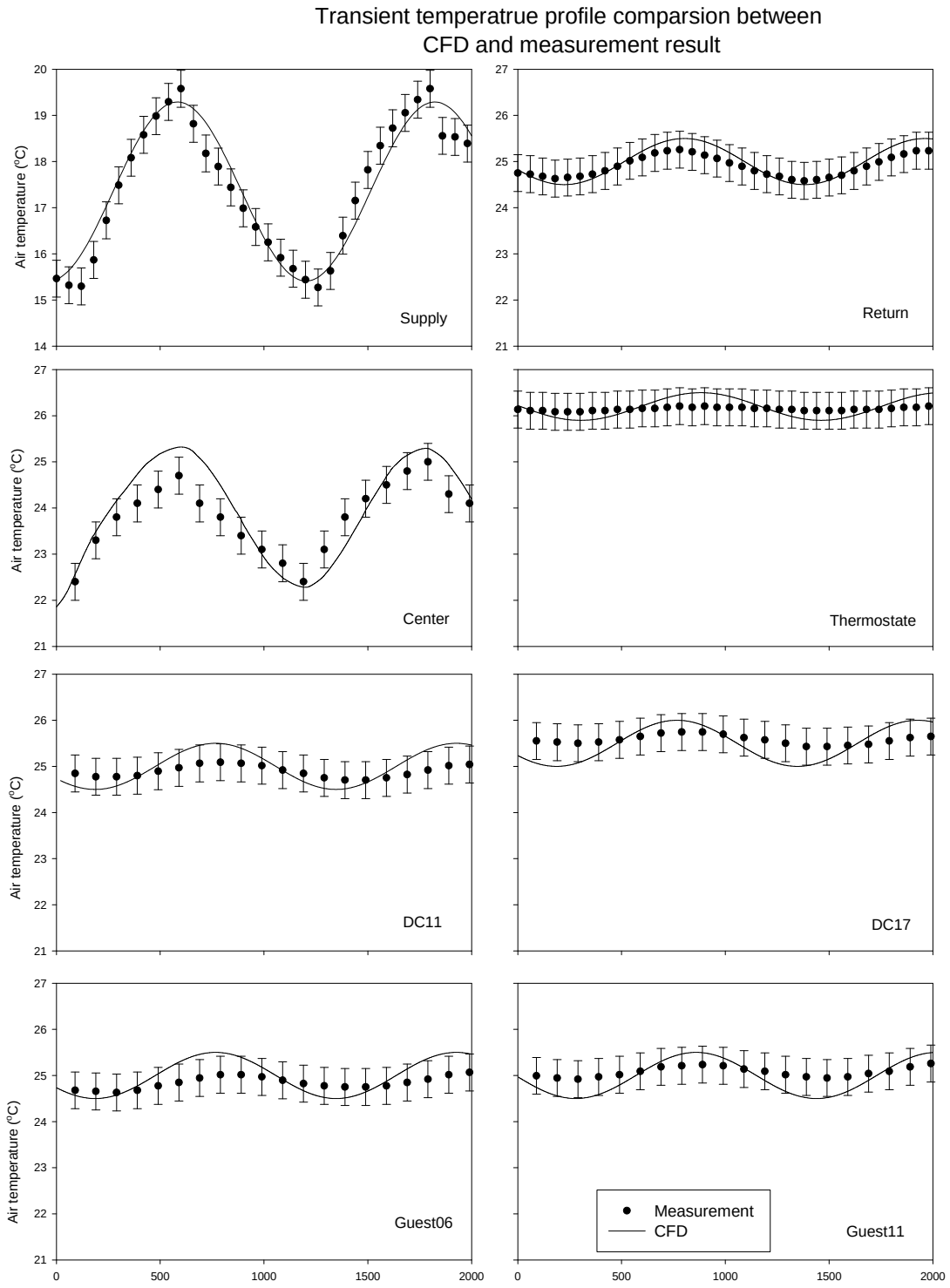

Figure 7.6: Temperature profile for the measured and the simulation result

The following graphs illustrate the result of the contour map of the temperature and the velocity profiles of different planes of the base case:

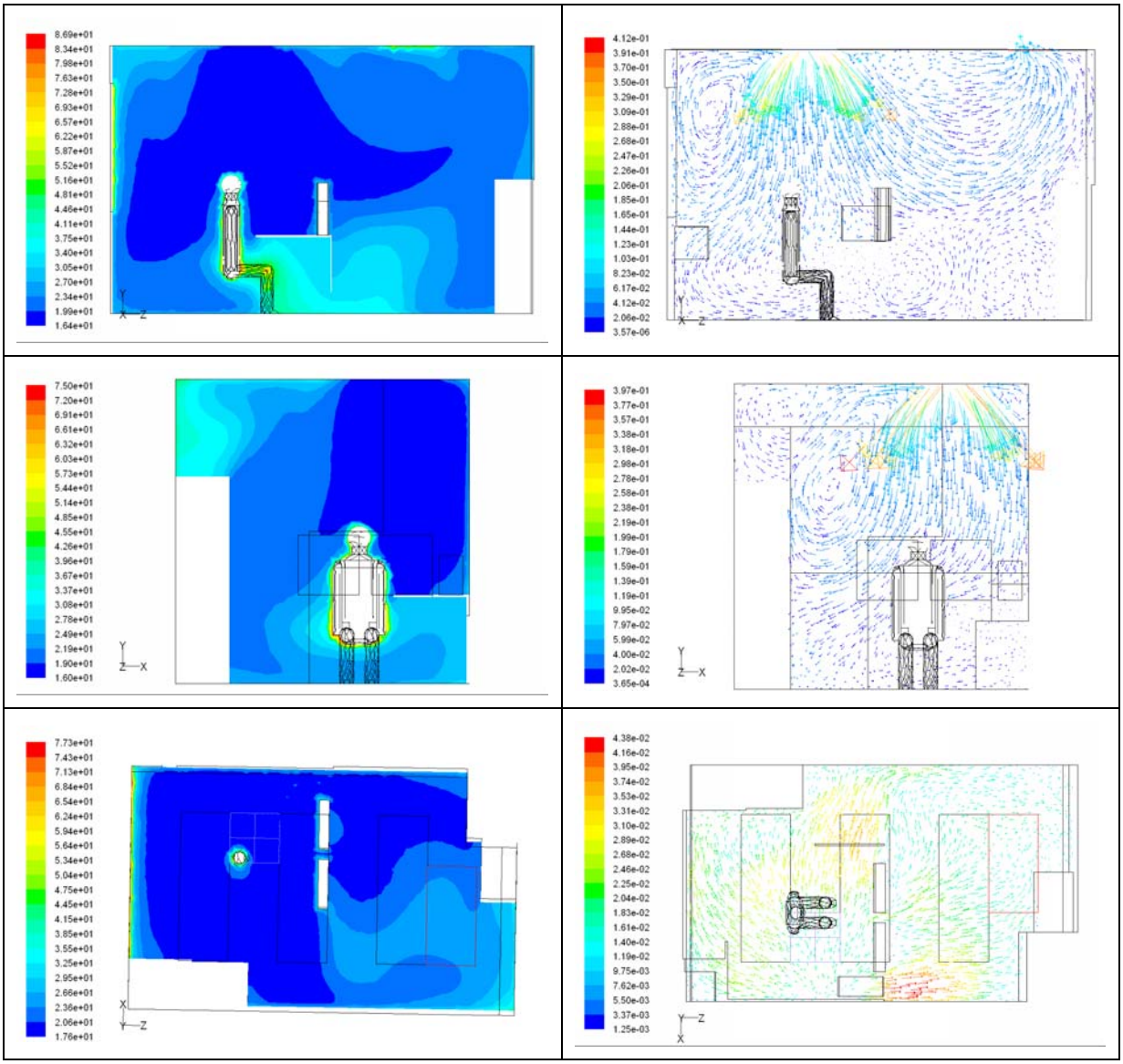

Figure 7.7: Temperature and the velocity contour of different planes of the base case.

7.4 Simulation of fluctuating airflow with different frequencies

Frequency spectrum analysis is much more useful than probability density analysis and autocorrelation coefficient in determining the dominant frequency and turbulence eddies' power density and corresponding frequency. According to the literature review in Chapter 1, the frequency spectrum of the velocity profile to the designated location plays a dominate position in the thermal comfort condition of the occupant. Therefore, one of the major criteria to represent the airflow characteristics at one point is the frequency spectrum of the transient velocity. Both the studies of Pedersen (1977) and Madsen (1984) demonstrated that maximum discomfort is found at about 0.5Hz. Fanger and Pedersen (1977) also reported that maximum discomfort was experienced when air velocity fluctuated at a frequency between 0.3 and 0.5Hz. Therefore, the fluctuating frequency of the velocity ranges from 0.2 to 0.001 Hz for simulating the harmonious fan coil unit. The maximum and minimum bounds of the simulated profile were derived from the measurement values as indicated in Chapter 6 (Figure 7.8). The simulation cases are summarized as follows:

Case	**Supply air temperature (^oC)**	**Frequency (Hz)**
A	17	0.2
B	17	0.01
C	17	0.02
D	17	0.001

Table 7.4: Summary of simulation cases

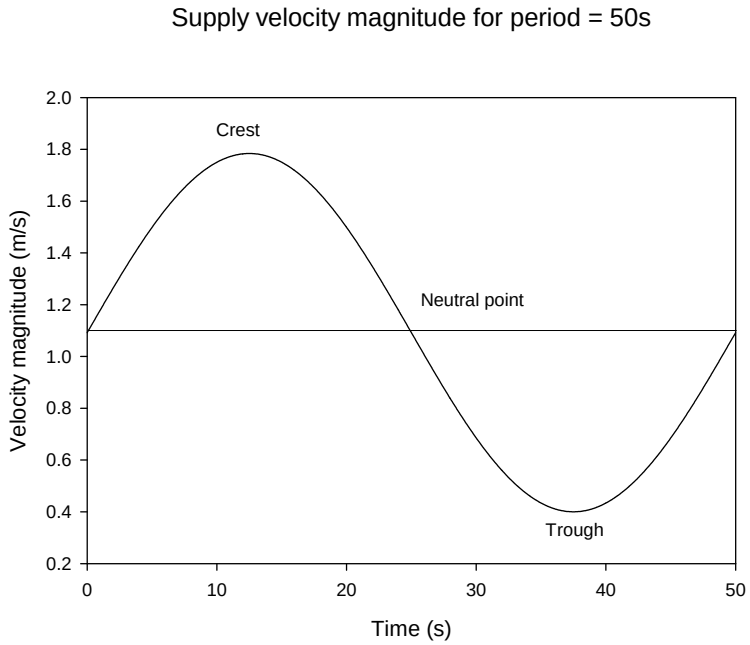

Figure 7.8: Supply velocity profile (0.2Hz)

0.2Hz **Crest** **Neutral** **Trough**

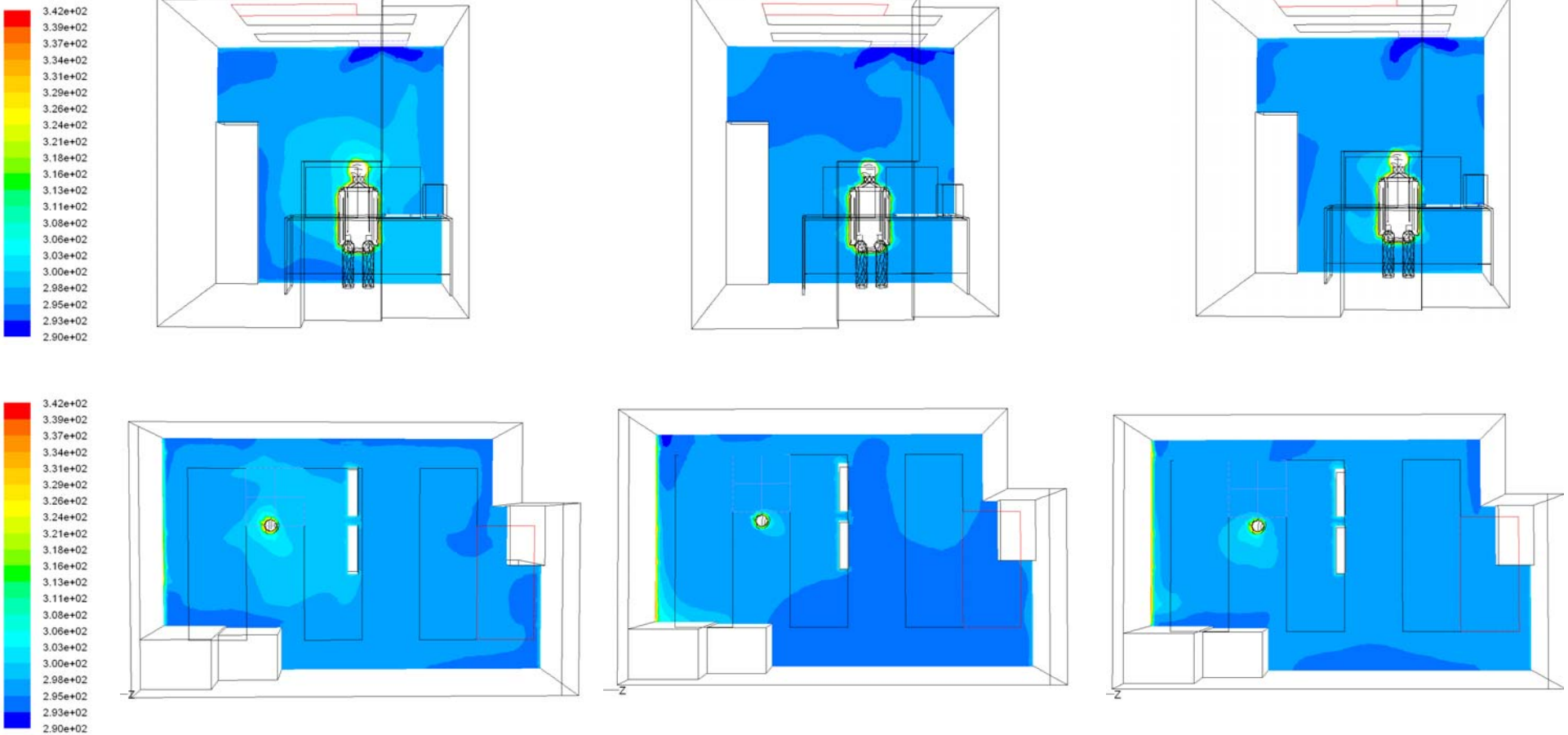

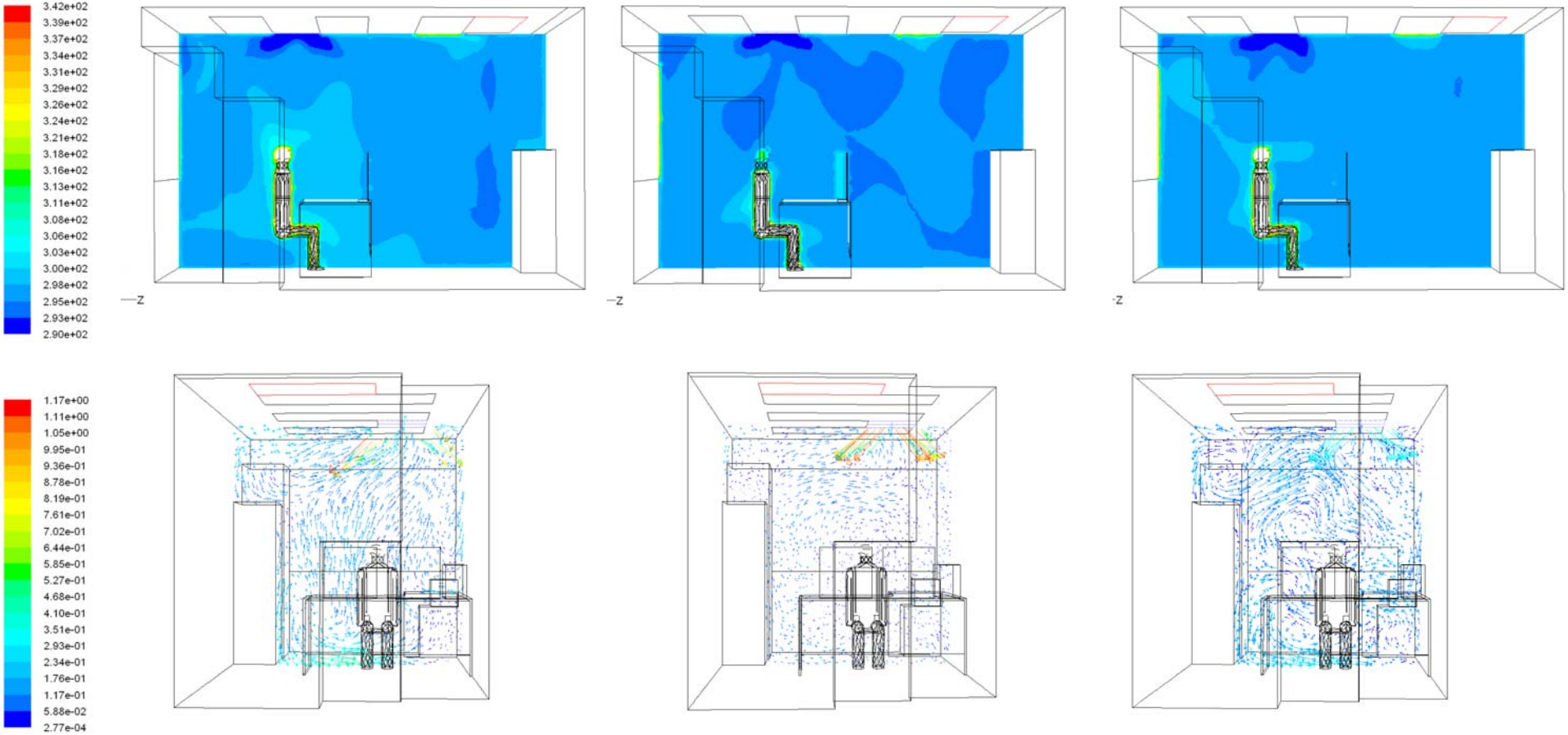
3.42e+02
3.39e+02
3.37e+02
3.34e+02
3.31e+02
3.29e+02
3.26e+02
3.24e+02
3.21e+02
3.18e+02
3.16e+02
3.13e+02
3.11e+02
3.08e+02
3.06e+02
3.03e+02
3.00e+02
2.98e+02
2.95e+02
2.93e+02
2.90e+02
1.17e+00
1.11e+00
1.05e+00
9.95e-01
9.36e-01
8.78e-01
8.19e-01
7.61e-01
7.02e-01
6.44e-01
5.85e-01
5.27e-01
4.68e-01
4.10e-01
3.51e-01
2.93e-01
2.34e-01
1.76e-01
1.17e-01
5.88e-02
2.77e-04

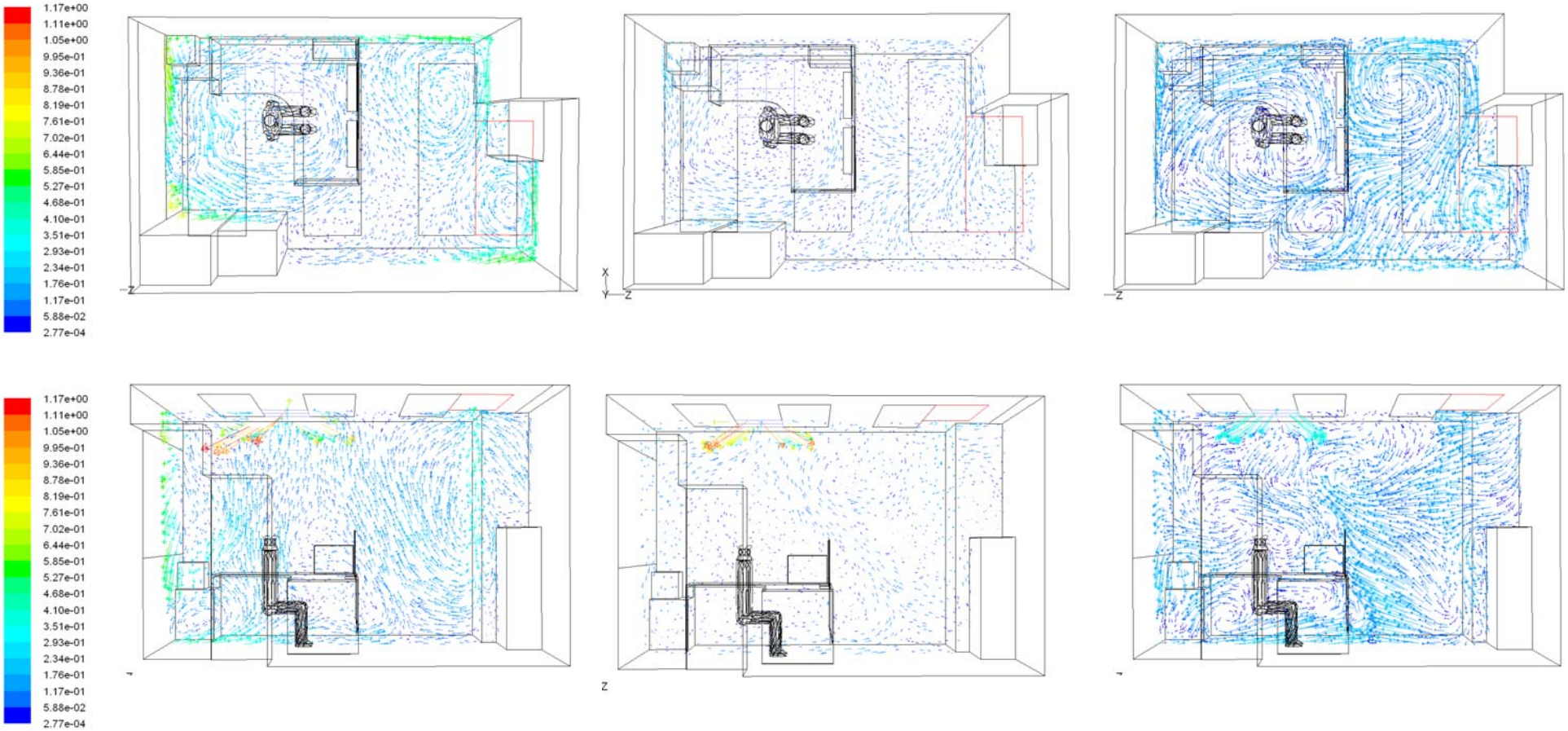

Figure 7.9: Contour of temperature and vector of velocity magnitude of different plan (0.2Hz)

The frequency of the sinusoidal airflow, generated from the UDF sine wave function, was 0.2 Hz, simulating the frequency of the new harmonious fan coil unit system design. The dominant frequencies of all cases at different locations were found to be about 0.2 Hz, which was perfectly compatible with the supply airflow fluctuations with various amplification of airflow amplitude, as illustrated in Figures 7.10-7.17.

To validate the transient simulation prior the application of this program in other design conditions, frequency spectrum analysis was employed to compare the frequency spectrum and dominant frequency consistence. The agreement between measured values and simulation results is very good that their coherent coefficient in most cases equals to 0.9. The computed turbulence intensity was not as good as that for the transient temperature and velocity profile; this may due to the measured location was located at the strong turbulence regions and at a higher air velocity.

7.5 Summary

Since indoor temperature and airflows were not uniformly distributed within space in most cases, the variation of thermal comfort parameters leads to the difference between occupied zone and thermostat location, which was often located outside the occupied zone. By determining the correlation of the comfort parameters between the thermostat location and the occupied zone or the room characteristics, it helpe to identify a better position for the thermal control sensor and to develop a better control for temporal and spatial distribution within space. For an enclosed room equipped with the

harmonious fan coil unit, the room thermal transient response and indoor air distribution were computed with user-defined function code incorporating the measured temperature and airflow profiles. With the transient response computed, the most suitable position

This research successfully used validated CFD model as a simulation tool to study the dynamic airflow and indoor temperature characteristic in designing a thermally comfort space as well as predicting the thermal condition in occupied or working zone.

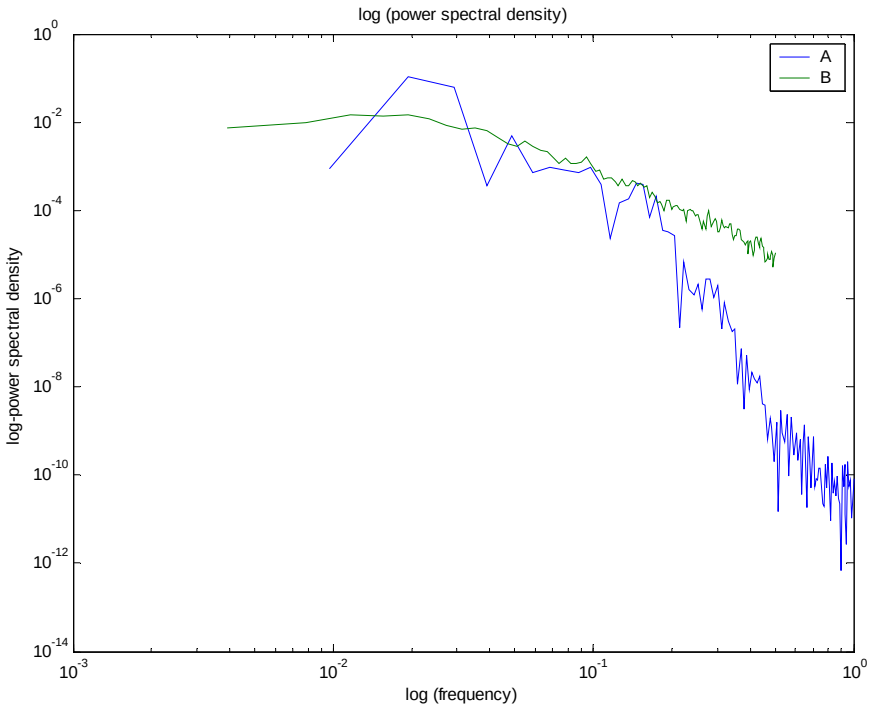

Figure 7.10: Airflow fluctuation characteristics comparison of simulation and measurement at the sitting position

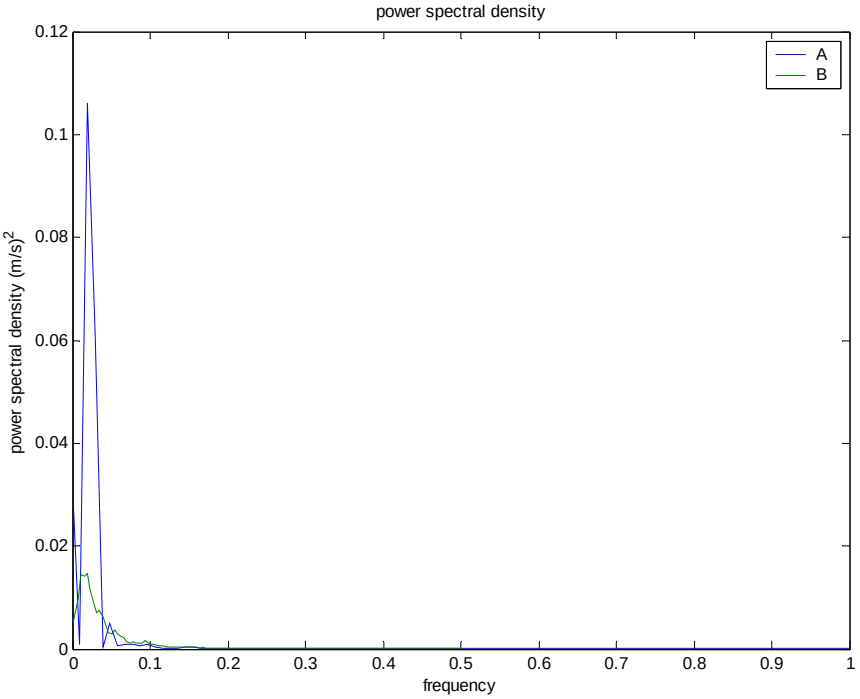

Figure 7.11: Airflow fluctuation characteristics comparison of simulation and measurement at the sitting position

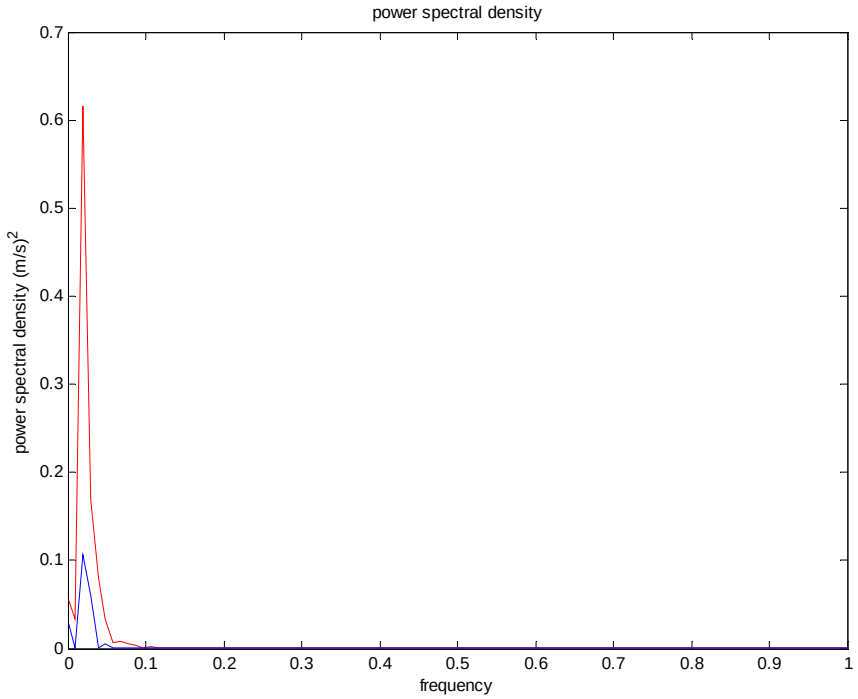

Figure 7.12: Airflow fluctuation of supply vs sitting location (0.2Hz)

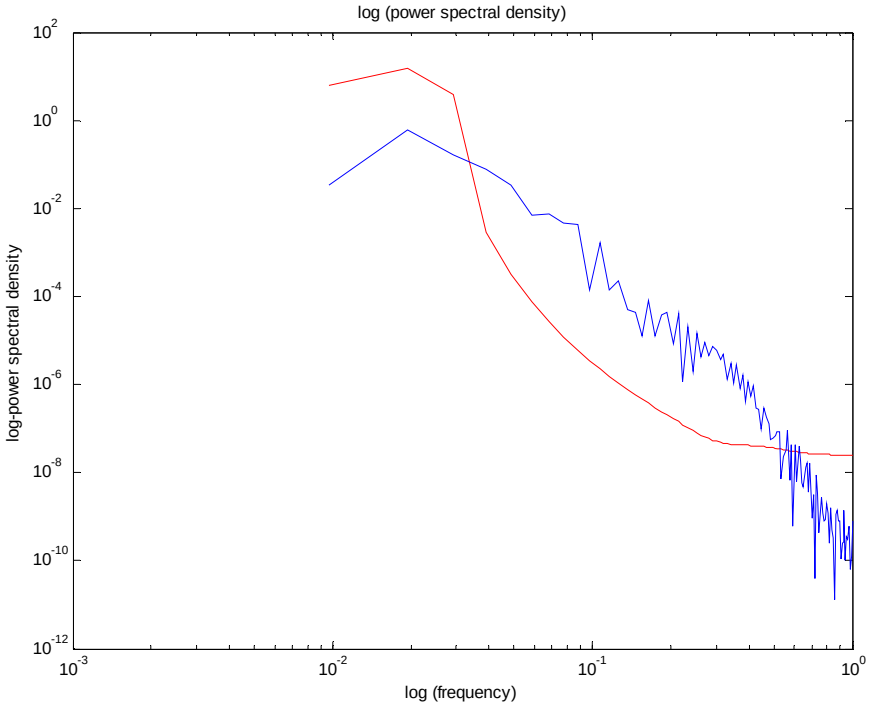

Figure 7.13: Airflow fluctuation of supply vs sitting location (0.2Hz)

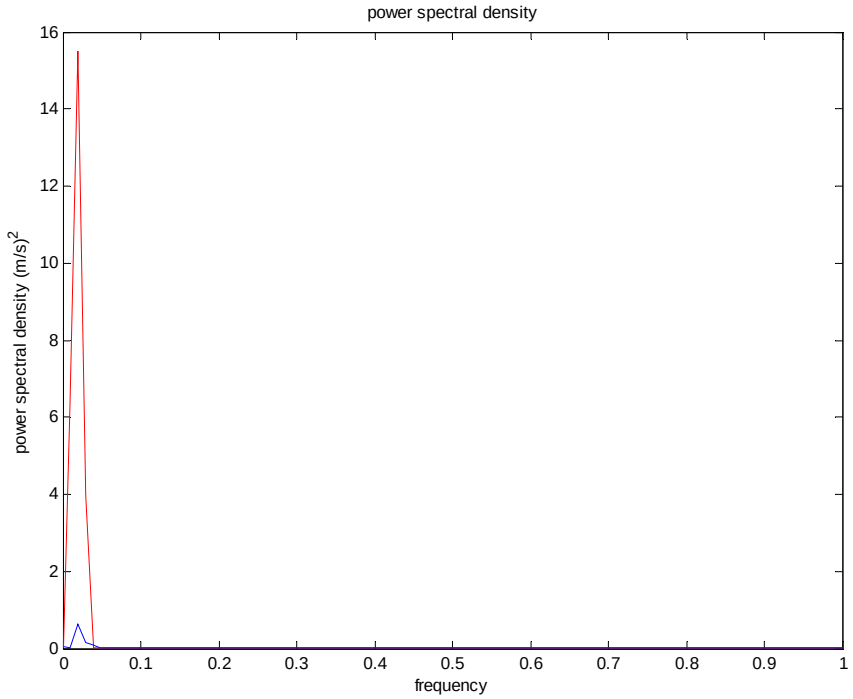

Figure 7.14: Power spectrum density of airflow fluctuation – air supply vs thermostat (0.2Hz)

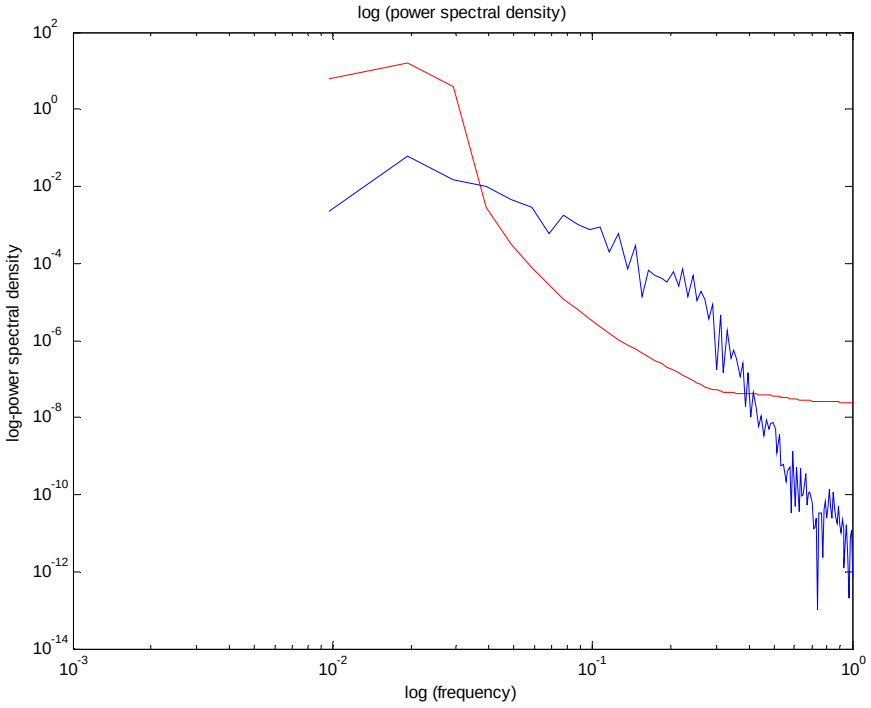

Figure 7.15: log- power spectrum density of airflow fluctuation – air supply vs thermostat (0.2Hz)

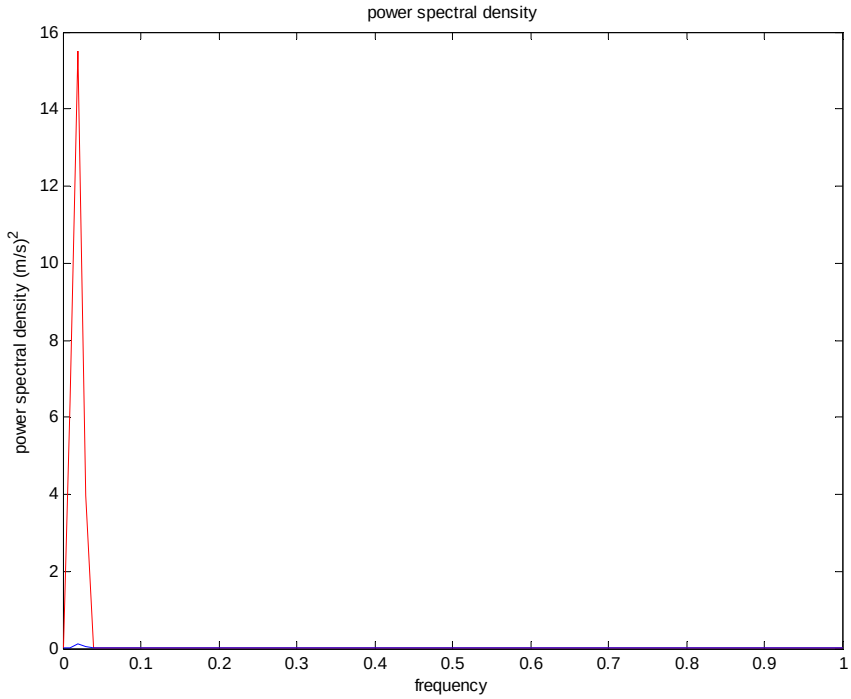

Figure 7.16: Power spectrum density of airflow fluctuation – thermostat vs sitting place (0.2Hz)

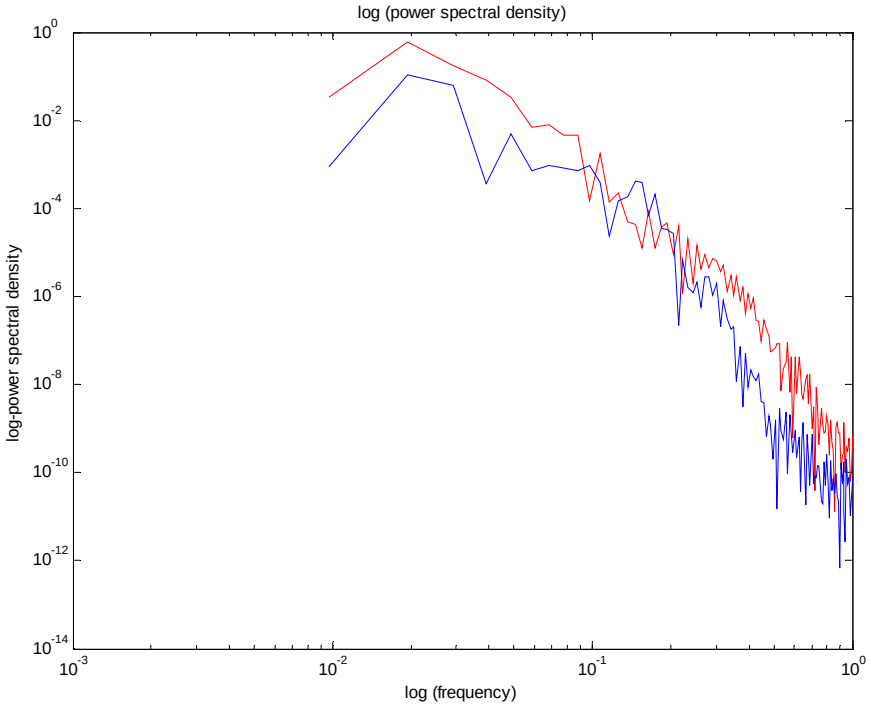

Figure 7.17: log-power spectrum density of airflow fluctuation – thermostat vs sitting place (0.2Hz)

CHAPTER 8: CONCLUSION

In June 2005, the Hong Kong government launched a "No freezing summer" campaign to urge the private sector to follow suit. However, 25.5^{o}C may not be everyone's preferred temperature, as each individual has his or her own clothing preferences and knowledge of thermal comfort and indoor quality. 25.5^{o}C scheme proposed by EMSD to Hong Kong residents is problematic. The major objective of the plan was simply setting the thermostat to 25.5^{o}C, and no further information was provided to the public. It created much public criticism about whether 25.5^{o}C is a comfortable temperature setting. The Hong Kong Economic Times reported that EMSD had to order fans to relieve staff complaints about warm office environments under the policy of 25.5^{o}C.

This research study provided supporting scientific results to escalate the indoor air temperature, making the Hong Kong indoor environment more environmental friendly. In fact, campaign as the above was not a simple scientific nor engineering matter. The intention of this study was neither to add pressure to the business sector nor to change their culture. A true sustainable thermal comfort is to ensure that the energy consumed is getting the intended level of satisfaction, and that the level of satisfaction takes into account of environmental ethics. The survey by Green Sense mentioned in Chapter 4 was a good example of how commercial sectors contradict in their motto of environmental friendliness and corporate culture due to the misunderstanding of thermal comfort. To correct the existing culture or simply "To right the wrongs", this study proposed solutions in the aspects of physiological, psychological and engineering efforts.

Physiological efforts included the understanding of Hong Kong clothing style, dressing culture and human behaviour. Psychological efforts took account of the education to public on their expectation and mind set of 'coolness' as well as the knowledge of true thermal comfort. Engineering aspect covered a wide range of proposal described in Chapters 5-7 to make the escalation of indoor temperature possible. Those efforts were summarized into an innovative 3-Steps protocol.

8.1 Proposed 3-Steps Protocol for Setting the Optimum Indoor Temperature

The strategic 3-steps protocol for sustainable thermal comfort setting and operation was proposed in this research and was a breakthrough for optimum thermal comfort control. It opens up the possibility of studies of system support and enhanced thermal comfort. The 3 steps were: setting of the optimum indoor air temperature, adjustment of clothing code and system enhancement. Step 1 covers the understanding of company culture in term of the demographic distribution of physical environmental parameters and preference or expectation of thermal comfort conditions in the premises. The understanding then turned into the adjustment of optimum air temperature set point based on the 10% or intended percentage of dissatisfaction. Step 2 proposed a proactive education of right clothing. This was expected to enable temperature to be lifted 2°C. Step 3 proposes engineering works including working together with architects to minimize unwanted infiltration, chilled water balancing to reduce temperature swing in space, and installing fan-assisted air-conditioning – a new harmonious fan coil unit system.

8.2 Clothing style of Hong Kong people

I_{cl} was found to have great impact in influencing thermal comfort control, which was very much ignored in practice of thermal comfort design. It caused a dilemma in controlling the indoor thermal comfort environment in air-conditioning offices. Also, due to an error in the initial perception of air-conditioning systems in the 1960s, indoor air temperatures are set erroneously low. Hong Kong people were adapted to their perception of “coolness” in indoor climate and the standard driven by themselves. The findings in the large scale survey by Chan et al. (1998) that Hong Kong was overcooled can now be explained.

The survey of the air temperature in banks by Green Sense agreed with the above hypothesis. A formal dressing code in the banks was perceived to give clients a formal and reliable reception. Unfortunately, clients were also exposed to an uncomfortable environment. This is due to an ignorance of a more in-depth understanding of the thermal comfort model. Chapter 4 provides clues to solve the problem.

Chapters 3 and 4 deal with the issues of users’ physiology in terms of sensation and psychology in terms of their habitual behavior and expectation to thermal comfort. The ‘thermal comfort performance’ with respect to I_{cl} also gives the whole scale of choices in deciding their company clothing culture and how to make changes of their expectation to promote a corporate image of environmental friendliness.

To be even more serious on sustainability (intelligent use of energy to optimize comfort, hence, to the benefit of the corporate throughput), appropriate enhancement to the physical environment, and in this study, an increase and harmonizing air flow, is an excellent alternative.

8.3 Development of harmonious fan coil system

Chapter 5 describes in detail design basis for the innovative harmonious fan coil system. It also points out that synergies of engineers, architects and even the users should all play roles (unfortunately, it also implies the deficiencies of the current roles of these people). Although it takes a great effort in conceiving the design, making it comes true through numerous meetings with the manufacturer, Facility Management Office, Campus Development Office, supervising the contractors, fine tuning the performance of the fan boxes and furnishing the control, it was demonstrated that the effort is worthwhile. The whole develop of harmonious fan coil unit system included gaining approval and getting the system finally installed, tested and commissioned, not only designing and testing the performance of the system, but also evaluating the overall satisfaction of the office staffs.

Chapter 6 demonstrated that the system was really able to provide the increase of velocity in air. It also demonstrates the capability of generating a varying flow. The auto-correlation technique as a signal process was successful in finding a very important air flow characteristics. The frequency behavior of the air flow pattern, as also found in several other studies quoted in Chapter 6 and 7, will be a

key factor in controlling sustainable thermal comfort. More interestingly, in this Chapter, it showed very clearly the deficiency of the current thermostat control system. Resources were put into the enhancement of thermostats without realizing that the small gain in swing in the thermostat was still not be able to reduce the amplified swing in space.

Chapter 5 and 6 opened up a new approach of sustaining high thermal comfort level. The design process and the testing methods all turned out to an integrated design process and testing and commissioning protocols for thermal comfort performances in air-conditioned offices.

8.4 CFD simulation

Transient simulation was carried out to simulate the dynamic air flow patter of the harmonious fan coil system. From the validation of the simulation result with the measurement, they showed an acceptable agreement. It demonstrated that CFD was an effective tool for the prediction of the dynamic situation of indoor environment.

From the result of the simulation, the power spectrum density, the turbulence intensity, and the effective frequency of acceleration were evaluated. It showed that the harmonious fan coil unit can provided an acceptable environment to the occupant with a rise in the temperature set point.

8.5 Further study

In this study, the relationship of the thermal sensation to the fluctuating velocity was based on literature review. Thermal sensation field survey was recommended to be carried out to understand the subjective thermal comfort satisfaction of the building occupant in such a system for any further enhancement.

For the CFD simulation, a dynamic tool for incorporate the influence of the external and internal environmental changes can be further developed. This can be achieved by coupling a building simulation program with CFD packages.

The HFCU system can be extended to any type of air side systems. It is still a prototype stage. Further study can turn the system into a commercial viable system for extensive use. Before that happens, the choice of fans, the configuration of the fan box and by-pass, and the control will all have to taken care of. Specifically, the harmonious nature, that is, the frequency of air flow fluctuation will be controlled by the air temperature as well.

Thermostat control is a high short-coming of thermal comfort control because it cannot dictate the air flow pattern. Hence, the amplification factor of the temperature swing is unpredictable. Careful ADPI commissioning will help. However, there are so many undetermined factors in any office make the control almost totally unsuccessful Therefore, thermostat control, especially the wall mounted configuration, should be a main area of research for any other study for sustainable thermal comfort control.

REFERENCE:

Alexander, D.K., 1996. *HTB2 – a model for the thermal environment of building in operation release 2, user manual*. Welsh School of Architecture, University of Wales College of Cardiff.

Asakai, M., Sakai Y., 1974. Cooling effect of car ventilators. *Bulletin of JSAE (Society of Automotive Engineers of Japan),*. No. 6, pp75-82.

ASHRAE, 2004. *ASHRAE Handbook – HVAC systems and equipment*, ASHRAE research.

ASHRAE, 2004. *ASHRAE Standard 55- Thermal Environmental Conditions for Human Occupancy*, ASHRAE.

ASHRAE, 2005. *ASHRAE Handbook – Fundamental*, ASHRAE research.

Auliciems, A., 1983. Psychophysical criteria for global thermal zones of building design, *International Journal of Biometeorology*, Vol., 26, pp. 69-86.

Awbi, H.B., Gan, G.,1994. Predicting air flow and thermal comfort in offices. *ASHRAE Journal*, Vol. 36, n2, pp.17–21.

Brager, G.S., de Dear, R., 2000. A standard for natural ventilation. *ASHRAE Journa*l, vol. 42, 21-28.

Bruel & Kjaer, 2007. http://www.bksv.com/2537.asp

Busch, J.F., 1990. Thermal responses to the Thai office environment. *ASHREA Transactions*, Vol., 96, n.1, pp. 859-972.

Busch, J.F., 1992. Tale of two populations : thermal comfort in air conditioned and naturally ventilated offices in Thailand, *Energy and Building*, Vol. 18, pp35-249.

Cena K., de Dear R., 2001. Thermal comfort and behavioural strategies in office buildings located in a hot-arid climate. *Journal of Thermal Biology*, Vol. 26, pp. 409-414

Cena, K., de Dear, R., 1999. Field study of occupant comfort and office thermal environments in a hot, arid climate. *ASHRAE Transactions*, Vol. 105, pp204-217.

Chan, D.W.T., Leung, P.H.M., Tam, C.S.Y., Jones, A.P. 2007. *Analysis Of Bacteria Species Present In A University Campus*. Building and Environment. (In Press)

Chan, W.T., Burnett, J., de Dear, R., Ng, C.H., 1998, A Large-scale Survey of Thermal Comfort in Office Premises in Hong Kong, *ASHRAE Technical Data Bulletin*, Vol. 14, n.1.

Cheong, K.W.D., Sekhar, S.C., Tham, K.W., Djunaedy, E., 1999. Airflow pattern in air-conditioned seminar room. *Indoor Air 99. Proceedings of the Eighth International Conference on Indoor Air Quality and Climate*, Vol. 2, pp. 54–59.

Chow, W.K., and Fung, W.Y., 1993. Numerical studies on the indoor air flow in the occupied zone of ventilated and air-conditioned space. *Building and Environment*, Vol. 31, n.4, pp. 319–344.

Chow, W.K., Wong, L.T., 1994. Experimental studies on air diffusion of a linear diffuser and associated thermal comfort indices in an air-conditioned space. *Building and Environment*, Vol. 29, n.4, pp523-530.

CNN, 2005. Hong Kong's cold war heats up, 2005.06.30.

Conceicao, E.Z.E., Lucio, M.J.R., Lourenco, T.M.C., Brito A.I.P.V., 2006. Evaluation of thermal comfort in slightly warm ventilation spaces in nonuniform environments. *HVAC&R Research*, July, Vol, 12, n.3, pp451-475.

CoolBiz, 2006. Japan Committee & Ministry of the Environment. http://www.team-6.jp/coolbiz/

de Dear R., 2004. Thermal comfort in practice, *Indoor air*, Vol. 14 (Suppl 7), pp. 32-39.

de Dear, R., 1998. A global database of thermal comfort field experiments. *ASHRAE Transactions*, Vol. 104, n.1

de Dear, R., Fountain, M.E., 1994. Field experiments on occupant comfort and office thermal environments in a hot-humid climate. *ASHRAE Transactions*, Vol. 100, pp457-475.

de Dear, R. and Brager, G.S., 2002. Thermal comfort in naturally ventilated buildings: revisions to ASHRAE Standard 55, *Energy and Buildings*, Vol. 34, pp549-561

de Dear, R., Ring, J.W., Fanger, P.O., 1993. Human experience of sudden environmental temperature transients. *Indoor Air*. Vol. 3, pp 181-192.

de Dear, R.J., Fountain, M.E., 1994. Field experiments on occupant comfort and office thermal environments in a hot-humid climate. *ASHRAE Transactions*, Vol. 100, n.2, pp. 457-475.

de Dear, R.J., Leow, R.J., Foo, S.C., 1991. Thermal comfort in the humid tropics: Field experiments in air conditioned and naturally ventilated buildings in Singapore. *International Journal of Biometeorology*, Vol. 34, pp. 259-265.

Donnini, G., Molina, J., Carlo, M., Lai, D.H.C., Lai, H.K., Chang, C.Y., Laflamme, M., Nguyen V.H., Haghighat, F., 1997. Field study of occupant comfort and office thermal environments in a cold climate. *ASHRAE Transactions*, Vol. 103, pp205-220.

DURRIDGE, 2006. http://www.durridge.com/RAD7.htm.

Ealiwa, M.A., Taki, A.H., Howarth, A.T., 2001. An investigation into thermal comfort in summer season of Ghadames, Libya, *Building and Environment*, Vol. 36, pp231-237.

EMSD, 2005. *Energy Witz*-Hong Kong EMSD Newsletter on Energy Efficiency and Related Matters, n. 8, pp. 14, Aug. 2005.

Fanger, P.O. et al, 1989. The impact of turbulence on draught. *Proceeding of XVII International conference of Refrigeration*, n.7.

Fanger, P.O., 1970. *Thermal Comfort Analyses and Applications in Environmental Engineering*, McGraw-Hill, London, New York.

Fanger, P.O., Lauridsen, J., Bluyssen, P., Clausen, G., 1988. Air Pollution sources in Offices and Assembly Halls, Quantified by the Olf Unit. *Energy and Buildings*. Vol. 12, pp7-19.

Fanger, P.O., Melikov, A.K., Hanzawa, H., Ring, J.W., 1988. Air turbulence and sensation of draught. *Energy and Buildings*. Vol. 12, pp 21-39.

Fanger, P.O., Pedersen, C.J.K., 1977. Discomfort due to air velocities in spaces, *Proceeding Meeting of Commission B1, B2 and E1 of the International Institute of Refrigeration*. Vol. 4, pp. 289-896.

Fishman, D.S., 1978. Subjective effects of air movement around the feet. *CIBS Symposium on Man environment and Buildings*, September.

Fountain, M., Arens, E., de Dear, R., Bauman, F., Miura, K., 1994. Locally controlled air movement preferred in warm isothermal environments. *ASHRAE Transactions*, Vol. 100, pp937-952.

Fountain, M.E., 1991. Laboratory studies of the effect of air movement on thermal comfort: A comparison and discussion of methods, *ASHRAE Transactions*, Vol. 97, n.1, pp. 863-873.

Fountain, M.E., 1993. Air movement and thermal comfort, *ASHRAE Journal*, August.

Gagge, A.P., Stolwijk, J.A.J., Nishi, Y., 1971. An effective temperature scale based on a simple model of human physiological regulatory response. *ASHRAE Transactions*, Vol.77, p.1, pp.247-262

Gan, G., 1995. Evaluation of room air distribution systems using computational fluid dynamics. Energy and Buildings, Vol. 23, n.2, pp. 83-93.

Gan, G., Groome, D.J., 1994. Thermal Comfort Models Based on Field Measurements. *ASHRAE Transactions*, No. 94-6-3, pp. 782-794.

Goldman, R.F., 1995. Extrapolating ASHRAE's Comfort Model. *HVAC&R Research*, Vol. 5,n.3, pp. 189-194.

Green Sense, 2007. Press conference, 2007.08.30.

Grimitlyn, M.I., Pozin, G.M., 1993. Fundamentals of optimizing air distribution in ventilated spaces. ASHRAE Transactions, Vol. 90, n. 1.

GVBChian, 2005. Global village of Beijing. http://www.gvbchina.org/EnglishWeb/00000GVB%20Express/(26%20Jun%202005)26%20Degrees%20Air-Conditioner%20Energy%20Reduction%20Campaign%20is%20launched.htm

Hanazawa, H., Melikow, A.K., Fanger, P.O., 1987. Airflow characteristic in the occupied zone of heated space, ASHRAE Transactions, Vol. 93, n. 1, 1987.

Hara, M. 1985. Relation between comfort and temperature air flow distribution in a heated room and comfort control. *Clima 2000*, Vol. 4, Indoor climate, Copenhagen, 1985.

Hardy, J.D., Stolwijk, J.A.J, Gagge, A.P., 1971. Comparative physiology of thermoregulation, Chapter 5, Vol. 2 pp.328-380.

Hayashi, T., Ishizu, Y., Kato, S., Murakami, S., 2002. CFD analysis on characteristics of contaminated indoor air ventilation and its application in the evaluation of the effects of contaminant inhalation by a human occupant. Building and Environment, Vol. 37, n. 3, pp. 219-330.

Hensen, J.L.M., 1990. Literature review on thermal comfort in transient conditions. Building and Environment, Vol. 25, n.4, pp. 309-316.

HKO, 2007. Hong Kong Observatory, http://ww/hko.gov.hk

Hong Kong Economic times, 2006. 新聞特寫-25.5°C 最舒服政府竟要買風扇 , *Hong Kong Economic times* (2006/07/14)

Huizenga, C., Zhang, H., Arens, E., 2001.; A model of human physiology and comfort for assessing complex thermal environments. *Building and Environment* Vol.36, pp.691-699.

Humphreys, M.A., 1975. Field studies of thermal comfort compared and applied. *Journal of the Institute of Heating and Ventilation Engineering*, Vol. 44, pp.5-27.

Humphreys, M.A., 1978. Outdoor temperatures and comfort indoors. *Building research and practice*, Vol. 6, n. 2, pp. 92-105.

Humphreys, M.A., 1979. The influence of season and ambient temperature on human clothing behavior. *Indoor climate*, Copenhagen: Danish Building Research.

Humphreys, M.A., 1996. Thermal comfort temperatures world-wide – the current position. *Renewable energy,* Vol. 8, pp.139-144.

ISO, 1995. ISO: 7730: Moderate thermal environments – determination of PMV and PPD indices and specification of the conditions for thermal comfort. International Standards Organization (ISO), Geneva.

Jones, B.W., Hsieh, K.,Hashinaga, M., 1986. The effect of air velocity on thermal comfort at moderate activity levels. *ASHRAE Transactions*, Vol. 92, Part 2B, pp 761-769.

Jones, P.J., O'Sullivan, P.E., 1987. *Development of a model to predict air flow and heat distribution in factories*. SERC Final Report.

Kimura, K., Tanabe, S., Iwata, T., 1994. Climate chamber studies for hot and humid regions. *Thermal comfort: past, present and future*, pp88-105.

Konz, S.A., Rosen, E., Gouch, H., 1982. The effect of air velocity on thermal comfort. *Proceeding of the Human factors society*. 27th Annual Meeting, Norfolk, VA. Human Factors Society.

Lu, W., Howarth, A.T., Adam, N., and Riffat, S.B., 1996. Modelling and Measurement of airflow and aerosol particle distribution in a ventilated two-zone chamber. *Building and Environment* Vol. 31, n.5, pp. 417–423.

Markatos, N.C., 1983. The computer analysis of building ventilation and heating problems. *Passive and Low Energy Architecture, Proceedings of the Second International PLEA Conference*, pp 667–675.

Mayer, E., 1987. Physical causes for draft: some new findings, ASHRAE Transitions, Vol. 93, pp 540-548.

Mayer, E., Schwab, R., 1988. Direction of low turbulent airflow and thermal comfort. *Proceedings of the Healthy Buildings*, 1988, Vol. 2, Stockholm, Sweden, pp. 577-582.

McIntyre, D.A., 1978. Preferred air speed for comfort in warm conditions. *ASHRAE Transactions*, Vol. 84, n. 2, pp. 264-277.

McIntyre, D.A., 1980. *Indoor Climate*. London.

McIntyre, D.A., Fanger, P.O., ValbJorn, O., 1979. The eddect of air movement in thermal comfort and sensation, *Indoor climate*, Copenhagen, Denmark.

Ming Poa, 2007. 深圳 1 日千人染感冒 疑天熱出入冷氣間溫差大, 2007.06.29

Mui, K.W., Chan, W.T., 2003. A new indoor environmental quality equation for air-conditioning building. *Architectural Science Review*, Vol. 48, pp1-6.

Mui, K.W., Chan, W.T., 2003. Adaptive comfort temperature model of air-conditioning building in Hong Kong. *Building and Environment*, Vol.38, pt.6, pp837-852.

Murakami, S., Kato, S., Zeng, J., 1997. Flow and Temperature Fields Around Human Body with Various Room Air Distribution: CFD Study on Computational Thermal Manikin-Part I. *ASHRAE Transactions*, Vol. 103, n.1, pp. 3

Murakami, S., Kato, S., Zeng, J., 1998. Numerical Simulation of Contaminant Distribution Around a Modelled Human Body: CFD Study on Computational Thermal Manikin: CFD Study on Computational Thermal Manikin-Part II. *ASHRAE Transactions*, Vol. 104, n.2, pp. 226

Nemecek, J., Grandjean, E., 1973. Results of an ergonomic investigation of large-scale offices. *Human Factors*. Vol. 15, n2, pp111-124.

Nicol, F., 1993. *Thermal comfort: A handbook for field studies toward an adaptive model*. London, UK: University of East London.

Nicol, F., 2004. Adaptive thermal comfort standards in the hot-humid tropics. *Energy and Building*, Vol. 36, pt. 7, pp.628-637.

Nicol, F., McCartney, K.J., 2001. SCATS: Final report – Public. Oxford Brookes University, UK.

Nielsen PV, 1974. *Flow in air-conditioned rooms*. Ph.D. Thesis, Technical University of Denmark.

Nilsson, H.O., Holmer, I., 2003. Comfort climate evaluation with thermal manikin methods and computer simulation models. *Indoor Air*, Vol. 13, n.1, pp. 28-37.

Olesen, B.W., Brager, G.S., 2004. A better way to predict comfort: the new ASHRAE standard 55-2004. *ASHRAE Journal*, August, pp. 20-26.

Petitjean, R., 2004. *Total hydronic balancing – A handbook for design and troubleshooting of hydronic HVAC system*. 3rd edition. Sweden.

Rohles, F.H., 1983. Ceiling fans as extenders of the summer comfort envelope. ASHRAE Transactions, Vol. 89, n. 1.

Rohles, F.H., Jones, B.W., 1983. A fan in winter. *Proceeding of the Human factors society*. 27th Annual Meeting, Norfolk, VA. Human Factors Society.

Rohles, F.H., Konz, S.A., Jones, B.W., 1982. Enhancing thermal comfort with ceiling fans. *Proceeding of the Human factor society*. 25th Annual meeting. Santa Monica, CA: Human Factors Society

Rohles, F.H., Woods, J.E., Nevins, R.G., 1974. The effects of air movement and temperature of the human sensation of sedentary man. *ASHRAE Transactions*, Vol. 80, Part1.

Rosen, E., Konz, S.A., 1982. Cooling with box fans. *Proceeding of the Human factors society*. 26th Annual Meeting, Seattle. Human Factors Society

Schiller, G.E., Arens, E.A., Bauman, F.S., Benton, C., Fountain, M., Doherty, T., 1988. A field study of thermal environments and comfort in office buildings. *ASHRAE Transactions*, Vol. 94, pp280-308.

SCMP, 2007. Band air-cons too cold, say greens. *South China Morning Post*, 2007.08.31.

Shortridge, 1992. *Airdata multimeter ADM-870 Operating manual*. Shortridge Instruments, Inc, Scottsdale, Arizona.

Shortridge, 2007. http://www.shortridge.com/flowhoods/cfm850-about.htm

Sigma plot, 2003. *Sigma Plot 8.0 User's guide*. SPSS Inc

So A., Tse B., Suen W., Lam K.K., Lo A., Yin R., Hu Q. A new energy efficient approach to air-side design for indoor air-conditioning systems. (In Press)

Somarathne, S., Seymour, M., Kolokotroni, M., 2005. Dynamic thermal CFD simulation of a typical office by efficient transient solution methods. *Building and Environmen*t, Vol. 40, pp 887-896.

Sonne, J.K. and Parker D.S. 1998. Measured ceiling fan performance and usage patterns: implications for efficiency and comfort improvement. *ACEEE summer study on energy efficiency in Building Proceeding*.

Sørensen, D.N., Nielsen,P.V., 2003. Quality control of computational fluid dynamics in indoor environments. *Indoor Air*, Vol. 13, n.1, pp.2-17.

Stolwijk, J.A.J., Hardy, J.D., 1966. Temperature regulation in Man – a theoretical study.

Takeya, N., Onishi, J., Koga, S.M., Izuno, M., Kitagawa, K., 1998. Computer effort saving methods in unsteady calculations of rooms airflows and thermal environments. *International conference on air distribution in rooms*, Stockholm, 1998.

Tanabe, S., 1994. Effects of air temperature, humidity, and air movement on thermal comfort under hot and humid conditions. ASHRAE Transitions, Vol. 10, n. 2.

Tanabe, S., Kimura, K., 1989. Importance f air movement for thermal comfort under hot and humid conditions. *Proceeding Second ASHRAE Far East Conference Air Conditioning in Hot Climates*, Kuala Lumpur. ASHRAE Inc., Altanta.

Teodosiu, C., Hohota, R., Rusaouen, G., Woloszyn, M., 2003. Numerical prediction of indoor air humidity and its effect on indoor environment. *Building and Environment*, Vol. 38, n.5, pp. 655-664.

Toftum, J., Melikov, A., Tynel, A., Bruzda, M., Fanger, P.O., 2003. Human response to air movement – Evaluation of ASHRAE's draft criteria (RP-843) HVAC&R Research, April, Vol. 9, n. 2, pp187-211.

TSI, 2000. *Model 8455/8465/8475 Air velocity transducer – Operation and Service Manual*. TSI Incorporated.

Tung, T.C.W., Burnett, J., Chan, D.W.T., 2006. Using the real time Radon-222 profile to quantify the specific radon production rate in an air-conditioned building. *Indoor and built environment*, Vol. 15, pt. 5, pp483-493.

Waters, R.A., 1986. *Air movement studies. Clean Room Design Seminar*, Institute of Mechanical Engineers, London.

Wu, H., 1989. The use of oscillating fans to extend the summer comfort envelope in hot arid climates, Proceeding of 2nd ASHRAE conference on air conditioning in hot climates.

Yamamoto, M.T, 1997. 1/f fluctuations in biological systems. *Proceeding of Annual International Conference of the IEEE Engineering in Medicine and Biology*, Chicago, USA. Pp 2692-2697.

Yang, J., Li, X., Zhao, B., 2004. Prediction of transient contaminant dispersion and ventilation performance using the concept of accessibility. *Energy and Buildings*, Vol. 36, pp293-299.

Ye, G., Yang, C., Chen, Y., Li, Y., 2003. A new approach for measuring predicted mean vote (PMV) and standards effective temperature (SET*). *Building and Environment*, Vol. 38, pp33-44.

Zhou, G., 1999. *Impact of frequency and airflow direction on sensation of draught*. PhD thesis ET-PhD-99-01. International centre for indoor environment and energy, Department of Energy Engineering, Technical University of Denmark.

Zhou, X., Quyang, Q., Lin, G., Zhu, Y., Impact of dynamic airflow on human thermal response. *Indoor air*, Vol. 16, pp 348-355.

Zhu, Y, 2000. *Research on the fluctuant characteristics of natural wind and mechanical winds*, Master thesis, Beijing Tsinghua University.

APPENDIX A: TEMPERATURE MEASUREMENT RESULTS

The following graphs show the temperature in four locations in the room, those are supply diffuser, thermostat, seat 1.1m height and breathing zone.

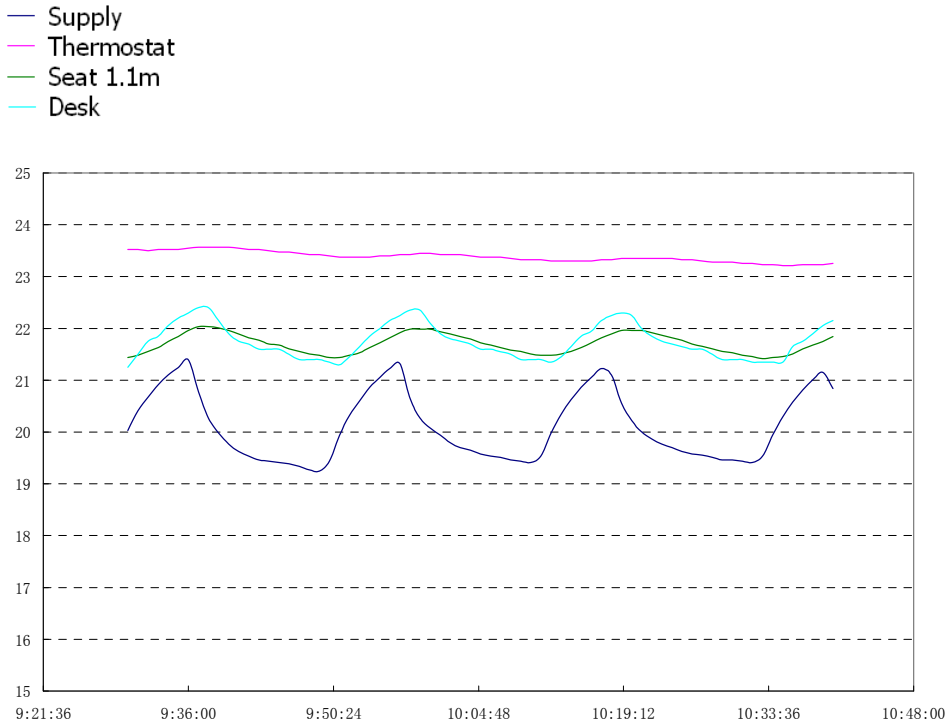

Figure A-1: Temperature profile of T_{set} = 22℃, FCU Speed = Low, Fan box freq = 45Hz

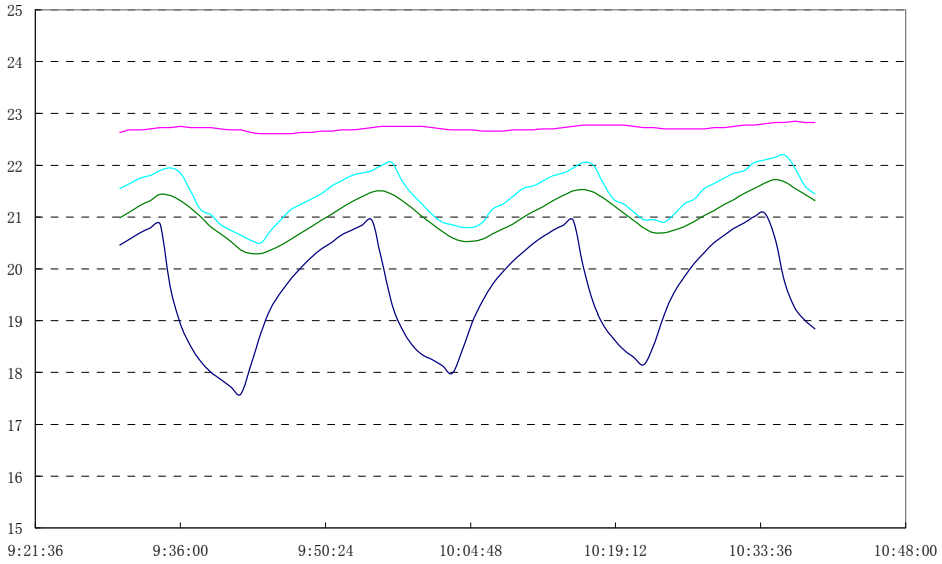

Figure A-2: Temperature profile of T_{set} = 22℃, FCU Speed = Low, Fan box freq = 35Hz

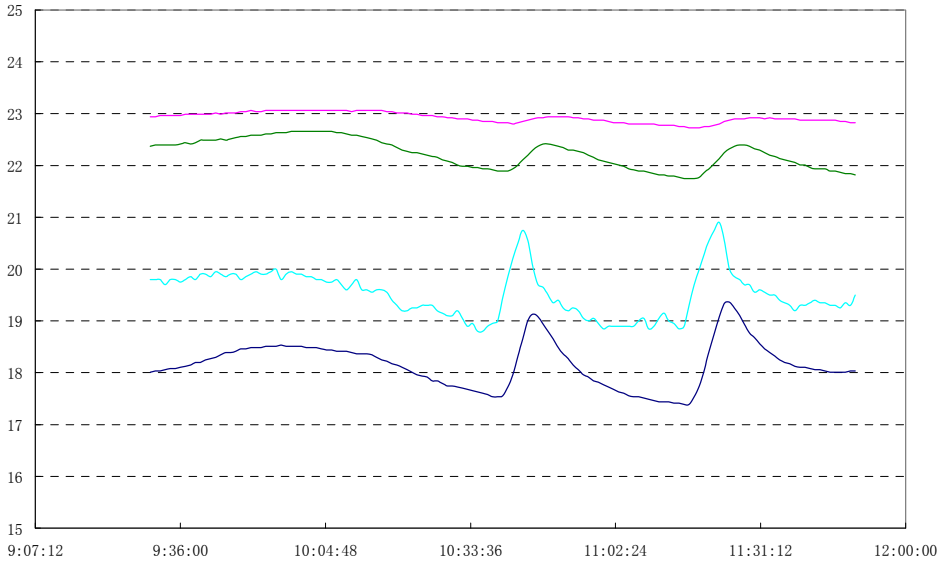

Figure A-3: Temperature profile of T_{set} = 22℃, FCU Speed = Low, Fan box OFF

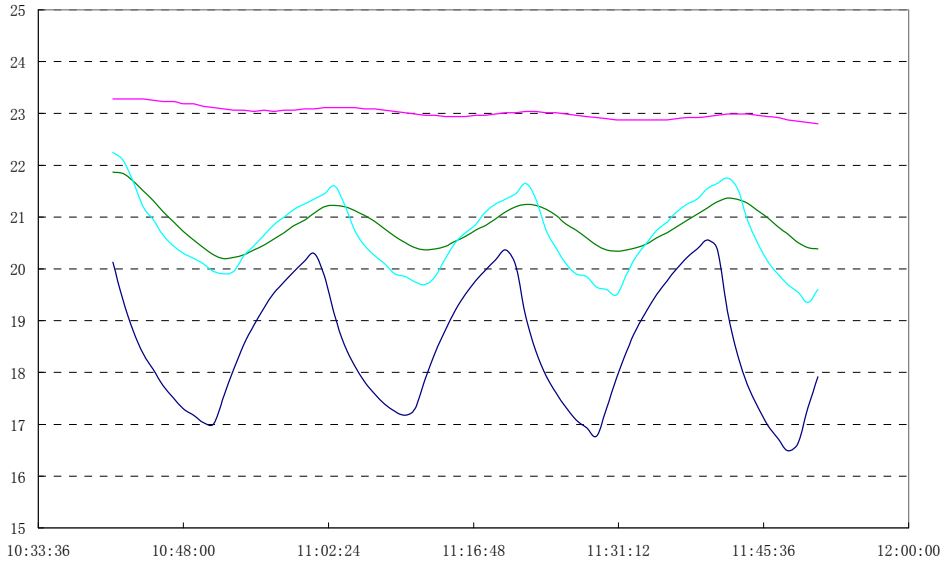

Figure A-4 Temperature profile of T_{set} = 22℃, FCU Speed = Medium, Fan box freq = 30Hz

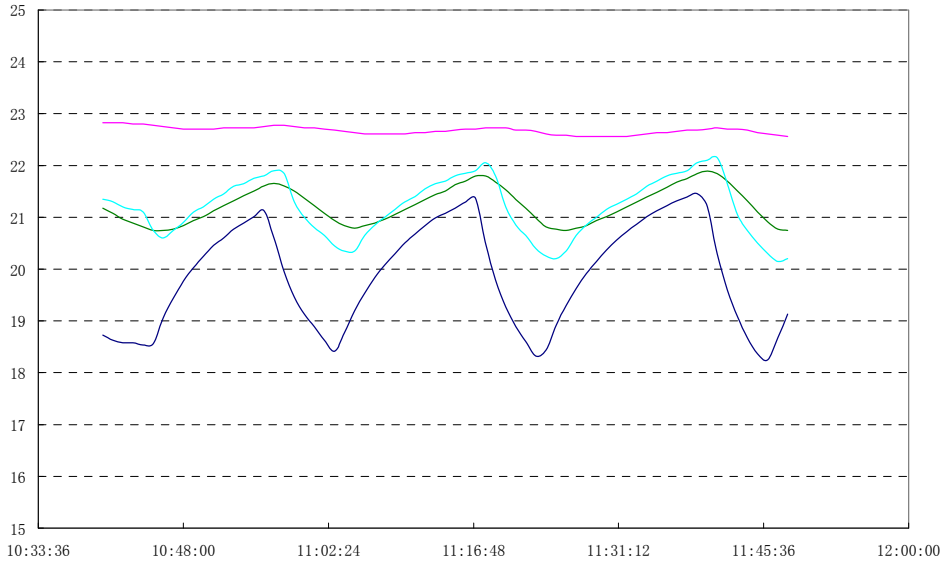

Figure A-5: Temperature profile of T_{set} = 22℃, FCU Speed = Medium, Fan box freq = 35Hz

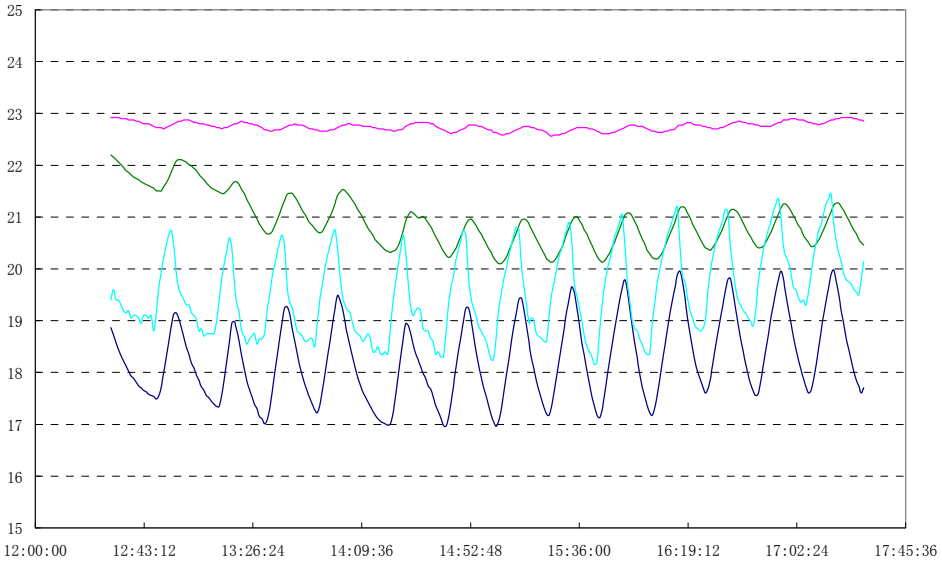

Figure A-6: Temperature profile of T_{set} = 22℃, FCU Speed = Medium, Fan box OFF

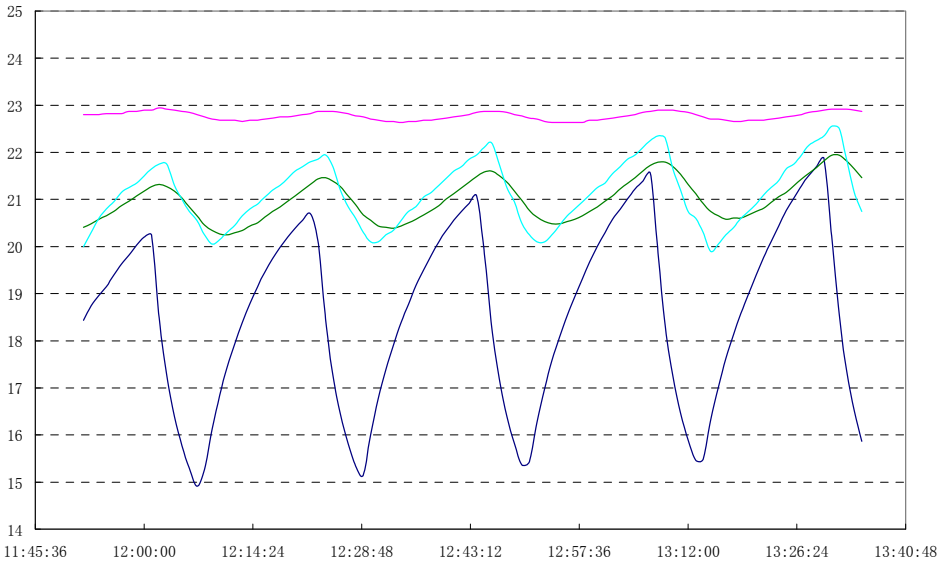

Figure A-7: Temperature profile of T_{set} = 22℃, FCU Speed = High, Fan box freq = 30Hz

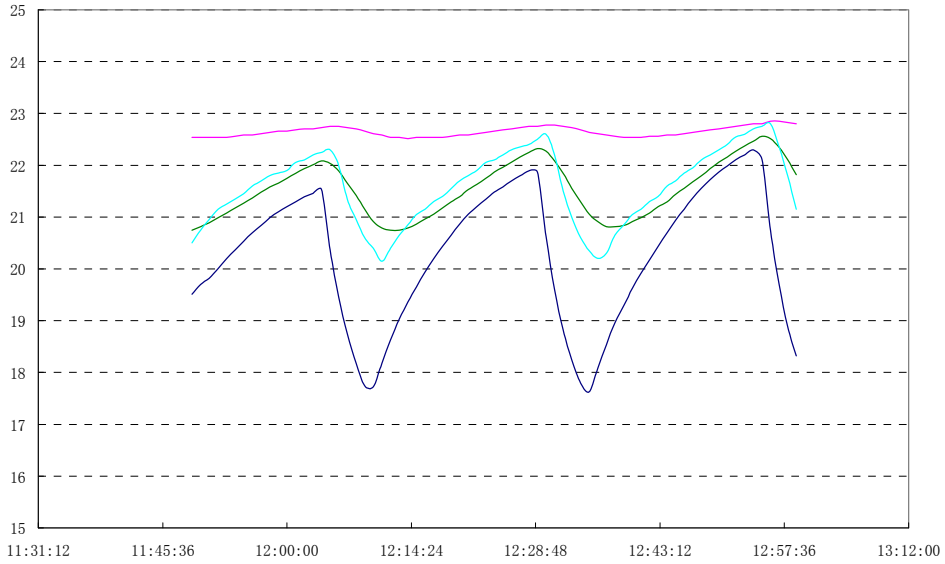

Figure A-8: Temperature profile of T_{set} = 22℃, FCU Speed = High, Fan box freq = 40Hz

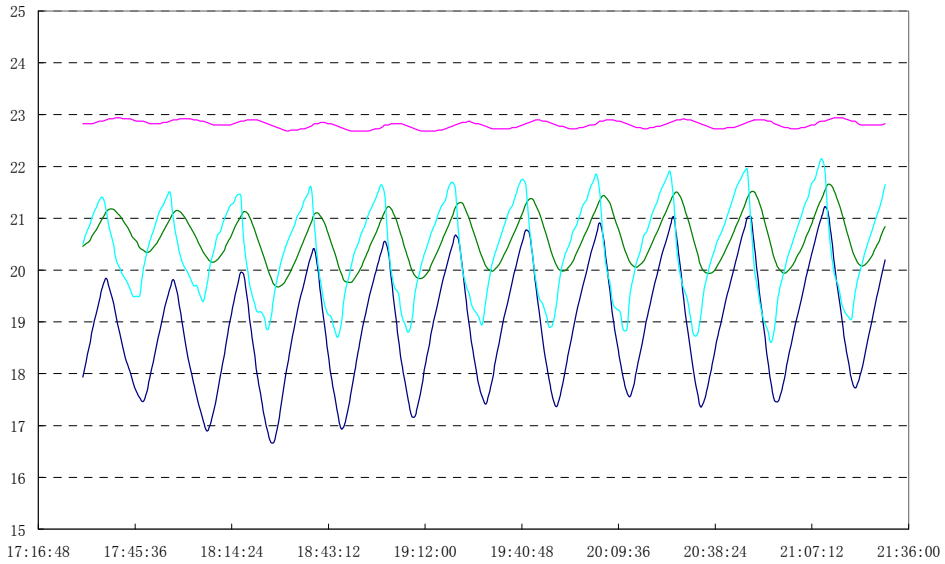

Figure A-9: Temperature profile of T_{set} = 22℃, FCU Speed = High, Fan box OFF

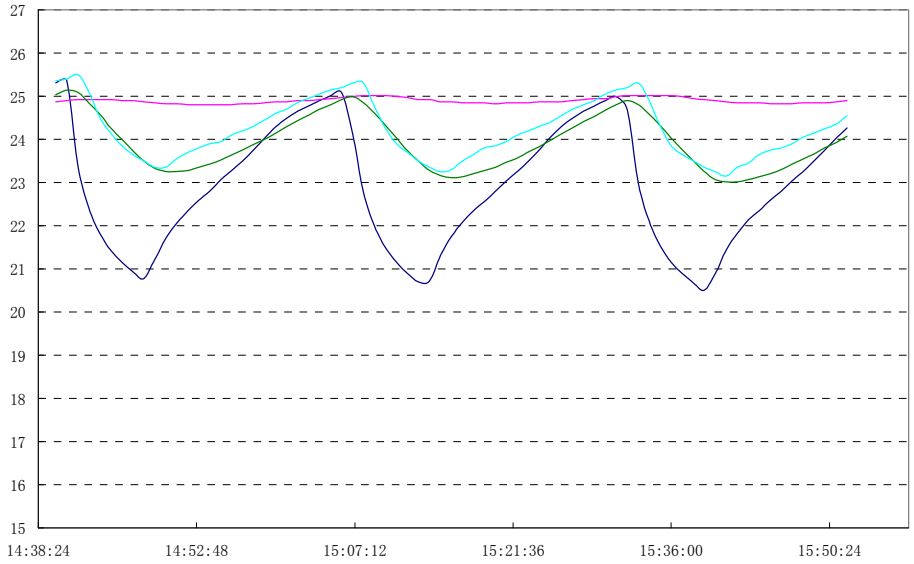

Figure A-10: Temperature profile of T_{set} = 24℃, FCU Speed = Low, Fan box freq = 45Hz

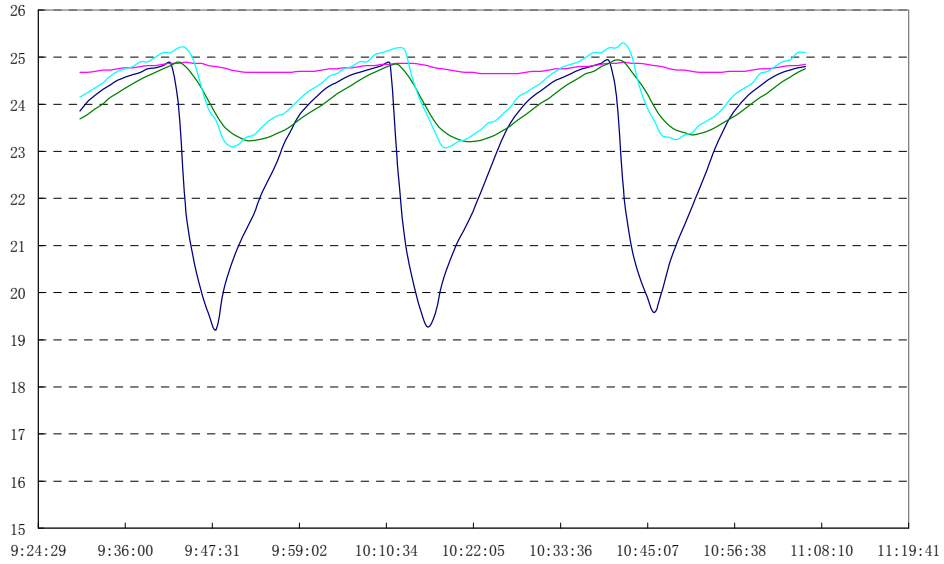

Figure A-11: Temperature profile of T_{set} = 24℃, FCU Speed = Low, Fan box freq = 35Hz

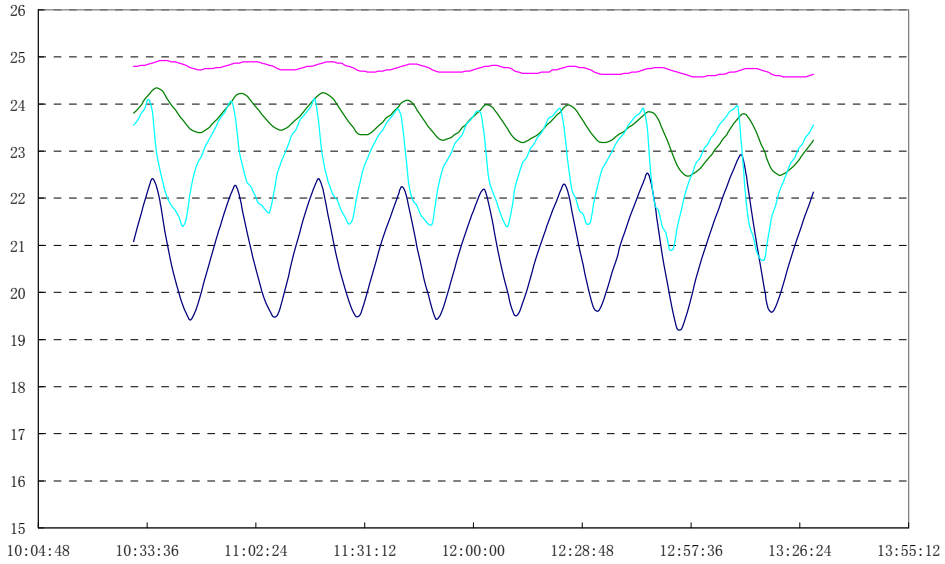

Figure A-12: Temperature profile of T_{set} = 24℃, FCU Speed = Low, Fan box OFF

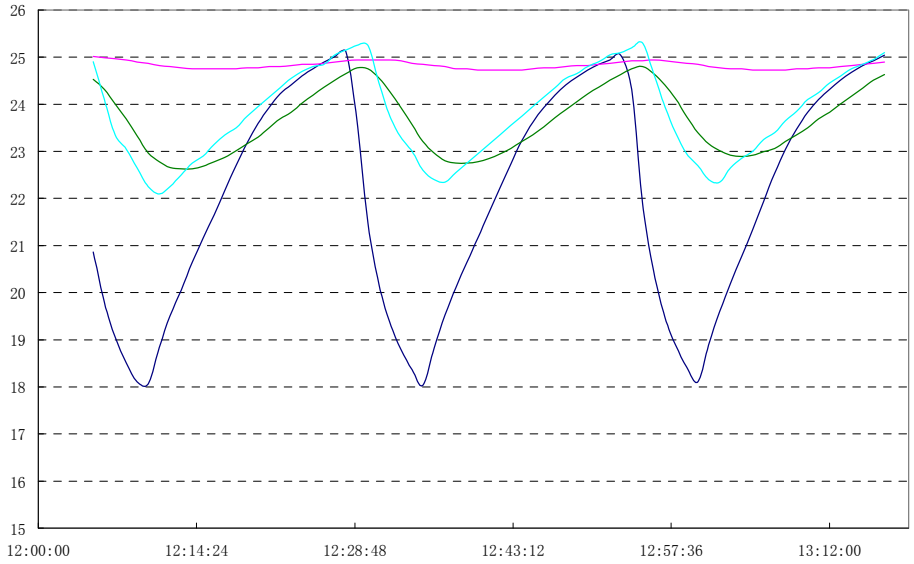

Figure A-13: Temperature profile of T_{set} = 24℃, FCU Speed = Medium, Fan box freq = 30Hz

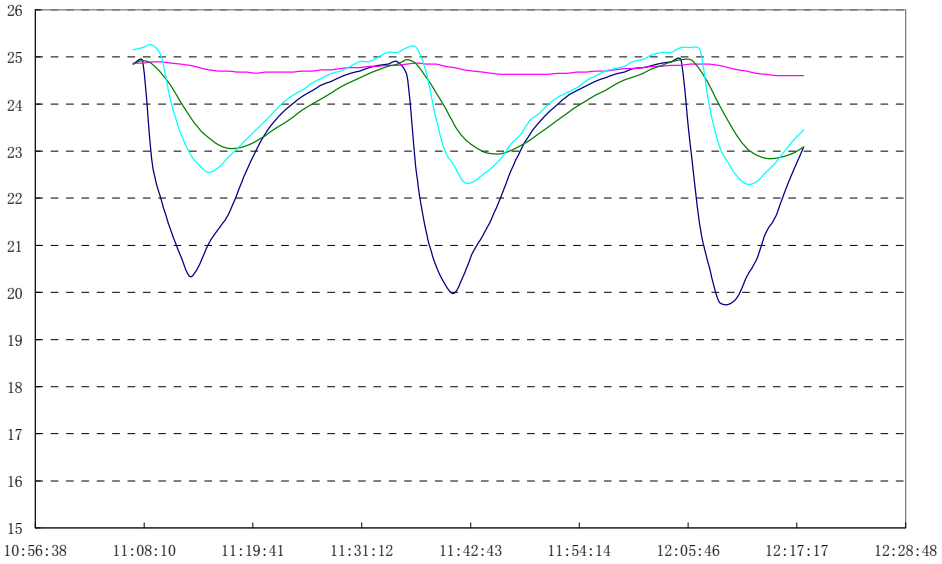

Figure A-14: Temperature profile of T_{set} = 24℃, FCU Speed = Medium, Fan box freq = 35Hz

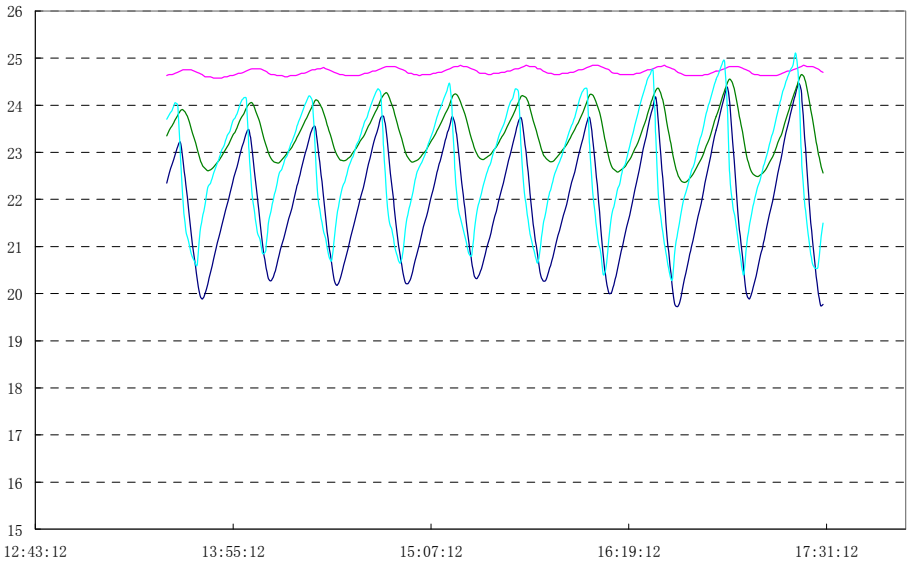

Figure A-15: Temperature profile of T_{set} = 24℃, FCU Speed = Medium, Fan box OFF

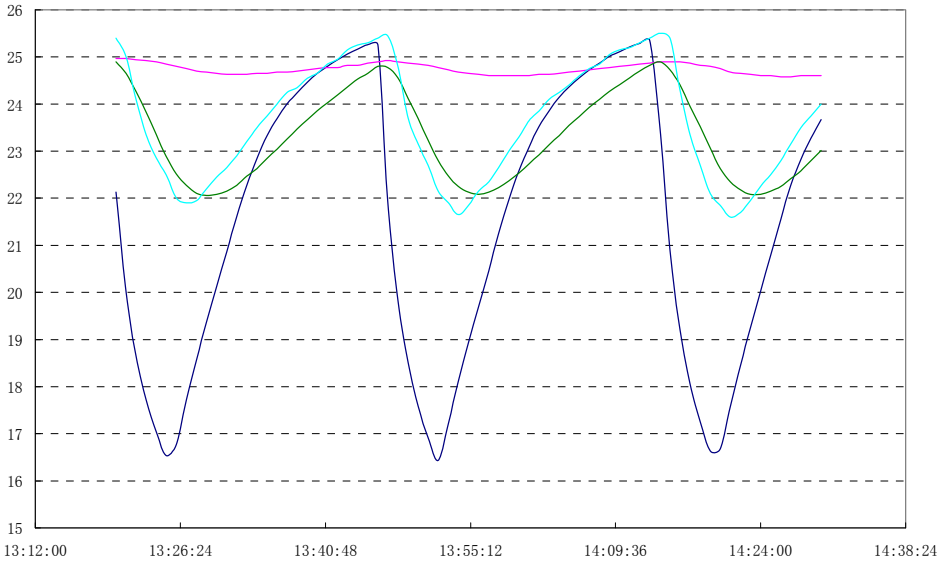

Figure A-16: Temperature profile of T_{set} = 24℃, FCU Speed = High, Fan box freq = 30Hz

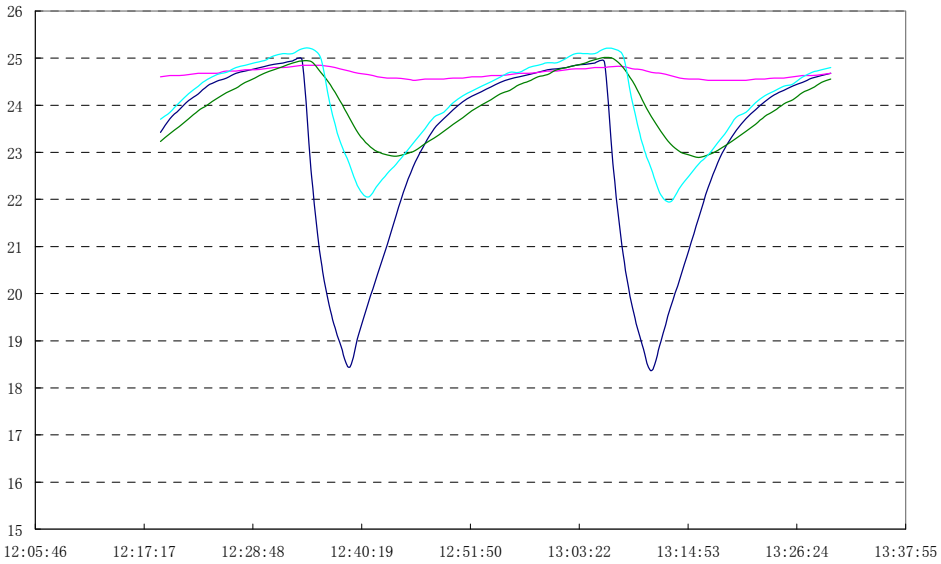

Figure A-17: Temperature profile of T_{set} = 24℃, FCU Speed = High, Fan box freq = 40Hz

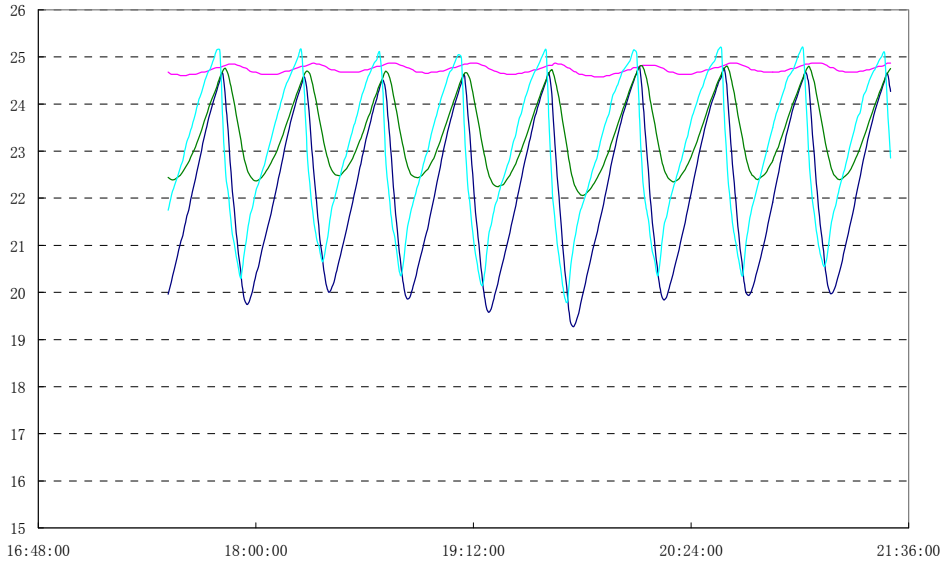

Figure A-18: Temperature profile of T_{set} = 24℃, FCU Speed = High, Fan box OFF

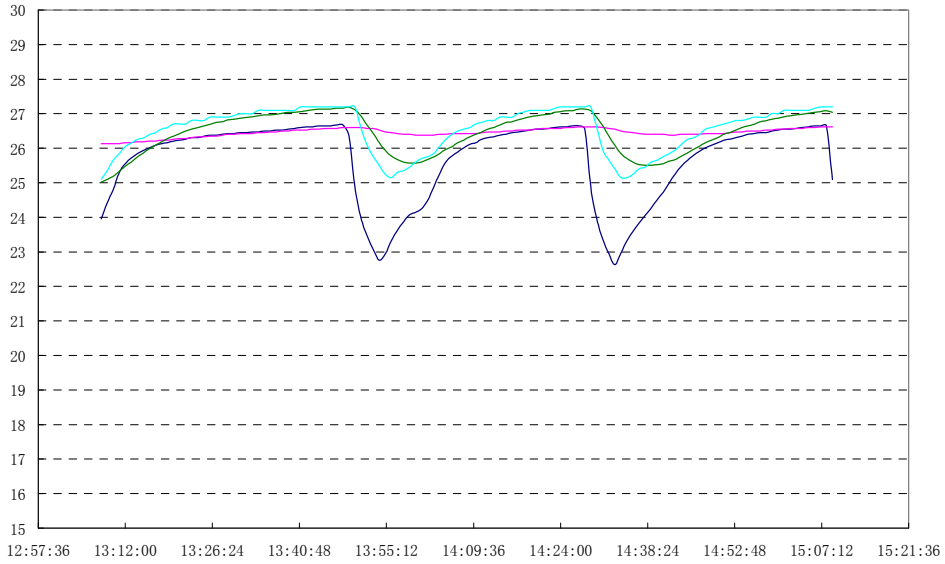

Figure A-19: Temperature profile of T_{set} = 26℃, FCU Speed = Low, Fan box freq = 45Hz

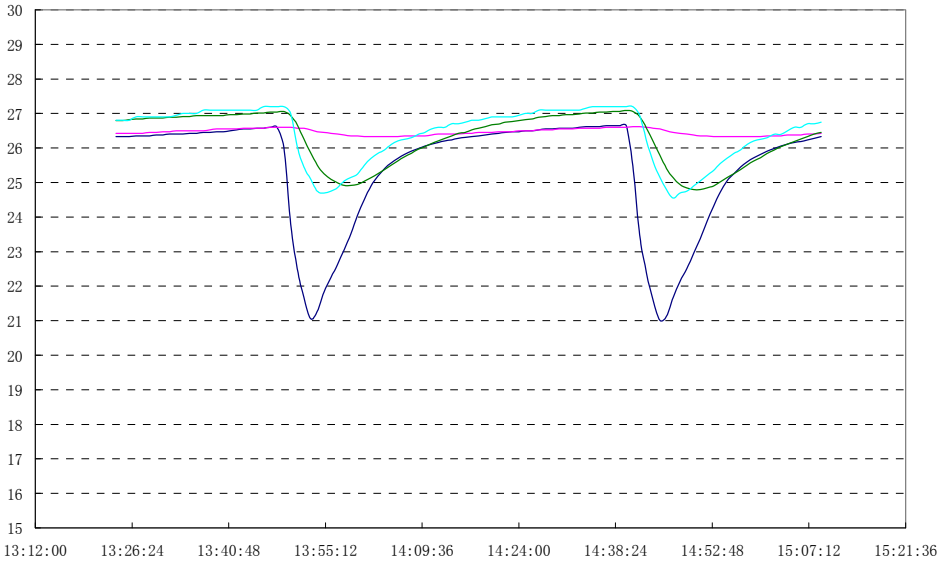

Figure A-20: Temperature profile of T_{set} = 26℃, FCU Speed = Low, Fan box freq = 35Hz

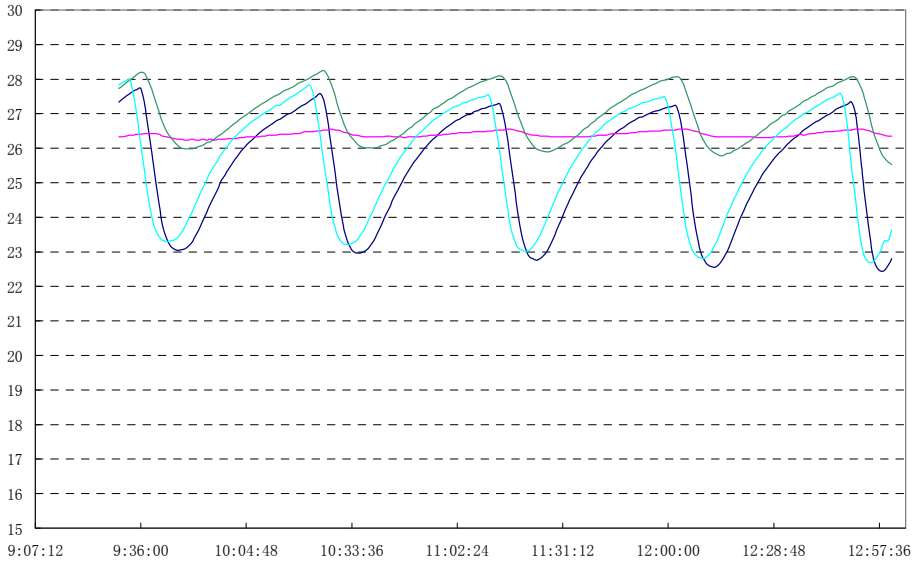

Figure A-21: Temperature profile of T_{set} = 26℃, FCU Speed = Low, Fan box OFF

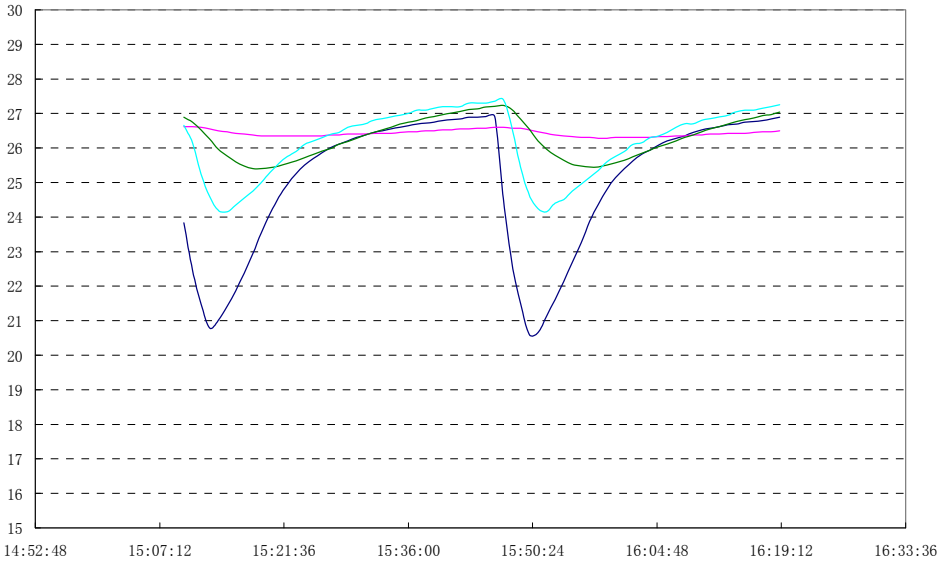

Figure A-22 Temperature profile of T_{set} = 26℃, FCU Speed = Medium, Fan box freq = 30Hz

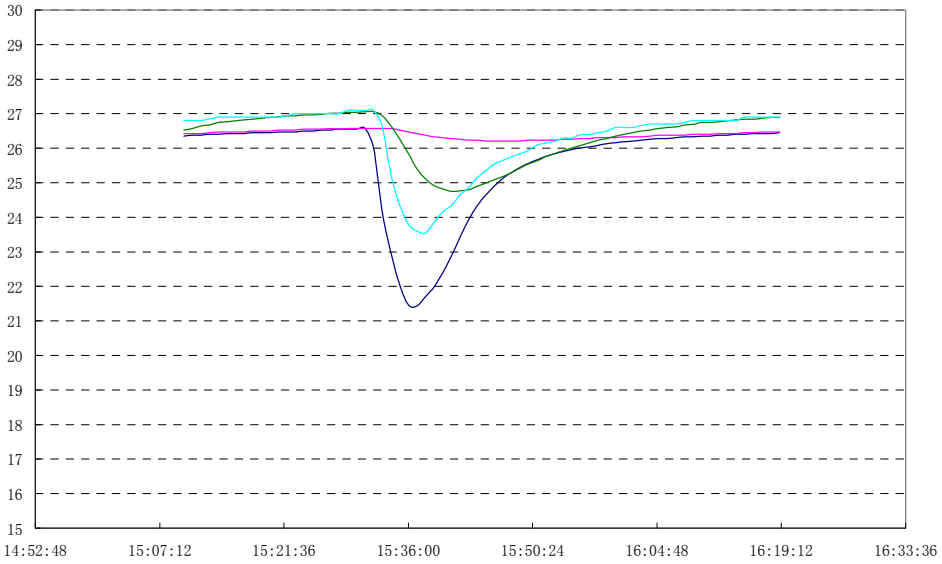

Figure A-23: Temperature profile of T_{set} = 26℃, FCU Speed = Medium, Fan box freq = 40Hz

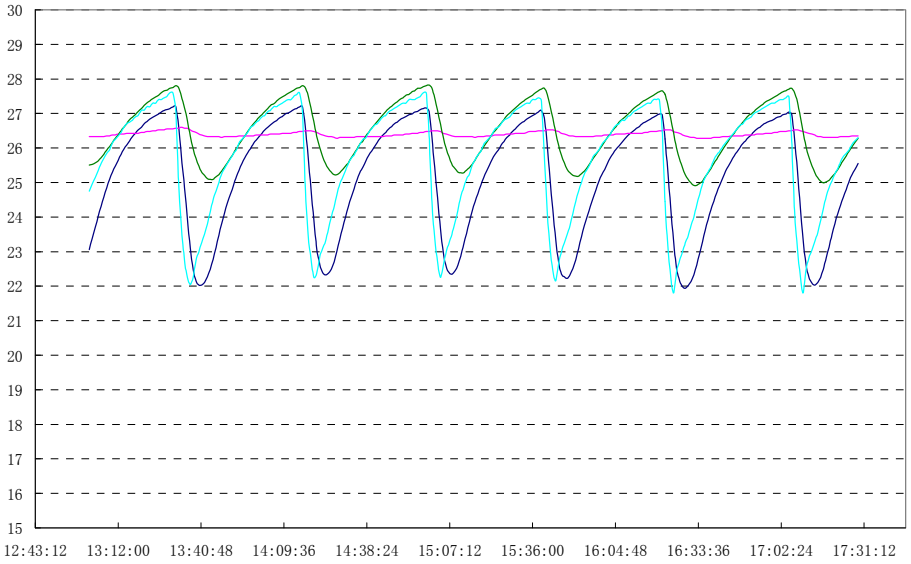

Figure A-24: Temperature profile of T_{set} = 26℃, FCU Speed = Medium, Fan box OFF

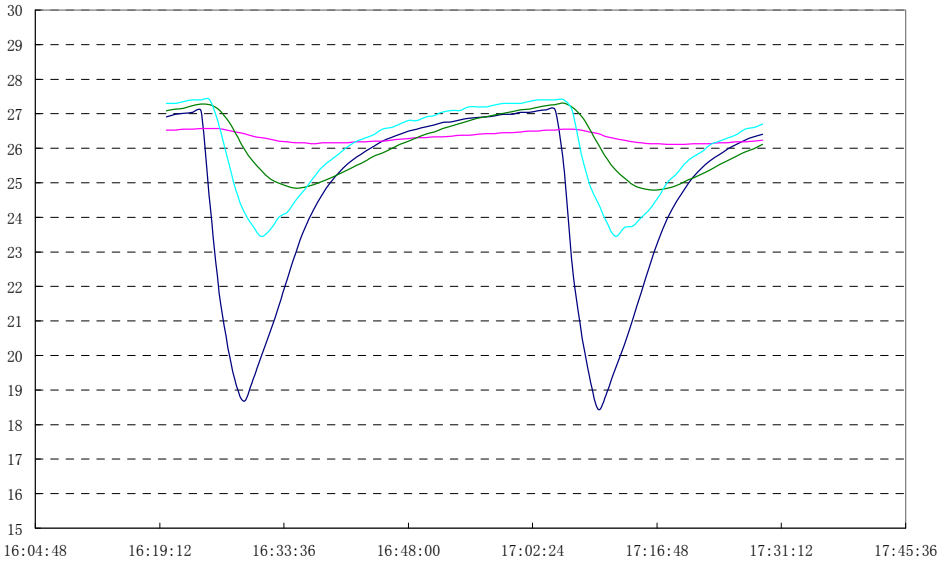

Figure A-25 Temperature profile of T_{set} = 26℃, FCU Speed = High, Fan box freq = 30Hz

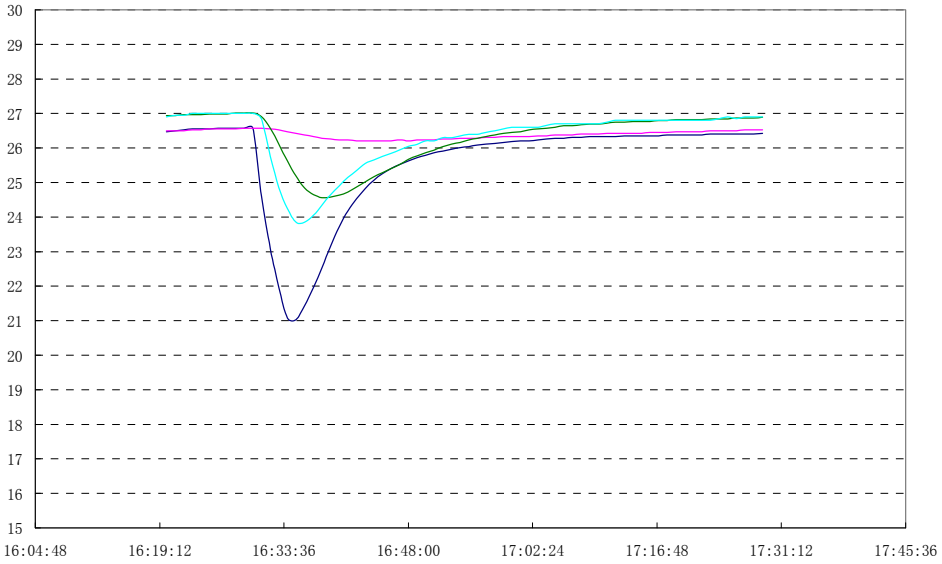

Figure A-26: Temperature profile of T_{set} = 26℃, FCU Speed = High, Fan box freq = 40Hz

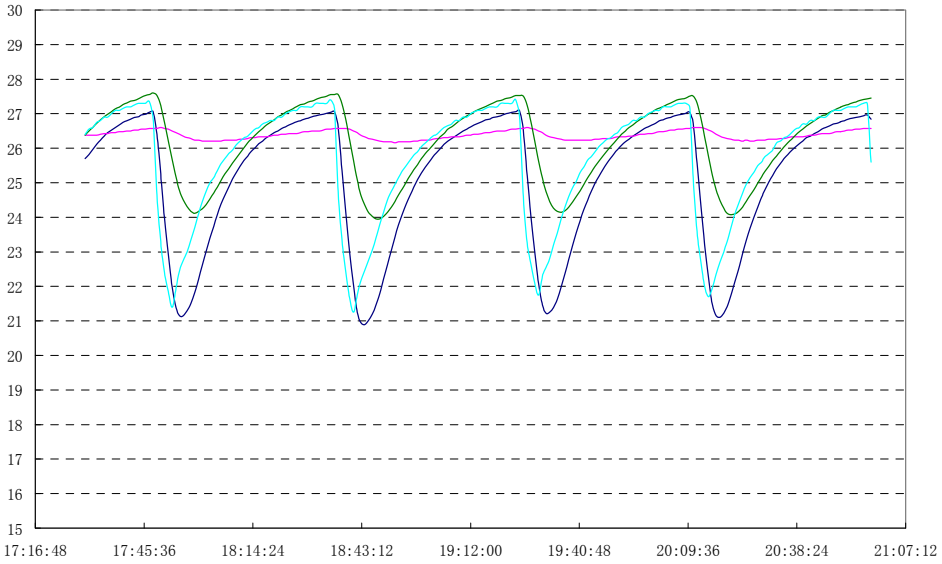

Figure A-27: Temperature profile of T_{set} = 26℃, FCU Speed = High, Fan box OFF

APPENDIX B - POWER SPECTRUM ANALYSIS FOR MEASUREMENT RESULTS

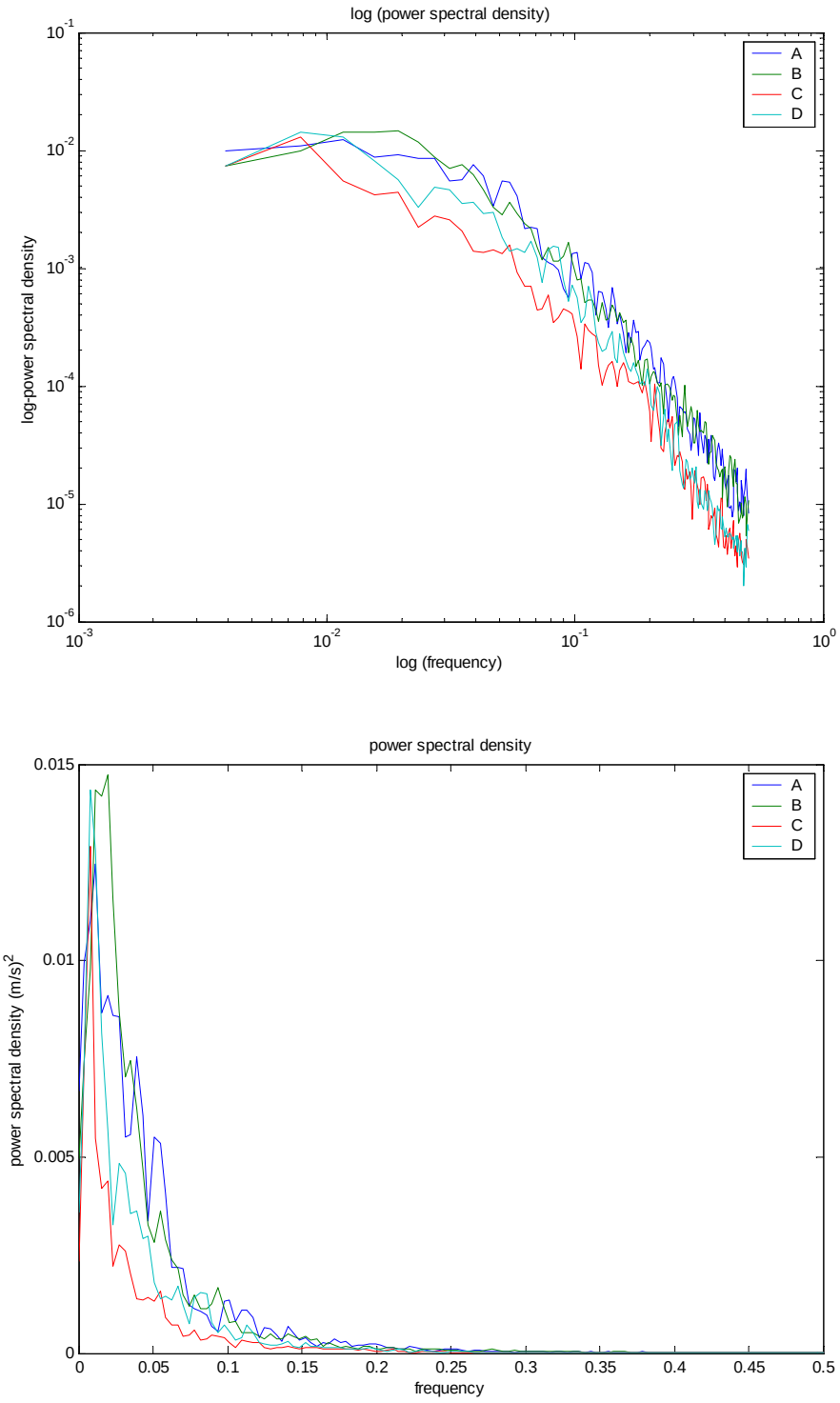

Figure B-1 Centrifugal fan 35Hz on power density of temperature and velocity records

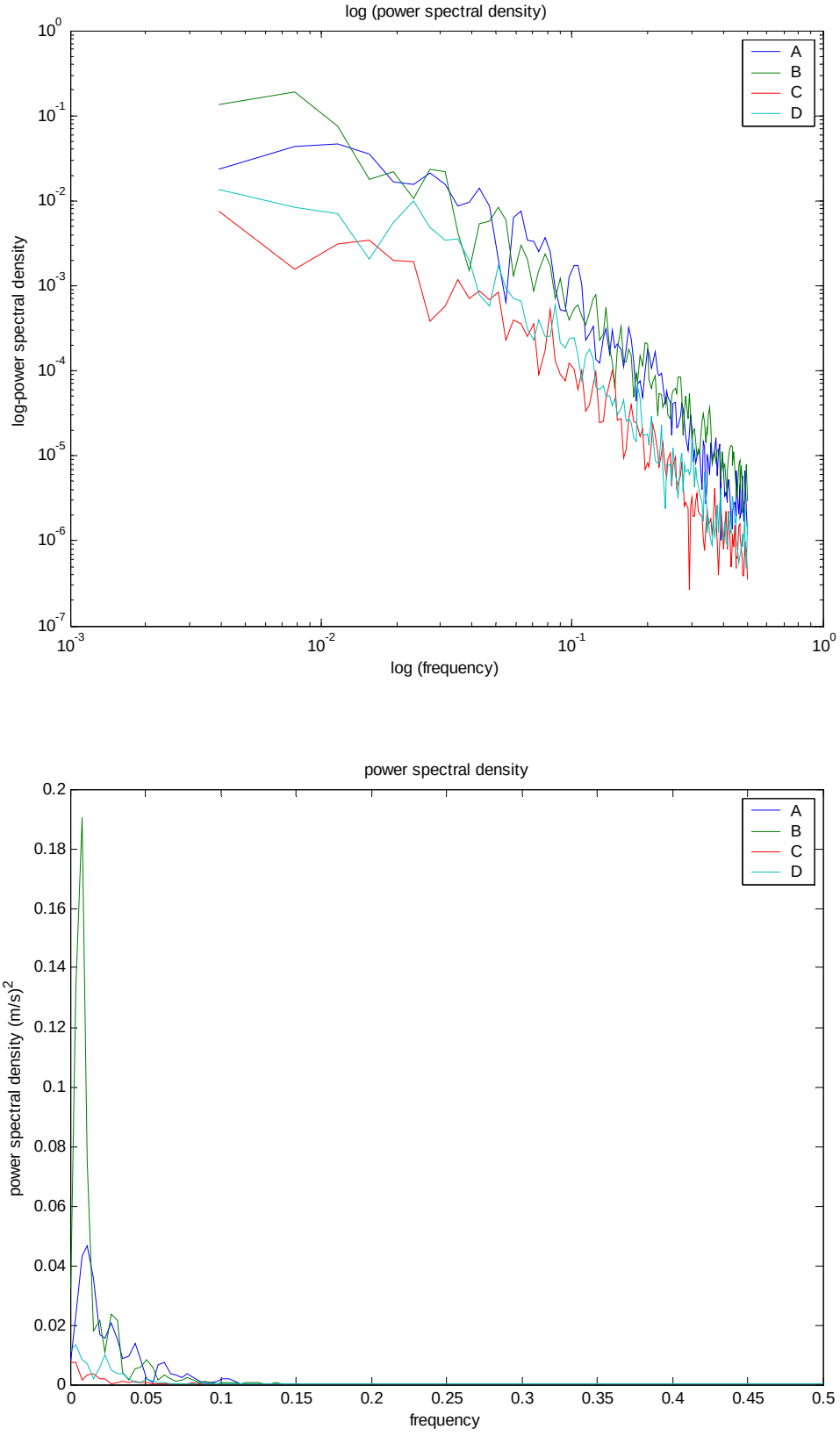

Figure B-2 Centrifugal fan OFF on power density of temperature and velocity records

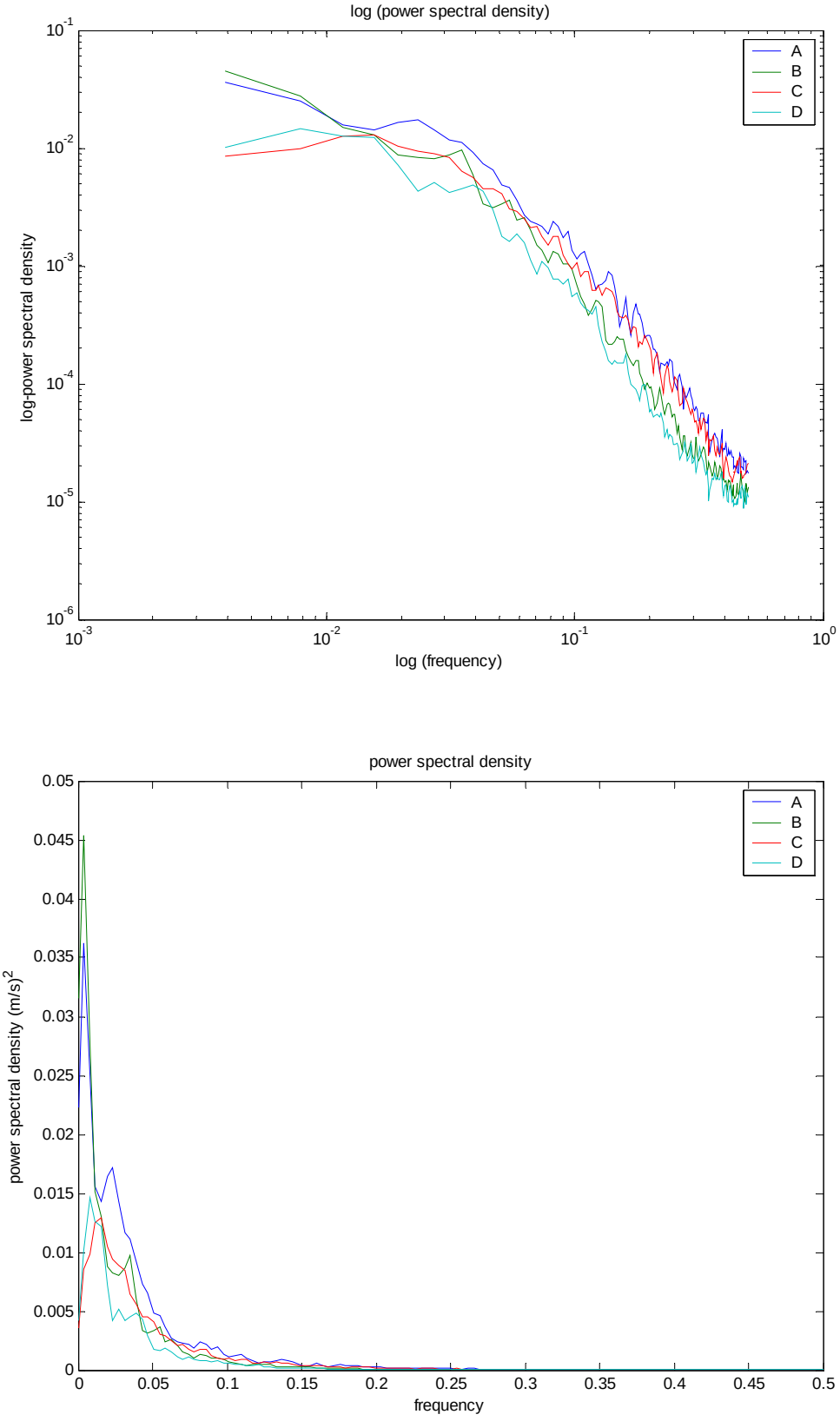

Figure B-3 Power density of temperature and velocity records with turbulence intensity 36.6% (Med,24C,15-30hz)

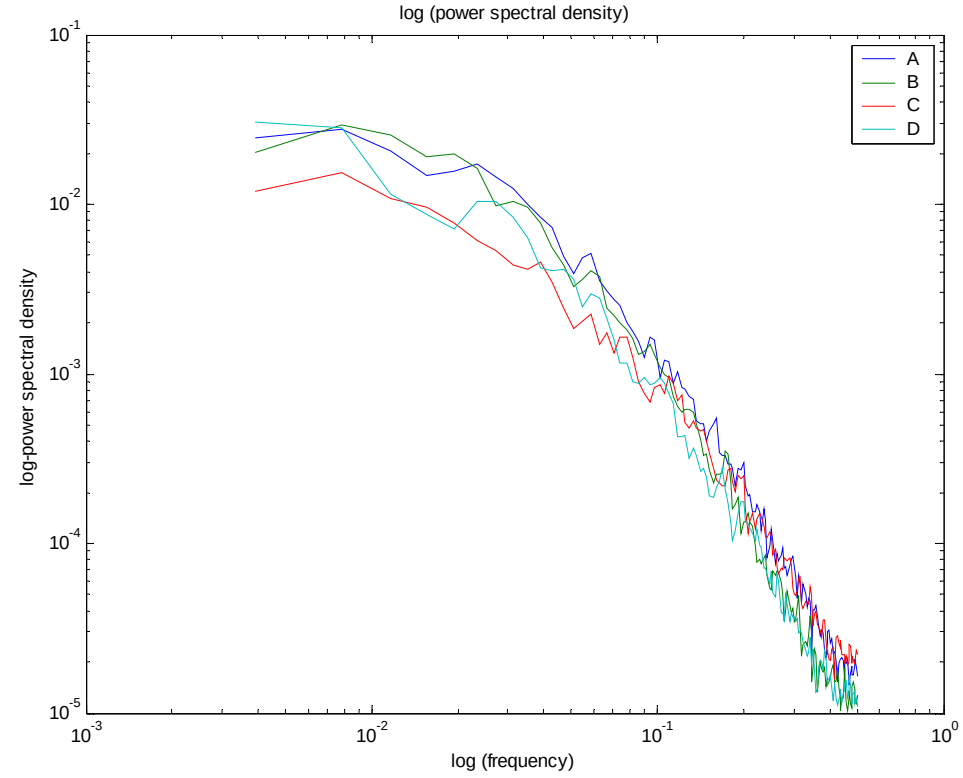

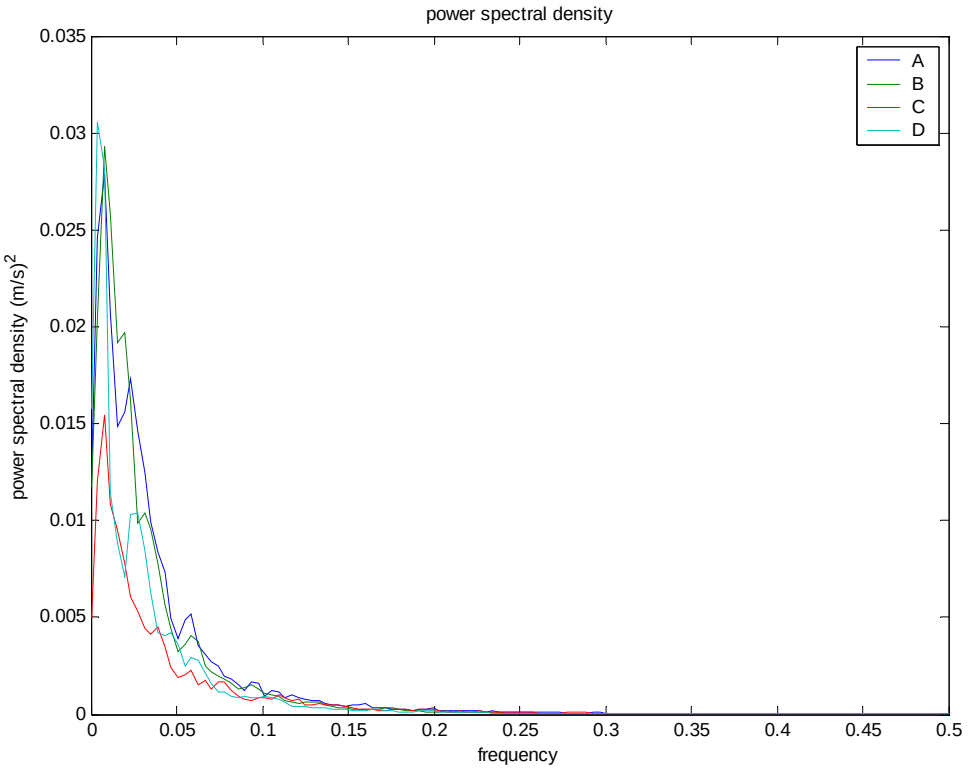

Figure B-4 Power density of temperature and velocity records with turbulence intensity 60.48% (Med,24C,15-45hz)

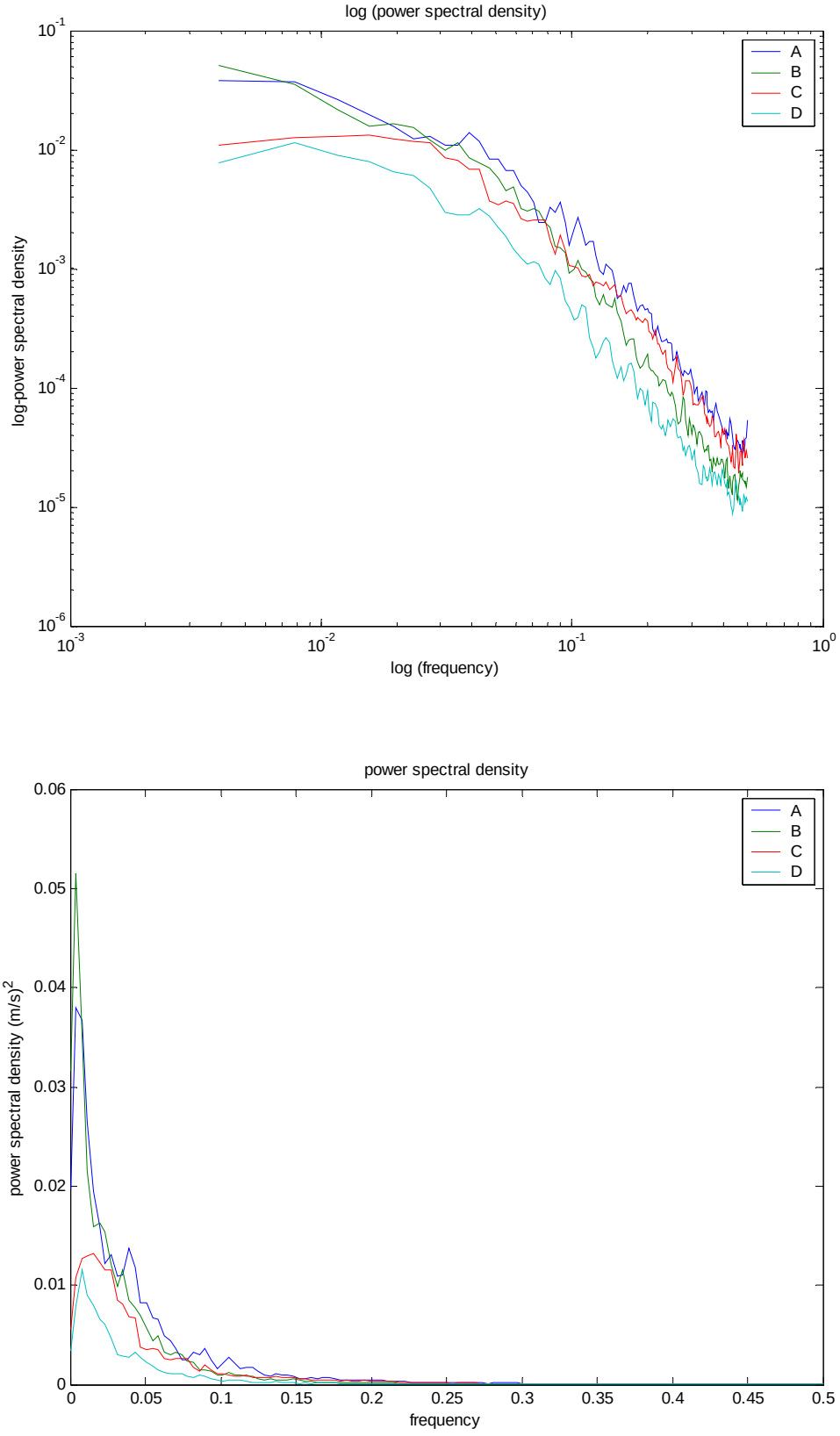

Figure B-5 Power density of temperature and velocity records with turbulence intensity 30.93% (Hi,24C,15-30hz)

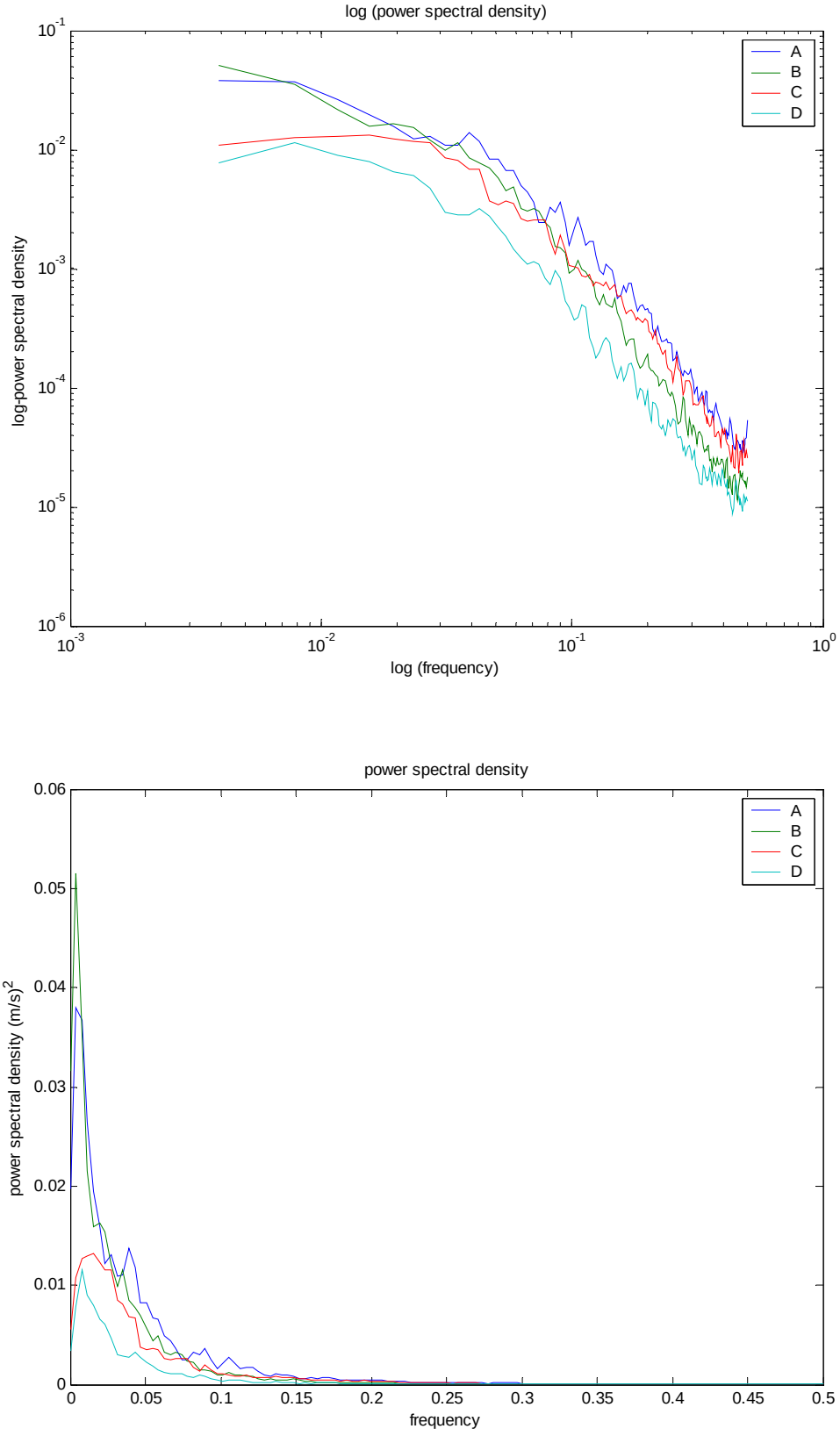

Figure B-6 Power density of temperature and velocity records with turbulence intensity

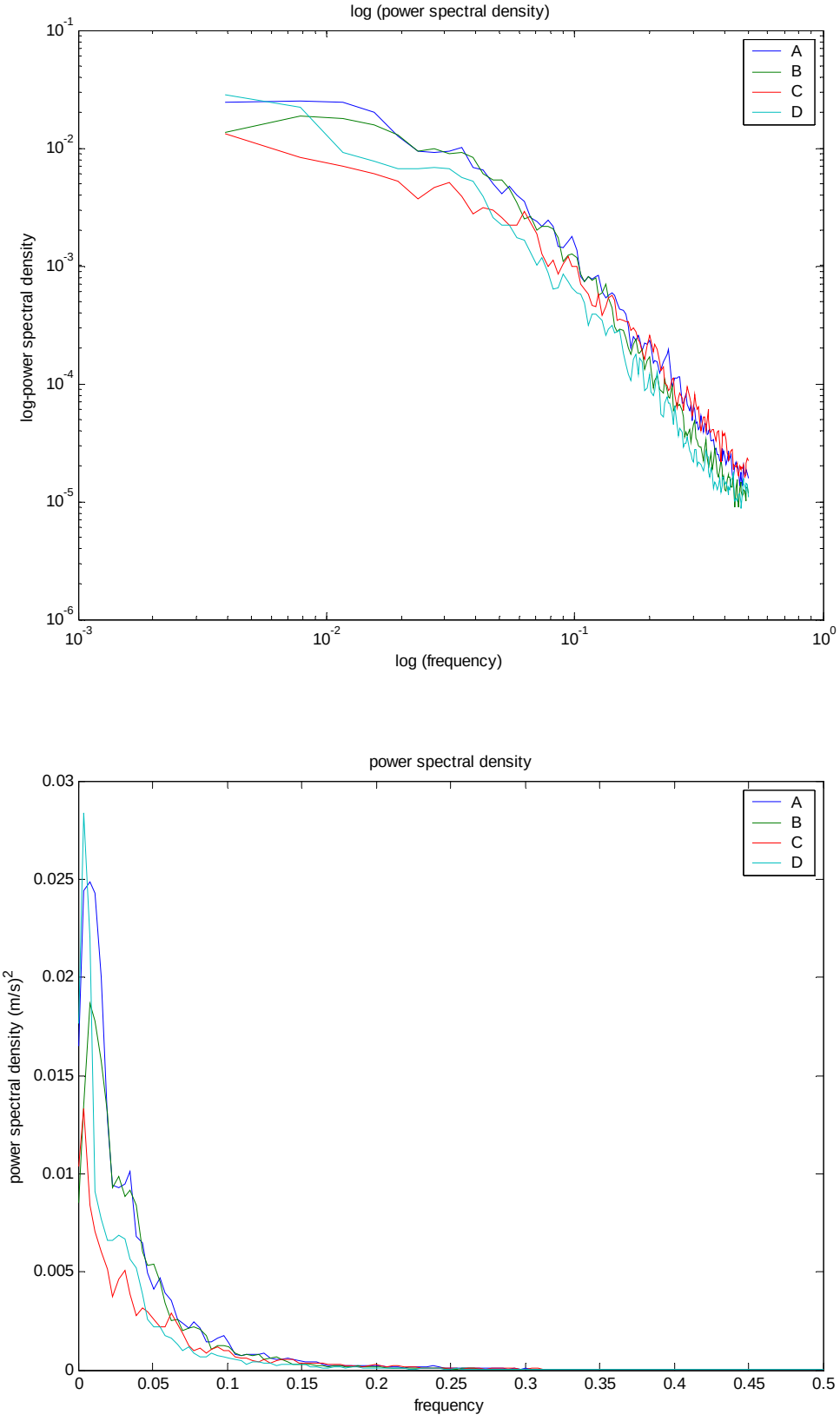

Figure B-7 Power density of temperature and velocity records with turbulence intensity 38.07% (Hi,24C,30-45hz)

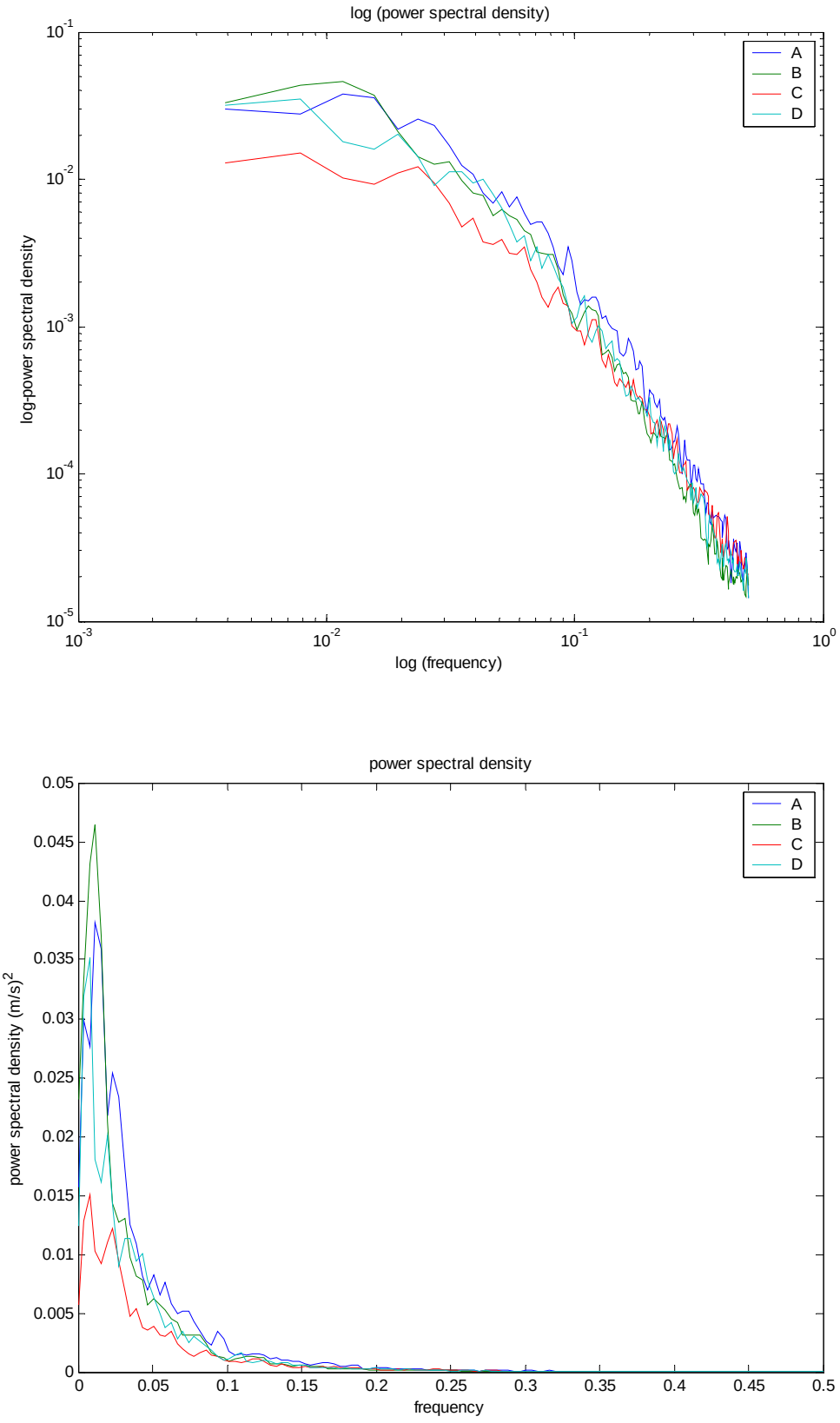

Figure B-8 Power density of temperature and velocity records with turbulence intensity 38.07% (Hi,24C,30-45hz)

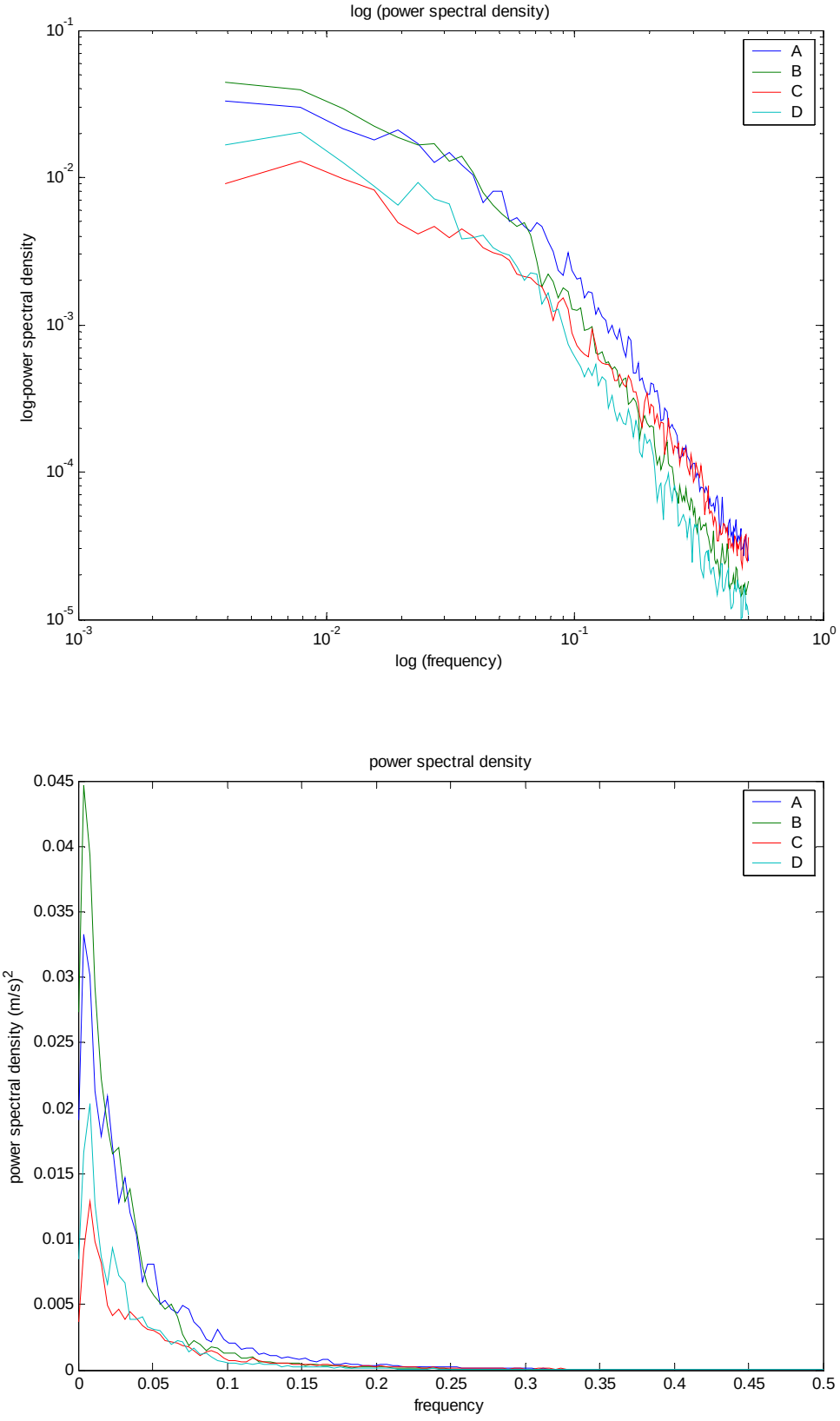

Figure B-9 Power density of temperature and velocity records with turbulence intensity 52.47% (Hi,24C,15-45hz)

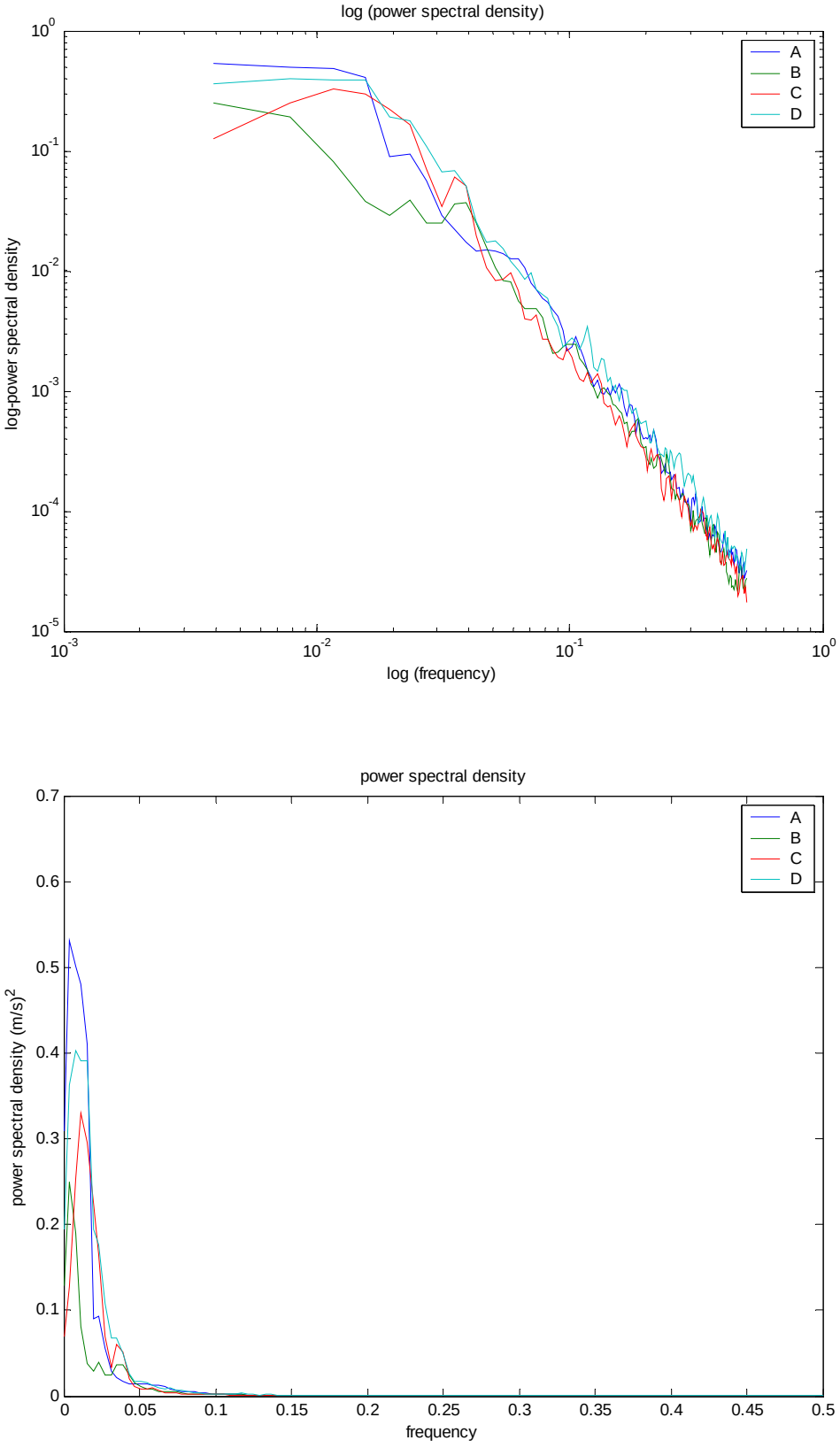

Figure B-10 Power density of temperature and velocity records with turbulence intensity52.47%(Hi,24C,15-45hz)

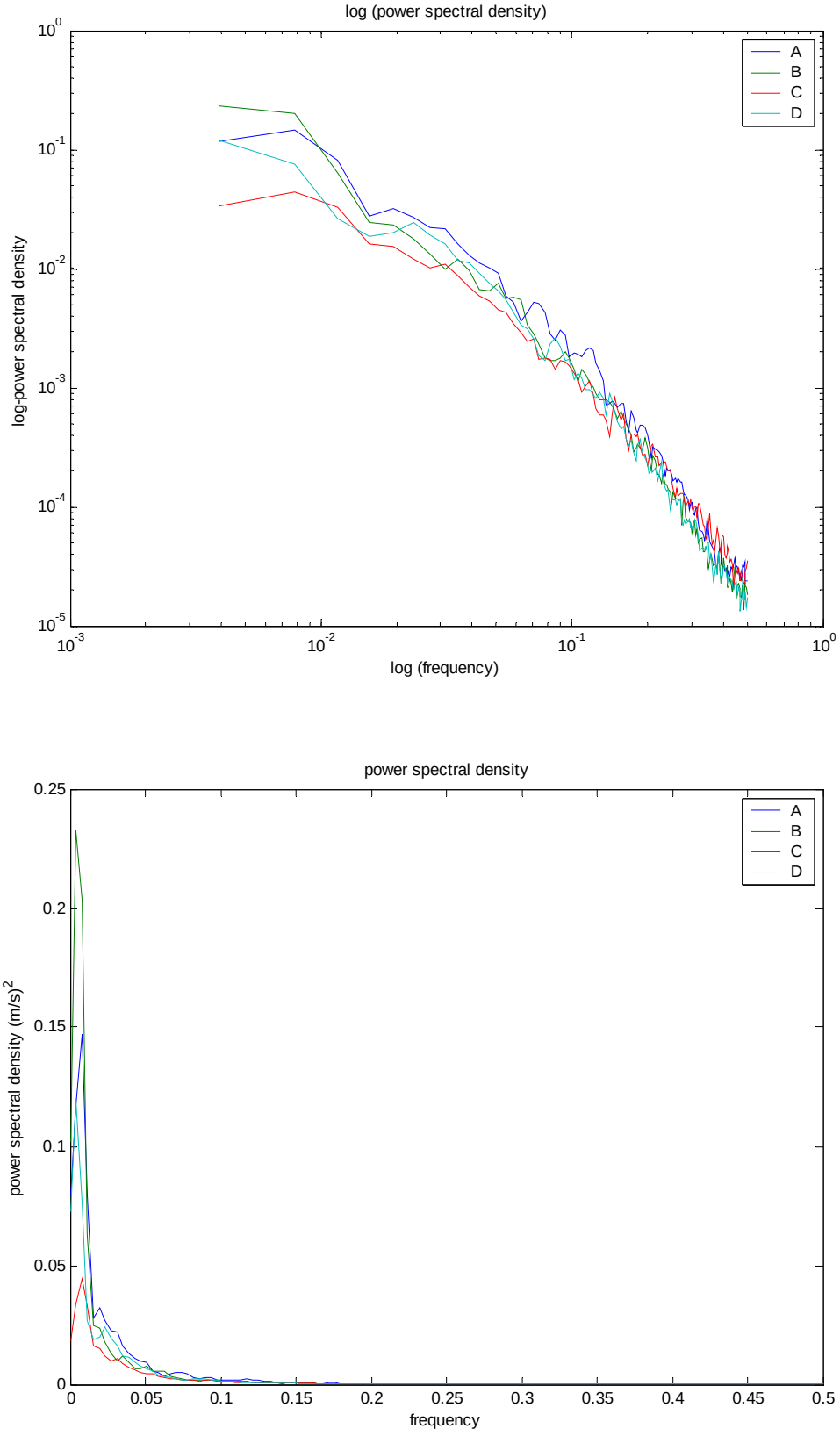

Figure B-11 Power density of temperature and velocity records with turbulence intensity 30.93%(Hi,24C,15-30hz)

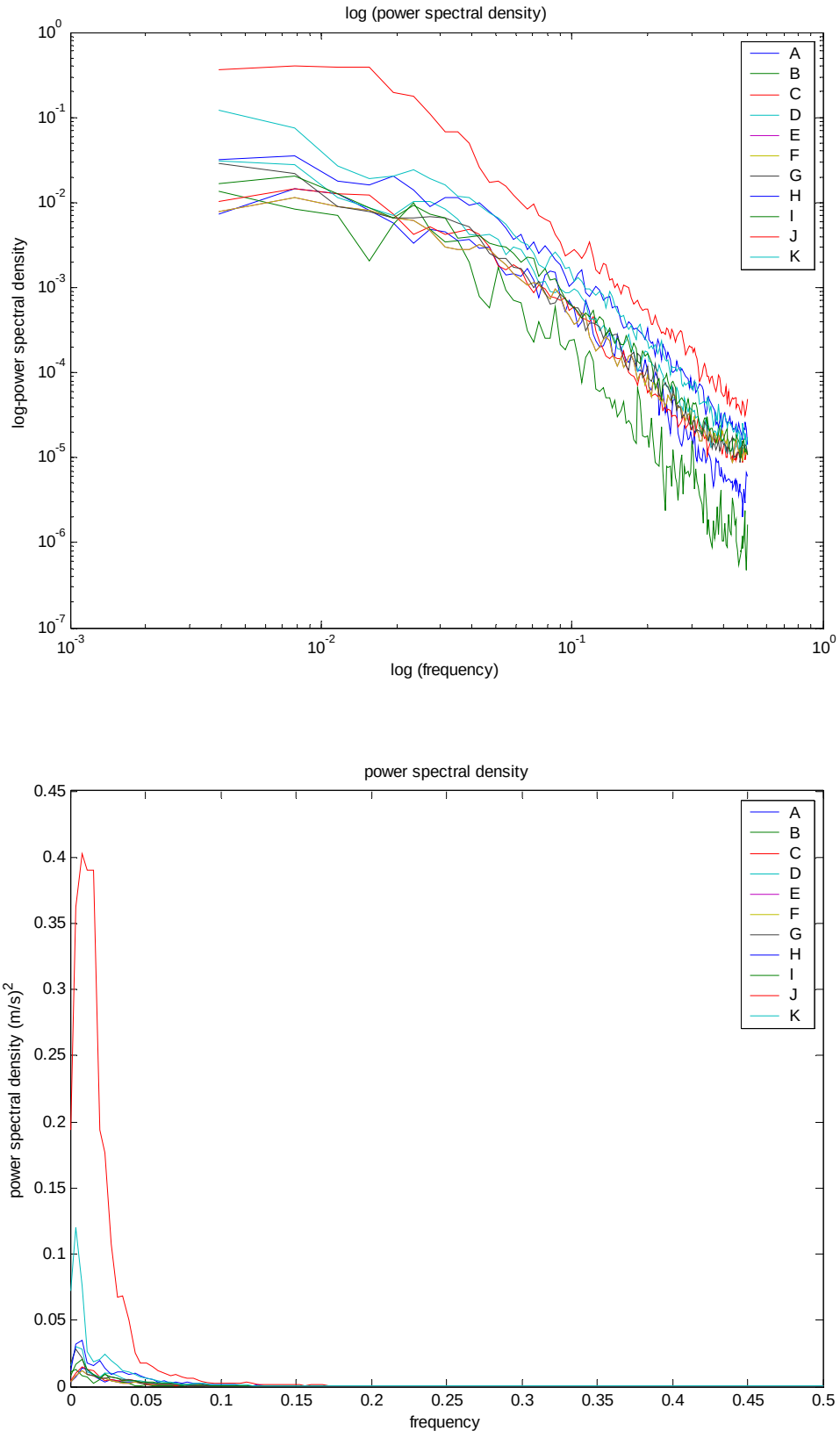

Figure B-12 Location guest 0.6 power density of temperature and velocity records

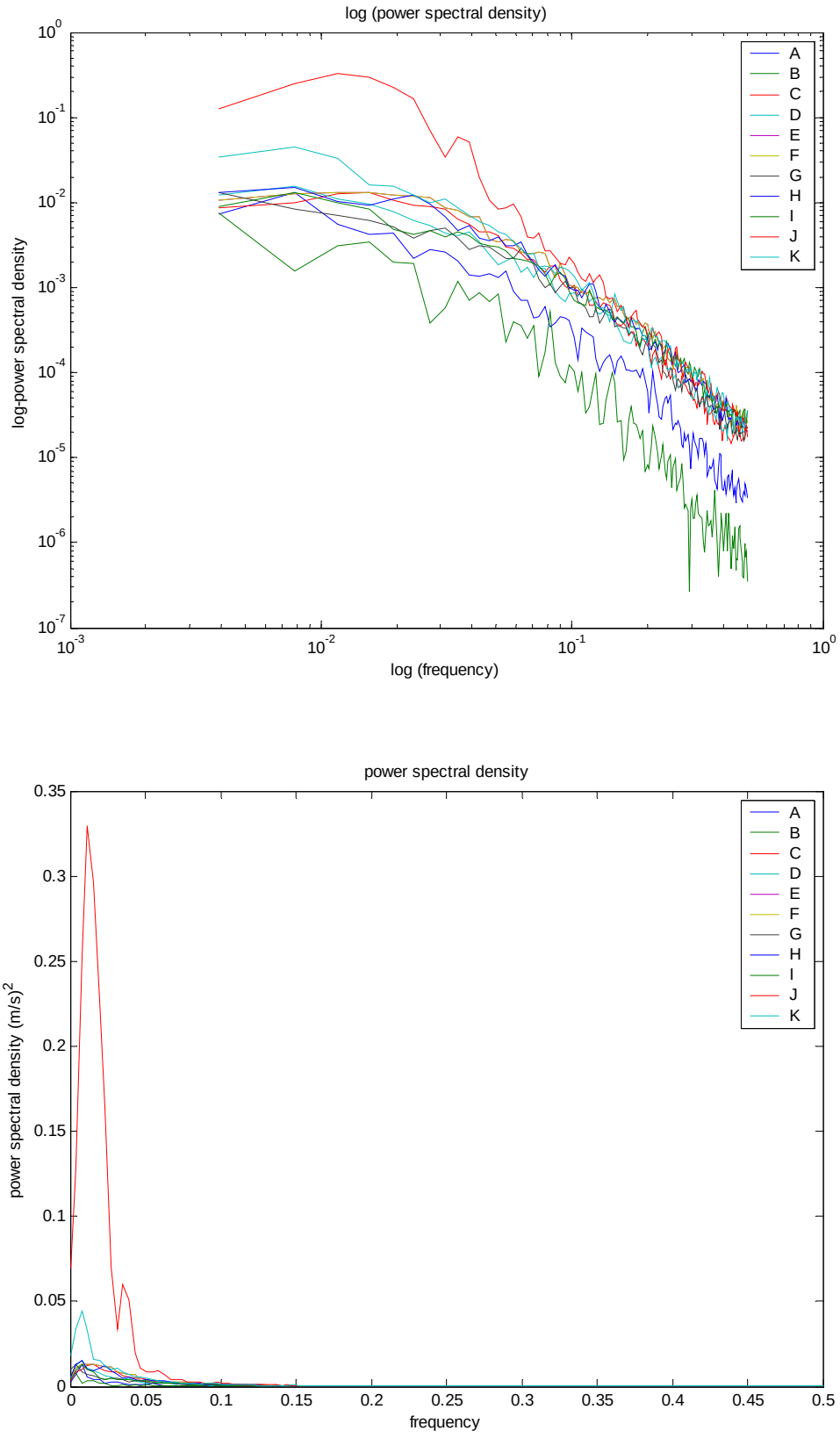

Figure B-13 Location guest 1.1 power density of temperature and velocity records

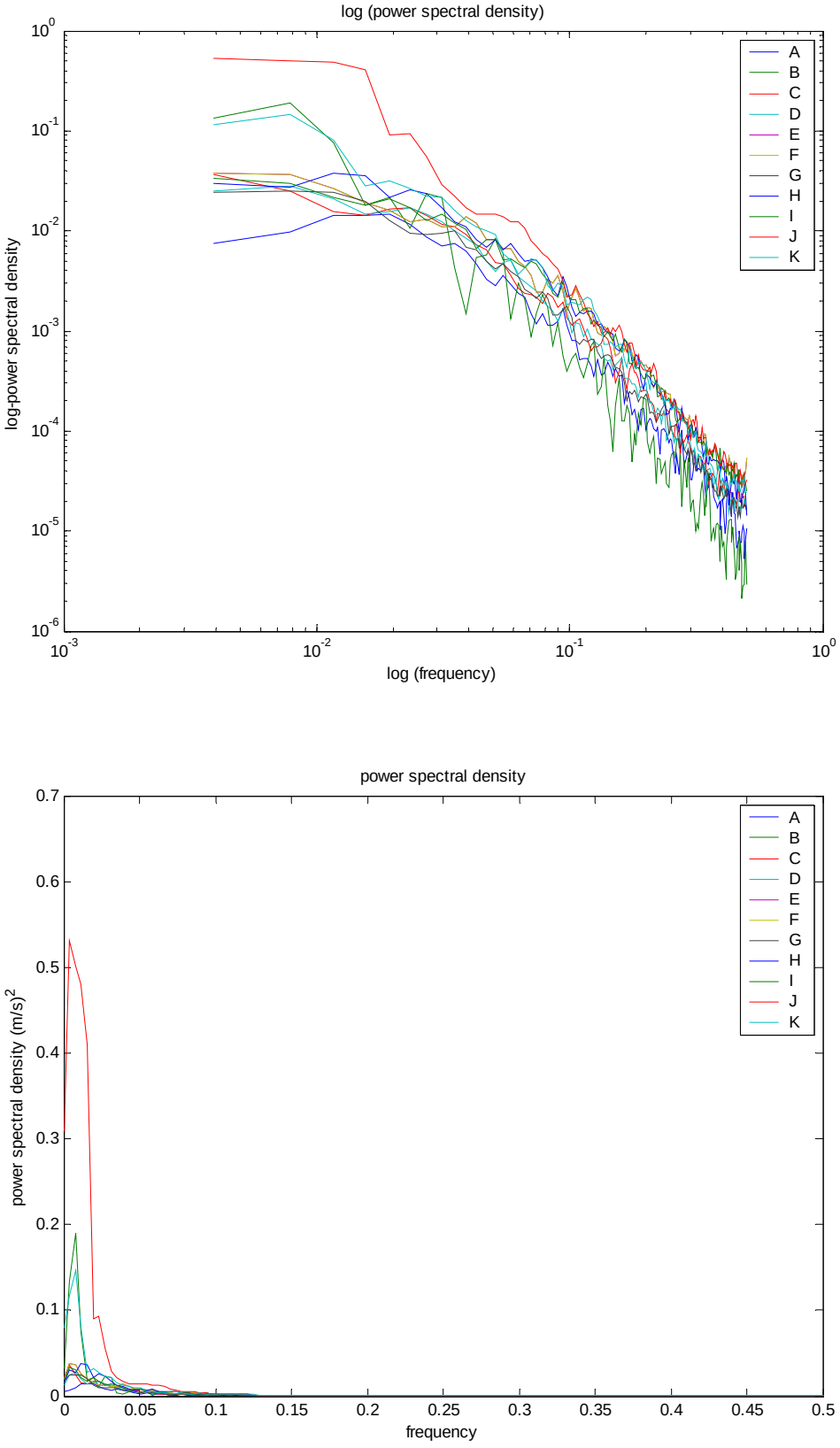

Figure B-14 Location sit 0.6 power density of temperature and velocity records

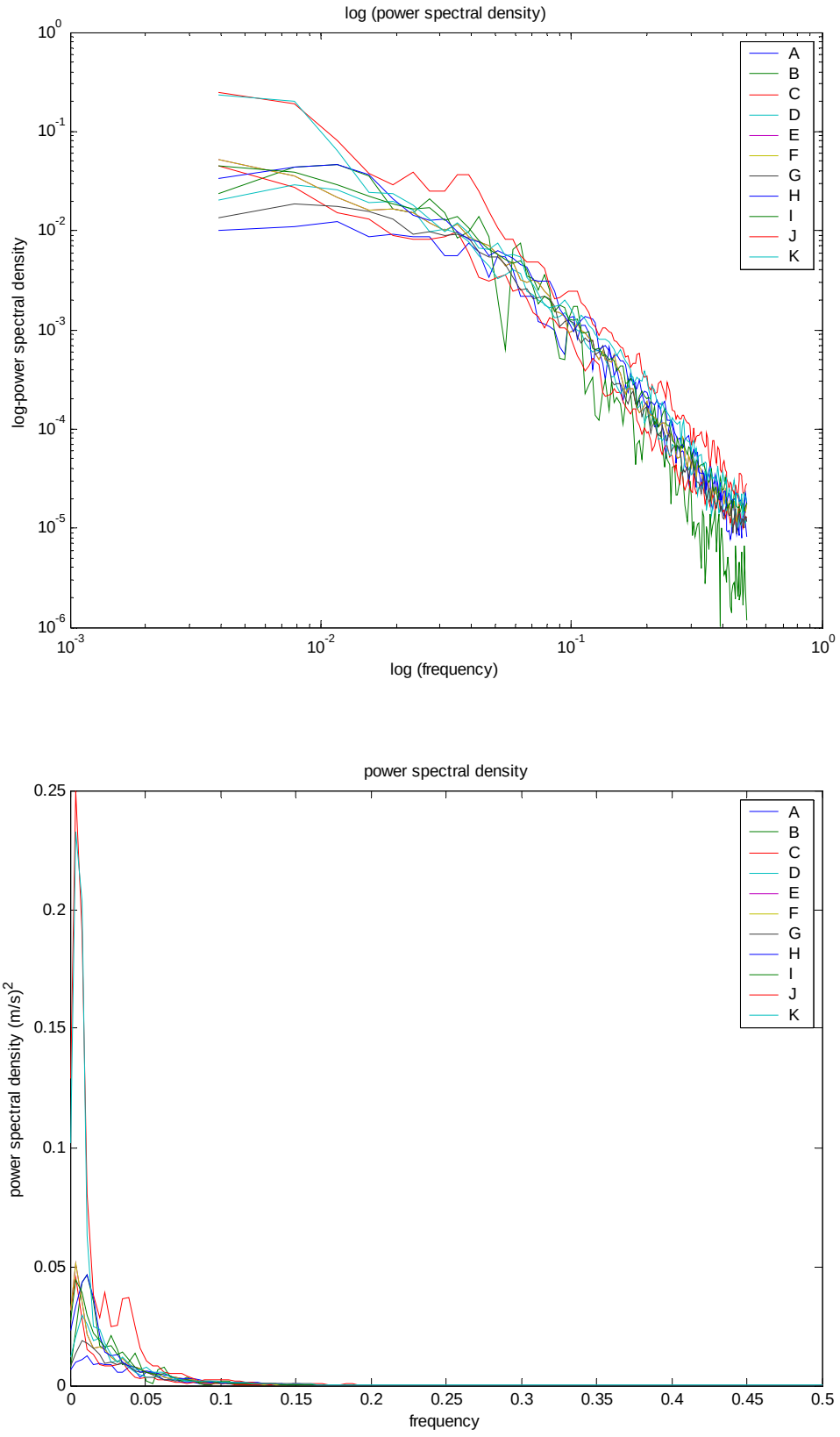

Figure B-15 Location sit 1.1 power density of temperature and velocity records

APPENDIX C – RELATIONSHIP BETWEEN AIR TEMPERATURE AND AIR VELOCITY

C.1 Correlation between air temperature and air velocity

HFCS (without centrifugal fan)

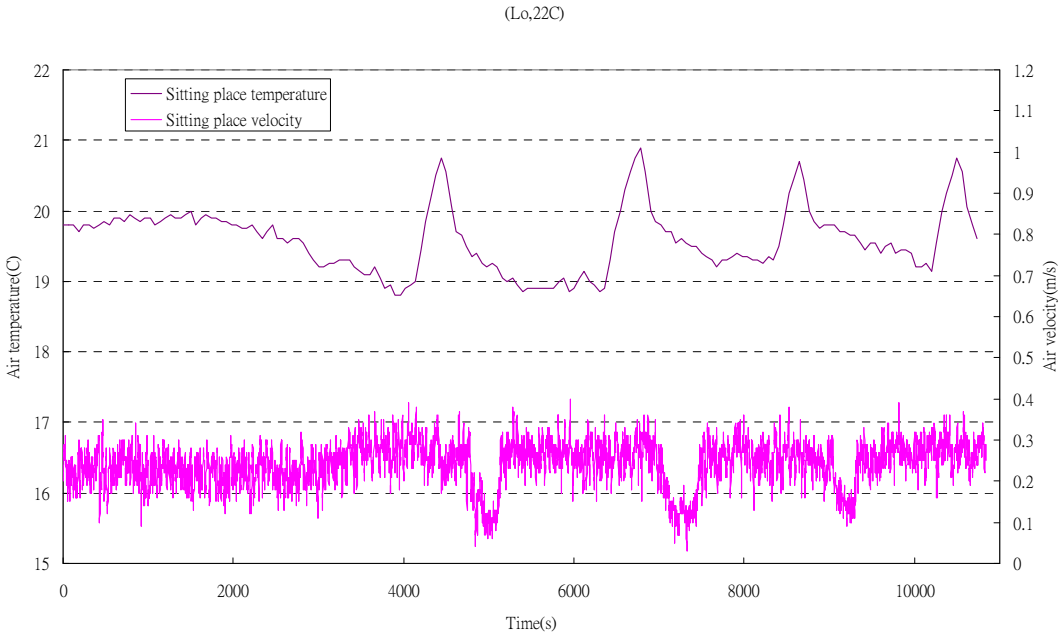

Figure C-1: Correlation between air temperature and air velocity at set point 22 ℃ and low fan speed.

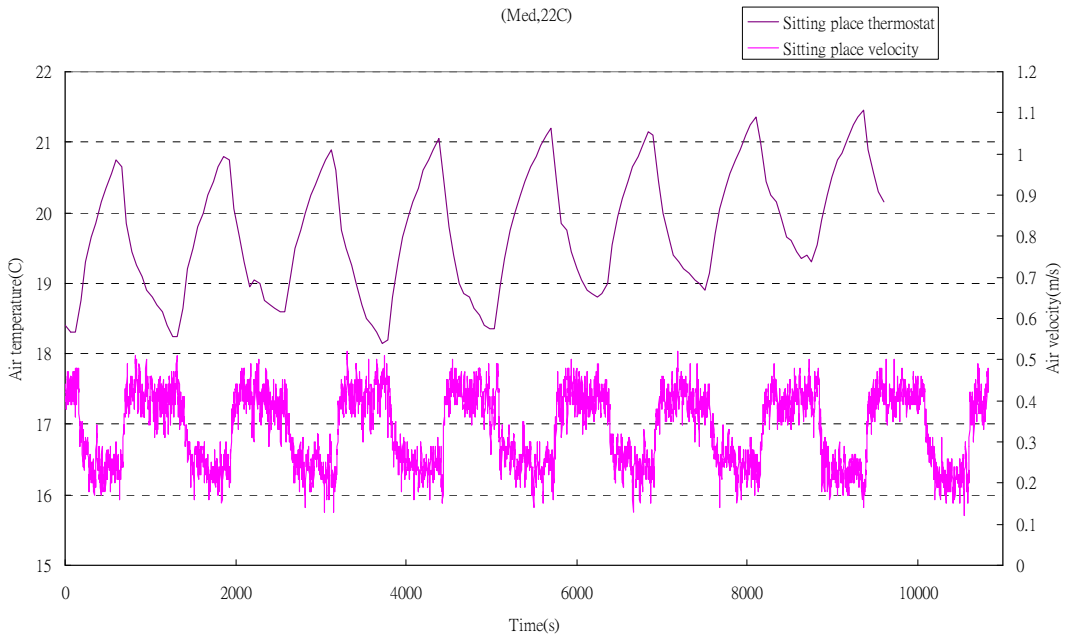

Figure C-2: Correlation between air temperature and air velocity at set point 22℃ and med fan speed.

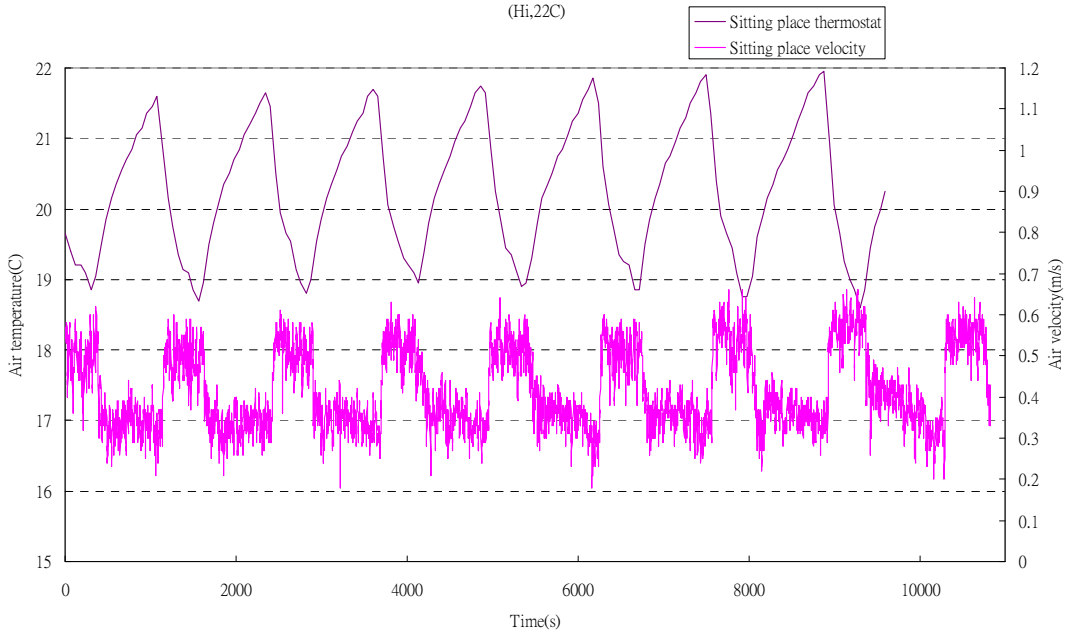

Figure C-3: Correlation between air temperature and air velocity at set point 22℃ and hi fan speed.

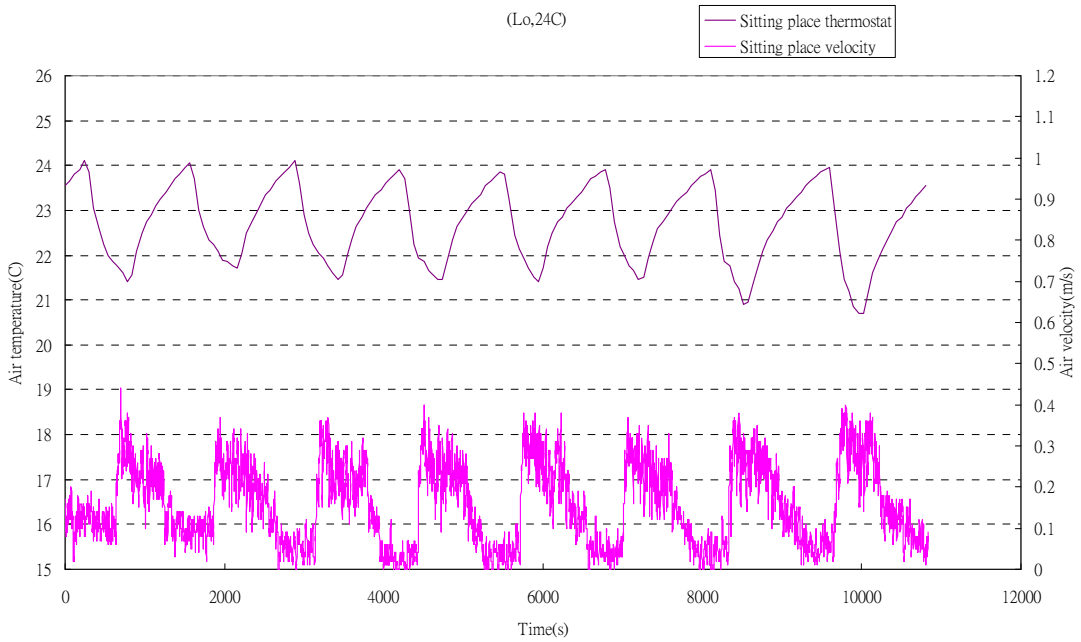

Figure C-4 Correlation between air temperature and air velocity at set point 24℃ and lo fan speed.

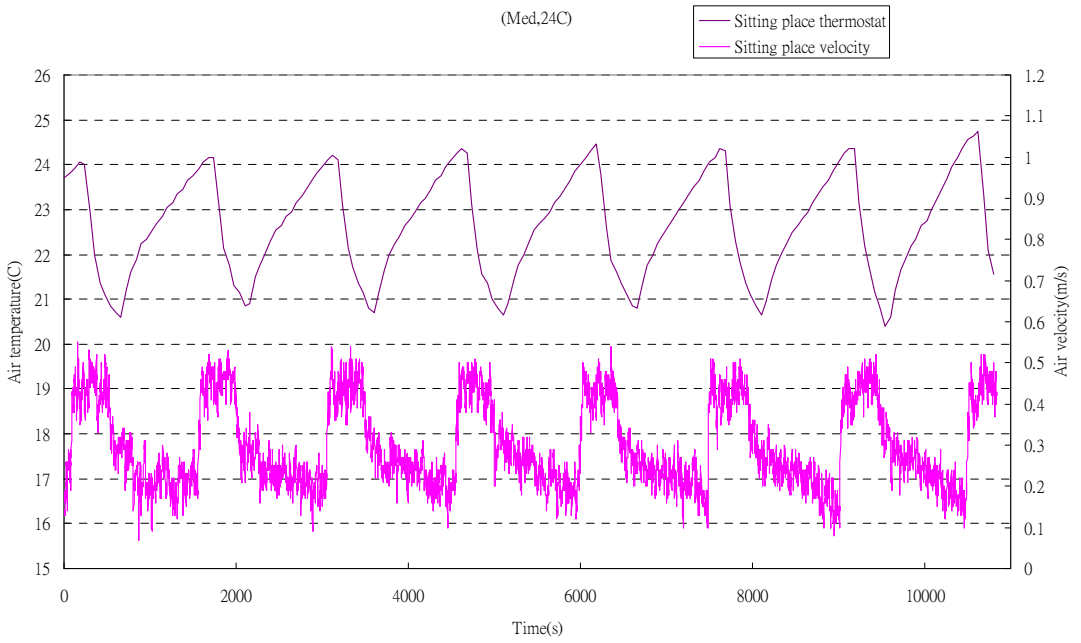

Figure C-5: Correlation between air temperature and air velocity at set point 24℃ and med fan speed.

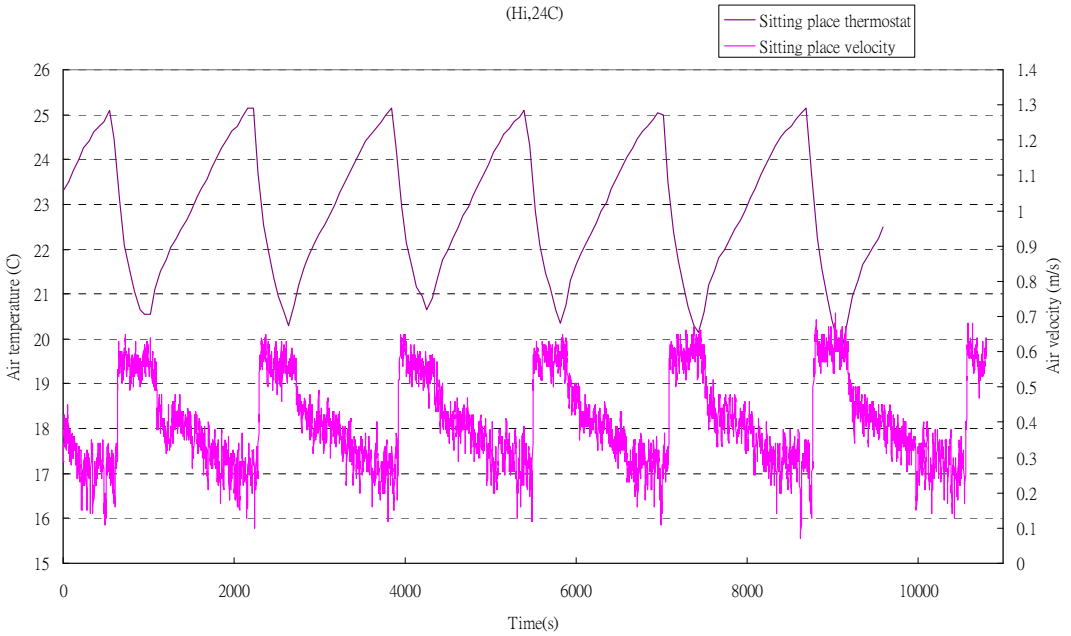

Figure C-6: Correlation between air temperature and air velocity at set point 24℃ and hi fan speed.

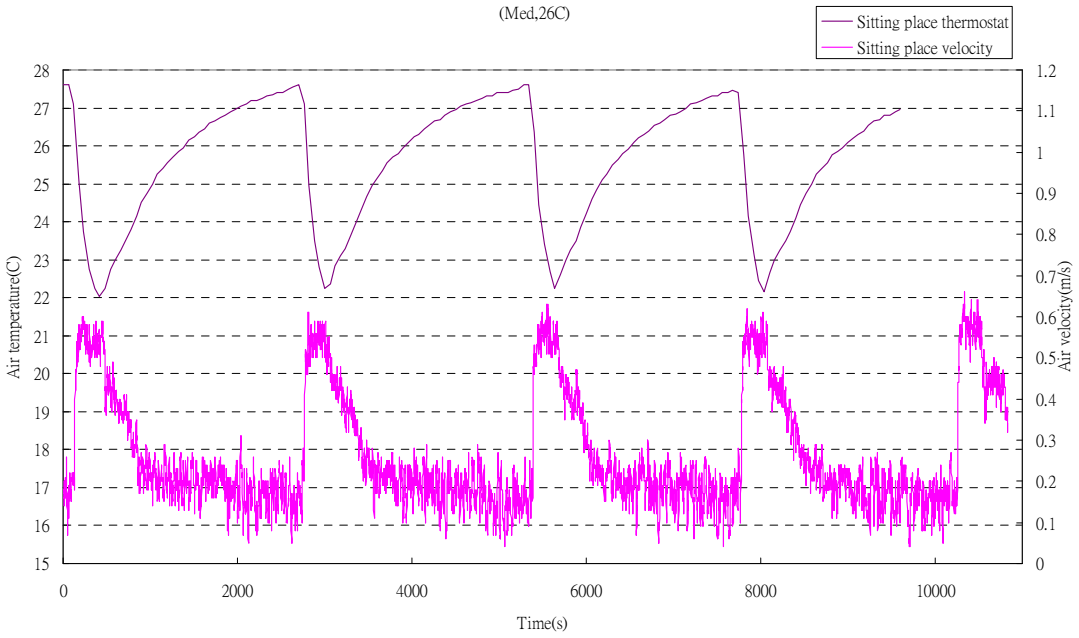

Figure C-7: Correlation between air temperature and air velocity at set point 26℃ and med fan speed.

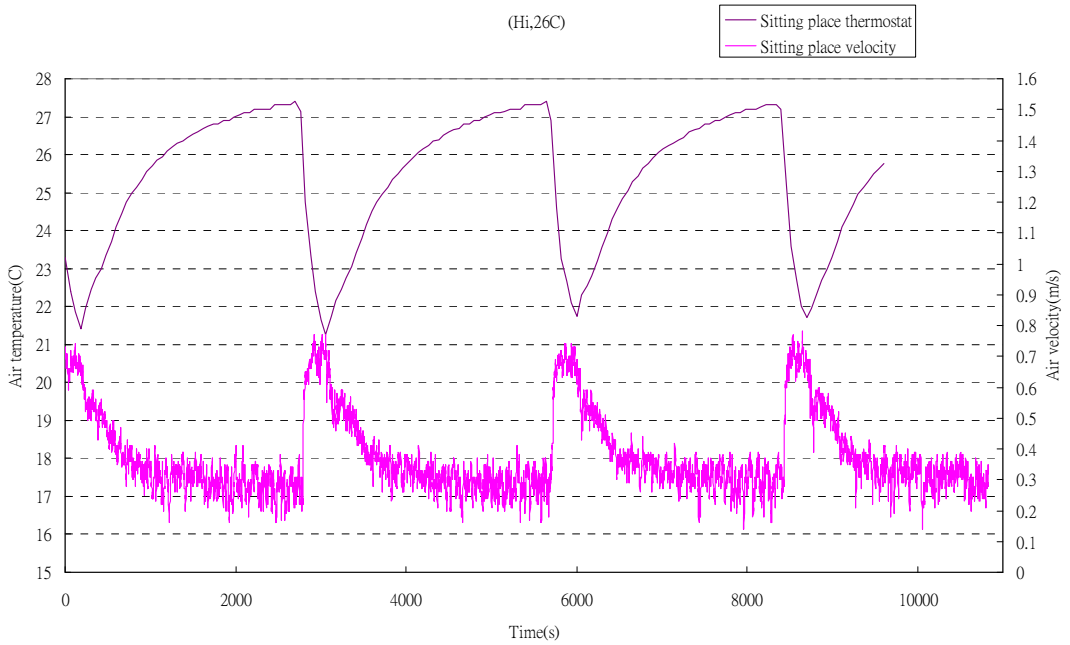

Figure C-8: Correlation between air temperature and air velocity at set point 26℃ and hi fan speed.

HFCS (with centrifugal fan)

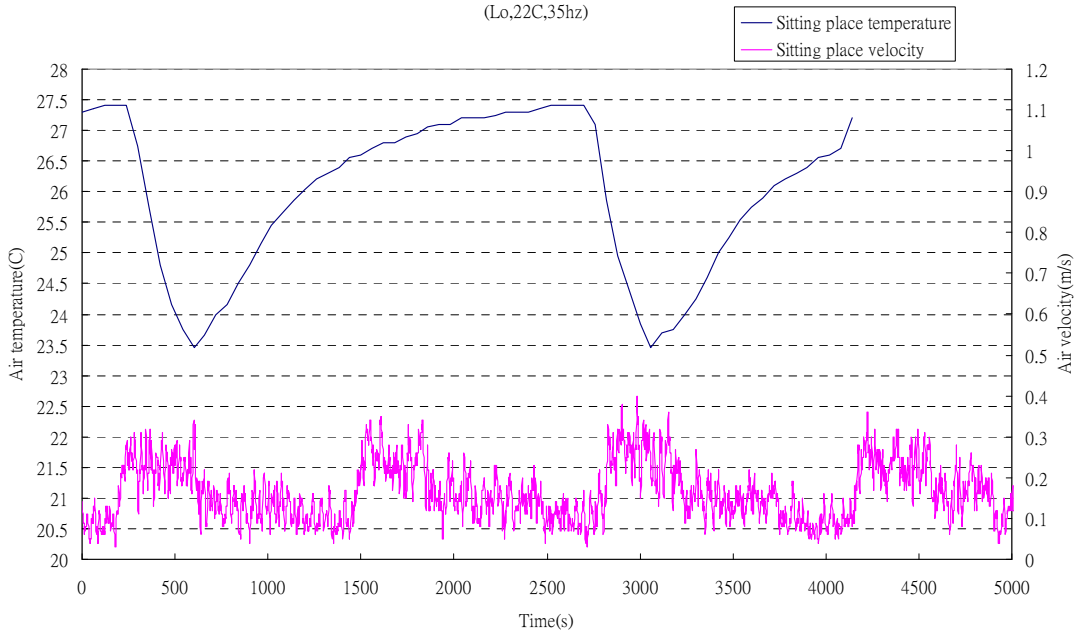

Figure C-9: Correlation between air temperature and air velocity at set point 22℃, 35Hz frequency and lo fan speed.

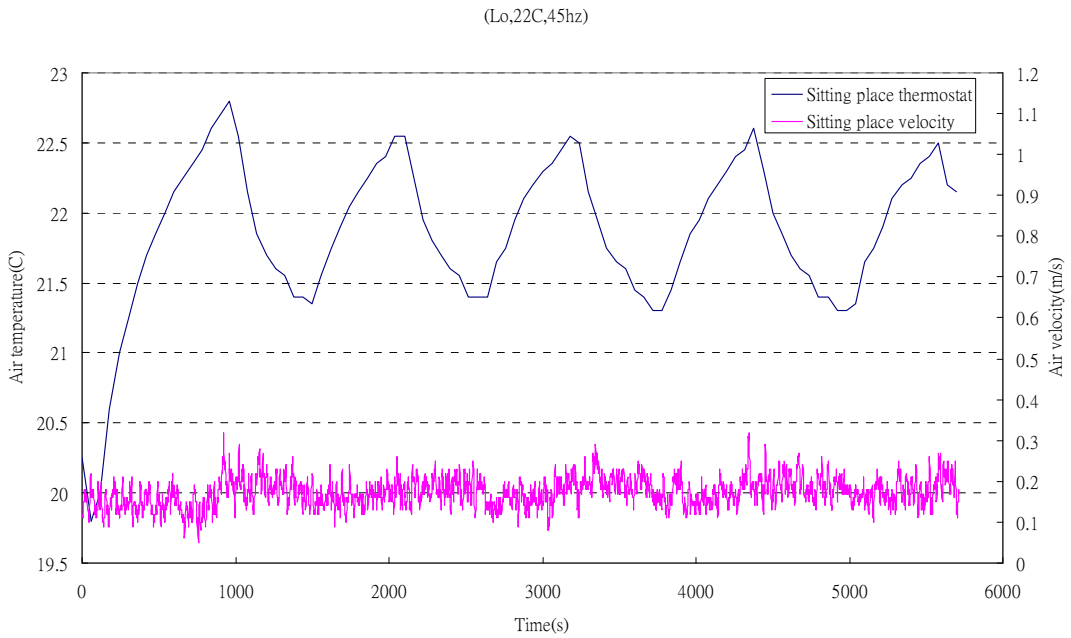

Figure C-10: Correlation between air temperature and air velocity at set point 22℃, 45Hz frequency and lo fan speed.

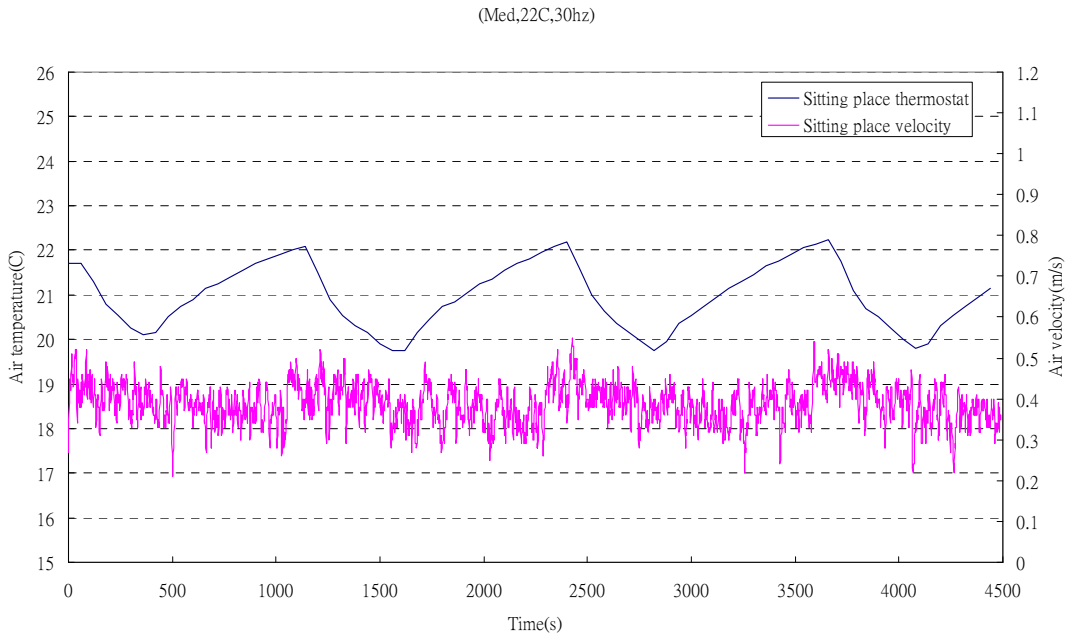

Figure C-11: Correlation between air temperature and air velocity at set point 22℃, 35Hz frequency and lo fan speed.

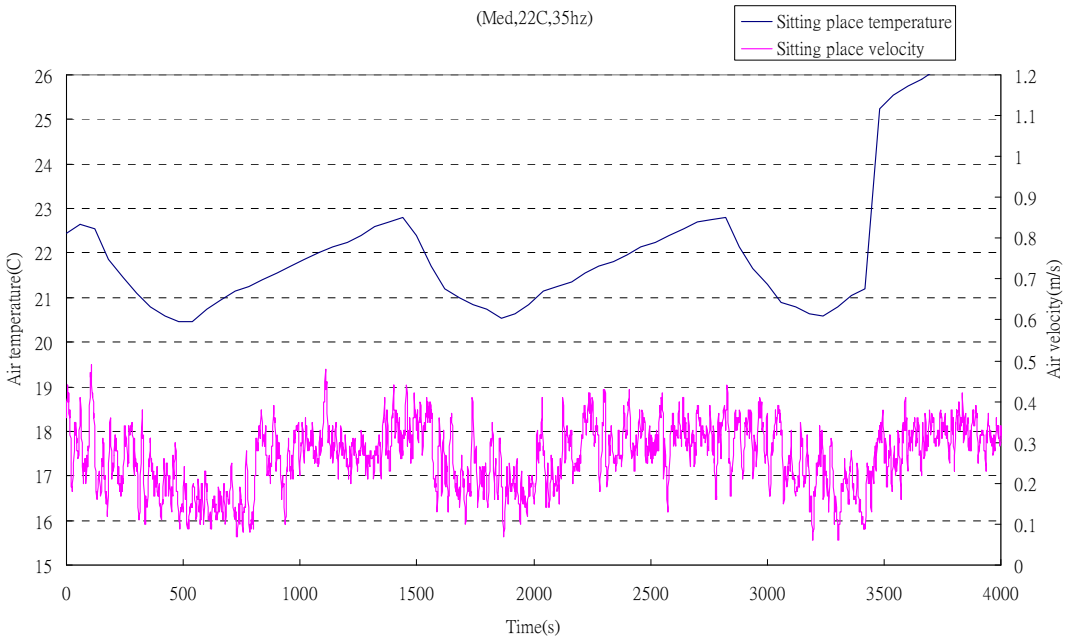

Figure C-12: Correlation between air temperature and air velocity at set point 22℃, 35Hz frequency and med fan speed.

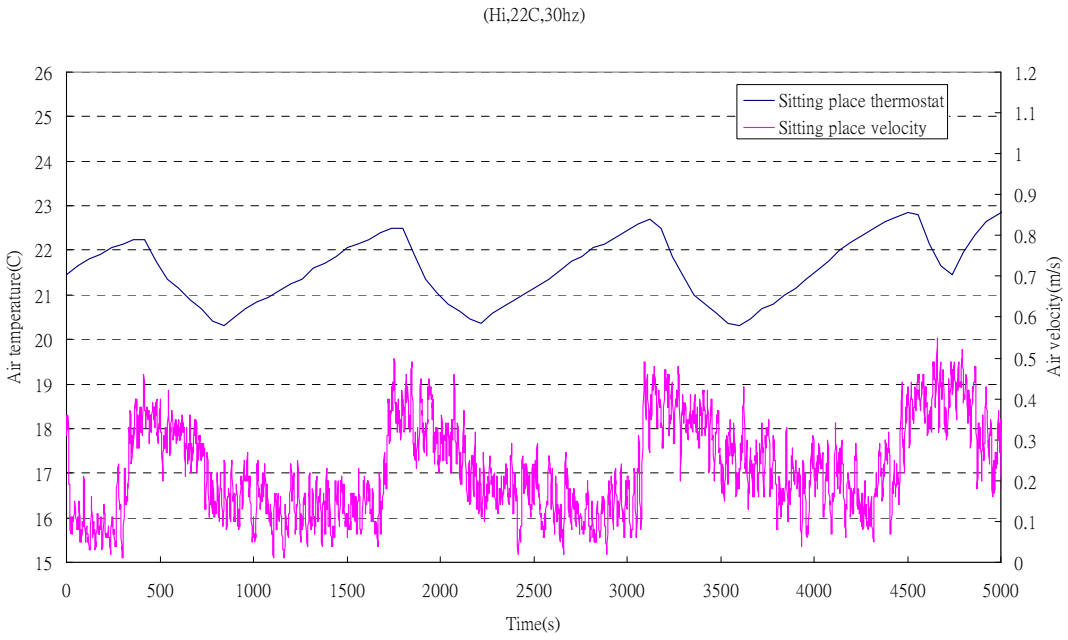

Figure C-13: Correlation between air temperature and air velocity at set point 22℃, 30Hz frequency and hi fan speed.

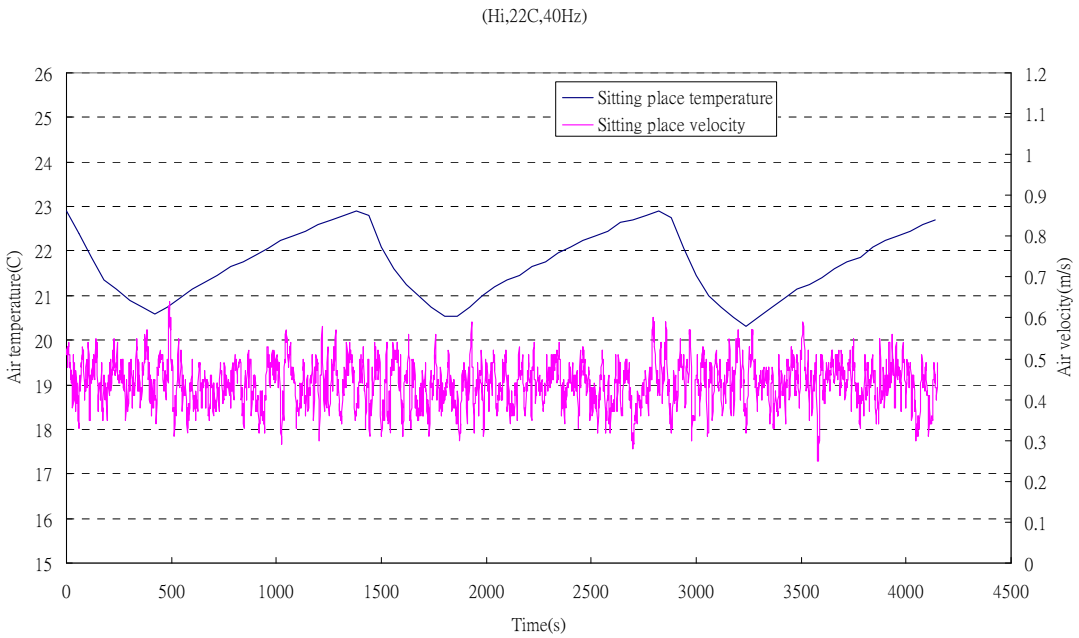

Figure C-14: Correlation between air temperature and air velocity at set point 22℃, 40Hz frequency and hi fan speed.

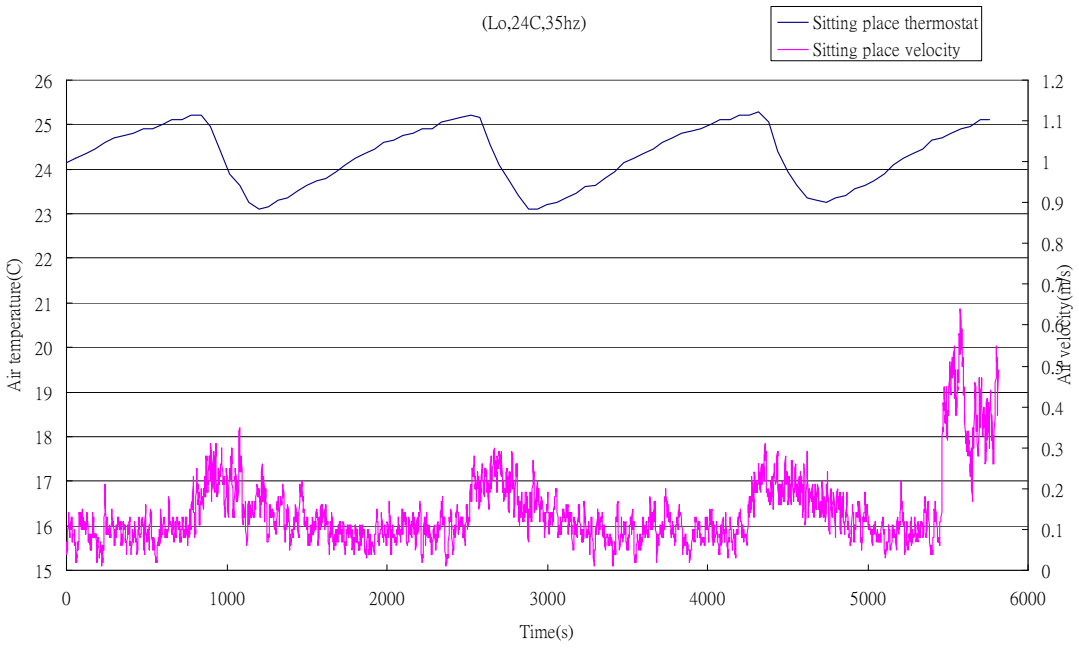

Figure C-15: Correlation between air temperature and air velocity at set point 24℃, 35Hz frequency and lo fan speed.

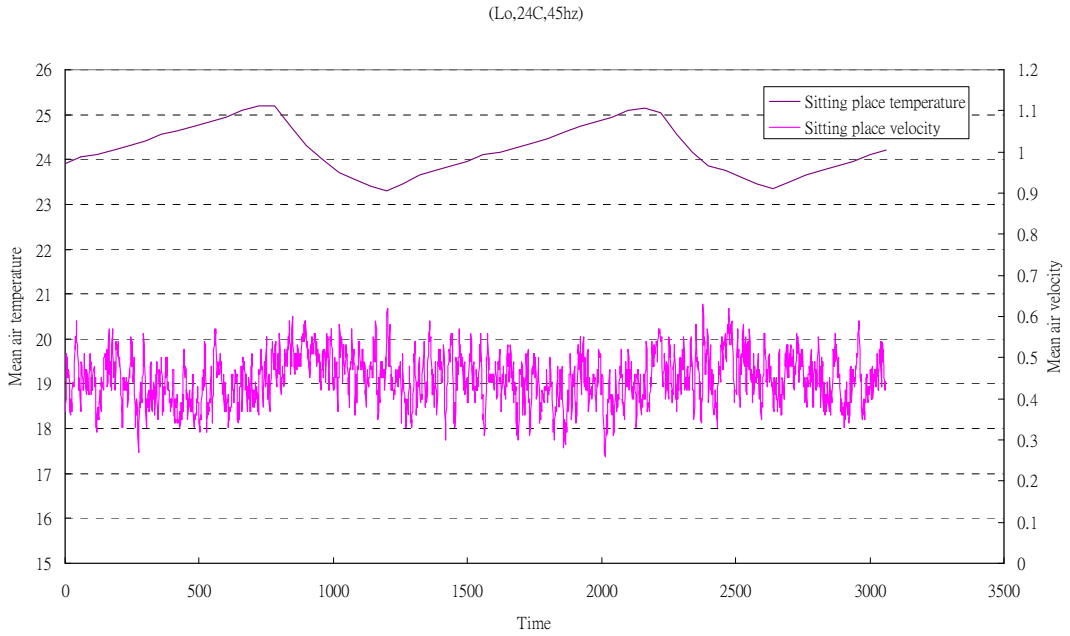

Figure C-16: Correlation between air temperature and air velocity at set point 24℃, 45Hz frequency and lo fan speed.

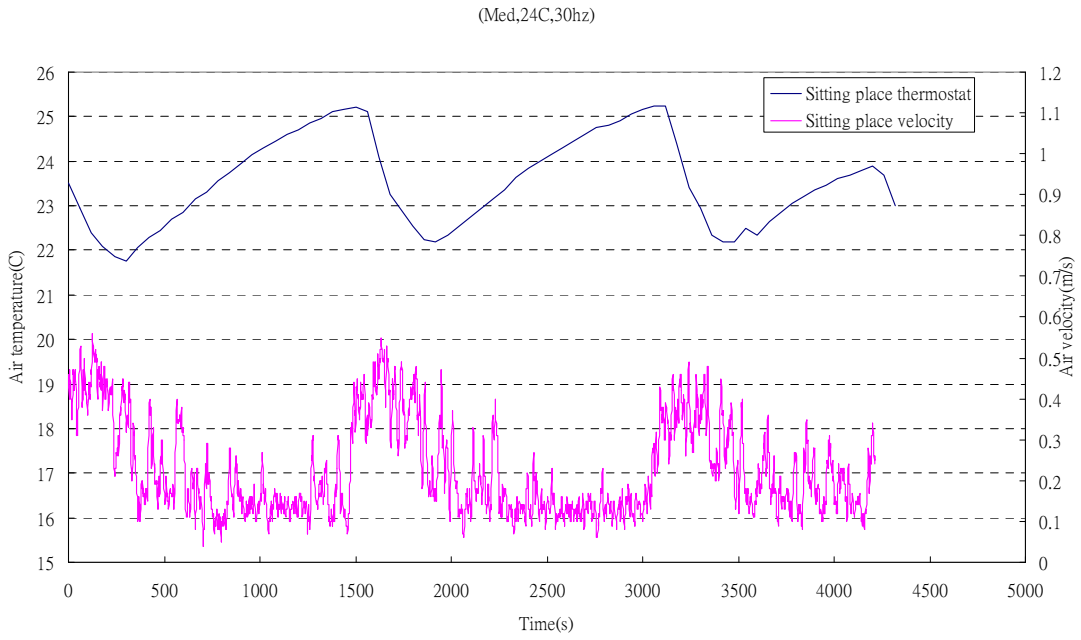

Figure C-17: Correlation between air temperature and air velocity at set point 24℃, 30Hz frequency and med fan speed.

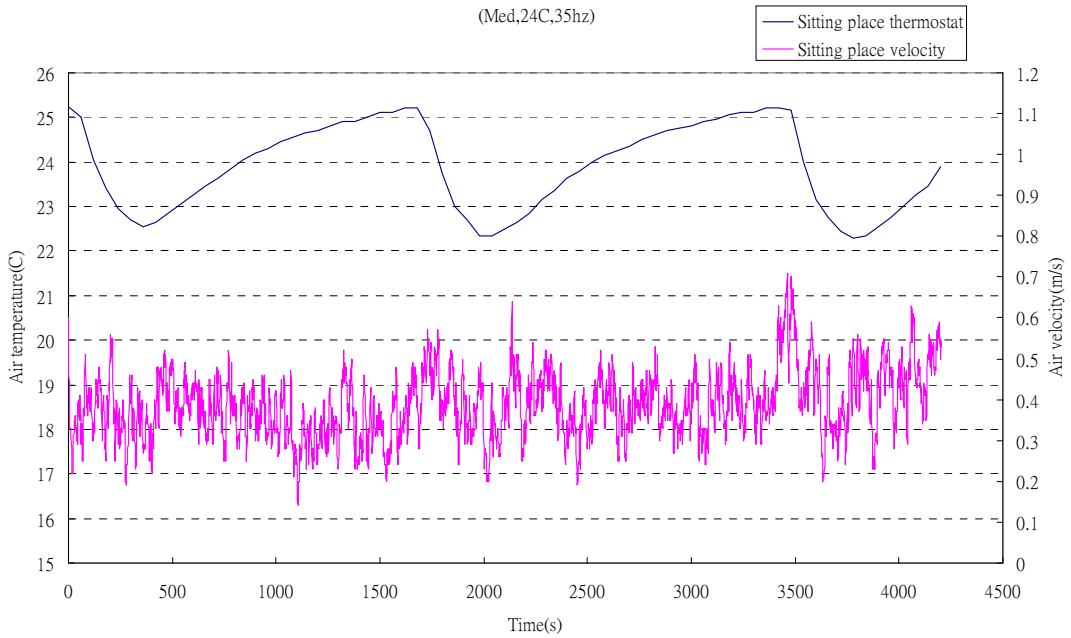

Figure C-18: Correlation between air temperature and air velocity at set point 24℃, 35Hz frequency and med fan speed.

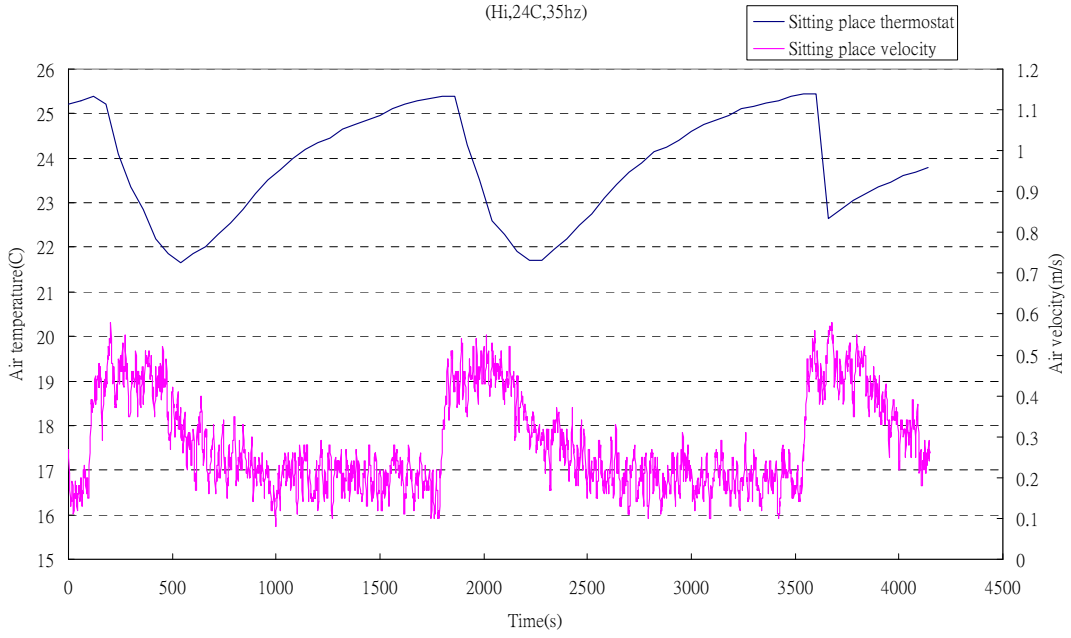

Figure C-19: Correlation between air temperature and air velocity at set point 24℃, 35Hz frequency and hi fan speed.

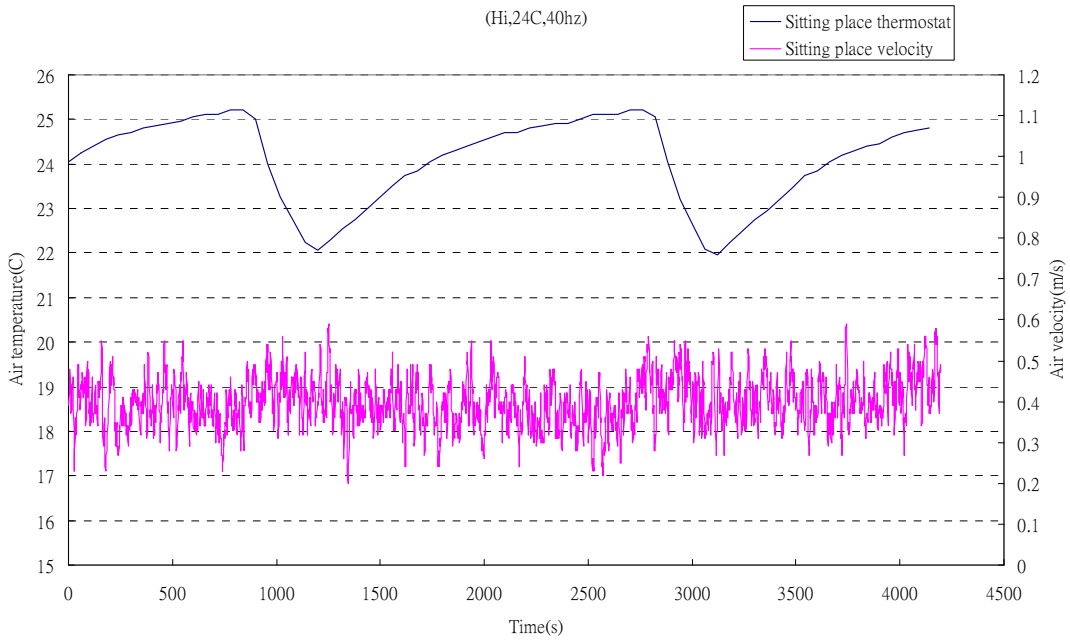

Figure C-20: Correlation between air temperature and air velocity at set point 24℃, 40Hz frequency and hi fan speed.

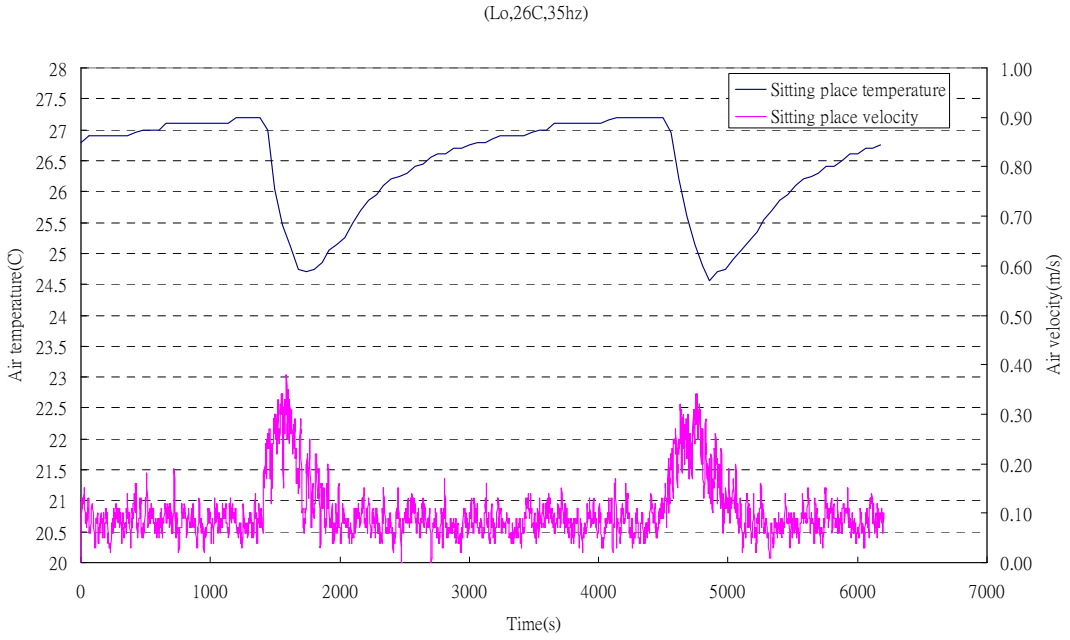

Figure C-21: Correlation between air temperature and air velocity at set point 26℃, 35Hz frequency and lo fan speed.

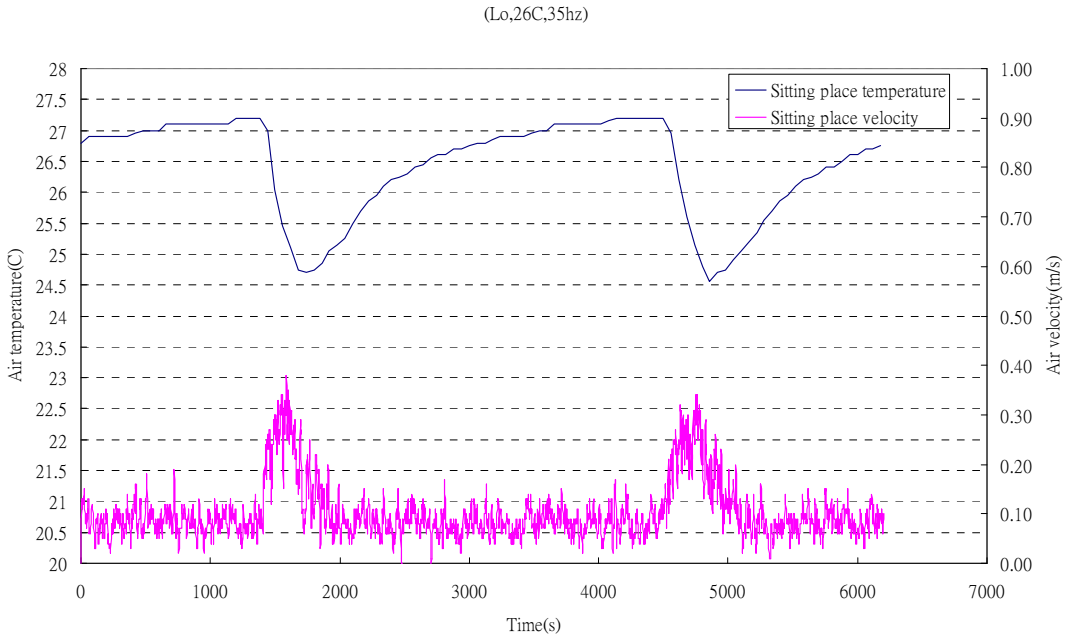

Figure C-22: Correlation between air temperature and air velocity at set point 26℃, 35Hz frequency and lo fan speed.

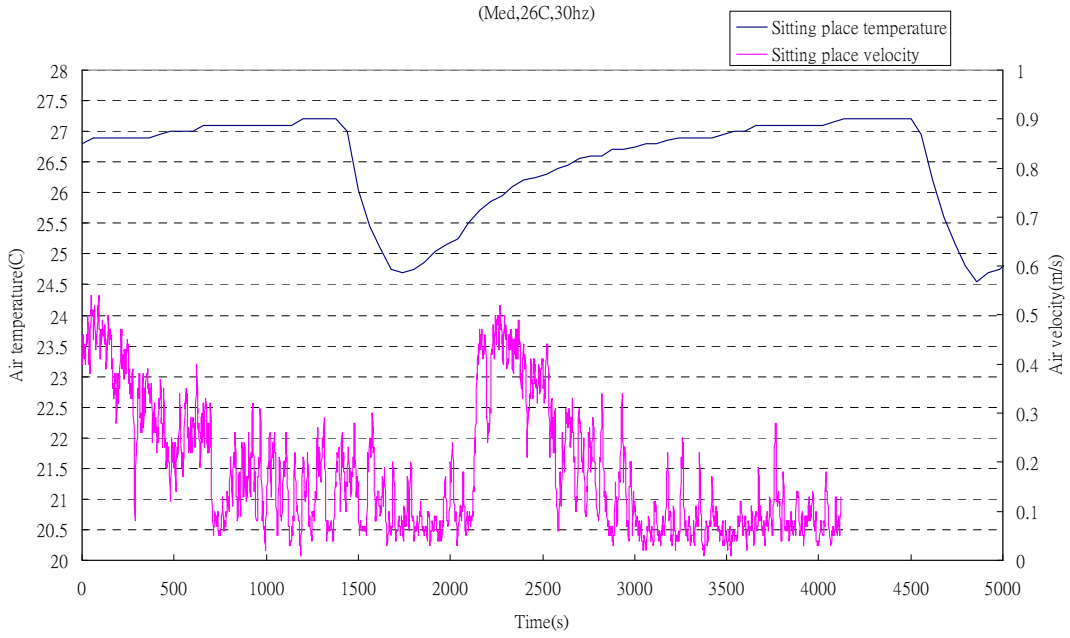

Figure C-23: Correlation between air temperature and air velocity at set point 26℃, 30Hz frequency and med fan speed.

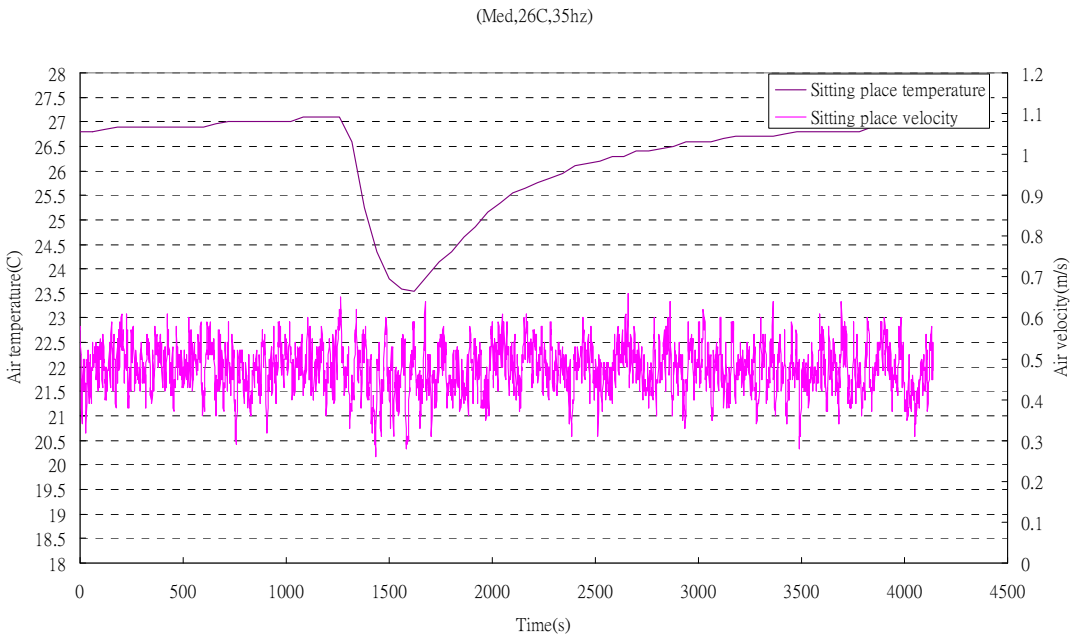

Figure C-24: Correlation between air temperature and air velocity at set point 26℃, 35Hz frequency and med fan speed.

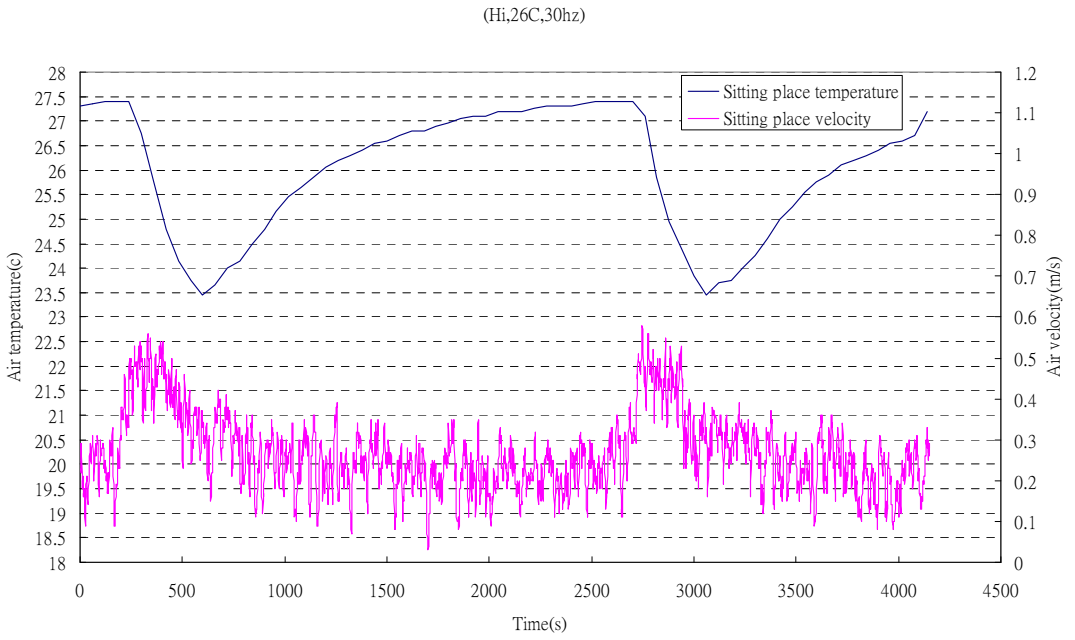

Figure C-25: Correlation between air temperature and air velocity at set point 26℃, 30Hz frequency and hi fan speed.

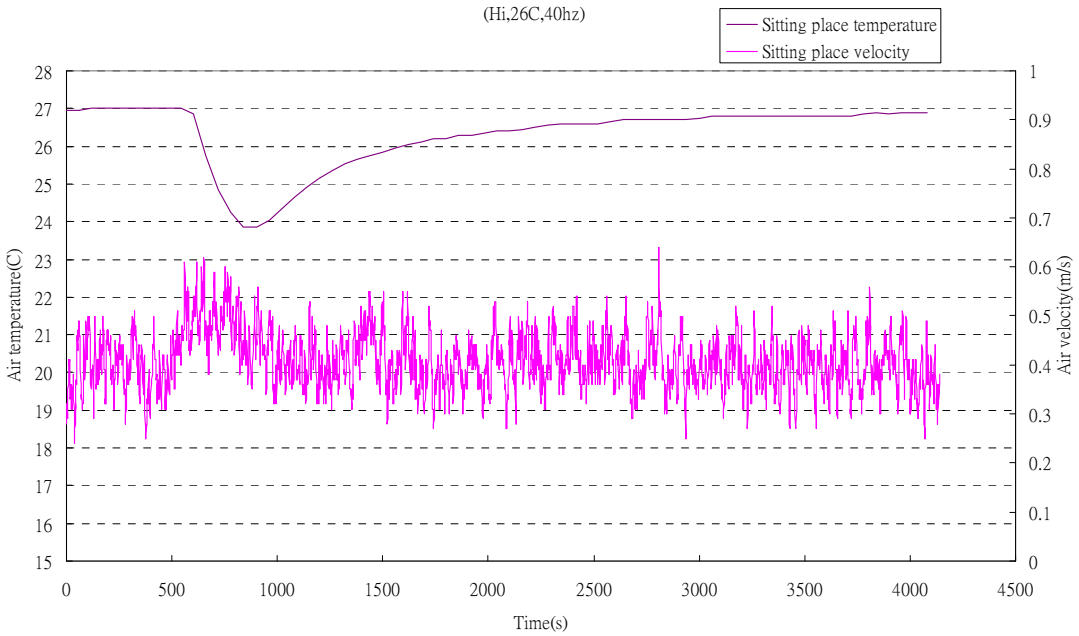

Figure C-26: Correlation between air temperature and air velocity at set point 26℃, 40Hz frequency and hi fan speed.

HFCS (with centrifugal fan and fluctuating frequency)

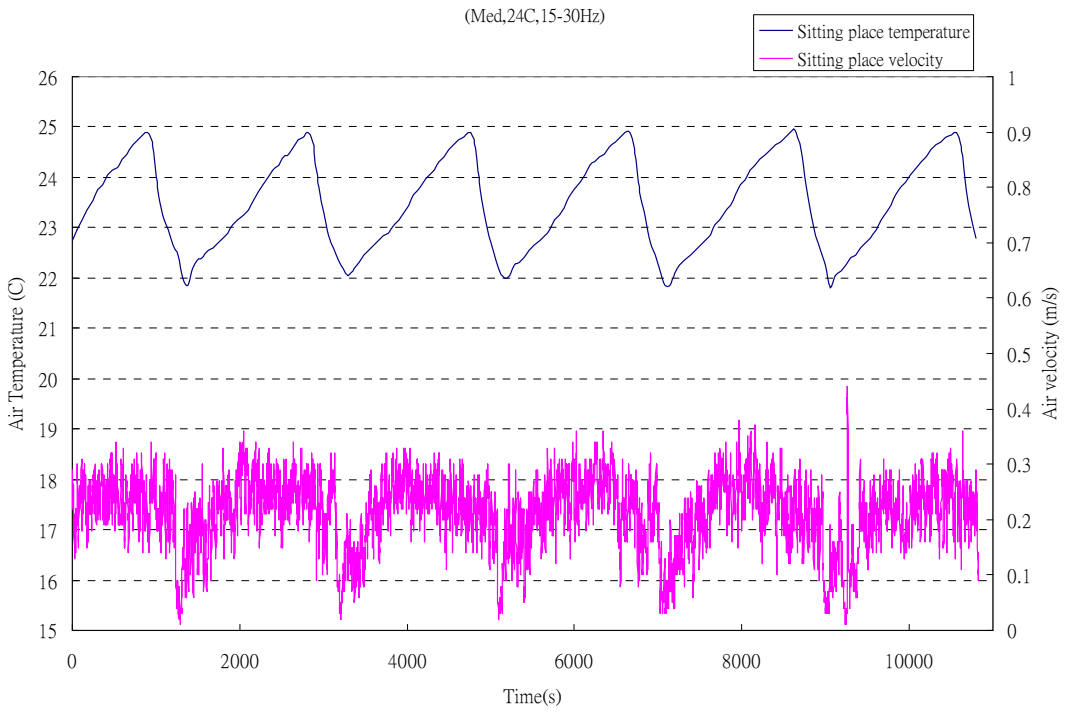

Figure C-26: Correlation between air temperature and air velocity at set point 24 ℃, 15 to 30Hz frequency and med fan speed.

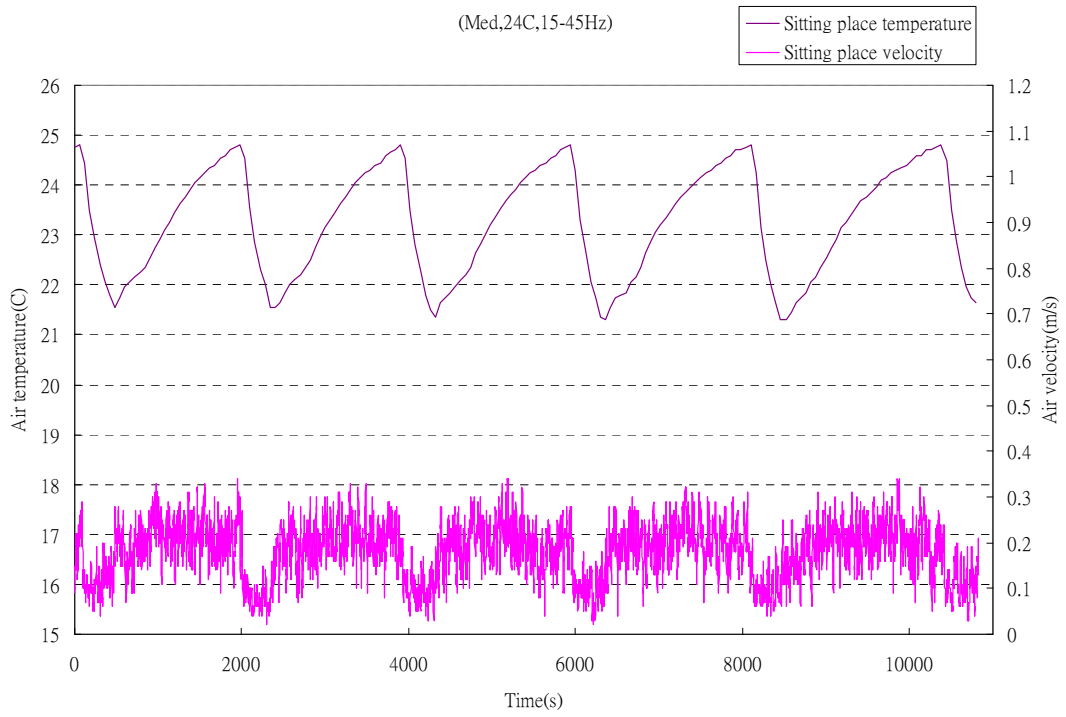

Figure C-27:Correlation between air temperature and air velocity at set point 24 ℃, 15 to 45Hz frequency and med fan speed.

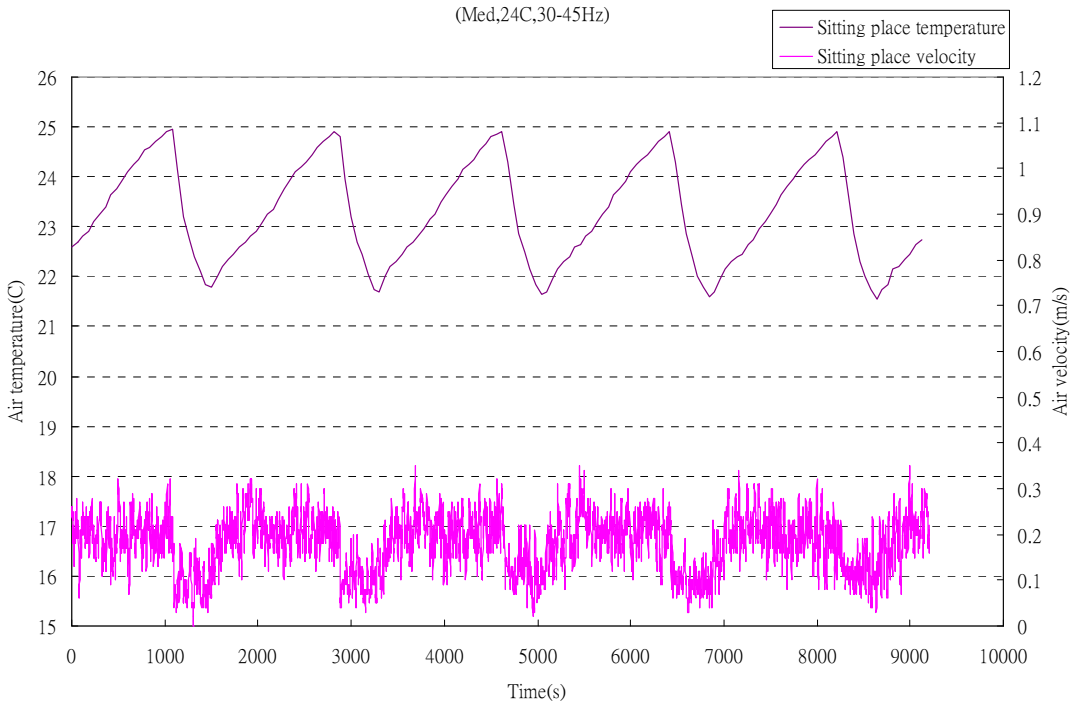

Figure C-28: Correlation between air temperature and air velocity at set point 24 ℃, 30 to 45Hz frequency and med fan speed.

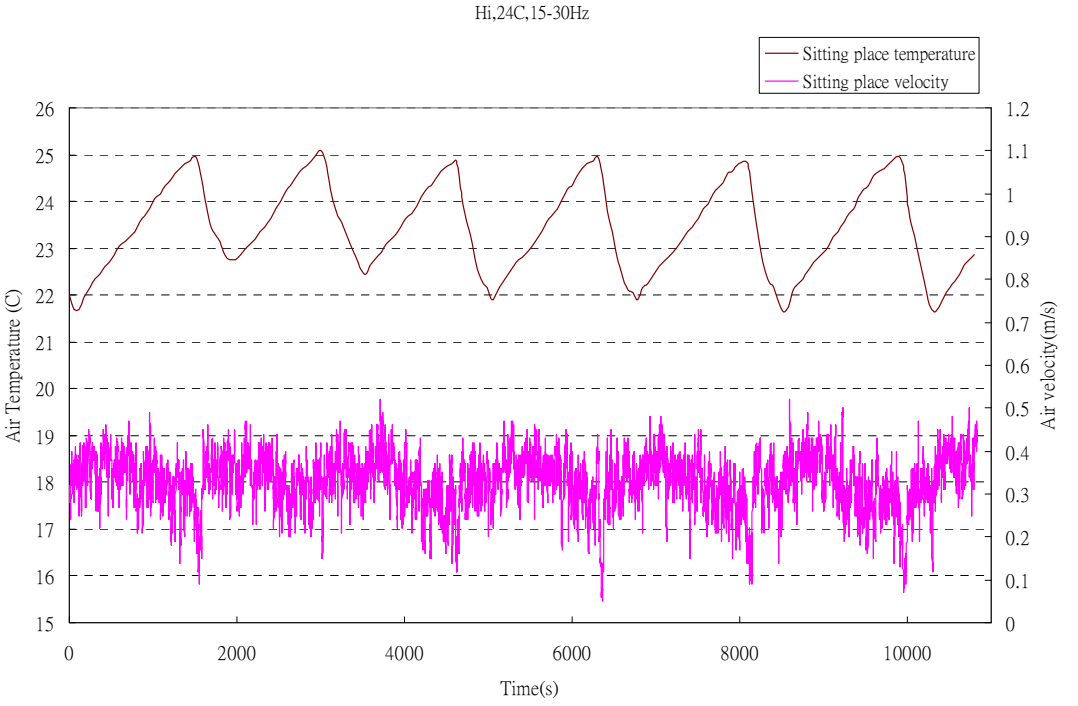

Figure C-29: Correlation between air temperature and air velocity at set point 24 ℃, 15 to 30Hz frequency and hi fan speed.

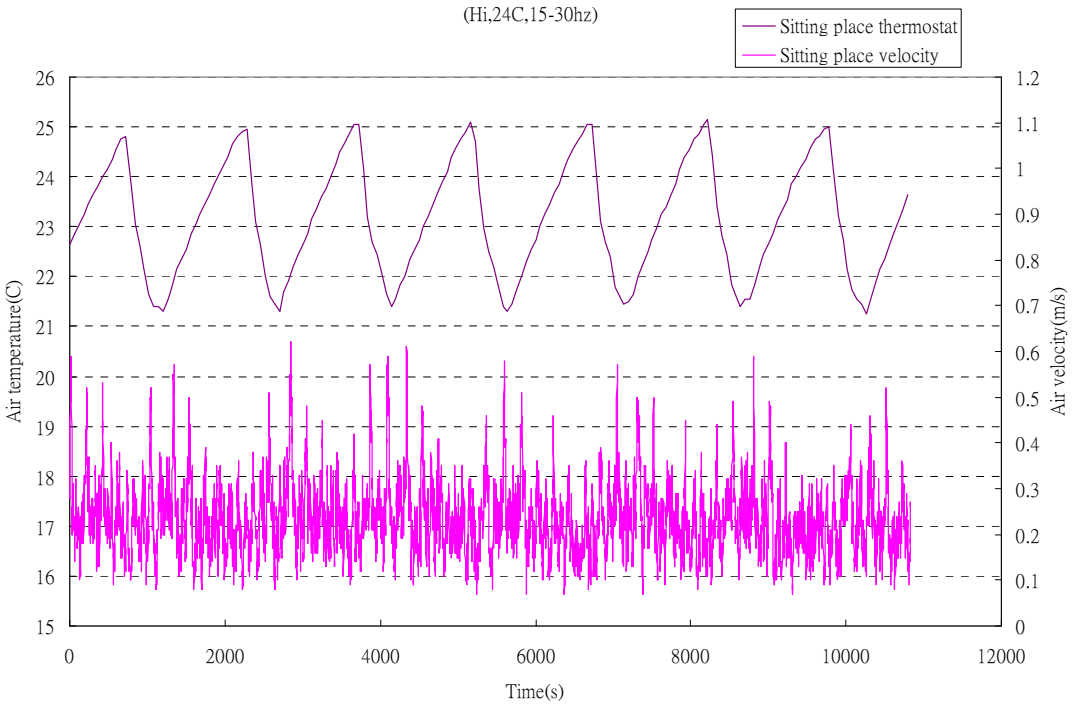

Figure C-29: Correlation between air temperature and air velocity at set point 24 ℃, 15 to 30Hz frequency and hi fan speed.

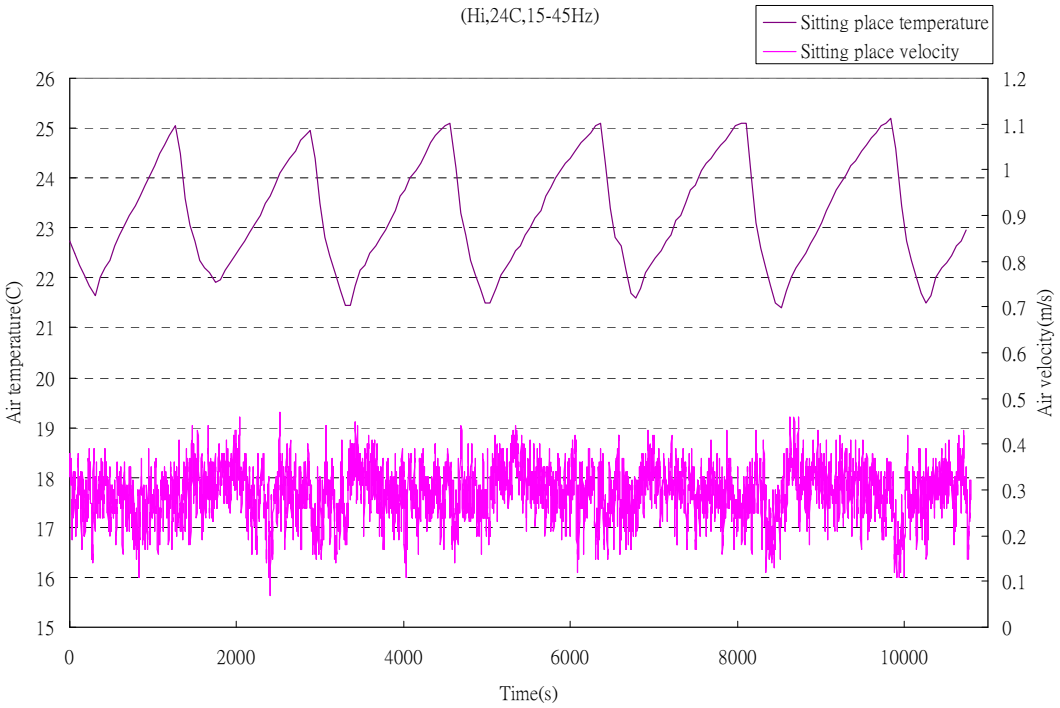

Figure C-30: Correlation between air temperature and air velocity at set point 24 ℃, 15 to 45Hz frequency and hi fan speed.

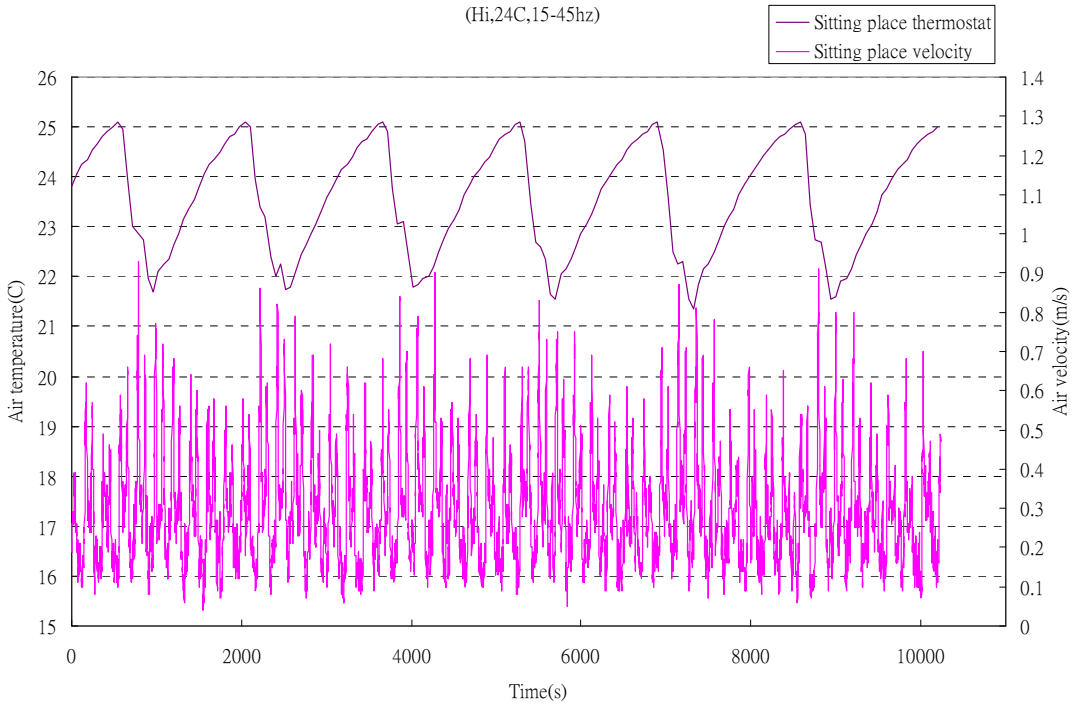

Figure C-31: Correlation between air temperature and air velocity at set point 24℃, 15 to 45Hz frequency and hi fan speed.

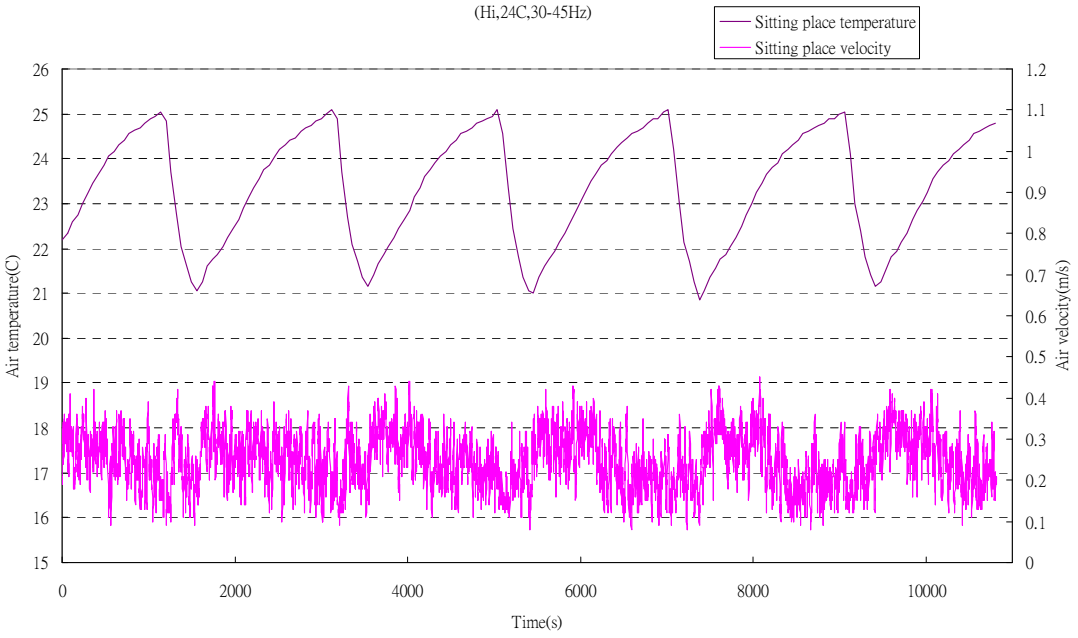

Figure C-32: Correlation between air temperature and air velocity at set point 24℃, 30 to 45Hz frequency and hi fan speed.

C.2 Relationship between mean air temperature and standard deviation of air velocity

HFCS (without centrifugal fan)

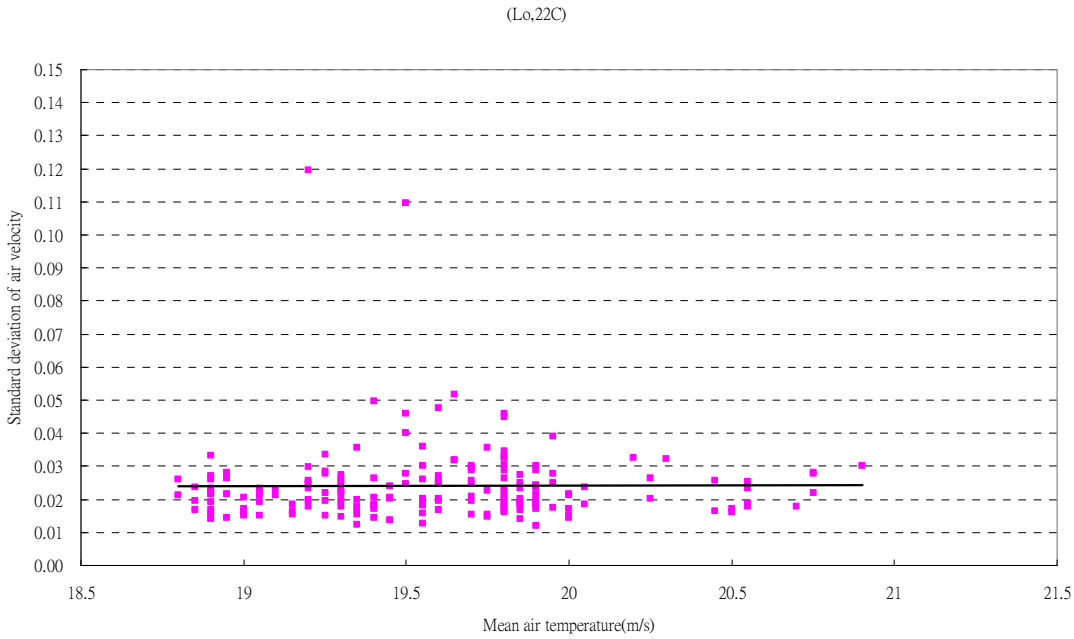

Figure C-33 : Relationship between mean air temperature and standard deviation of air velocity at set point 22 ℃ and low fan speed.

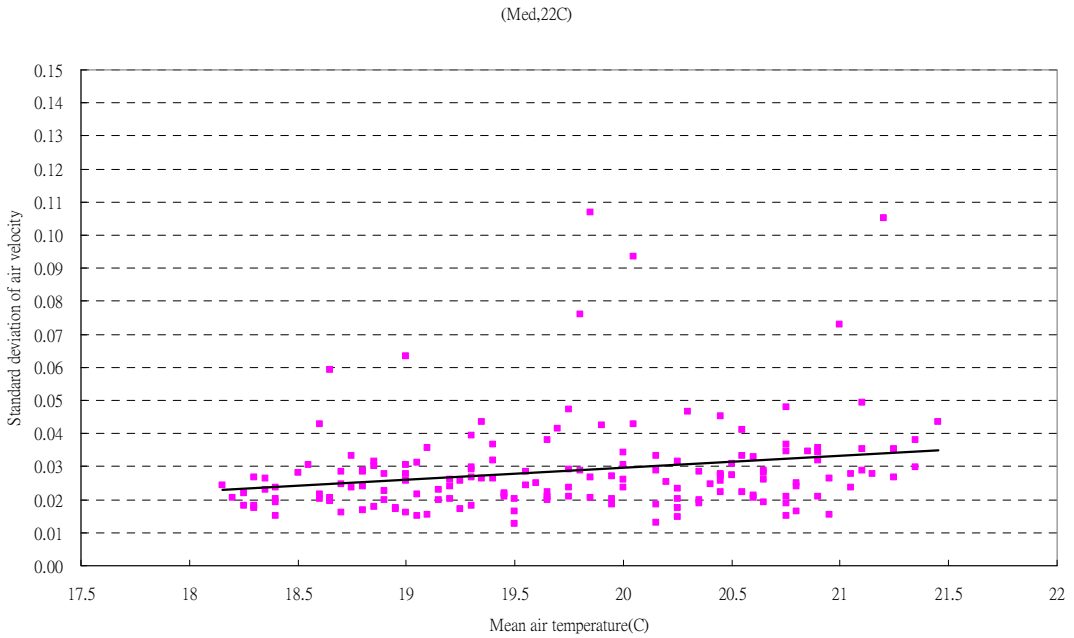

Figure C-34: Relationship between mean air temperature and standard deviation of air velocity at set point 22 ℃ and med fan speed.

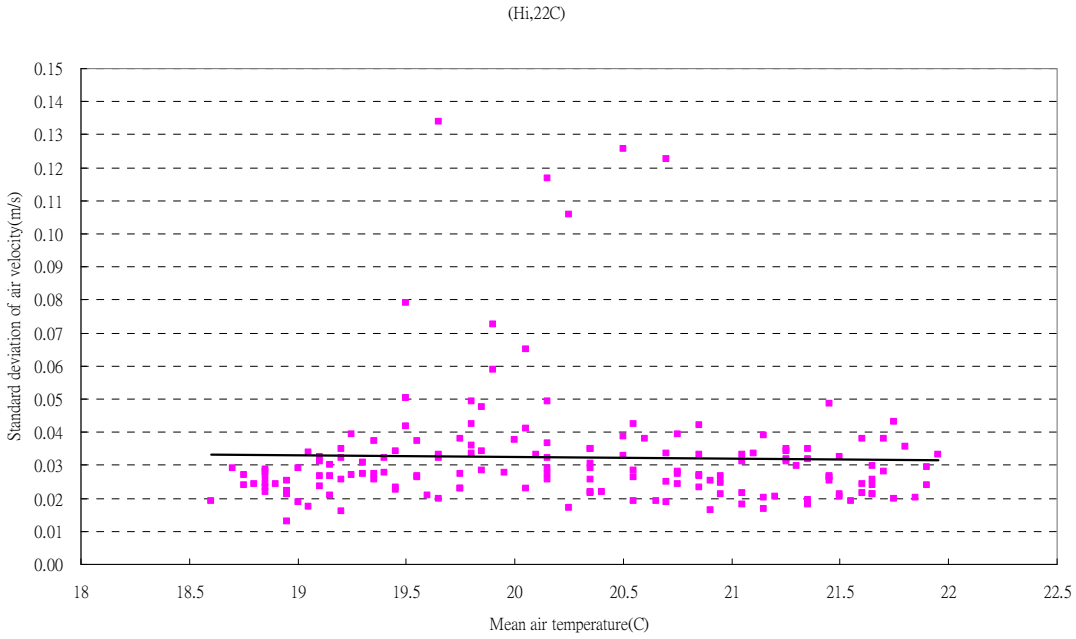

Figure C-35 : Relationship between mean air temperature and standard deviation of air velocity at set point 22 ℃ and hi fan speed.

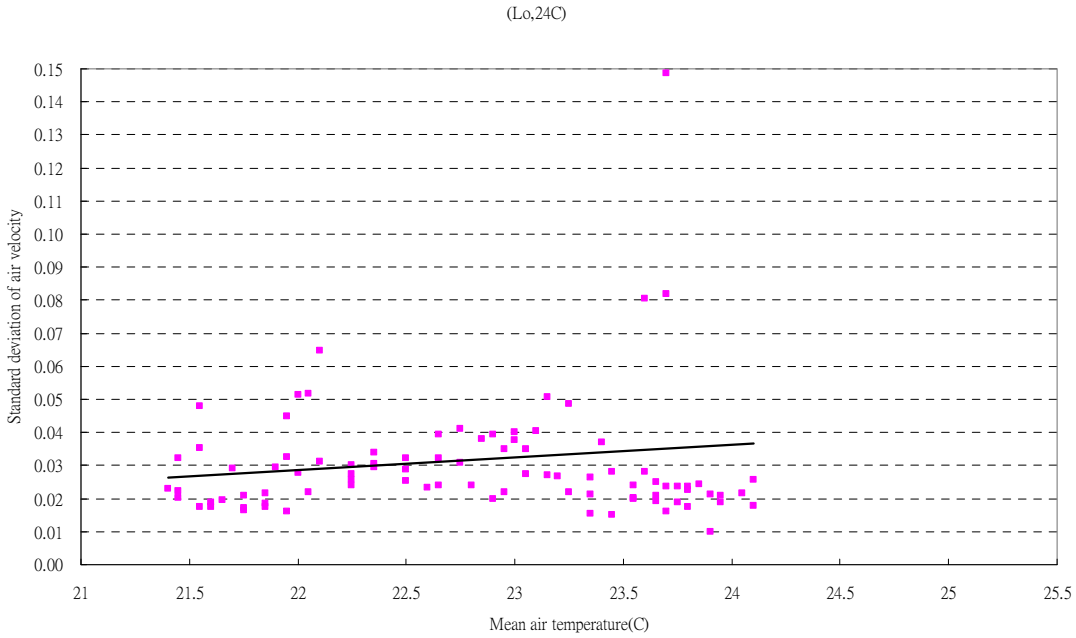

Figure C-36 : Relationship between mean air temperature and standard deviation of air velocity at set point 24 ℃ and low fan speed.

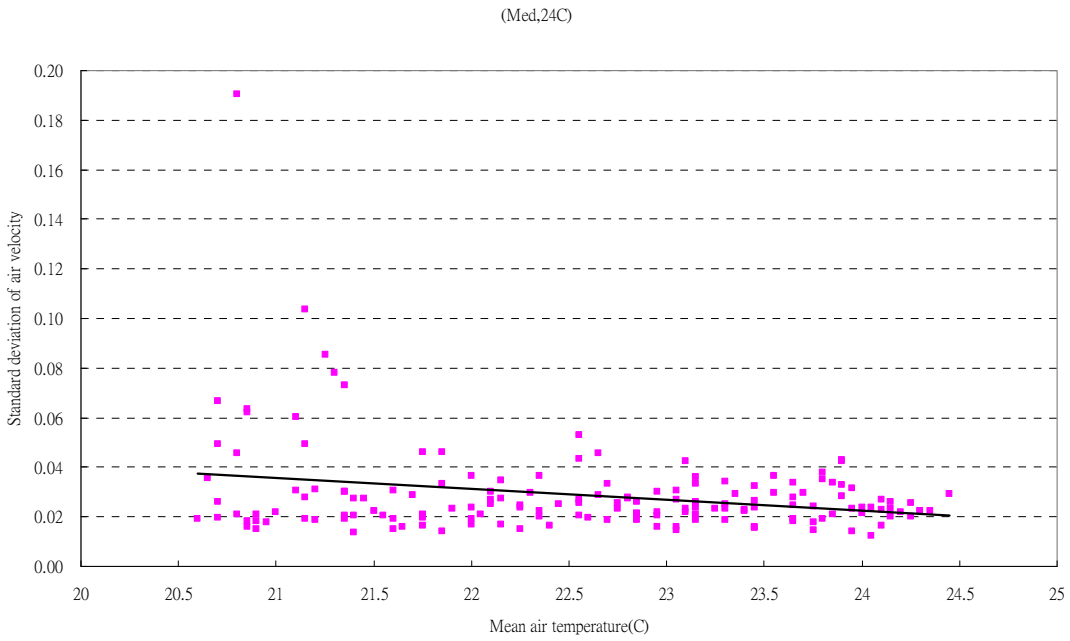

Figure C-37 : Relationship between mean air temperature and standard deviation of air velocity at set point 24 ℃ and med fan speed.

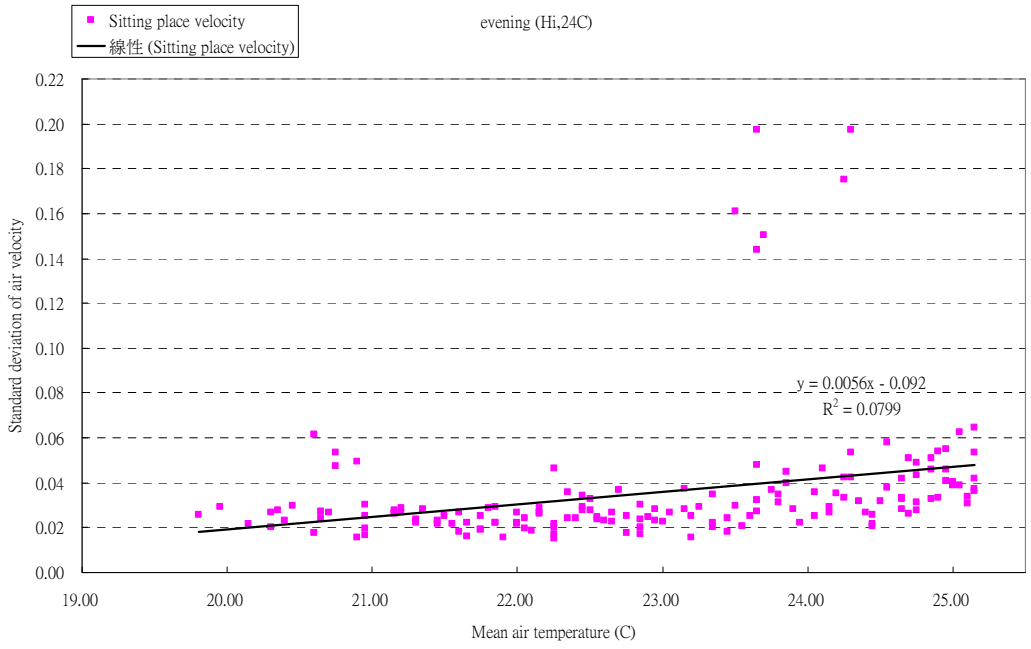

Figure C-38 : Relationship between mean air temperature and standard deviation of air velocity at set point 24 ℃ and hi fan speed.

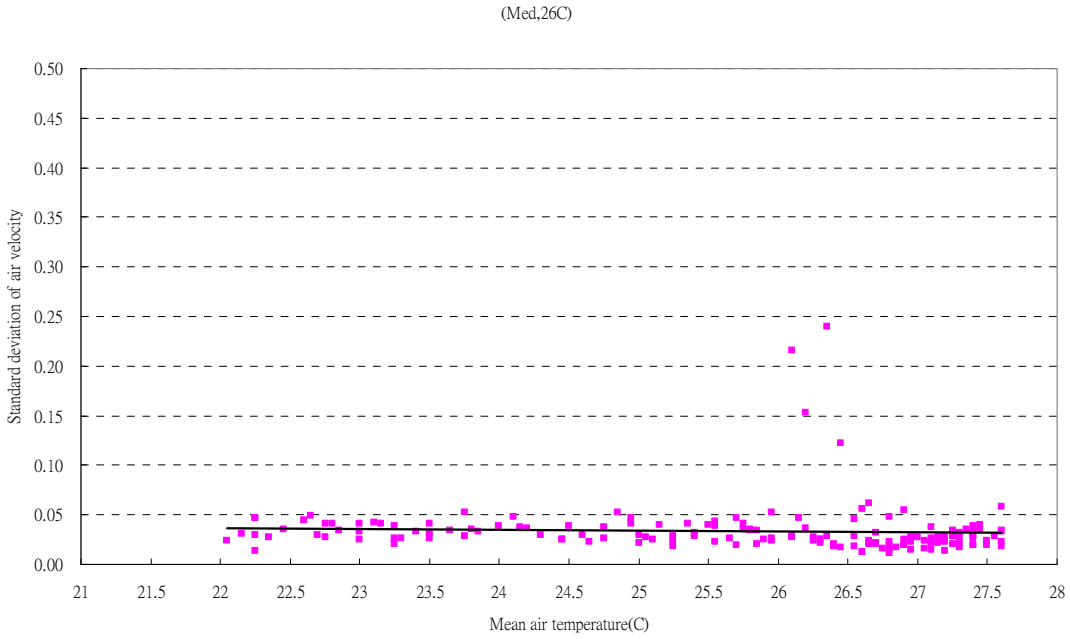

Figure C-39 : Relationship between mean air temperature and standard deviation of air velocity at set point 26 ℃ and med fan speed.

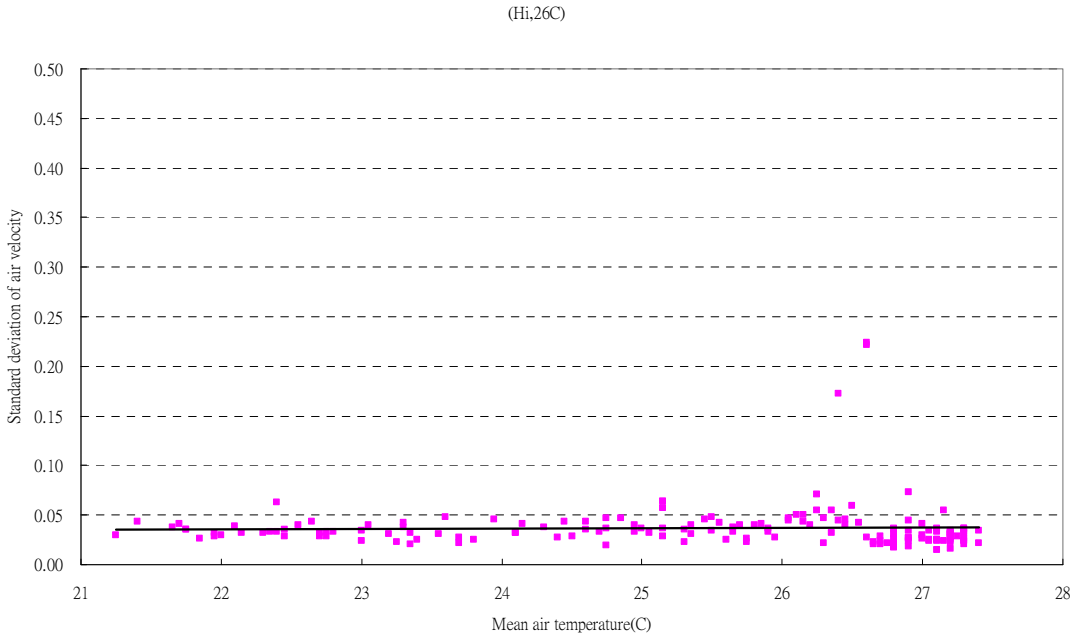

Figure C-40 : Relationship between mean air temperature and standard deviation of air velocity at set point 26 ℃ and hi fan speed.

HFCS (with centrifugal fan and fluctuating frequency)

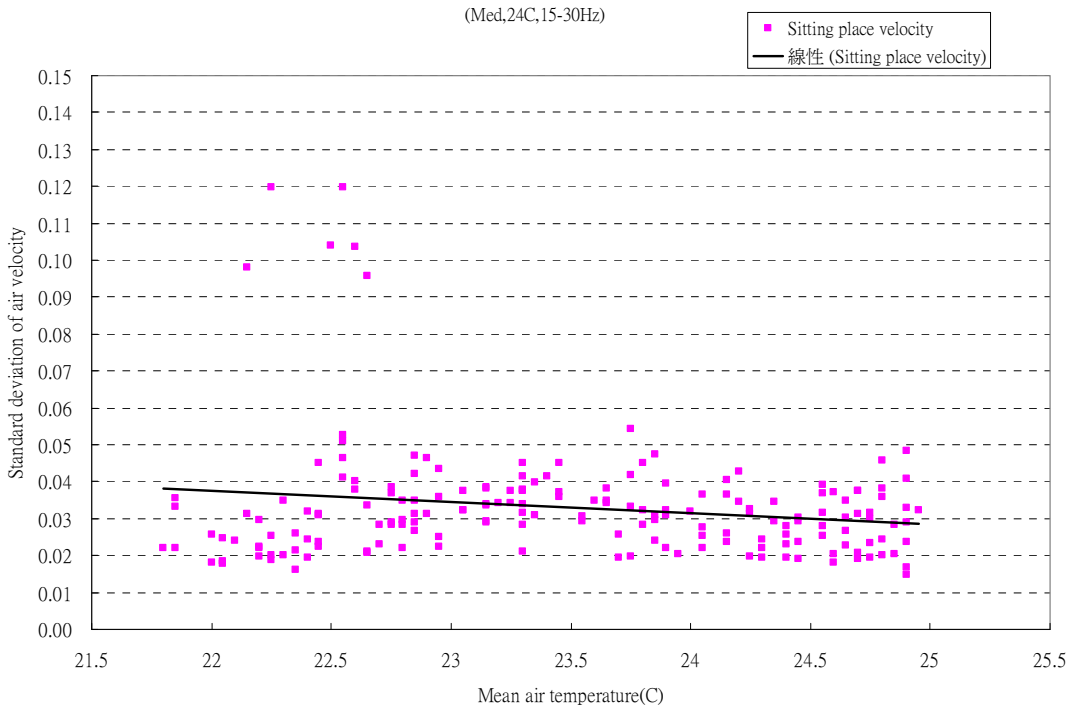

Figure C-41 : Relationship between mean air temperature and standard deviation of air velocity at set point 26 ℃, 15-30Hz and med fan speed.

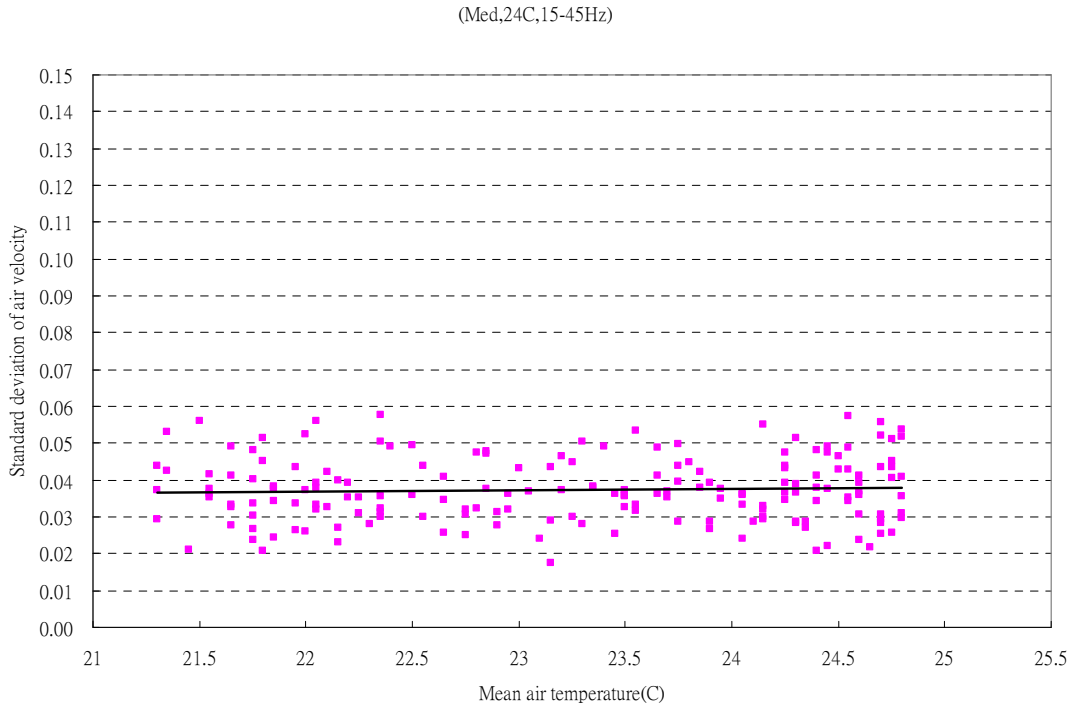

Figure C-42 : Relationship between mean air temperature and standard deviation of air velocity at set point 24 ℃, 15-45Hz and med fan speed.

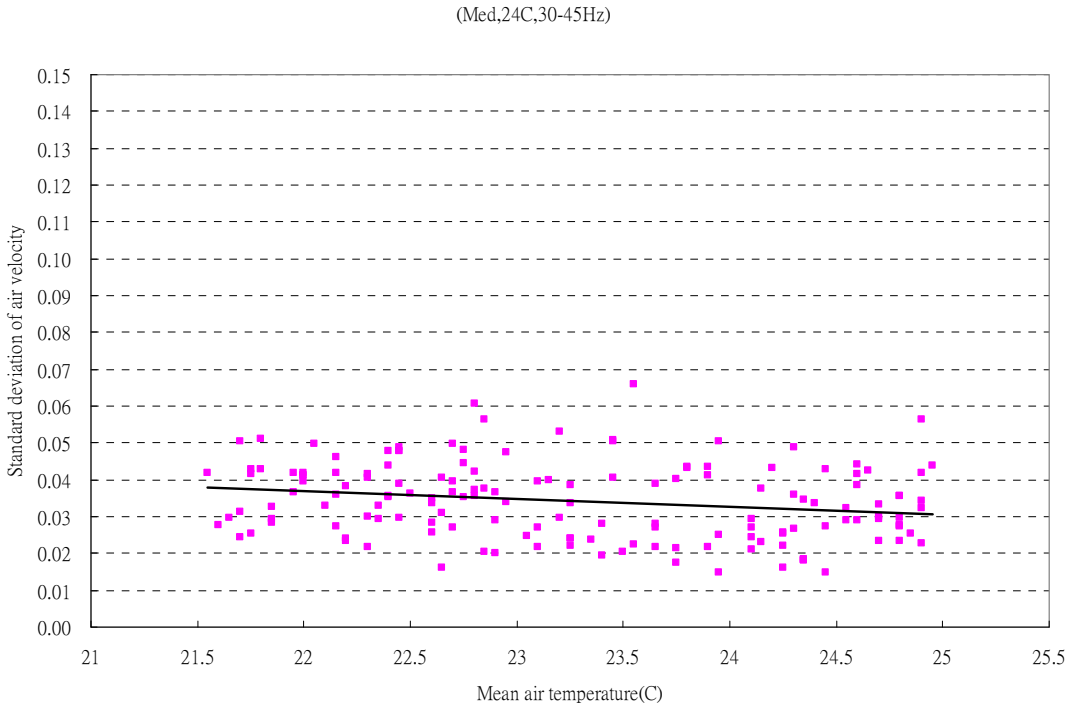

Figure C-43 : Relationship between mean air temperature and standard deviation of air velocity at set point 24 ℃, 30-45Hz and med fan speed.

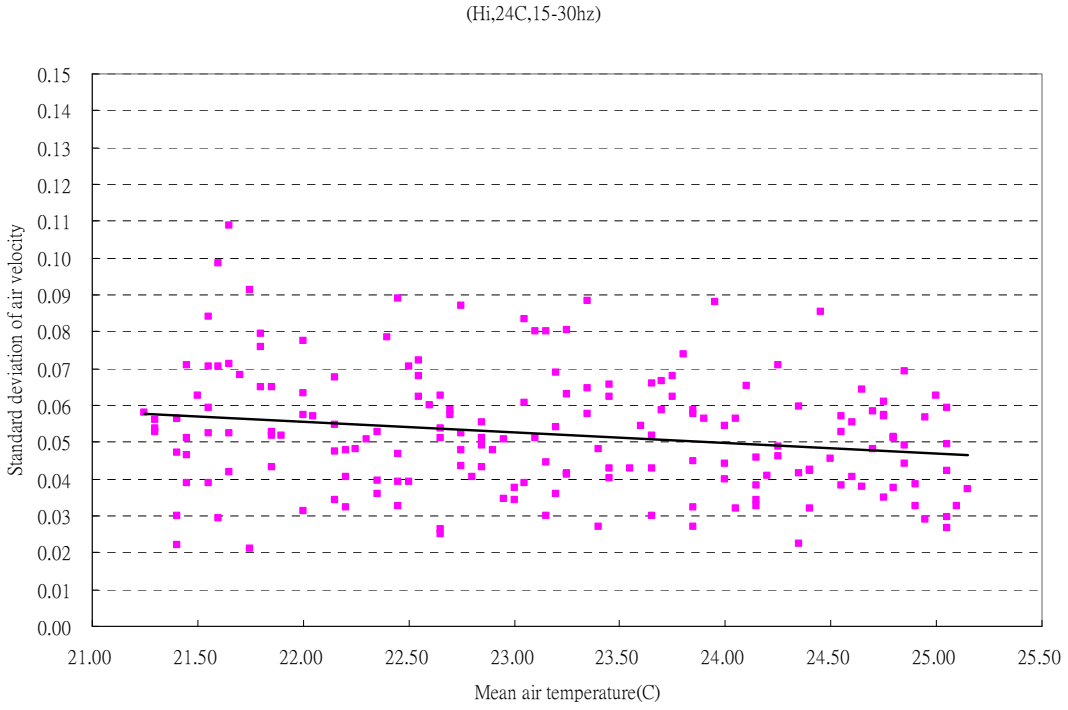

Figure C-44 : Relationship between mean air temperature and standard deviation of air velocity at set point 24 ℃, 15-30Hz and hi fan speed.

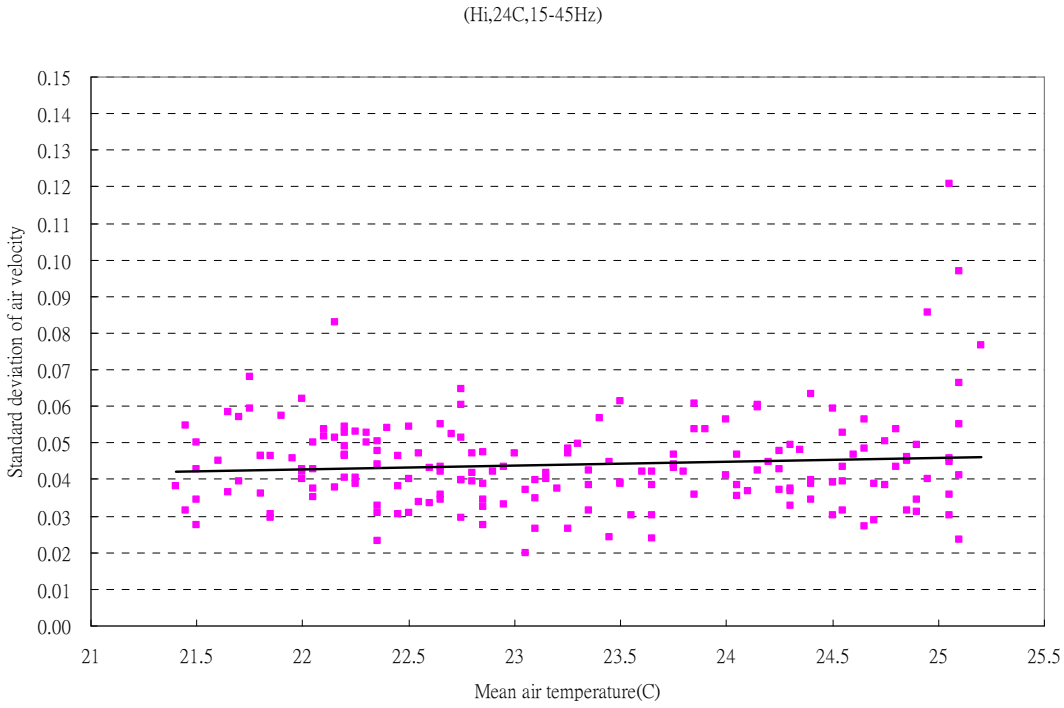

Figure C-45 : Relationship between mean air temperature and standard deviation of air velocity at set point 24 ℃, 15-45Hz and hi fan speed.

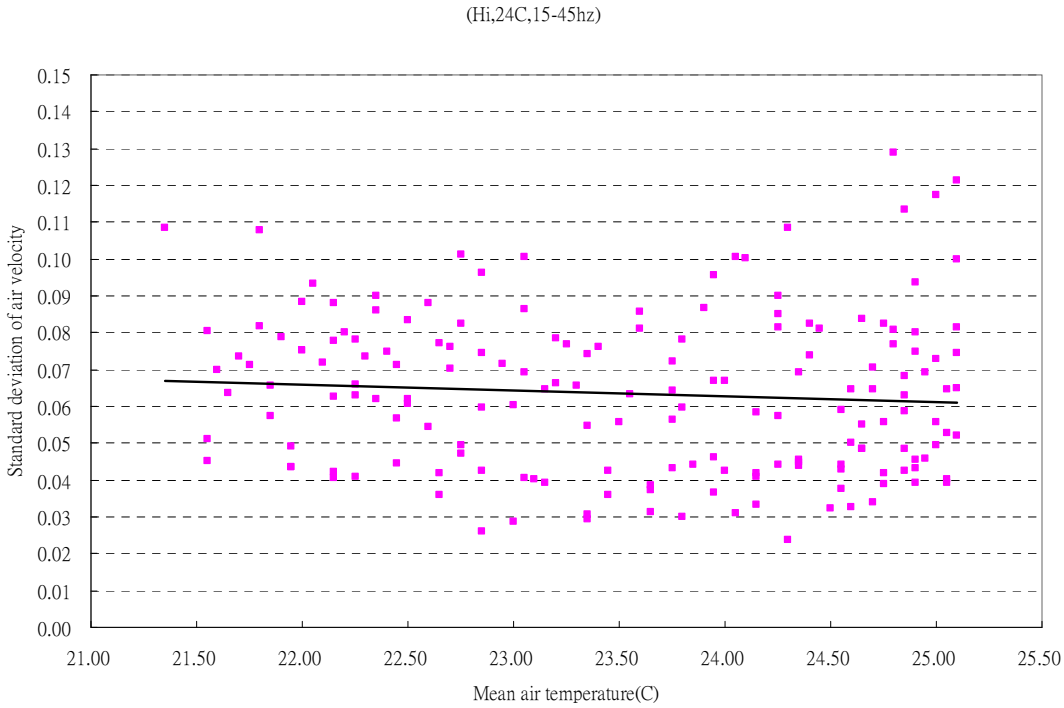

Figure C-46 : Relationship between mean air temperature and standard deviation of air velocity at set point 24 ℃, 15-45Hz and hi fan speed.

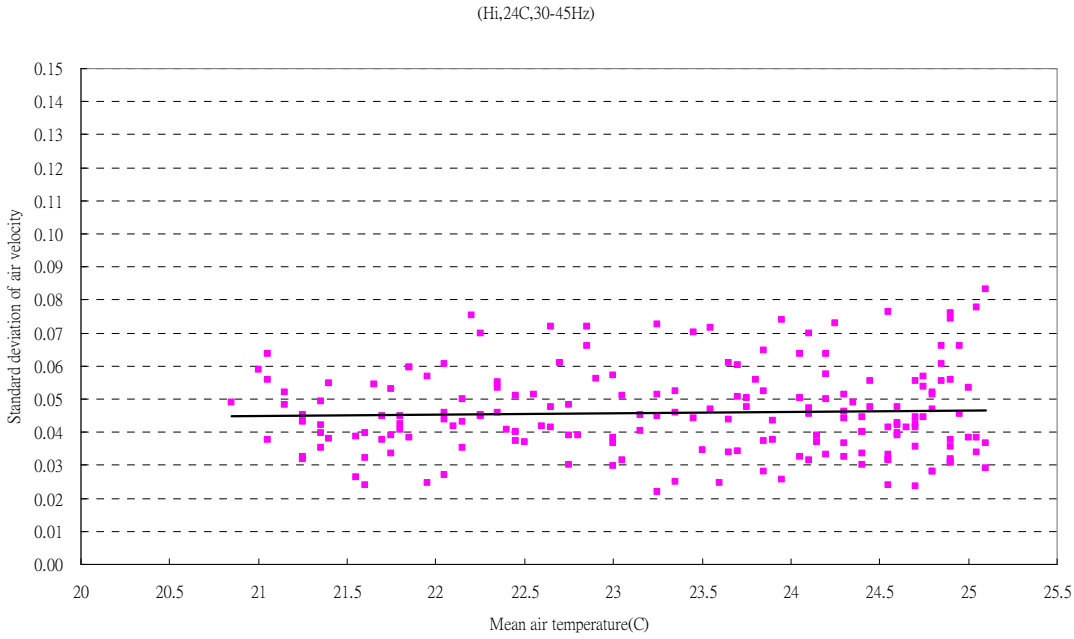

Figure C-47 : Relationship between mean air temperature and standard deviation of air velocity at set point 24 ℃, 30-45Hz and hi fan speed.

C.3 Relationship between mean air temperature and mean air velocity

HFCS (without centrifugal fan)

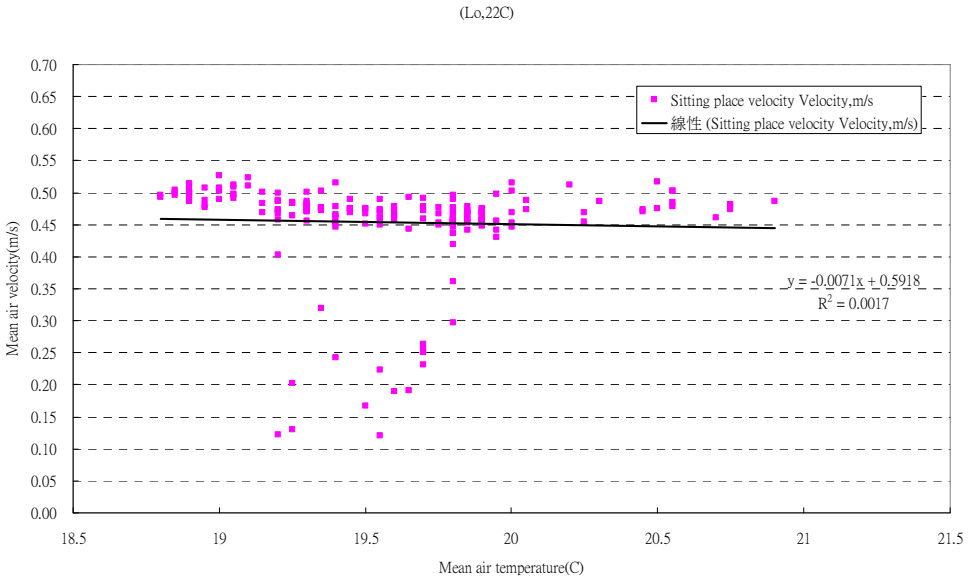

Figure C-48 : Relationship between mean air temperature and mean air velocity at set point 22 ℃ and low fan speed.

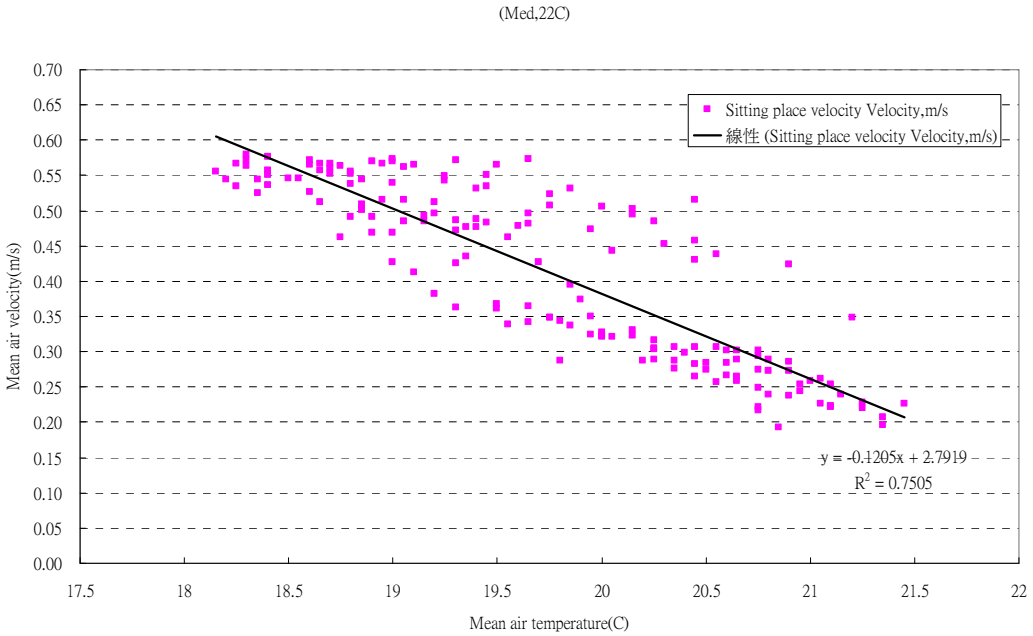

Figure C-49 : Relationship between mean air temperature and mean air velocity at set point 22 ℃ and med fan speed.

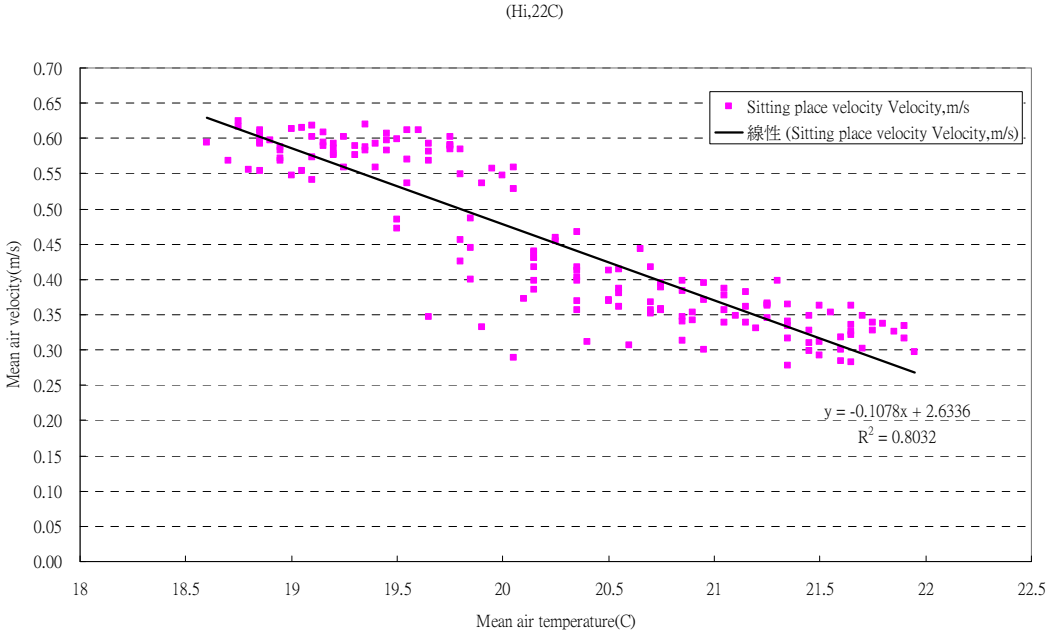

Figure C-50 : Relationship between mean air temperature and mean air velocity at set point 22 ℃ and hi fan speed.

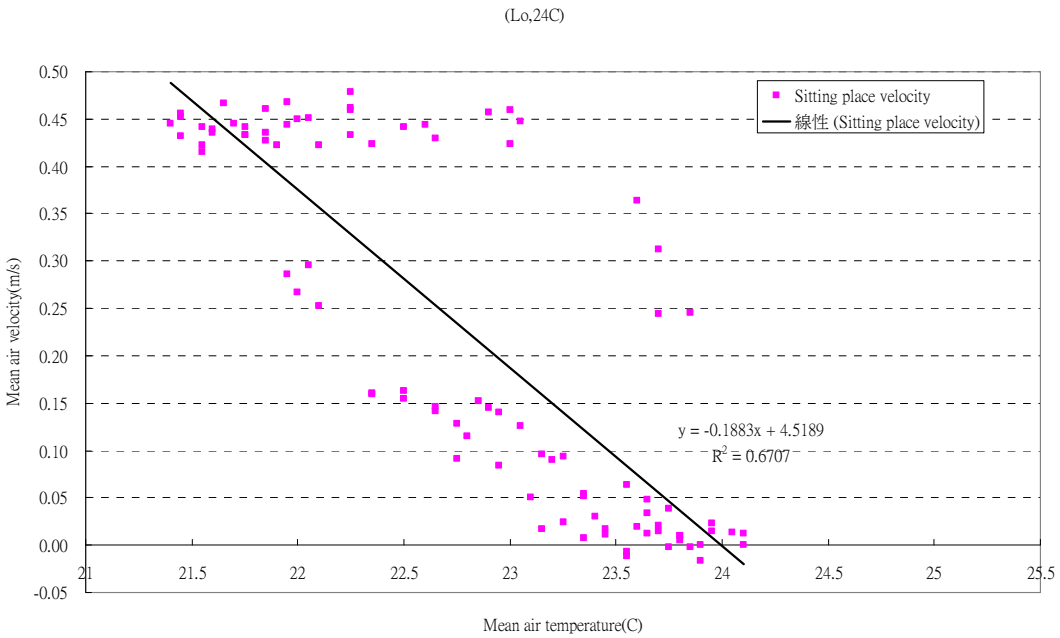

Figure C-51 : Relationship between mean air temperature and mean air velocity at set point 24℃ and low fan speed.

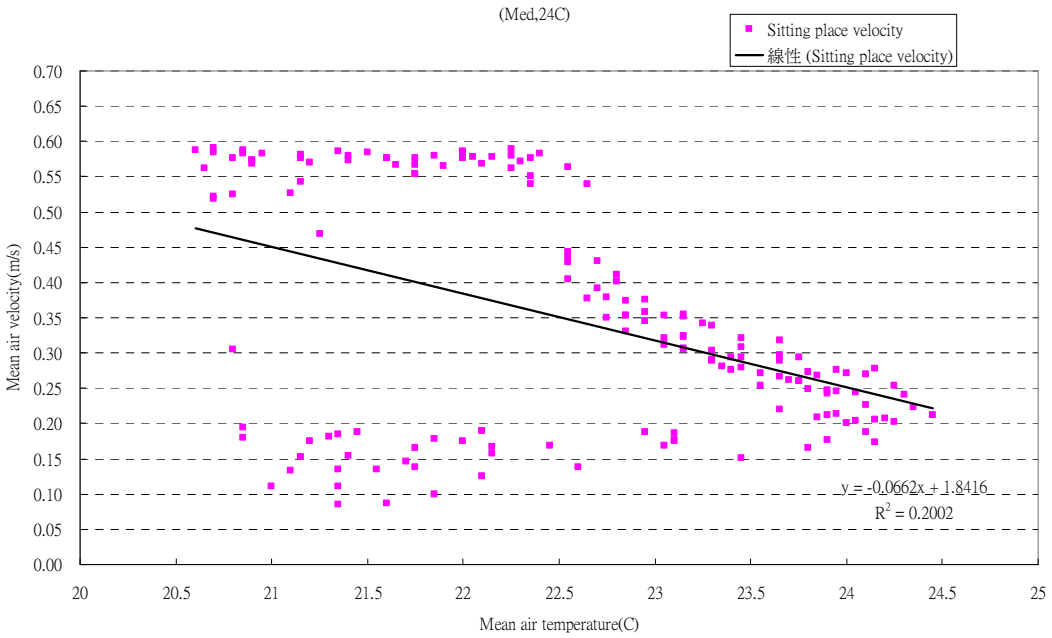

Figure C-52 : Relationship between mean air temperature and mean air velocity at set point 24℃ and med fan speed.

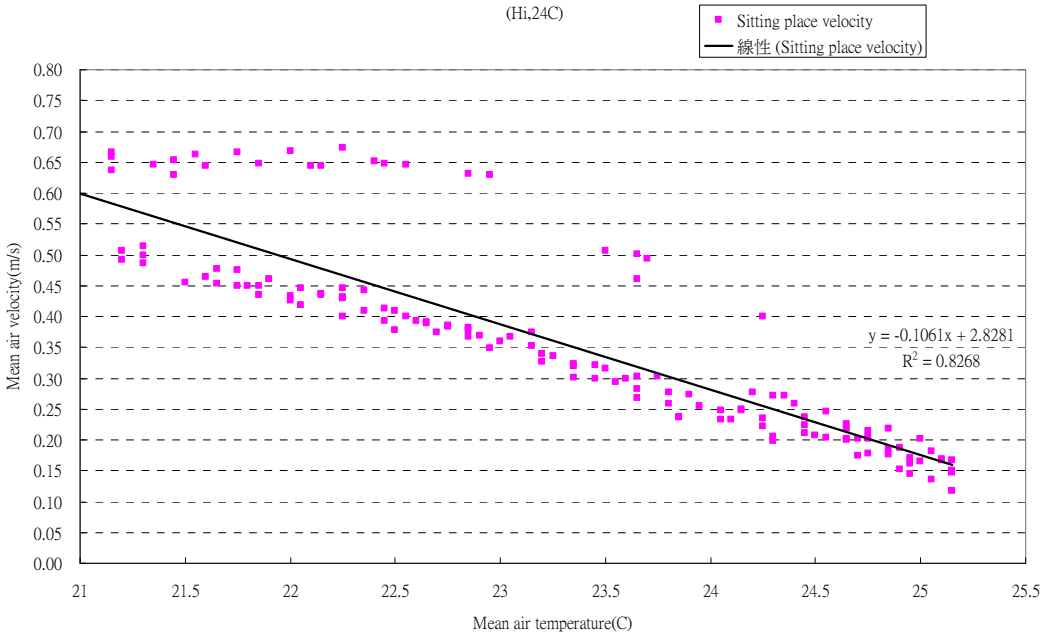

Figure C-53 : Relationship between mean air temperature and mean air velocity at set point 24 ℃ and hi fan speed.

HFCS (with centrifugal fan and fluctuating frequency)

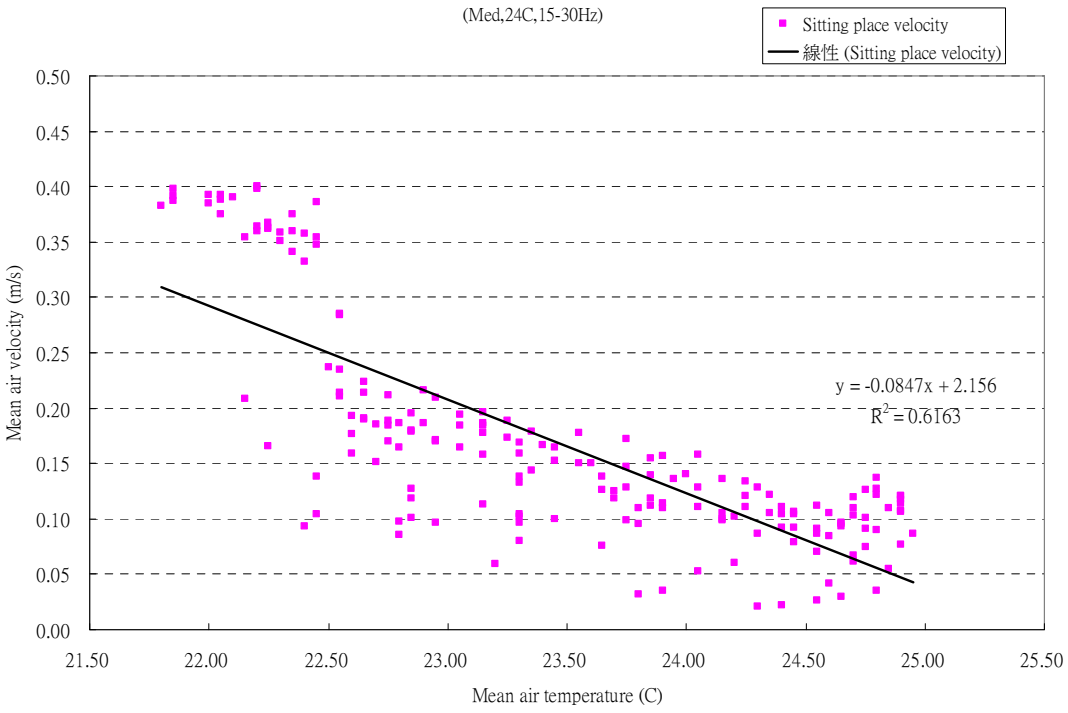

Figure C-54 : Relationship between mean air temperature and mean air velocity of air velocity at set point 24 ℃, 15-30Hz and med fan speed.

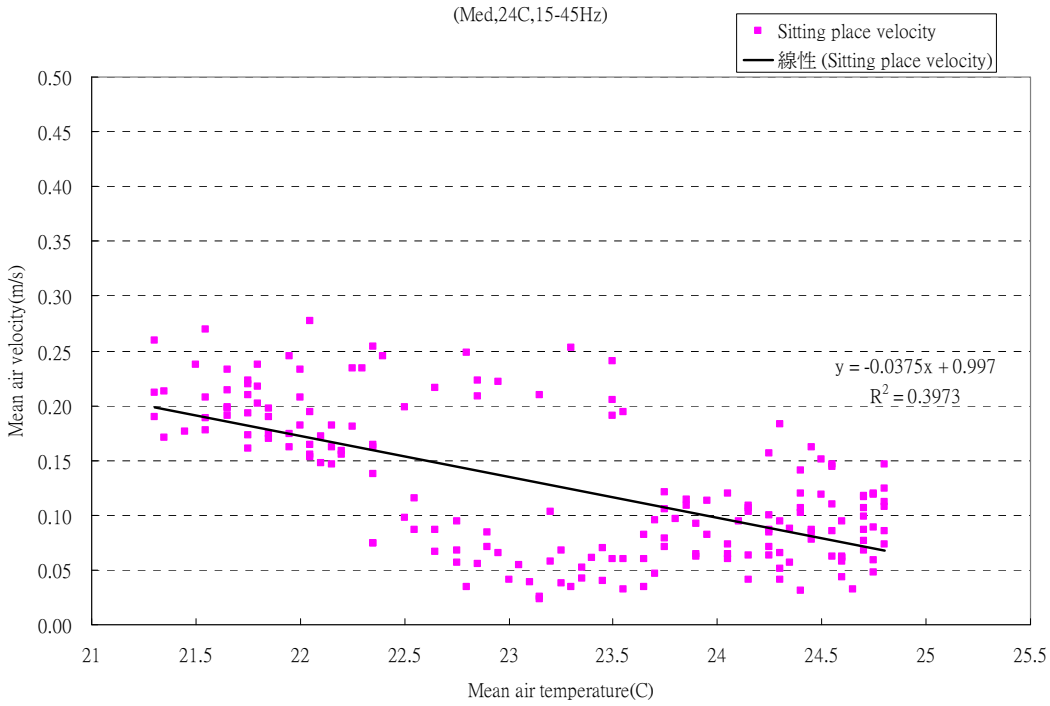

Figure C-55 : Relationship between mean air temperature and mean air velocity of air velocity at set point 24 ℃, 15-45Hz and med fan speed.

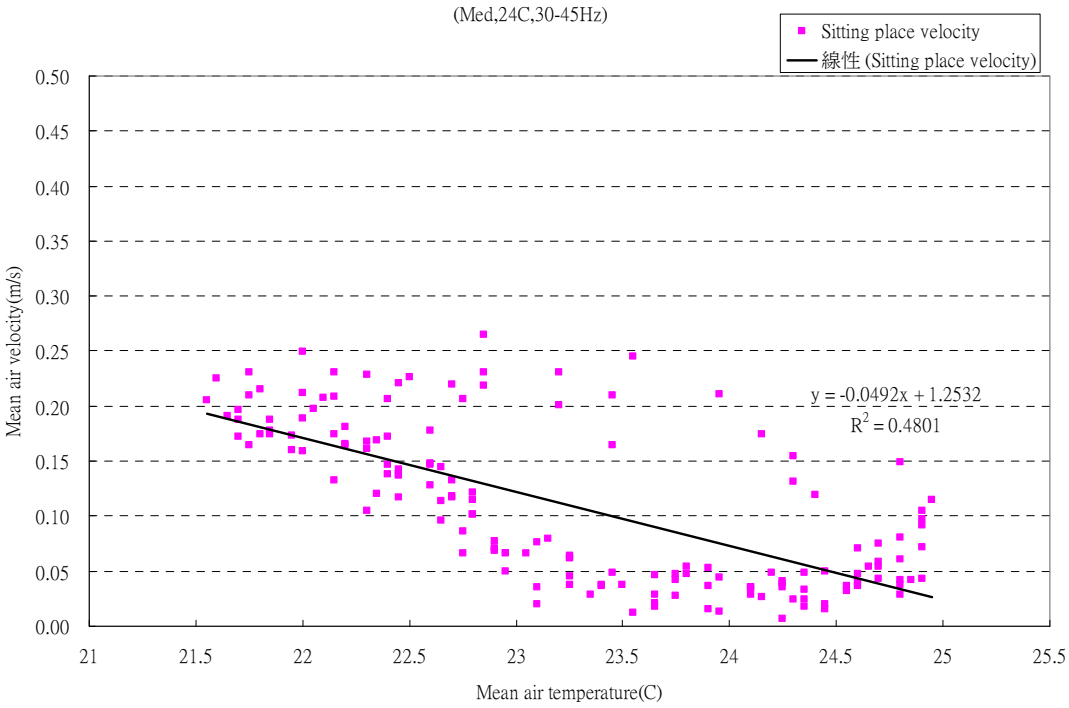

Figure C-56 : Relationship between mean air temperature and mean air velocity of air velocity at set point 24 ℃, 30-45Hz and med fan speed.

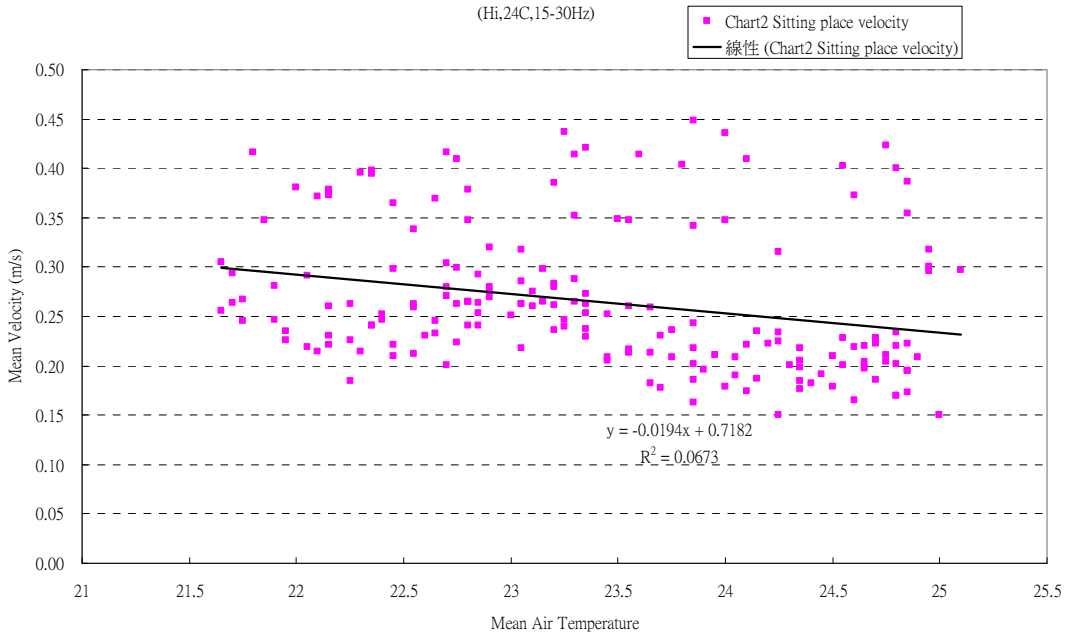

Figure C-57 : Relationship between mean air temperature and mean air velocity of air velocity at set point 24 ℃, 15-30Hz and hi fan speed.

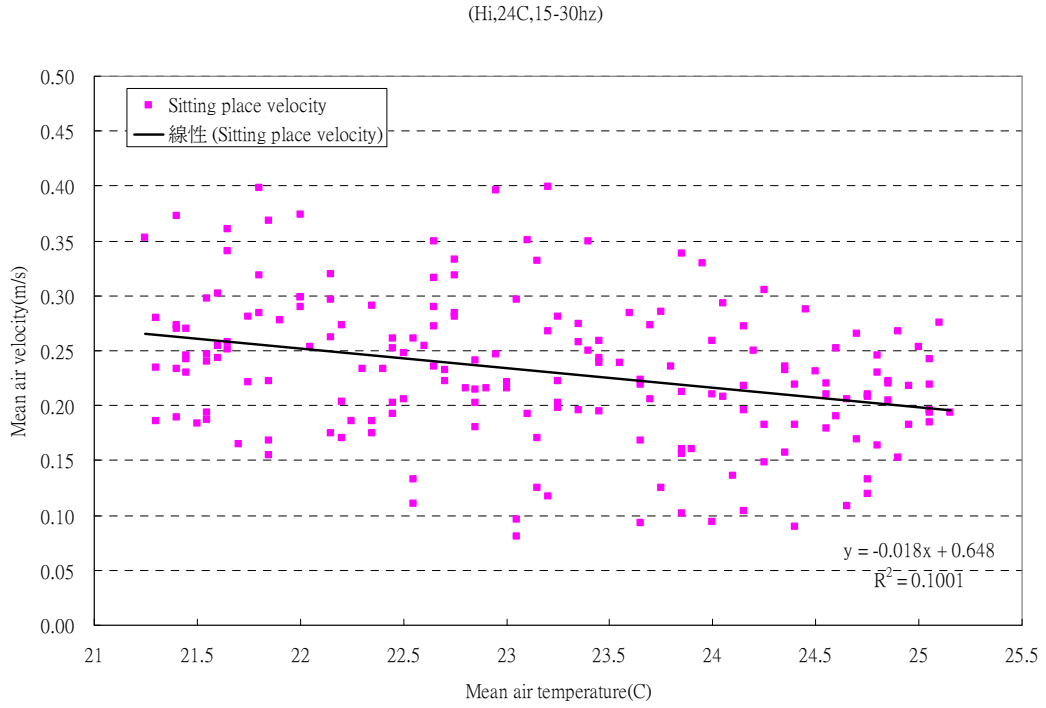

Figure C-58 : Relationship between mean air temperature and mean air velocity of air velocity at set point 24 ℃, 15-30Hz and hi fan speed.

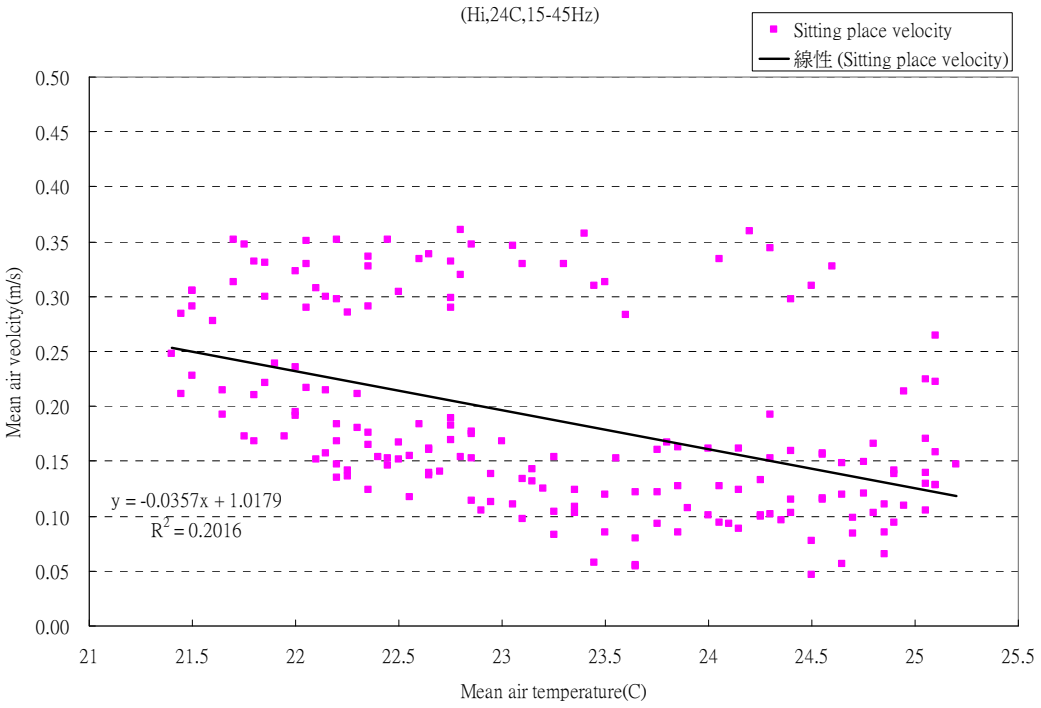

Figure C-59 : Relationship between mean air temperature and mean air velocity of air velocity at set point 24 ℃, 15-45Hz and hi fan speed.

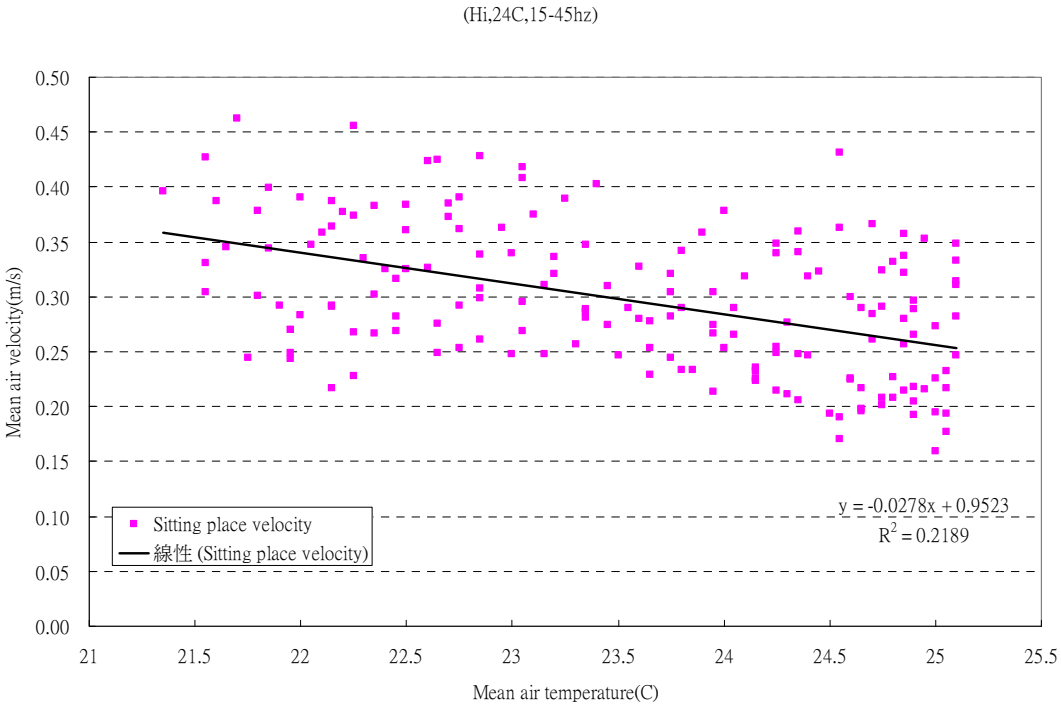

Figure C-60 : Relationship between mean air temperature and mean air velocity of air velocity at set point 24 ℃, 15-45Hz and hi fan speed.

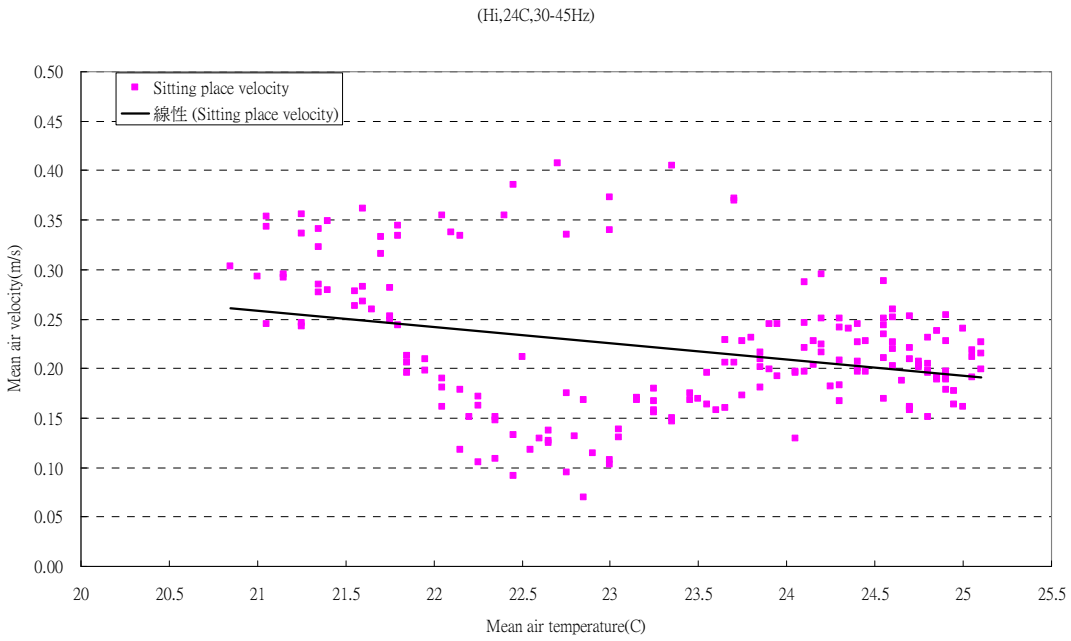

Figure C-61 : Relationship between mean air temperature and mean air velocity of air velocity at set point 24 ℃, 30-45Hz and hi fan speed.

APPENDIX D: CFD GOVERNING EQUATION

The following conservation equations for mass and momentum have been used to solve the steady flow problem. The equation for conservation of mass can be written as

$$\frac{\partial}{\partial x_i}\left(\rho u_i\right) = S_m \tag{D.1}$$

The above equation is valid for incompressible as well as compressible flows. The sources S_m is the mass added to the continuous phase from the dispersed second phase (e.g. due to the vaporization of liquid droplets) and by any other user-defined source.

Conservation of momentum for the *i*th direction in an inertial reference frame is written as

$$\frac{\partial}{\partial x_i}\left(\rho u_i u_j\right) = -\frac{\partial p}{\partial x_i} + \frac{\partial \tau_{ij}}{\partial s_j} + \rho g_i + F_i \tag{D.2}$$

where τ_{ij} is the shear stress tensor which is given by

$$\tau_{ij} = \left[\mu\left(\frac{\partial u_i}{\partial x_j} + \frac{\partial u_j}{\partial x_i}\right)\right] - \frac{2}{3}\mu\frac{\partial u_i}{\partial x_j}\delta_{ij} \tag{D.3}$$

The second term on the right hand side is the effect of volume dilation or calculating the pressure. This method is derived from the SIMPLE algorithm of Patankar and Spalding (Patankar, Spalding, 1972).

For turbulent flow, the flow variables are decomposed into mean and fluctuating components and substituted in the above instantaneous equation. Taking the time average yields the averaged momentum equation as

$$\frac{\partial}{\partial x_j}\left(\rho u_i u_j\right) = -\frac{\partial p}{\partial x_i} + \frac{\partial}{\partial x_i}\left[\mu\left(\frac{\partial u_i}{\partial x_j} + \frac{\partial u_j}{\partial x_i} - \frac{2}{3}\delta_{ij}\frac{\partial u_i}{\partial x_j}\right)\right] + \frac{\partial}{\partial x_j}\left(-\rho\overline{u_i' u_j'}\right) \qquad \text{(D.4)}$$

The continuity equation remains the same.

Addition terms, $\left(-\rho\overline{u_i' u_j'}\right)$ appear that represent the effect of turbulence and needs to be modeled in order to get closer solutions (Wilcox, 2000).

In turbulent flows, small, high frequency fluctuations are present even in a steady flow, and to account for these, time-averaging procedure is employed, which results in additional terms. These additional terms need to be expressed as calculable quantities for closure solution. The standard $k-\varepsilon$ model will be used in the simulation of most indoor air flow simulation as suggested by Chen (Chen, Srebric, 2002), a semi-empirical model based on model transport equations for

the turbulent kinetic energy 'k' and its dissipation rate 'ε'. The standard $k-\varepsilon$ model is as follows:

Kinematic eddy viscosity:

$$\nu_T = \frac{C_\mu k^2}{\varepsilon} \tag{D.5}$$

Turbulent kinetic energy:

$$\frac{\partial k}{\partial t} + u_j \frac{\partial k}{\partial x_j} = \tau_{ij} \frac{\partial u_i}{\partial x_j} - \varepsilon + \frac{\partial}{\partial x_j}\left[\left(\nu + \frac{\nu_T}{\sigma_k}\right)\frac{\partial k}{\partial x_j}\right] \tag{D.6}$$

Dissipation rate:

$$\frac{\partial \varepsilon}{\partial t} + u_j \frac{\partial \varepsilon}{\partial x_j} = C_{\varepsilon 1} \frac{\varepsilon}{k} \tau_{ij} \frac{\partial u_i}{\partial x_j} - C_{\varepsilon 2} \frac{\varepsilon^2}{k} + \frac{\partial}{\partial x_j}\left[\left(\nu + \frac{\nu_T}{\sigma_\varepsilon}\right)\frac{\partial \varepsilon}{\partial x_j}\right] \tag{D.7}$$

Closure coefficients and auxiliary relations:

$C_{\varepsilon 1}$=1.44, $C_{\varepsilon 2}$=1.92, C_μ=0.09, σ_ε=1.3, σ_k=1.0, $\omega = \frac{\varepsilon}{C_\mu k}$ and $\ell = \frac{C_\mu k^{\frac{3}{2}}}{\varepsilon}$

However, according to the Chen's research (Chen, 1995), renormalization group (RNG) $k-\varepsilon$ model is more accurate then the standard $k-\varepsilon$ for all indoor simulations conducted for this project. The RNG $k-\varepsilon$ model was developed by Yakhot and Orszag (Yakhot et al., 1986). The equation for the eddy viscosity

still uses those in the standard $k-\varepsilon$, but applies a modified coefficient, $C_{\varepsilon 2}$, which is:

$$C_{\varepsilon 2} \equiv \tilde{C}_{\varepsilon 2} + \frac{C_\mu \lambda^3 \left(\frac{1-\lambda}{\lambda}\right)}{1+\beta\lambda^3}, \lambda \equiv \frac{k}{\varepsilon}\sqrt{2S_{ij}S_{ji}} \qquad \text{(D.8)}$$

RNG has different closure coefficients as the standard, they are:

$C_{\varepsilon 1}$=1.42, $C_{\varepsilon 2}$=1.68, C_μ=0.085, σ_ε=0.72, σ_k=0.72, β=0.012, λ_o=4.38.

For the near-wall treatment, non-equilibrium wall functions are adopted here as the Reynolds number is low to the near wall region. On the other hand, RNG only works under a high Reynolds number. The non-equilibrium wall function is different from the standard wall function in two ways: the treatment of the mean velocity, which is sensitized to the pressure gradient, and the two-layer based concept for turbulence kinetic energy ($\overline{G}_k$, $\bar{\varepsilon}$) calculation.

y_v is the dimensionless thickness of the viscous sub layer

$$y_v \equiv \frac{\mu y_v^*}{\rho C_\mu^{1/4} k_p^{1/2}}, \quad y_v^* = 11.225 \qquad \text{(D.9)}$$

The mean velocity is calculates as:

$$\frac{\hat{U} C_\mu^{1/4} k_p^{1/2}}{\tau_\omega / \rho} = \frac{1}{0.4187} \ln\left(9.793 \frac{\rho C_\mu^{1/4} k_p^{1/2} y_p}{\mu}\right) \qquad \text{(D.10)}$$

where

$$\hat{U} = U - \frac{1}{2}\frac{dp}{dx}\left[\frac{y_v}{\rho\kappa\sqrt{k}}\ln\left(\frac{y}{y_v}\right) + \frac{y - y_v}{\rho\kappa\sqrt{k}} + \frac{{y_v}^2}{\mu}\right] \tag{D.11}$$

As mentioned before, the non-equilibrium wall function divided the region into 2 sub-layers, when $y \prec y_v$, $\tau_t = 0, k = \left(\frac{y}{y_v}\right)^2 kp$ and $\varepsilon = \frac{2\nu k}{y^2}$, on the other hand, when $y > y_v$, $\tau_t = \tau_w, k = kp, \varepsilon = \frac{k^{3/2}}{C_l y}$

$$\overline{G_k} \equiv \frac{1}{y_n}\int_0^{y_n} \tau_t \frac{\partial U}{\partial y} dy = \frac{1}{\kappa y_n}\frac{\tau_\omega^2}{\rho C_\mu^{1/4} k_p^{1/2}}\ln\left(\frac{y_n}{y_v}\right) \tag{D.12}$$

$$\bar{\varepsilon} \equiv \frac{1}{y_n}\int_0^{y_n} \varepsilon dy = \frac{1}{y_n}\left[\frac{2\nu}{y_v} + \frac{k_p^{1/2}}{C_l}\ln\left(\frac{y_n}{y_v}\right)\right]k_p \tag{D.13}$$

Discretization method

For calculating pressure, the SIMPLE algorithm is adopted, while for the others, second-order upwind is applied.

The basic steps for the SIMPLE (semi-implicit method got pressure-linked equations) are shown in the following flow chart:

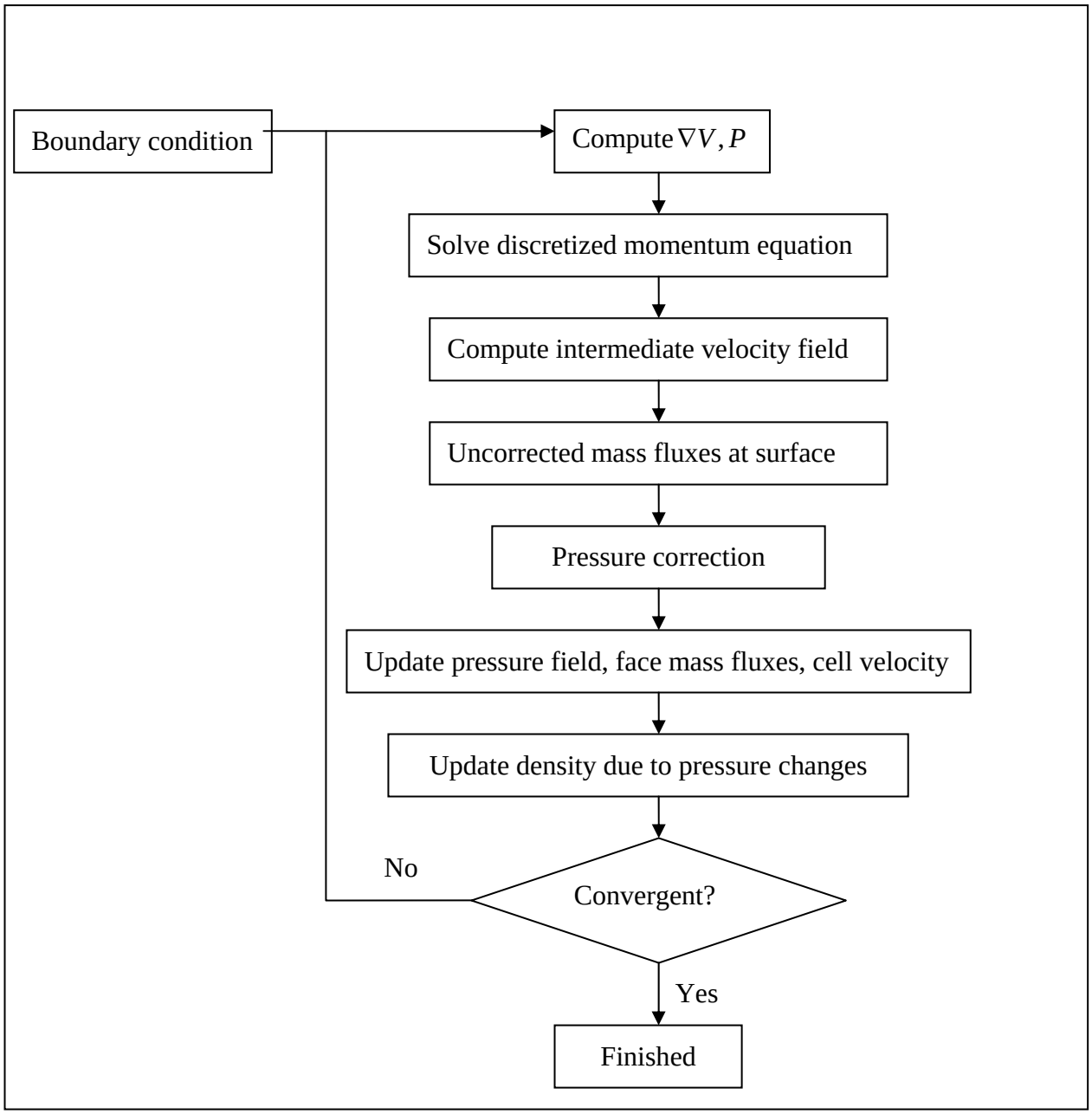

Figure D.1: Calculation procedure of SIMPLE algorithm

Second-order upwind first calculates the average of the parameter ϕ between two adjacent cells, then uses the two cell average ($\tilde{\phi}_f$) to calculate the gradient of the parameters to the upstream cell, $\nabla\phi$ by taking volume average of the $\tilde{\phi}_f$:

$$\nabla\phi = \frac{1}{V}\sum_{f}^{N_{face}} \tilde{\phi}_f \vec{A} \qquad \text{(D.14)}$$

Then the new face value is calculated by the summation of the old value ϕ plus the gradient times the displacement of the centroids ($\nabla \vec{s}$).

$$\phi_f = \phi + \nabla\phi \cdot \nabla\vec{s} \qquad \text{(D.15)}$$

Unlike first-order upwind and power-law scheme, the second-order upwind takes more cell values into consideration, and thus a higher accuracy is expected. When compared to the QUICK scheme, second-order upwind can save computational time. Consequently, this scheme provides an optimum between computational time and accuracy level.

Boundary types

Wall

The input variables for the wall are heat flux and surface temperature. For the human surface, only surface temperature is applied, as by inputting heat fluxes, an unreasonable surface temperature may occur.

Velocity inlet

For the boundary condition of the velocity inlet, the input variables for all the simulations include velocity magnitude and direction, temperature, and the parameter for determining the turbulence. In all the simulation cases described in

this thesis, the inputs to specify the turbulence are the intensity and hydraulic diameter method. The intensity I is defined as:

$$I \equiv \frac{rms(V)}{\overline{V}} = 0.16\left(\mathrm{Re}_{D_H}\right)^{-1/8} \cdot 100\% \qquad \text{(D.16)}$$

In most of the cases, the I is set to be 5%.

The hydraulic diameter is calculated by the area and the perimeter of the opening:

$$D_H = \frac{4A}{U} \qquad \text{(D.17)}$$

In most of the cases, the I is set to be 5%.